STUDY OF BIOMASS GASIFIER-ENGINE SYSTEMS WITH INTEGRATED FEED DRYING FOR POWER AND CHP

JOHN GRAHAM BRAMMER

Doctor of Philosophy

Aston University

February 2001

Aston University

STUDY OF BIOMASS GASIFIER-ENGINE SYSTEMS WITH INTEGRATED FEED DRYING FOR POWER AND CHP

JOHN GRAHAM BRAMMER

Doctor of Philosophy
2001

SUMMARY

Biomass gasification systems for the production of electricity suffer from a number of technical disadvantages at smaller scales, notably the presence of tars in the fuel gas, low overall efficiency and high capital cost. This study addresses biomass gasifier-engine systems for power and combined heat and power (CHP) in the size range 0.5-2.0 dry tonnes per hour (roughly equivalent to 0.5-3.0 MW_e). By the use of system modelling, it seeks to identify efficiency and cost optima from a wide range of system configurations and operating conditions.

The need to dry biomass feedstocks before they can be gasified can place a large energy and capital cost burden on smaller-scale systems. Drying may not always be unavoidable, but as biomass moisture content to the gasifier increases, the quality of the product gas deteriorates along with the overall performance of the whole system. Particular emphasis is therefore given in the study to the integration of biomass drying, with the type of dryer and the source of heat considered in detail.

The system model is spreadsheet-based, with individual worksheets corresponding to models of system components. This approach allows easy modification of the model, and rapid generation of results. Most of the system components are explicitly modelled on a continuous basis, rather than being represented as fixed processes based on user-supplied data. Wherever possible, data supplied by manufacturers or taken from real systems is used in the construction of the sub-models, particularly in the derivation of cost functions.

In addition to the emphasis on drying integration, the study also considers the alternatives of high-temperature slagging and conventional gasification (the former allowing the consideration of air oxygen enrichment), both with suitable provision for the delivery of a low-tar product gas. In the case of slagging gasification, the potential for supplying oxygen-enriched air to the engine as well as the gasifier is also examined.

2

DEDICATION

To Caroline, my wife.

ACKNOWLEDGEMENTS

TABLE OF CONTENTS

APPENDICES

LIST OF FIGURES

LIST OF TABLES

14

SYMBOLS AND ABBREVIATIONS

Primary Symbols

A	area	m^2
ACB	annual cost of biomass	£'000 p.a.
ACC	annual cost of capital	£'000 p.a.
AF	annuity factor	
AP	annual profit	£'000 p.a.
AR	annual revenue	£'000 p.a.
C, C_n	constants	
c	specific heat capacity	J/kgK, kJ/kgK
COD	chemical oxygen demand	mg/l
COE	cost of electricity	£/kWh
d	discount rate	%
DC	delivered cost	£/dt (£ per dry tonne)
DPC	direct plant cost	£'000
EC	equipment cost	£'000
EP	electricity price	£/kWh
F	gasifier equipment cost factor	
f, g	functions	
FC	fixed charge	£'000 p.a.
H	enthalpy	kJ/kg
ΔH	enthalpy of reaction/combustion	MJ/kg, MJ/Nm^3
HHV	higher heating value	MJ/kg, MJ/Nm^3 (dry basis u.o.s.)
HP	heat price	£/kWh
i	inflation rate	%
IPC	installed plant cost	£'000
l	project lifetime	years
L	labour requirement	persons per shift
LC	lease charge	£'000 p.a.
LF	learning factor	
LHV	lower heating value	MJ/kg, MJ/Nm^3 (dry basis u.o.s.)
LR	learning ratio	

M	mass	kg, t
m	mass flow	kg/s, t/h, dt/h (dry tonnes per hour)
N	number of units	
OOC	other operating costs	£'000 p.a.
P	power (electrical,mechanical)	kW, MW
Q	heat flow, thermal input	kW, MW
StS	settleable solids	mg/l
T	temperature	°C, K
ΔT	temperature difference	K
t	time, period	s, h
TPC	total plant cost	£'000
U	heat transfer coefficient	W/m^{2}K
V	volume	m^3
v	interstitial velocity	m/s
W	volume flow rate	m^3/s, Nm^3/s
X	moisture content (dry basis)	% (kg moisture per 100kg dry solid)
x	distance	m
Y	absolute humidity	kg/kg (kg moisture per kg dry gas)
Z	regenerator length	m
ϕ	mean diameter	mm
Λ	reduced length	
Π	reduced period	
λ	equivalence ratio (air:fuel)	
η	efficiency	% (LHV basis u.o.s.)
[]	concentration	vol. frac. (u.o.s.)

Subscripts and Superscripts

A	air	AR	actual reaction
B	dry biomass	B	brake thermal
C	cooling or sealing water	c	cycle
d	drying	E	electricity
EA	equilibrium approach	ER	equilibrium reaction

G	gas	H	heat
I	indicated	L	loss
NG	natural gas	O	oxygen
OV	*overall*	P	regenerator packing
PG	product gas	T	total
v	volumetric	V	vapour
W	water in CHP system	i, j, m, n, r, s	integers

LOCATION	LOCATION SUBSCRIPT		
	Inlet	Overall/Mean	Outlet
Ambient	-	0	-
Reception/storage/screening	-	1	-
Dryer	2	3	4
Dryer burner	5	-	6
Air oxygen enrichment plant	-	7	8
Gasifier	9	10	11
Cold regenerator	12	13	14
Hot regenerator	15	-	16
Product gas water heater	17	18	19
Product gas quench (including WWT)	-	20	-
IC engine	21	22	23
Engine coolant radiator	24	25	26
Engine coolant water heater	27	28	29
Engine exhaust gas water heater	30	31	32
Electrical grid connection	33	34	-
Heat customer	35	-	-
Total plant	-	36	-

Abbreviations

AOEP	Air Oxygen Enrichment Plant
BCD	Band Conveyor Dryer
BIGCC	Biomass Integrated Gasification Combined Cycle
BGES	Biomass Gasifier Engine System
CHP	Combined Heat and Power
CI	Compression Ignition
ECR	Engine Coolant Radiator
ECWH	Engine Coolant Water Heater
EEGWH	Engine Exhaust Gas Water Heater
GC	Grid Connection
HHV	Higher Heating Value
LHV	Lower Heating Value
IC(E)	Internal Combustion (Engine)
IGCC	Integrated Gasification Combined Cycle
MVR	Mechanical Vapour Recompression
PGQ	Product Gas Quench
PGWH	Product Gas Water Heater
PSA	Pressure Swing Adsorption
RCD	Rotary Cascade Dryer
RCIB	Rotary Cascade Dryer with Integral Burner
RFSG	Reverse Flow Slagging Gasifier
RSS	Reception, Storage, Screening
SI	Spark Ignition
SRC	Shore Rotation Coppice
UGETC	Updraft Gasifier with External Tar Cracking
VOC	Volatile Organic Compound
VSA	Vacuum Swing Adsorption

1 INTRODUCTION

1.1 Background

The term *biomass* was originally coined by biologists to denote the weight of plant and animal material per unit area of land [1]. However, since the oil crises of the 1970s spurred vigorous interest in alternatives to oil, the term has also come to mean any plant or animal material of recent origin, for use particularly as a source of energy. This latter is the sense in which the term *biomass* is used not only here, but more and more commonly in industry, agriculture and government around the world.

The use of such material as a source of energy is however nothing new. Wood was one of the first fuels to be used by man, and remains to this day the principal source of energy in large parts of the developing world, combusted to produce heat for cooking and heating in open fires or relatively simple stoves and grates. In recent times, biomass as a fuel for the production of heat and power on an industrial rather than domestic scale has received a great deal of attention, particularly as it represents a renewable source of energy (provided it is grown and harvested sustainably) with the potential to address many of the pollution problems associated with the use of fossil fuels [2]. Among these are the emission of oxides of nitrogen and particularly sulphur which give rise to acid deposition. Most importantly however, the use of sustainably grown biomass for energy is "carbon-neutral" - that is to say the carbon emissions to the atmosphere from the conversion system (in the form of gaseous carbon dioxide) are balanced by the carbon uptake from the atmosphere during the growing cycle of the biomass; and atmospheric carbon dioxide is believed to be one of the principal causes of global warming [3].

In December 1997, coinciding with the Kyoto Summit on climate change, the European Commission published its white paper "Energy For The Future: Renewable Sources of Energy" [4], stating the aim of doubling the share of energy from renewable sources in total energy consumption in the European Union from 6% in 1995 to 12% by 2010. Nearly 85% of this additional contribution is projected to come from biomass sources including the organic fraction of municipal solid wastes (Figure 1.1) [4]. This represents a tripling of present energy consumption from biomass in the European Union from 45 Mtoe (million tonnes oil equivalent) to 135 Mtoe. Electricity production from renewables is

forecast to double over the same period, with electricity production from biomass accounting for over 60% of the increase. Also, of the additional 90 Mtoe of energy consumption from biomass sources, nearly 30 Mtoe is projected to come from combined heat and power (CHP) systems operating on solid biomass feedstocks, either residues from forestry and agriculture or dedicated "energy crops". A CHP system is one which supplies electrical power and heat simultaneously, the heat usually being in the form of steam or hot water. The concept is currently attracting a great deal of interest because of the very high fuel utilisation efficiencies that may be achieved compared with systems for power production alone, although a customer must exist for the heat produced.

Figure 1.1 Renewables Share of Energy Consumption - European Union [4]

Individual countries are adopting similar targets for increased use of renewable energy in general and biomass in particular. The UK has recently announced an ambition to generate 10% of its electricity from renewable sources by 2010, and biomass is expected to play a major part [5]. Outside the European Union, the United States Department of Energy's Biopower Program aims to establish 17 GW_e of new biomass generating capacity by 2018, bringing the contribution from biomass to about 7.5% of total electricity [6].

These are very ambitious targets to achieve in a short time-scale. There is therefore much activity within the European Union and elsewhere on work to bring bio-energy systems for

power and CHP to a state of commercial readiness as rapidly as possible. Because of the low energy density of biomass as a fuel at the point of collection (compared, say, with natural gas or coal), transportation costs limit economic plant sizes to far below those based on fossil fuels. A value around 100 MW$_e$ is often quoted as an upper limit [7]. A significant fraction of the new capacity required if governments' targets are to be met will however be at scales very much smaller than this, in the region of a few megawatts. At this scale plants would supply heat and power to local small-to-medium scale industry and residential groupings with surplus electricity sold to the public distribution grid [3,4].

The present work focuses on this smaller scale of bio-energy system, with an electrical output of between 0.5 and 2.5 MW$_e$ (corresponding approximately a biomass consumption in the range 0.5 to 2.0 dt/h). The range has been chosen to exclude "on-farm" systems of up a few hundred kW$_e$ where cost minimisation considerations often dictate the use of sub-optimum, often recycled components. It also corresponds to the target application range of one of the main system components in the study, the development of which has provided the financial support for this work (see Section 1.4).

The traditional technology option for power or CHP from biomass has been conventional combustion, in usually either a fluidised bed or moving grate combustor, with a boiler raising steam to drive a back-pressure or condensing steam turbine [8]. Emissions from this type of system (including CO, NO$_x$, particulates) can however be high [9], and at the small scale of interest considered in this work the steam turbine becomes very expensive [10]. Thermal efficiencies (fuel in to electricity out) are also low, usually well below 20% at smaller scales [11], and even in a CHP system it is economically sensible to maximise the electricity output provided surplus can be sold to the distribution grid, as electricity is a much higher value product than heat.

1.2 The Biomass Gasifier-Engine System

Air-blown gasification combined with an internal combustion (IC) engine for power production is widely held to be a leading modern technology option for power or CHP from biomass at scales of up to 5 MW$_e$ [7,12,13]. This arrangement, referred to henceforth as a biomass gasifier-engine system or BGES, has the potential for overall efficiencies to

21

electricity of 25% or more at a substantially lower capital cost than the steam-cycle alternative [14,15].

The system extent may be defined as from the delivery of feedstock to the plant, through to supply of electricity to the local grid (and in the case of CHP, supply of heat to the purchasing body). Within the system, the biomass is first dried if necessary, and then reacted in a gasifier, usually of the fixed bed type (see Section 5.1.1), with typically about a third of the oxidant necessary for complete combustion. A low heating value product gas is produced with CO and H_2 as the primary combustible components, and this is then combusted with air in the IC engine. Heat may be recovered, for example from the engine exhaust and cooling water, and from the hot product gas from the gasifier prior to combustion in the engine.

The IC engine operating in this mode can achieve substantially higher electrical efficiencies than either a steam turbine or a simple-cycle gas turbine at this scale and at lower cost [16]. Combined cycle gas turbine configurations are receiving much attention at larger scales, but are widely regarded as economically practical at scales of typically 20 MW_e and above [12].

A number of systems have been built and operated on the BGES principle [14,17,18,19,20], usually for power production only, and these are described in Section 6.1.2. Successful commercial operation has however been difficult to achieve thus far. There have been two principal reasons. The first of these is the presence of excessive levels of tars in the gasifier product gas which can seriously limit the life of engine components. The removal of tars from the product gas to a level acceptable for use in engines (Section 6.1.1.1) is difficult and expensive, as well as representing a loss of useful chemical energy, and can also give rise to a further effluent disposal problem in the form of water from wet scrubbers [21,22].

The extent of tars in the product gas is related to gasifier design and operating conditions (see Section 5.1.2). One approach to the problem is to design a gasifier in which the gasification reactions take place either at high temperature and/or under the influence of a catalyst, so that the tars are cracked to permanent gases. In a fixed-bed gasifier this may be achieved by one or more of the following methods:

- elevation of the temperature of the gasification zone within the reactor by the use of pre-heated and/or oxygen-enriched air as the gasifying agent (resulting in slagging operation)

- provision of an external thermal reactor supplied with secondary air

- provision of an external catalytic reactor, supplied with secondary air if necessary

The use of oxygen-enriched air also leads directly to a higher heating value product gas, which has the potential to improve engine efficiency by increasing power output, and also to reduce the capital cost of the gasifier and particularly the engine by reducing the size of equipment required. Oxygen-enriched air may also be fed to the engine as the comburent, offering similar potential improvements in efficiency and cost.

The prospect of a net reduction in the electricity production cost of this type of system addresses the second reason for its lack of commercial success - economic viability. Up to now, BGESs have required considerable public subsidy, except in certain specialised cases where the feedstock is at or near zero cost and the location is remote or poorly served by other energy options. If the use of oxygen-enriched air has the potential to reduce system capital cost and improve overall efficiency, it can bring about a reduction in the electricity production cost. Oxygen enrichment has in the past usually been discounted as an option because of the electricity requirements and cost of the air separation equipment necessary to provide the oxygen. However, costs have fallen considerably in recent years (Section 7.2).

1.3 Biomass Drying

The moisture content of the feedstock directly affects the operation of biomass gasifiers through the effect it has on reaction rates, reaction temperatures and product gas heating value. Most biomass feedstocks suitable for gasification would be likely to have a moisture content on delivery to the plant in the range 40-120% on a dry basis, depending on the type, location, and storage duration. Many gasifiers however require a substantially lower moisture content for satisfactory operation (Section 5.1.1), and in any case the

23

quality of the gasifier product gas generally improves as feed moisture is reduced. A drying operation is therefore often necessary, and in a gasifier aiming to operate at high temperatures and deliver a high heating value product gas, moisture content of the feedstock may be expected to be a critical parameter due to the energy costs of evaporation.

Drying is an energy-intensive operation, and a dryer can represent a significant capital outlay. Sources of heat are available within the overall process to accomplish drying, although these are already in demand in a CHP system for meeting the heat load. A number of technologies exist which are suitable for the drying of biomass, but the integration of these into a system of this type presents complex issues of performance and cost optimisation which have rarely been subjected to rigorous analysis.

Throughout this work, biomass moisture content is quoted on a dry basis, defined as mass of water divided by mass of bone dry solid, expressed as a percentage (% db). It should be noted that values are also commonly quoted on a wet basis, i.e. mass of water divided by mass of wet solid (% wb).

1.4 Work Scope and Objectives

In a BGES there is a strong degree of interaction between the drying process, the extent of air oxygen enrichment, gasifier performance and overall system performance, and a modelling approach is required if the system is to be analysed, understood and optimised. The primary objective of the present work is:

- the development of a model of a biomass gasifier-engine system (BGES) for power or CHP, and its use to study the performance and cost characteristics of a small-scale system for both power and CHP with an electrical output of between 0.5 and 2.5 MW$_e$. Particular attention is given to the integration of feed drying, and to the potential use of a high-temperature slagging gasification process with provision for air pre-heating and oxygen enrichment.

The evaluation of system performance and cost involves the optimisation of configurations against certain criteria, and the comparison of different configurations on a consistent basis.

Both systems incorporating a high-temperature slagging gasifier and a non-slagging gasifier with external tar cracking are considered. In the former case, the system incorporates gasifier air pre-heating through heat exchange with the hot product gas, as well as an air separation unit for supplying oxygen-enriched air to both the gasifier and the engine. The gasifier design concepts are also evaluated independently (Section 5.3).

A range of strategies for the energy integration of drying are proposed and evaluated, with particular emphasis on CHP applications where the energy sources which may be used for drying are also in demand for the export of heat. There is also a detailed examination of the subject of feed drying in biomass gasification systems in general, covering both the drying process and available drying technologies. [Note: the term *biomass gasification system* is used throughout this thesis to mean any system for the production of power or CHP incorporating biomass gasification].

The work is a consolidation and extension of tasks carried out by the author as part of a 3-year European Commission JOULE project (JOR3-CT97-0130, "Reverse-flow Slagging Gasifier"), in which Aston University is a partner together with Biomass Technology Group (BTG), KEMA and Kara of the Netherlands and CIEMAT-CEDER of Spain. The Reverse-flow Slagging Gasifier (RFSG) is a novel design concept originated by BTG, and is described in Section 5.1.3. The design is evaluated through the use of models in Section 5.3. The primary aim of the JOULE project is to develop such a gasifier at pilot scale. Aston University has responsibility for a number of aspects within the overall project including the integration of drying, gasifier modelling, operation of engines on low heating value gas, and system techno-economic evaluation.

1.5 Thesis Structure

After the present introductory chapter, Chapter 2 describes the methodology used, and Chapter 3 contains a review of previous system studies.

Thereafter the thesis addresses individual system modules separately before going on to address the system model and its application.

Chapter 4 addresses the dryer, discussing suitable dryers for a BGES before going on to discuss the dryer sub-model. This chapter is supported by Appendix 1 - see below.

Chapter 5 then addresses the gasifier, discussing biomass gasifier design before describing the gasifier sub-model and its application in an evaluation of the RFSG concept.

Chapter 6 then addresses the IC engine and discusses design and performance issues and operational history, before describing the engine sub-model.

The remaining system modules to be included explicitly in the system model are addressed in Chapter 7, with sub-sections given to reception/storage/screening, air oxygen enrichment plant, heat recovery plant and product gas quench.

Chapter 8 describes the operation of the system model, including the integration of the individual modules, and the calculation of overall system parameters (in particular economic parameters). The chapter concludes by discussing the application of the model in the study of the system concept, and how the results are to be presented. Chapter 9 then presents and discusses the results of the study.

Finally conclusions are presented in Chapter 10, along with suggestions for further work.

There are two appendices. Appendix 1 contains a review of drying technologies for biomass gasification systems in general. Appendix 2 contains the system model worksheets.

2 METHODOLOGY

This chapter describes the methodology employed in carrying out the system study, including the choice of system configurations and the rationale behind their selection, the boundary conditions employed and process variables considered, and the basis of the economic analysis incorporated into the system model.

Besides the gasifier and the IC engine, the BGES incorporates a dryer, an optional air separation plant for oxygen enrichment, and (for CHP applications) heat recovery from the hot product gas, the engine exhaust and the engine cooling system (Figure 2.1). The great majority of engine-based CHP systems export heat as hot water [23], as the energy in the engine cooling water circuits whose temperature is usually too low for the production of steam may then be effectively utilised [24] (see Section 6.1.1.4). This is assumed here.

Each of the blocks in Figure 2.1 represents a system module (Section 2.2).

2.1 Sources of Surplus Energy in a BGES

The primary energy pathway in a BGES is from chemical energy in solid biomass to gaseous chemical energy via the process of gasification, thence to mechanical energy in an IC engine and finally to electrical energy in an electrical generator. At various points in the system, however, energy is available which cannot contribute directly to the production of electricity, but which can be used for evaporative drying, or in the case of CHP applications water heating. These energy sources are the following (Figure 2.2):

- surplus biomass (undersize particles unsuitable for supply to the gasifier), combusted to generate hot exhaust gas (chemical energy)

- hot gasifier product gas, cooled prior to the IC engine inlet (thermal energy)

- hot exhaust gas from the IC engine (thermal energy)

- Hot coolant from the IC engine cooling circuits (thermal energy)

27

RECEPTION, SCREENING

| wet biomass

DRYER

| dry biomass

GASIFIER ← OXYGEN ENRICHMENT

| hot fuel gas

HEAT RECOVERY ⇨ heat out to district heating scheme

GAS QUENCH

| cold flue gas

ENGINE ⇨ electrical power out via grid connection

| hot flue gas & hot water

HEAT RECOVERY ⇨ heat out to district heating scheme
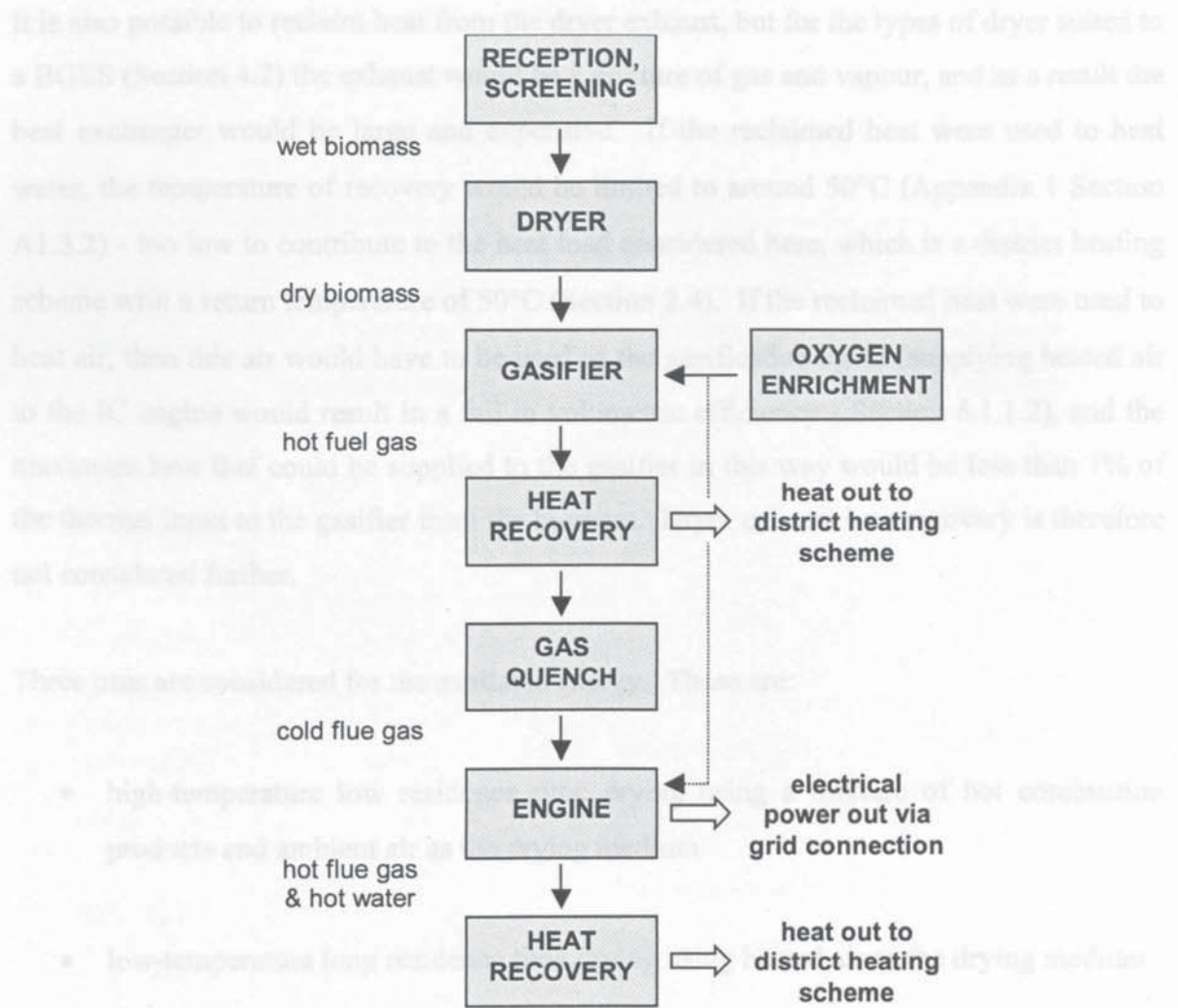
Figure 2.1 Biomass gasifier-engine system (CHP configuration)

biomass → DRYER → biomass → GASIFIER → product gas → ENGINE → exhaust gas

DRYER ⇩ SURPLUS BIOMASS (CHEMICAL)

GASIFIER ⇩ PRODUCT GAS (THERMAL)

ENGINE ⇩ ENGINE COOLANT (THERMAL)

EXHAUST GAS (THERMAL)
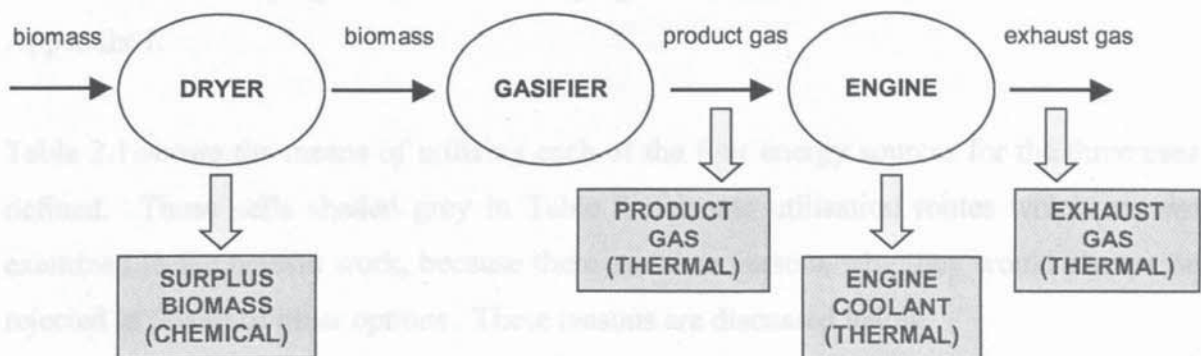
Figure 2.2 Sources of energy in a BGES

It is also possible to reclaim heat from the dryer exhaust, but for the types of dryer suited to a BGES (Section 4.2) the exhaust would be a mixture of gas and vapour, and as a result the heat exchanger would be large and expensive. If the reclaimed heat were used to heat water, the temperature of recovery would be limited to around 50°C (Appendix 1 Section A1.3.2) - too low to contribute to the heat load considered here, which is a district heating scheme with a return temperature of 50°C (Section 2.4). If the reclaimed heat were used to heat air, then this air would have to be used as the gasification agent (supplying heated air to the IC engine would result in a fall in volumetric efficiency - Section 6.1.1.2), and the maximum heat that could be supplied to the gasifier in this way would be less than 1% of the thermal input to the gasifier from the biomass. Dryer exhaust heat recovery is therefore not considered further.

Three uses are considered for the available energy. These are:

- high-temperature low residence time drying using a mixture of hot combustion products and ambient air as the drying medium

- low-temperature long residence time drying using heated air as the drying medium

- for CHP applications, the export of heat to a district heating scheme in the form of hot water (Section 2.4).

The reasons underlying the choice of drying media are discussed in Section 4.2 and Appendix 1.

Table 2.1 shows the means of utilising each of the four energy sources for the three uses defined. Those cells shaded grey in Table 2.1 denote utilisation routes which are *not* examined in the present work, because there are clear reasons why they would always be rejected in favour of other options. These reasons are discussed below.

The remaining utilisation routes are all examined; the italicised figures denote the relevant system configuration numbers (see Table 2.2).

29

Table 2.1 Utilisation of energy sources in a BGES
(grey cells: not considered in this study,
italic numbers: system configuration in Table 2.2)

ENERGY SOURCE	UTILISATION ROUTE		
	Drying (combustion prod.)	Drying (heated air)	Hot water generation
Surplus biomass	via biomass burner *7-12*	via biomass burner, gas/gas heat exch.	via biomass burner, gas/liquid heat exch. *7, 9, 11*
Product gas (thermal)	via gas/gas heat exchanger	via gas/gas heat exchanger	via gas/liquid heat exchanger *1, 3, 5, 7, 9, 11, 13, 15, 17*
Hot engine exhaust gas	direct *1-12*		
Hot engine coolant	not possible	via liquid/gas heat exchanger *13-18*	

Most of the rejected utilisation routes require gas-to-gas heat exchange. This tends to be expensive, requiring large heat exchange surface areas. Problems of cross-leakage or external leakage arise if a rotary regenerator is used, which is the cheapest and most effective option for gas-to-gas heat exchange of this type [25].

Exhaust gas from the IC engine or the biomass burner can be used directly for drying rather than by heating air via a heat exchanger. If heated air drying is required, it is better provided from the IC engine coolant radiator, which is a necessary part of the engine installation for all configurations (Section 6.2.3.2).

As regards the use of hot product gas for drying, there is the risk of leakage of a flammable gas either into the atmosphere or into the drying air stream, representing both a hazard and an energy loss.

30

Finally, the heating of combustion products using the IC engine coolant is not possible, as the maximum coolant temperature will always be less than the combustion products temperature at entry to the dryer (see Sections 6.2.2 and 7.3.2.1).

As Table 2.1 shows, sensible utilisation routes exist both for drying and for CHP for each of the four energy sources except the thermal energy of the product gas. The optimal allocation of energy between these competing demands in CHP applications is a key point for consideration.

It is assumed here that all of the product gas in a given system is used to produce electricity for sale to the local grid, and that the customer for the heat in a CHP application is able and willing to purchase all of the heat offered by the system. In real CHP applications where the heat demand is likely to be prescribed and variable over time, it may make economic sense to combust some of the product gas directly for the production of heat.

2.2 System Modules

The BGES model (referred to henceforth as the "system model") is a spreadsheet model, with individual linked worksheets containing sub-models of the various system modules (Figure 2.1). A justification for the choice of a spreadsheet model is given in Section 8.1.

The system model contains the following module sub-models (see Figure 2.1), which in various configurations allow the energy integration options of Table 2.1 to be evaluated, as well as the relative performances of the slagging and non-slagging gasifiers and the merits of using oxygen-enriched air both in the slagging gasifier and the IC engine:

- Reception/storage/screening

- Biomass dryer
  1. Rotary dryer (combustion products)
  2. Rotary dryer with burner – (combustion products)
  3. Band dryer (heated air)

31

- Air oxygen enrichment plant

- Gasifier
  1. Slagging gasifier (Reverse-Flow Slagging Gasifier - RFSG)
  2. Non-slagging gasifier (Updraft Gasifier with External Tar Cracking - UGETC)

- Product gas quench (including waste water treatment)

- IC engine

- Heat recovery
  1. Product gas heat recovery (water heater)
  2. Engine coolant heat recovery (air heater - radiator)
  3. Engine coolant heat recovery (water heater)
  4. Engine exhaust gas heat recovery (water heater)

- Grid connection

Reasons for the selection of the dryer types are discussed in Section 4.2 and Appendix 1.

Each of the module sub-models includes performance calculations where necessary, as well as functions for capital and production costs relating to that system component (see Chapter 8). Sub-models for the dryer, gasifier, engine and heat recovery plant modules contain explicit process calculations; those for the remaining modules comprise correlations of some process variable with costs and power requirements. For all system modules excepting the gasifiers, sub-models are based on plant commercially available at present. It is assumed that tar levels are sufficiently low from both gasifier types for additional tar removal to be unnecessary (see Section 5.4).

2.3 System Configurations

A total of 18 basic system configurations are modelled, corresponding to the options of three dryer types, two gasifier types, the optional use of air oxygen enrichment, and either

power-only operation or CHP operation. These are defined in Table 2.2. The configurations and associated flow pathways are illustrated in Figures 2.3-2.14. The CHP configurations show a hot water network connected to a heat load (the district heating scheme); the rationale behind the network configuration is explained in Section 8.3. It is also an option to select operation of the IC engine on either ambient or oxygen-enriched air if an air separation plant is present (Section 6.2), but this option has been omitted from Table 2.2 for clarity.

Key to Figures 2.3 - 2.14

————	biomass
————	air or oxygen-enriched air
••••••••••	product gas
– – – –	combustion products
————	hot water
[dashed box]	optional plant item

RS	reception, storage, screening
BS	buffer store
RFSG	reverse-flow slagging gasifier
UGETC	updraft gasifier with external tar cracking
PGWH	product gas water heater
QW	quench scrubber and waste water treatment
ECWH	engine coolant water heater
EEGWH	engine exhaust gas water heater

Table 2.2 System configurations to be modelled

Configuration (Figure No.)	Dryer Type	Gasifier Type	Air Separation Plant	Output Type
1 (2.3)	rotary	RFSG	yes	CHP
2 (2.4)				power-only
3 (2.3)			no	CHP
4 (2.4)				power-only
5 (2.5)		UGETC		CHP
6 (2.6)				power-only
7 (2.7)	rotary with burner	RFSG	yes	CHP
8 (2.8)				power-only
9 (2.7)			no	CHP
10 (2.8)				power-only
11 (2.9)		UGETC		CHP
12 (2.10)				power-only
13 (2.11)	band	RFSG	yes	CHP
14 (2.12)				power-only
15 (2.11)			no	CHP
16 (2.12)				power-only
17 (2.13)		UGETC		CHP
18 (2.14)				power-only
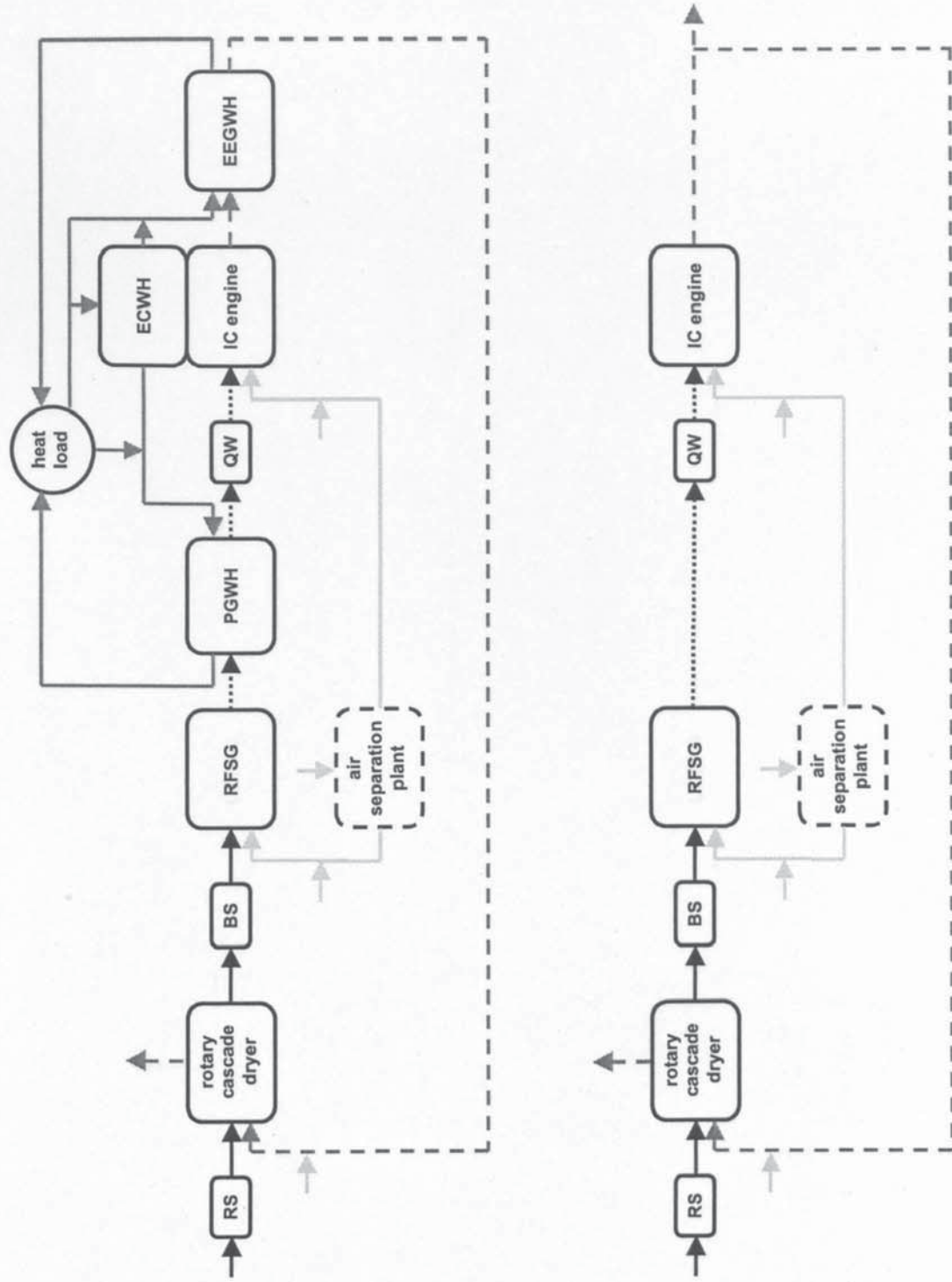
Figure 2.3
Configurations 1 and 3 -
rotary dryer, RFSG, CHP

Figure 2.4
Configuration 2 and 4 -
rotary dryer, RFSG,
power only

35
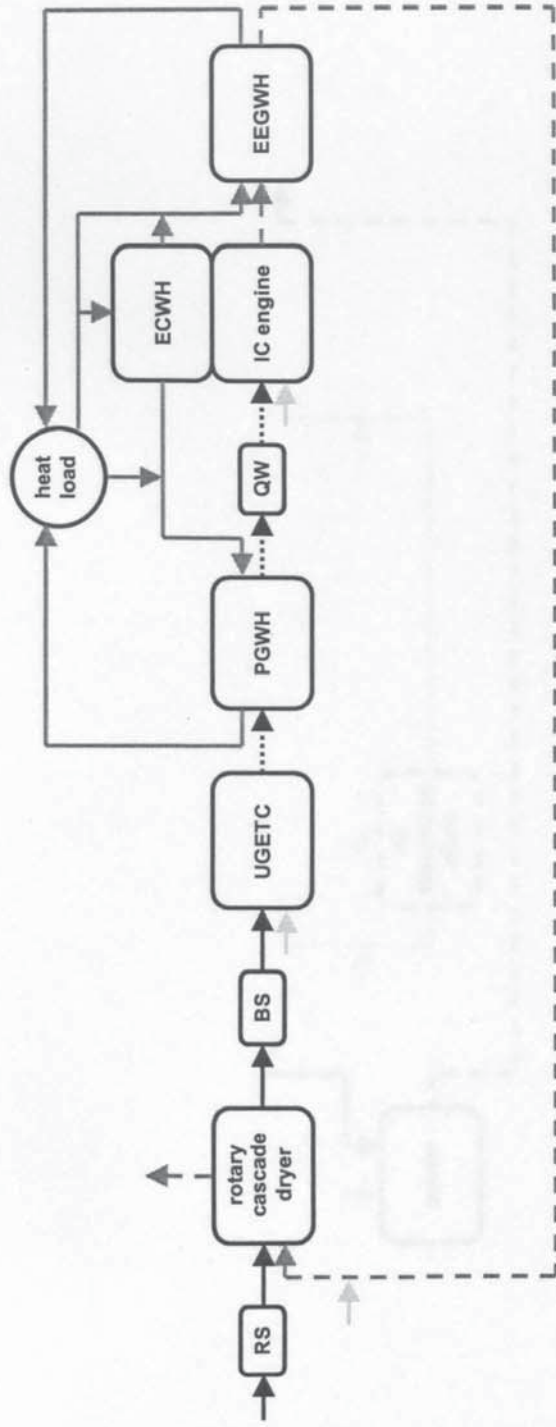
Figure 2.5
Configuration 5 -
rotary dryer, UGETC, CHP
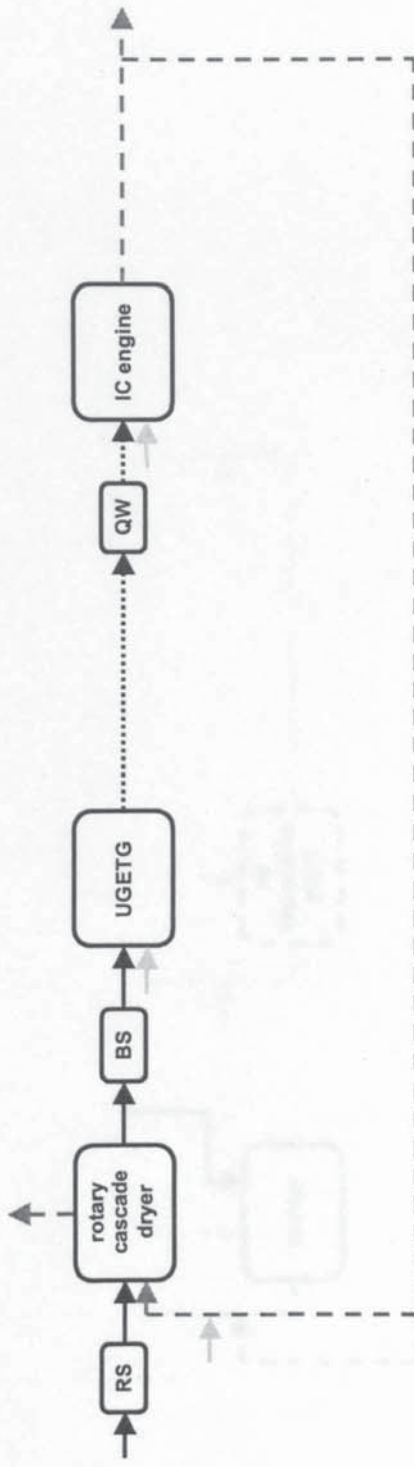
Figure 2.6
Configuration 6 -
rotary dryer, UGETG,
power only

36
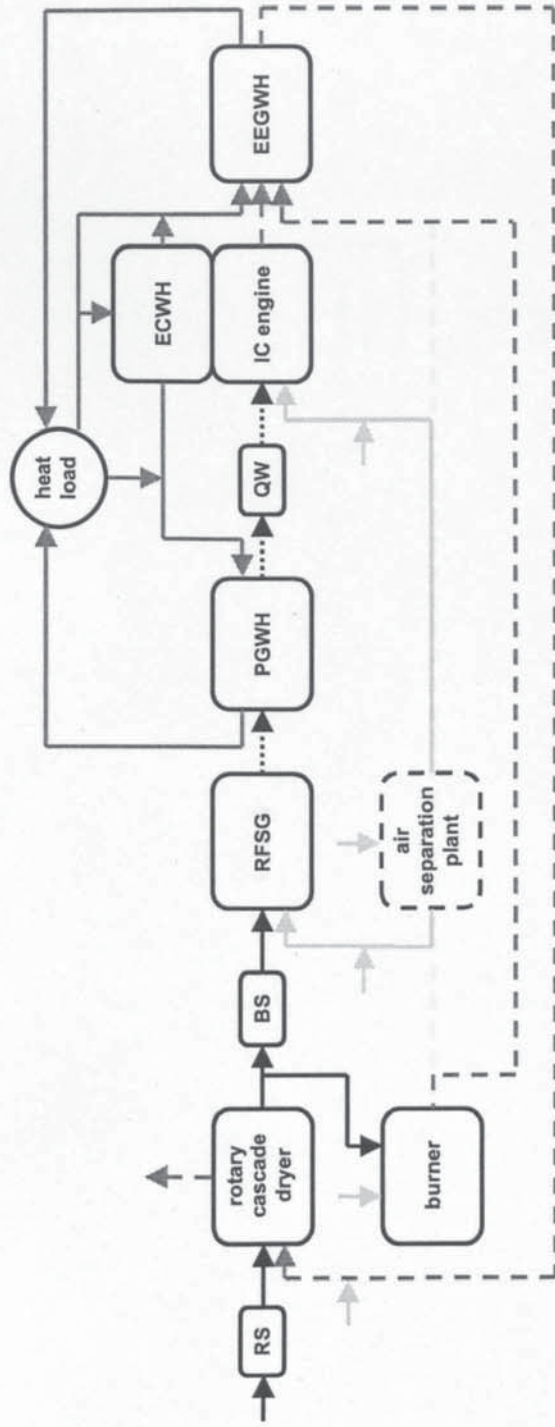
Figure 2.7
Configurations 7 and 9 -
rotary dryer with burner,
RFSG, CHP
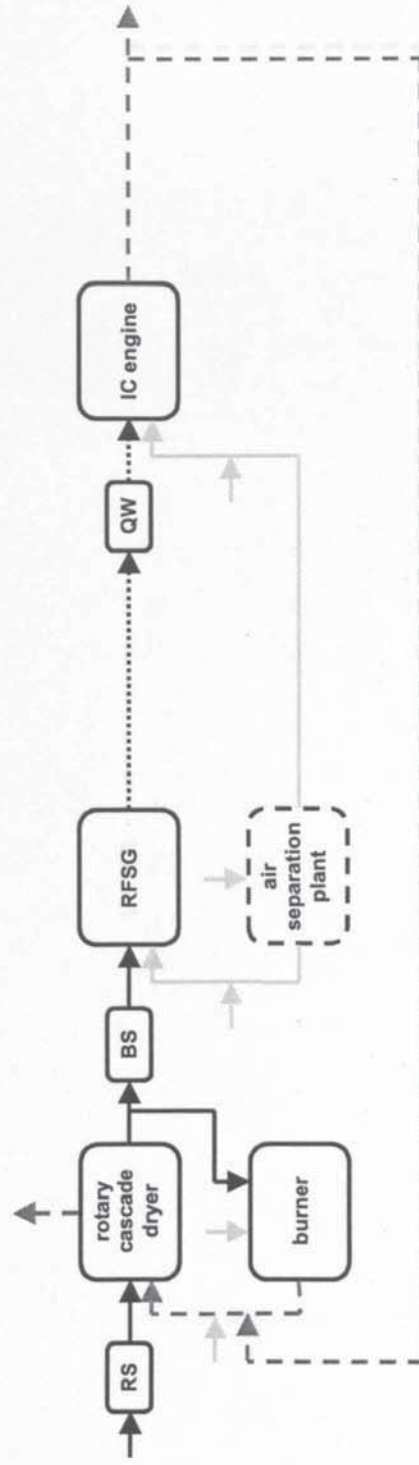
Figure 2.8
Configuration 8 and 10 -
rotary dryer with burner,
RFSG, power only

37
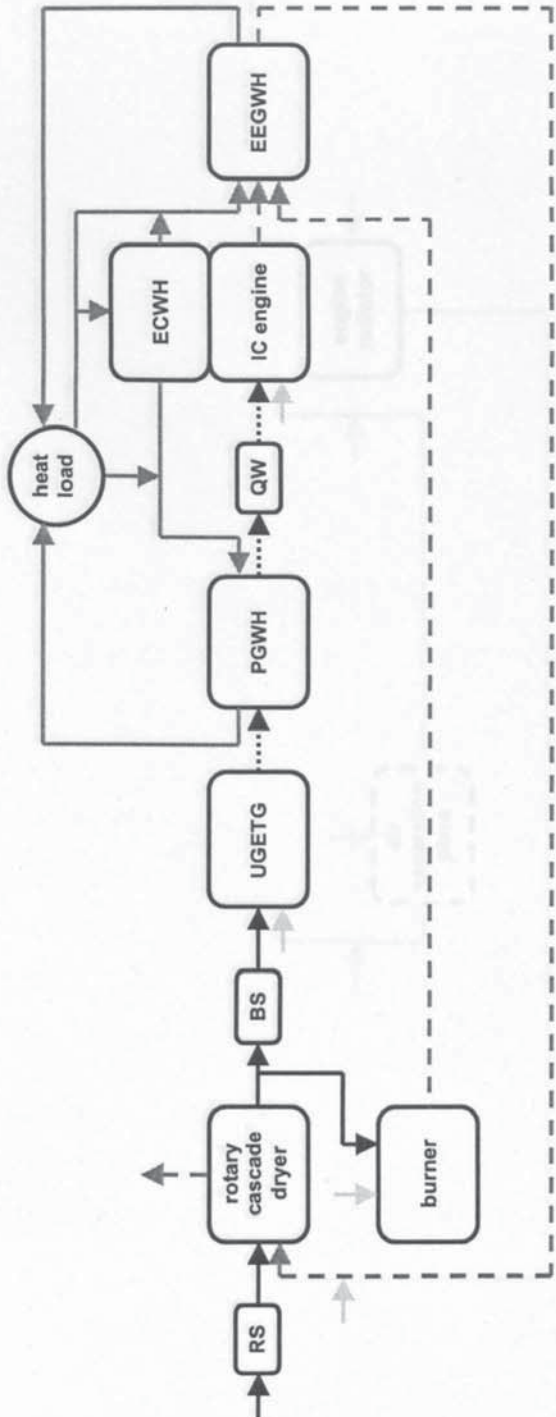
Figure 2.9
Configuration 11 -
rotary dryer with burner,
UGETC, CHP
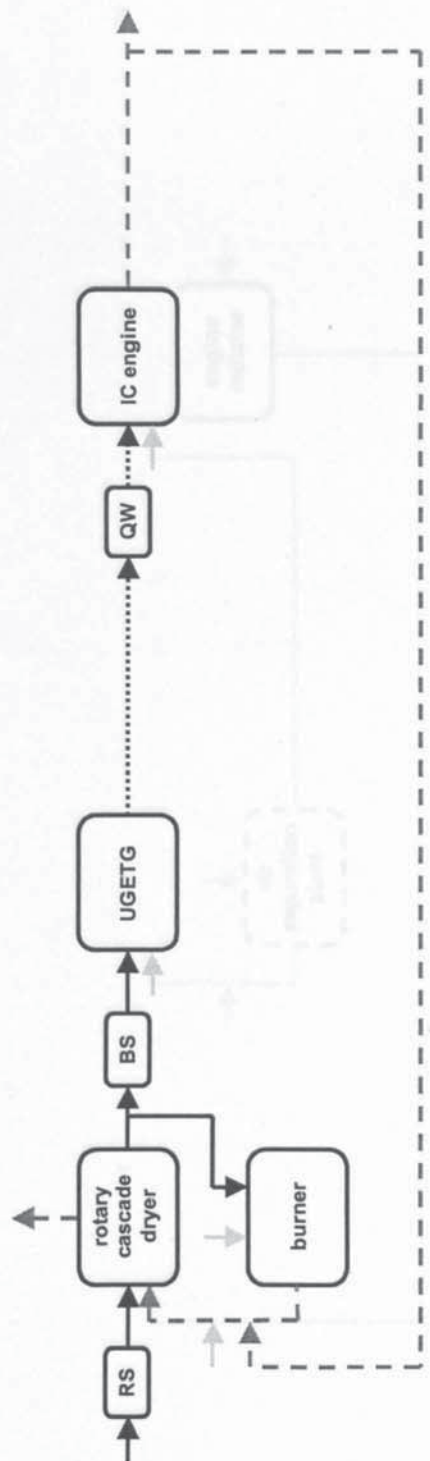
Figure 2.10
Configuration 12 -
rotary dryer with burner,
UGETG, power only

38
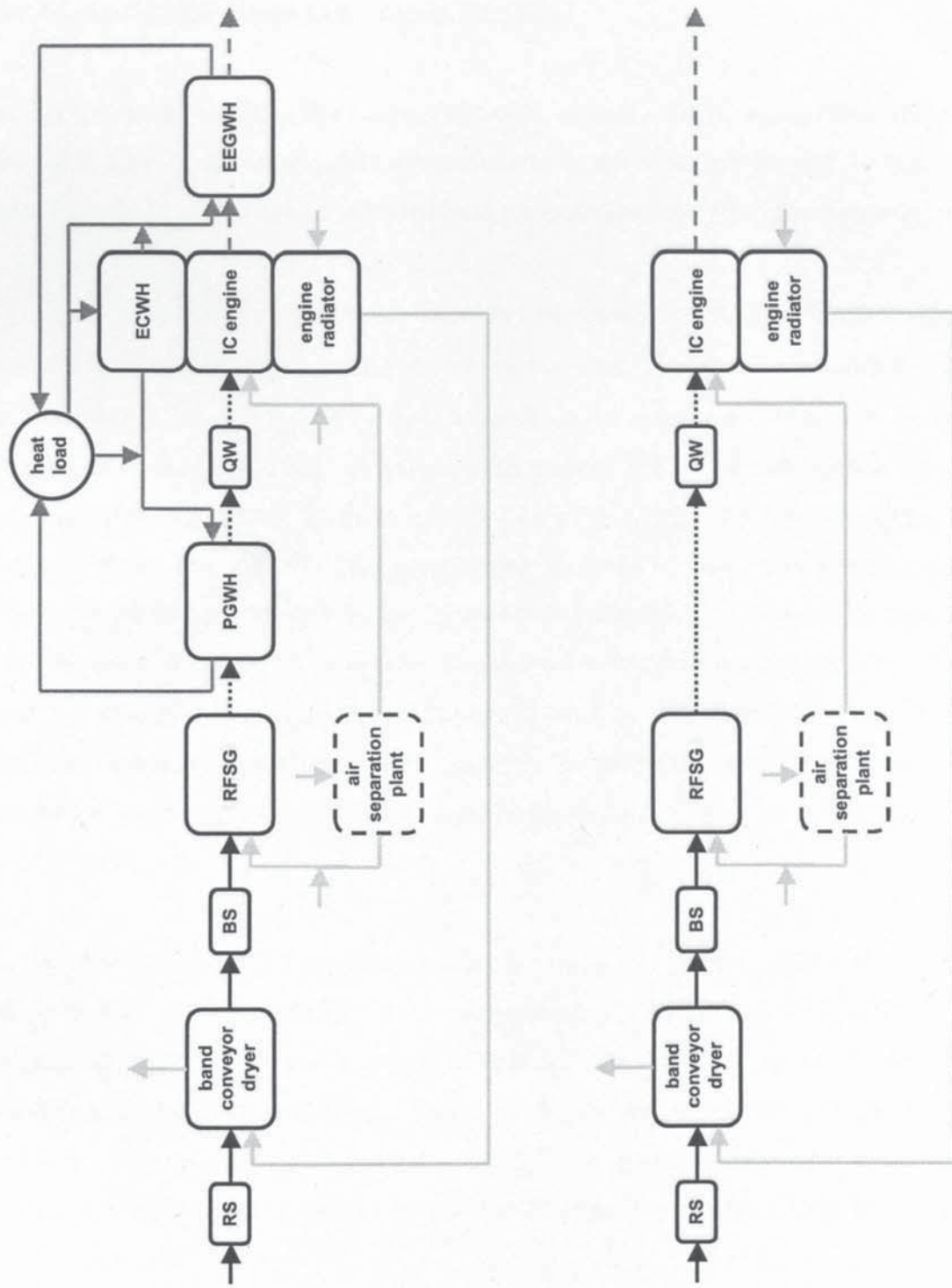
Figure 2.11
Configurations 13 and 15 -
band dryer, RFSG, CHP

Figure 2.12
Configurations 14 and 16-
band dryer, RFSG,
power only

39

2.4 Boundary Conditions and Process Variables

The system model includes the entire conversion system – that is to say, from the point at which the feed is delivered (and payment made to the supplier) through to the point at which electricity and/or heat is exported (and payment received from the customer).

The model is operated as a single enterprise, selling electricity to the grid and, in the case of a CHP application, heat in the form of hot water at ... barg to a district heating scheme [26, 27, 28]. The return water from the scheme is assumed to be at 50°C ... addition of any make-up water by the scheme [28]. Costs associated with piping and associated equipment for the transmission of hot water from the boundary of the system to the customer in a CHP scheme are not included in the system model; these costs are assumed to have been met by the customer and are reflected in the price paid for the heat (see Section ...). The system is assumed to operate continuously at an annual capacity factor of ... actual annual generation divided by that which could be achieved by continuous running at maximum plant capacity, assuming an annual availability of 90% (number of operating hours divided by total hours in year). These figures are arbitrary but representative. [ ]

The broader the scope of the system model, the greater the complexity of its construction and operation (see Chapter 3). It has therefore been necessary to fix the biomass dry composition and ... biomass moisture (both process and product), air oxygen content, biomass dryer and biomass delivered cost to be the key process line variables. The fixing of biomass dry composition is justified in that this is remarkably constant for what are chemically quite similar woody or herbaceous biomass types, particularly across a low energy range [30].

The actual biomass type has been chosen in consultation with the BGUL-B project group to be short rotation coppice (SRC) poplar, in the form of whole-tree chips. SRC poplar as a leading candidate for biomass energy plantations in Europe [31, 32], and wood chips are well suited in terms of ... feed for fixed bed gasifiers (see Section ...). SRC poplar is also fairly typical of woody biomass in terms of composition and combustion characteristics. Table 2.3 gives the ... properties of SRC poplar, whilst tree ... used in this study ...

Figure 2.13
Configuration 17 –
band dryer, UGETG, CHP

Figure 2.14
Configuration 18 –
band dryer, UGETC,
power only

2.4 Boundary Conditions and Process Variables

The system model includes the entire conversion system - that is to say, from the point at which the feed is delivered (and payment made to the supplier) through to the point at which electricity and/or heat is exported (and payment received from the customer).

The system is modelled as a stand-alone enterprise, selling electricity to the grid and, in the case of a CHP application, heat in the form of hot water at 100°C and 1 barg to a district heating scheme [26,27,28]. The return water from the scheme is assumed to be at 50°C after the addition of any make-up water by the scheme [29]. Costs associated with piping and associated equipment for the transportation of hot water from the boundary of the system to the customer in a CHP scheme are not included in the system model; these costs are assumed to have been met by the customer and are reflected in the price paid for the heat (see Section 8.2.2). The system is assumed to operate continuously at an annual capacity factor of 0.8 (total annual generation divided by that which could be achieved by continuous running at maximum plant capacity), including an annual availability of 90% (number of operating hours divided by total hours in year). These figures are arbitrary but representative.

The broader the scope of the system model becomes, the more complex its construction and operation (see Chapter 8). It has therefore been decided to fix the biomass dry composition and allow biomass moisture (both pre- and post-dryer), air oxygen content, biomass input and biomass delivered cost to be the key process flow variables. The fixing of biomass dry composition is justified in that this is remarkably constant for most raw (i.e. chemically unconverted) woody or herbaceous biomass types, particularly purpose-grown energy crops [30].

The actual biomass type has been chosen in consultation with the JOULE project group to be short rotation coppice (SRC) poplar, in the form of whole-tree chips. SRC poplar is a leading candidate for future energy plantations in Europe [31,32], and wood chips are well suited in terms of size as a feed for fixed bed gasifiers (see Section 5.1.1). SRC poplar is also fairly typical of a woody biomass in terms of composition and physical characteristics. Table 2.3 gives the key properties of SRC poplar whole tree chips used in this study

(referred to henceforth as the "standard" biomass); these have either been taken from the literature or determined experimentally at the laboratories of CIEMAT-CEDER in Spain as part of the JOULE project. The 0.4% by weight of nitrogen has been ignored for modelling purposes, leaving a biomass molar composition (dry ash free) of $CH_{1.53}O_{0.66}$.

Table 2.3 Properties of SRC poplar whole tree chips [33,34,35]

Chip volumetric mean diameter (mm)	30
Chips <10mm mean diameter (% wt)	15
Bulk density (kg/m³, dry)	135
Specific heat capacity (KJ/kgK, dry)	1.4
Volatile matter (wt% dry)	78.6
Fixed carbon (wt%, dry)	19.1
Ash content (wt%, dry)	2.3
Carbon content (wt%, dry)	48.4
Hydrogen content (wt%, dry)	6.2
Oxygen content (wt%, dry)	42.5
Nitrogen (wt%, dry)	0.4
Lower heating value (MJ/kg, dry)	18.21
Lower heating value (MJ/kg, dry ash free)	18.64

Volumetric mean diameter ϕ_v is defined as:

$$\phi_v = \sqrt[3]{\frac{6\sum_{n=1}^{n=N} V_n}{\pi N}} \qquad (2.1)$$

where V_n is the volume of the nth particle in a population of N particles. It is assumed that only particles of mean diameter above 10mm are acceptable for a fixed bed gasifier (see Section 5.1.1); those below this size must be removed prior to the gasifier.

Lower heating value (LHV) of a fuel refers to the heating value when the water in the products is in the vapour phase; higher heating value (HHV) to that when the water in the

products is in the liquid phase. Either can be used in a study such as this provided that the basis is consistent throughout and the definition is understood. The LHV is used here. The value quoted in Table 2.3 refers to moisture-free fuel; LHVs are quoted on this basis throughout.

The key process variables have the following ranges associated with them:

- biomass feed rate: 0.5-2.0 dt/h, equivalent to 2.5 -10 MW_{th} thermal input (or about 0.5 - 2.5 MW_e assuming an overall efficiency of 20-25%).

- biomass delivered cost: £20/dt-£80/dt (unscreened). Rösch and Kaltschmitt [18] give a current cost for chipped SRC poplar at the plant gate in the range 7.2-11.6 ECU/GJ (1998 prices), converting to £75-£145/dt. For a small-scale system, transportation costs (included in these figures) would be at the lower end of the range considered by Kaltschmitt, so that a sensible range of current cost for the present application might be £75-£110/dt. With familiarity and technological development in the growing of SRC poplar, and the availability of fiscal incentives and subsidies, these costs would be expected to have reduced by the time a tenth plant is built (see Section 2.5.2); if a range of possible cost reductions from 25% to 75% is considered, this translates into a cost range of about £20-£80/dt.

- biomass moisture content before drying: 50-100% db (this allows for varying degrees of pre-delivery drying - see Appendix 1 Section A1.2)

- biomass moisture content after drying: 10-50% db for the RFSG, 10-100% db for the UGETC (see Sections 5.1.3, 5.1.4, Appendix 1 Section A1.5.2)

- air oxygen concentration: 21-60% by volume. The upper limit dictated by the air separation technology would be 90% - see Section 7.2. However, the RFSG design concept stipulates a maximum O_2 concentration of 60%, for reasons given in Section 5.1.3. Higher air oxygen concentrations are considered in the gasifier design evaluation study of Section 5.3.

- capital cost (equipment cost) of the RFSG 1.0-1.5 times that of the UGETC (see Section 5.4.2.1).

Standard atmospheric conditions of 15°C, 101.3 kPa and 80% relative humidity have been assumed throughout. Ambient air is assumed to contain 21% oxygen by volume. Water is assumed to have a constant specific heat capacity of 4.188 kJ/kgK. Polynomial temperature functions have been used for the specific heat capacities of various gases, and for the vapour enthalpy of steam at various pressures, based on a standard reference [36].

2.5 Economic Analysis

The base year for the study was chosen to be 1998, this being the year during which most of the manufacturers' cost data were collected. All cost data are therefore presented in 1998 GB£. The following exchange rates have been used:

- 1 US$ = 0.62 GB£

- 1 ECU (or €) = 0.68 GB£

An inflation rate of 3% is assumed. This has been used to adjust all non-1998 cost data. The project lifetime is taken to be 20 years. A nominal "cost of money" discount rate of 12% is used, in line with a recent UK government review of renewable energy technologies [5].

2.5.1 Capital Cost

The measure of capital cost used in the present work is total plant cost (*TPC*), that is to say the total amount of capital required to finance the total system to the point at which it is ready to operate. *TPC* may be calculated for each system module before a summation to give the overall *TPC*; this allows the apportioning of costs between each module to be easily extracted and is the practice adopted here.

The calculation of *TPC* begins with the purchase cost (delivered to the plant gate) of the major plant items comprising each system module (the "equipment cost" - *EC*). It is assumed that all plant items are bought new. Increments are then added for erection, instrumentation, piping and ducting, associated electrical equipment, structures and buildings, civil works and lagging, to give a direct plant cost (*DPC*). These increments are often specific to the system module, direct plant cost is therefore calculated before costs of the modules are aggregated. Engineering design and management overheads are then added to give an installed plant cost (*IPC*), and finally commissioning costs, contractor's fees, interest during construction and a contingency element are added to give total plant cost. These increments are less specific to system modules, being usually approximated as fixed percentages of direct plant cost

Where cost data utilised in the present work were not in the form of total plant costs, appropriate conversions have been performed. This has been done using factors published by the IChemE [37] and adapted by Bridgwater [38]. For converting from equipment cost to direct plant cost, the following relationship was used:

$$DPC = EC \left(1 + \sum C_3 C_1 EC^{C_2} \right) \qquad (2.2)$$

where costs are expressed in US\$ (1991), and values for the constants C_1, C_2 and C_3 are given in Table 2.4 [38]. The adjustment C_3 is unity unless selected otherwise. Multiplication factors for the conversion of direct plant cost to total plant cost are given in Table 2.5 [38,39]. A contingency of 10% has been selected, in line with a previous comparable economic study [40], although the selection of a value is somewhat arbitrary and values from 0% to 50% have been used [39].

For each module where equipment cost has to be converted to total plant cost in this manner, a simplified relationship has been obtained by applying the factors described above to a wide range of equipment costs and performing regression analysis on the results to arrive at a power law expression of the form:

$$TPC = x EC^y \qquad (2.3)$$

The power law form is sensible from consideration of Equation 2.2 which is a summation of power laws, recognising that TPC is related to DPC by a constant multiplier.

Table 2.4 Equipment cost conversion factors [38]

Aston University

Illustration removed for copyright restrictions

Table 2.5 Conversion of direct plant cost to total plant cost [38,39]

Item	Range	Factor Used
Engineering, design and supervision	10-20% *DPC*	0.15 *DPC*
Management overheads	5-20% *DPC*	0.1 *DPC*
Installed plant cost (IPC)		1.25 *DPC*
Commissioning	1-10% *IPC*	0.05 *IPC*
Contingency	0-50% *IPC*	0.1 *IPC*
Contractor's fee	5-15% *IPC*	0.1 *IPC*
Interest during construction	7-15% *IPC*	0.1 *IPC*
Total plant cost (TPC)		1.35 *IPC*
		1.69 *DPC*

2.5.2 Learning Effects

It is assumed that the aggregated total plant cost arrived at by the method thus far outlined is equivalent to that of a first plant. A BGES may be regarded as a new process, and as such its capital cost is likely to fall over time as more plants are built and experience accumulated. A constant learning factor (*LF*), defined as the cost reduction (%) when production is doubled, is a well-documented phenomenon in process industries where values of between 20 and 30 are commonly observed [41]. The same phenomenon is also held to apply to plant replication, and has been used in the analysis of biomass gasification systems [42].

Considering the *i*th and the *j*th plants, their total plant costs TPC_i and TPC_j are related by the learning factor in the following manner:

$$\frac{TPC_j}{TPC_i} = \left(\frac{j}{i}\right)^{\frac{\ln(1-0.01LF)}{\ln(2)}} \tag{2.4}$$

47

This ratio is referred to as the learning ratio (*LR*). A learning factor of 20% has been used in the present work [40, 42], so that:

$$LR = \frac{TPC_j}{TPC_i} = \left(\frac{j}{i}\right)^{-0.322}$$

(2.5)

In order to allow for some maturation of the technology, the tenth plant has been chosen as a basis for quotation. Therefore, a learning ratio of $10^{-0.322}$ or 0.476 has been applied to *all* module costs to arrive at the reported values. This is felt to be a sensible choice for enabling a comparison of BGES costs with those of mature (n^{th} plant) technologies, avoiding the over-pessimistic impression obtained from using first-of-a-kind costs while not projecting too far into the future.

In practice, not all system modules will be at the same level of maturation. It might be reasonable for example to regard biomass gasifier capital cost as first-of-a-kind, but conventional IC engine capital cost as largely mature. On the other hand, IC engines operating on low-CV gasifier product gas are largely unproven and widely viewed as requiring substantial development. This study is primarily concerned with comparing different configurations and operating points for a single plant type with the same basic set of system modules. Differentiation between system modules on the basis of maturity is therefore less important than if the main objective were to compare different plant types. As the application of learning factors is highly subjective and inexact, a module-specific approach is held to be unjustified.

Learning ratio is applied at the system module level prior to aggregation, so that a breakdown of total plant cost (and ultimately electricity production cost) by system module is straightforward.

2.5.3 Production Costs

Production costs on an annual basis are composed of operating costs, which comprise feedstock costs, labour, utilities, maintenance and overheads, and a charge for capital. The cost of electricity supplied can then be derived by dividing the production cost by the

annual amount supplied in kWh to give a cost in p/kWh or £/kWh. Where heat is sold in a CHP scheme, the revenue from the heat sales is first deducted from the production cost. Feedstock cost is a key process variable in the present study (see Section 2.4). The plant operator's profit has been ignored, as this work aims primarily to compare system configurations and operating points - hence the calculated cost of electricity is strictly a break-even cost of electricity. The remaining elements are discussed in the following sections.

2.5.3.1 Annual Cost of Capital

In economic evaluations of investment decisions, it is normally assumed that the full amount of the capital required to establish the project is borrowed, and must be repaid over the loan period (although in practice lending institutions would expect a proportion of the funds to be provided through equity). The loan period is often taken to be the lifetime of the project. A fixed charge (FC) may be calculated, being the levelised annual amount paid in nominal terms over the lifetime of the project which would be just equal to the capital outlay when discounted to present values and summed using a discount rate d, also known as the "cost of money". FC is given by:

$$\frac{FC}{TPC} = d\left(\frac{(1+d)^l}{(1+d)^l - 1}\right)$$ (2.6)

where l is the lifetime of the project (assumed the same as the loan rate). The fixed charge is constant in nominal terms throughout the lifetime of the project. In order to give an average annual cost of capital (ACC) in real terms, the present value of the series of FCs must be calculated using an assumed inflation rate i, and the total divided by the project lifetime:

$$ACC = \left(\frac{FC}{l}\right)\left(\frac{1}{i}\right)\left(\frac{(1+i)^l - 1}{(1+i)^l}\right)$$ (2.7)

Combining Equations 2.6 and 2.7 gives an annuity factor AF, also known as a fixed charge rate:

$$AF = \frac{ACC}{TPC} = \left(\frac{1}{l}\right)\left(\frac{d}{i}\right)\left(\frac{(1+d)^l}{(1+i)^l}\right)\left(\frac{(1+i)^l - 1}{(1+d)^l - 1}\right) \qquad (2.8)$$

Using an inflation rate of 3%, an arbitrary but representative project lifetime of 20 years and a discount rate of 12%:

$$AF = 0.0996 \qquad (2.9)$$

As with learning ratio, annuity factor is applied at the system module level prior to aggregation so that total production cost can be easily broken down by system module.

2.5.3.2 Labour

The labour requirement per shift is calculated for each system module (see relevant sections).

Following previous comparable economic studies [39,40], a five shift arrangement is assumed and the labour rate including social costs but excluding overheads is set at £20,000 per person per annum.

2.5.3.3 Utilities

All power requirements are assumed to be met from the gross output of the plant (i.e. they are parasitic). Power requirements for the dryer and the oxygen enrichment plant are relatively large, and are calculated separately (see Sections 4.3 and 7.2). The remaining parasitic power demand, covering fans, pumps etc., is taken to be 5% of the gross generator output [40]. Utilities required for plant start-up (electricity, natural gas) have been ignored.

The cost of make-up water in CHP schemes is assumed to be met by the heat customer. The costs associated with cooling and seal water for air separation and with water for

quenching are both calculated (see Sections 7.2.3, 7.4). The cost of water used is £0.785/m^3 [43].

The cost associated with fuel requirements for on-site feedstock handling vehicles is calculated (see Section 7.1).

2.5.3.4 Maintenance and Overheads

Annual maintenance and overheads (including insurance, taxes, rent etc.) are calculated as a percentage of total plant costs.

Previous comparable economic studies of bio-energy systems have used values in the range 1-4% for maintenance and 4-8% for overheads [16,39,40]; the present study arbitrarily uses 4% for both in the absence of better information.

3 PREVIOUS SYSTEM STUDIES

3.1 Introduction

This section carries out a review of the literature on system studies comparable to that of the present work. Its purpose is to place the present study in context and demonstrate its novelty, while also critically reviewing the approaches taken by other authors in similar studies, and presenting key results from those studies for comparison with those of the present work.

The present study involves the construction of a system model - that is a model of a multi-element (or multi-module) process which aims to predict system outputs from system inputs by representing the modules of the system and their interconnections. The system in this case is an industrial process for the production of electricity (or combined heat and power), taking as its input the delivery of a biomass feedstock from an external supplier, and as its output the supply of electricity and heat to an external customer. A key feature of the system is the upgrading of the feedstock by the process of gasification.

The scope of the review has therefore been defined as the modelling of biomass gasification systems for power or CHP. This covers a reasonable number of studies with a high degree of relevance to the present work. A further narrowing of scope might be contemplated on the basis of scale (and by implication the choice of prime mover), but this is considered too limiting as there have only been a small number of modelling studies considering biomass gasification systems in the range 0.5-2.5 MW_e based on IC engines.

3.2 Biomass Gasification System Studies

Biomass gasification system studies vary in form, depending on the particular study's objectives. These variations are usually to be found in the level of technical and economic detail contained within the module sub-models (and therefore the range of input parameters for which the system response can be tested). Previous studies have in general either sought to compare the performance and/or the economics of different gasification-based systems [e.g. 44,45,46,47,48,49], or to compare the performance and/or the economics of gasification-based systems against other bio-energy systems [e.g. 39,40,50,51,52]. Most

often these comparisons are performed either at the known design point of the systems in question, or at some arbitrary scale selected for the purpose of the study. Less often, comparisons are made across a range of scales.

Rarely however do these studies attempt to optimise the design and operating conditions of the systems being compared, which is the principal concern of the present study. They are concerned to develop accurate performance and particularly cost estimates for actual or proposed systems, but they are not concerned with understanding or improving the design of those systems. Even when design issues are addressed, studies are frequently limited by resources to a small number of cases, particularly if specialised process flow software is being used which can be costly to configure and run.

The most relevant previous studies of biomass gasification systems for power or CHP are now discussed, grouped in subsections corresponding to the originating organisation.

3.2.1 Aston University

The Bio-Energy Research Group at Aston University in the U.K. has been active for many years in the techno-economic analysis of bio-energy systems. For example, dedicated models have been developed to analyse fast pyrolysis systems (BLUNT, [53]) and systems for the production of liquid fuels from gasification (AMBLE, [54]). Both models include technical representations of the key processes (in the form of mass energy balances) as well as cost functions. At the time, the models were written in Fortran; today, they could be more conveniently implemented on spreadsheets.

The key work considering biomass gasification systems for the production of electricity or CHP was carried out by Toft [40] between 1993 and 1995. In his PhD thesis, Toft presents a thorough study of the techno-economics of four separate biomass-to-electricity systems, two of which are gasification-based. The study aimed to compare the systems on the basis of overall efficiency, capital cost and cost of electricity. The four systems considered were combustion in a conventional steam cycle, atmospheric gasification with a dual-fuel IC engine (i.e. a BGES), fast pyrolysis with a dual-fuel IC engine, and pressurised gasification in a combined cycle.

The system boundaries were from chipped wood feed (pre-transport), through to delivery of electricity at point of connection to the grid. Each system was evaluated over a range of scales from 1-100 MW_e, with all other input parameters remaining fixed. Also, at selected scales, feed costs were varied from 0-80 US$/dt and availabilities from 50-100%. Sensitivity studies were also conducted of certain key parameters, particularly financial parameters and component efficiencies.

A spreadsheet-based model was developed for the analysis. The model was intended to compare very different systems on a consistent basis as a function of system scale, and not to consider system design or optimisation. Representations of the various system components were based predominantly on correlations developed from available performance and cost data. The gasification process was not modelled; instead the gasifier was represented by empirical correlations of cold gas efficiency and cost with biomass input. While the data used to obtain these correlations was reliable, they were insufficiently comprehensive to permit the effects of different biomass moisture contents to the gasifier to be considered - one of the principal concerns of the present study.

The IC engine was represented in a similar way, using empirical correlations of efficiency and cost with thermal input. In the case of the gasification combined cycle option, no attempt was made to model the combined cycle; again, the model relies on efficiency and cost correlations which are inevitably tentative as a consequence of the extremely limited empirical data available at the time.

Because of these simplistic representations, the study made no attempt to consider the effects of change in feedstock, gasifier operating conditions or prime mover operating conditions. Nevertheless, the cost analysis was thorough and great care was taken to compare systems on a consistent basis. All capital costs of system modules are brought to a common Total Plant Cost basis which includes equipment cost including associated instrumentation and connections, installation, all engineering and contractors' costs, and contingency. Learning effects are also treated thoroughly, with the more novel technologies treated both on a current-cost and future-cost (10th plant) basis, and with learning effects applied both at a system level and in some cases at a component level. This rigorous treatment is important when comparing different systems with widely

differing levels of technological maturity, as is the case here, although it is less important in the present study for the reasons already discussed in Section 2.5.2.

A single biomass type was considered, namely a generic wood with a lower heating value (LHV) of 19.3 MJ/kg dry and a nominal delivered moisture content of 100% db. The dryer was assumed to be of the rotary type (Appendix 1 Section A1.7.3), delivering a fixed final moisture content of 17.6% db. A fixed value of flue gas energy requirement per unit of water evaporated was assumed, and a simple check was made to see whether sufficient was available. Dryer capital cost was correlated empirically with biomass input and water evaporation rate. Oxygen enrichment of the gasification air was not considered.

Some results for the BGES configuration are presented in Table 3.1. Unfortunately, the smallest scale for which detailed data were presented was 5 MW$_e$ - rather higher than the maximum of 2.5 MW$_e$ being considered in the present study. All costs are on a 1995 basis. Capital cost was a total plant cost (see Section 2.5.1). Feed cost before transport was 40 US$/dt, discount rate was 10%, plant availability was 90% and load factor was 1.0. Diesel consumption in the dual fuel engine was 5% of total thermal input.

Table 3.1 BGES performance and cost - Toft [40]

Aston University

Illustration removed for copyright restrictions

For a feedstock cost of 80 US$/dt, the cost of electricity from a 5 MW$_e$ system (1st plant) rose to 0.213 US$/kWh. At a system size of 10 MW$_e$, a 10% increase in feed moisture content (to 110% db) resulted in a 0.91% increase in cost of electricity, while a 10% reduction in feed moisture content (to 90% db) resulted in a 0.78% drop in cost of electricity.

Toft's model was subsequently incorporated into the Bioenergy Assessment Model (BEAM) developed under the IEA Bioenergy Agreement, Tasks IX and X [55,56]. BEAM extends Toft's model to consider the complete biomass production process (rather than simply allocating a feed cost as in Toft's model), and also to consider biomass-to-ethanol systems.

3.2.2 Electric Power Research Institute

In 1992 the Electric Power Research Institute in the United States initiated an in-depth strategic analysis of biomass and waste fuels and power technologies, in order to develop consistent performance and cost data and to identify market deficiencies and opportunities [50,57,58]. The systems analysed include co-firing with coal in utility boilers, stoker boilers fired with wood, municipal solid waste and refuse-derived fuel, wood-fired circulating fluid bed boilers, the Whole Tree Energy concept, and wood-fired gasification combined cycle. These are compared with coal-fired boilers and natural gas combined cycle.

The performance/cost analysis was carried out using a spreadsheet-based techno-economic model, BIOPOWER. BIOPOWER contains individual spreadsheets for each technology option, in which data are entered and calculations performed. Performance is calculated from energy/mass balances, sometimes combined with performance correlations (as for example with the gas turbine). Economic parameters from correlations established by the EPRI investigators.

The biomass gasification system analysis considers two combined cycle technologies, each at a scale of 100 MW_e - a current technology option using an industrial gas turbine, cold gas clean-up and a wood-fired rotary dryer, and an advanced technology option using an aeroderivative gas turbine, hot gas clean-up and a direct-contact steam dryer. The gasifier is modelled assuming equilibrium of the water-gas shift reaction and a specified product gas temperature, together with a specified char conversion efficiency and a specified tar production. The wood-fired dryer does not make use of the flue gases from the combined-cycle heat recovery steam generator; it has a dedicated combustor burning wood and gasifier char. The steam dryer takes superheated steam from the heat recovery steam

generator at the appropriate temperature and pressure, and returns saturated steam to the heat recovery steam generator afterwards.

The study uses a total plant cost including major equipment, installation, general facilities, land and civil works, engineering (10% of installed equipment) and contingency (15% of installed equipment). The intention of the study was to evaluate the technical and economic status of the evaluated technologies at the time of the study, so that current costs are used throughout with no consideration of learning factors.

In their summary of the EPRI analysis, McGowin and Wiltsee report costs of electricity of 9.5 USc/kWh and 6.9 USc/kWh for the current and advanced options respectively (1994 prices), for a wood cost of around US$41/dt at a delivered moisture content of 50% db. This compares with a cost of electricity of 3.9 USc/kWh for natural gas combined cycle.

The BIOPOWER model is thorough and easily understood. It relies heavily however on user input data (for example to specify component efficiencies) and uses relatively simple representations of processes. There are no options for different equipment types within each system, and there are no attempts reported to optimise the design of the individual systems in any way. In particular, the influence of biomass moisture content on the gasification process and the economic consequences of drying have not been addressed. Also the study was aimed at large-scale systems, and no attempt was made to apply the methodology to systems anywhere close to the scale range of the present study.

3.2.3 Energy Options Ltd.

Heaton [59], working for Energy Options Ltd, a small U.K. consultancy, carried out a study for DGXII of the European Commission between 1986 and 1987, with the objective of evaluating the technology, application and economic viability of systems in the range 1-6 MW_e. He chose therefore to restrict the study to BGESs, incorporating both downdraft and fluid bed gasifiers and both SI and dual fuel CI engines. Six systems were evaluated, covering a range of scales and gasifier-engine combinations. As part of the study, two separate Fortran models were developed, one to determine performance and one to determine costs; however, these models relied on correlations of empirically-derived overall process parameters - none of the component processes was modelled analytically.

Each of the six configurations was modelled at a single design point only, as dictated by the limited empirical data utilised. This was sufficient for the purposes of the study which was principally to establish the economic status of such systems. However, without more empirical data (which were probably unavailable in any case) it would not have been possible to vary process parameters such as biomass moisture content to the gasifier, which are of particular interest in the present study.

The feedstock was wood chips (type unspecified), with a delivered moisture content of 35% db. This is a rather low figure for virgin wood, even allowing for on-farm drying, and appears to be a compromise between SRC sources and dry waste-wood sources (although this is not explicitly stated). A rotary dryer was assumed with an exit moisture content of 25% db.

Some results are summarised in Table 3.2. The delivered feedstock cost was £35/dt, plant availability was 94.7% and average load factor 0.75. Costs are 1986 values.

Table 3.2 BGES performance and cost - Heaton [59]

Capital cost is described as "installed", but no definition is given in the published report. Data have been obtained from manufacturers where possible. It is also unclear whether any learning factor was applied, whether efficiency was on a lower or higher heating value basis, and what discount rate was used, as appendices which may contain some of these data could not be obtained. All costs are on a 1986 basis.

3.2.4 National Renewable Energy Laboratory

The National Renewable Energy Laboratory in the United States have carried out a number of modelling studies of biomass gasification systems over recent years, usually considering large scale systems and using the ASPEN PLUS process simulator to calculate system performance. ASPEN PLUS is widely used for system performance studies in all process industries and is becoming popular for the modelling of power generation systems. However, it is best suited to large-scale systems with high levels of complexity. Its merits, particularly with regard to suitability for the present study, are discussed in Section 8.1.

Craig and Mann [44] used ASPEN PLUS to determine the efficiency and cost of the production of electricity only, in large scale (>30 MW$_e$) biomass integrated gasification combined cycle (BIGCC) systems. The aim was to establish the status of such systems, not to explore their design characteristics.

Three BIGCC systems were analysed; one incorporating a pressurised fluid bed gasifier, one incorporating an atmospheric fluid bed gasifier, and one incorporating a twin-bed indirectly heated gasifier. In the case of the pressurised fluid bed gasifier and the twin-bed gasifier, operational data available from product development units were regressed to construct user-specified gasifier models within ASPEN PLUS for gas yield, composition and temperature. In the case of the atmospheric fluid bed gasifier, no data were available and the gasifier was modelled within ASPEN PLUS as a quasi-equilibrium reactor with fixed reactant ratios taken from a comparable system. This is likely to have resulted in inaccuracies, as equilibrium assumptions when applied to fluid bed gasifiers (particularly short residence time circulating types) tend to result in an underestimation of methane content and an overestimation of cold gas efficiency.

Within the three basic systems, a number of alternative configurations were evaluated including two specific gas turbine types and two product gas cooler types. Not all options were modelled for all systems. The biomass feedstock was either maple or poplar, depending on the gasifier type. Feedstock composition and flow rate were fixed for each gasifier-turbine combination. The flow rates were selected to give the product gas flow required to achieve the turbine design firing temperature. Air oxygen enrichment was not considered.

A rotary dryer was assumed, with a fixed final moisture content of 12.4% db for the pressurised and indirectly heated gasifiers and 20.5% db for the atmospheric gasifier. The drying medium was flue gas from the heat recovery steam generator, combined with the products of combustion from a small dedicated biomass combustor as required, and mixed with ambient air to achieve a fixed dryer inlet temperature of 204°C (deemed low enough to avoid the risk of fire).

As part of the study, a separate investigation of the effect of feedstock moisture and air pre-heat on the performance of the indirectly heated twin-bed gasifier was carried out. In this gasifier, char from the gasification reactor is transported to a separate combustion reactor where it is burnt in air, thereby heating sand which is returned to the gasification reactor as the source of heat for steam-only gasification. It was concluded that a moisture content of higher than 12.4% db could be used while still maintaining the temperatures necessary for gasification; however this option was not explored using a full ASPEN PLUS simulation.

Economic analyses were carried out of the various system configurations, assuming the nth production plant (i.e. mature technology). The base year for costing was 1990. Capital costs were based on actual equipment costs where possible; elsewhere they were capacity-factored from actual equipment costs. A total plant cost was used including installed process plant equipment cost, general facility costs (10% of process plant cost), engineering fees (15% of process plant cost) and contingency (16.5% of process plant cost). A plant capacity factor of 80% was assumed.

Net power outputs were in the range 55-132 MW$_e$, and net system efficiencies (LHV basis) were in the range 35-40%. Total capital costs were in the range 1100-1700 US$/kW (1990), and electricity costs were in the range 0.051-0.063 US$/kWh (1990), based on a biomass gate cost of 42 US$/dt.

The techno-economic analysis of the system incorporating a twin-bed indirectly heated gasifier (specifically the Battelle/FERCO gasifier [60]) carried out by Craig and Mann was updated in 1997, and incorporated in a detailed life-cycle analysis of a conceptual BIGCC installation based on the Battelle/FERCO gasifier (Mann and Spath [61]).

3.2.5 Princeton University

The Center for Energy and Environmental Studies at Princeton University in the United States has been active in the area of bio-energy systems analysis for many years, and has produced many publications.

In a techno-economic study of biomass gasification combined cycle systems featuring aero-derivative gas turbines by Consonni and Larson [47,48], three systems were compared, one based on atmospheric air-blown fluid bed gasification (the TPS gasifier), one on pressurised air-blown fluid bed gasification (the Bioflow gasifier), and one on twin fluid bed gasification (the Battelle/FERCO gasifier). The feedstock was a generic wood with a moisture content of 100% db, dried to about 18% db in each case in a rotary dryer using the gas turbine exhaust gases after the heat recovery steam generator. The systems were modelled at net power outputs in the range 25-30 MW_e, a scale more suited to European applications than that adopted for the EPRI and NREL studies referred to above.

An internally-developed flowsheeting code [62] was used for the performance analysis. The gasification process was not modelled; instead a product gas composition was assumed from manufacturers' data, and a mass/energy balance performed. Overall efficiencies in the range 41-45% were obtained (LHV basis) - high compared with other studies, reflecting the higher efficiency of the aero-derivative gas turbines.

Costs of electricity were calculated only in a very approximate way and few details are given. Values in the range 4.9-5.7 USc/kWh are quoted.

A study by Hughes and Larson [63] looked at the effect of biomass moisture level both at delivery to the dryer and delivery to the gasifier on overall performance in a wood chip fired combined cycle power plant of about 40 MW_e, with a pressurised circulating bed gasifier and a flue gas dryer using the exhaust gas from the heat recovery steam generator. The study was concerned only with the effects on cycle power output and efficiency, and did not consider costs.

Again, the centre's internally-developed flowsheeting code [62] was used for the performance analysis. The pressurised fluid bed gasification process was not modelled in detail as reactions are far from equilibrium. Instead, a constant gasifier temperature was assumed, and a mass/energy balance performed to calculate the product gas flow rate for feeds of different moisture content. A measured product gas composition was used for the 15% moisture cases. At all other moisture contents the composition had to be estimated; however, it was shown that this did not affect product gas heating value or cycle efficiency significantly.

Some results are presented in Figure 3.1. Overall system efficiency (HHV basis) is plotted against wood moisture content to the gasifier, for five different pre-dryer wood moisture contents.

Aston University

Illustration removed for copyright restrictions

Figure 3.1 Effect of feed moisture content on system overall efficiency [63]

There is an improvement in system overall efficiency for any decrease in the feed moisture content to the gasifier at a given pre-dryer moisture content. At a given feed moisture content to the gasifier, there is an improvement in efficiency with reducing pre-dryer moisture content up to the point where there is a surplus of heat remaining in the heat recovery steam generator exhaust gas which cannot be utilised elsewhere.

3.2.6 Technical Research Centre of Finland (VTT)

The Technical Research Centre of Finland (VTT) has been active in the techno-economic assessment of bio-energy systems for many years, and is one of the leading centres in this area having conducted many studies [e.g. 39,46,64,65,66,67]. The centre has developed a strong competence in the application of the ASPEN PLUS process simulator to bio-energy systems in general and biomass gasification systems in particular, and most published studies involve its use. Two studies are of particular interest as they include consideration of BGESs, and these are now discussed.

In a study conducted within the IEA Bioenergy Agreement, Solantausta et al [39,66] aimed to model and evaluate the cost and performance of new power production concepts employing woody biomass as fuel. A total of fifteen gasification-based cases were modelled using the ASPEN PLUS process simulator. These covered a capacity range of 5-60 MW_e and included atmospheric and pressurised combined cycles, a steam-injected gas turbine (STIG) cycle and a BGES cycle. Both power-only and CHP modes were considered for most configurations (although not for the BGES, which was power-only).

Each power-only configuration was modelled at two or three capacities, using flue gas drying in each case. The CHP cases were all modelled at 30 MW_e, but those cases incorporating pressurised gasification (combined cycle and STIG) were run with both flue gas and steam drying options. Flue gas drying assumed a rotary dryer; steam drying assumed a pressurised fluid bed dryer (Appendix 1 Section A1.7.5.1).

A single wood feedstock was used for all cases, with a moisture content of 100% db. Both dryer types delivered a final moisture content of 17.6% db. These moisture contents were not varied at any stage of the investigation. Two gasifier product gas compositions were used, one for atmospheric and one for pressurised gasification. These did not vary from one case to the next. It does not appear that a gasification model was used; however no details were given as to how the gas compositions were obtained. Oxygen enrichment of the gasification air was not considered.

Two BGES cases were run, one at 5 MW$_e$ and one at 25 MW$_e$. Each incorporated an atmospheric air-blown fluid bed gasifier and a dual fuel diesel engine. Diesel pilot flow was around 9% of total thermal input in each case. Results are given in Table 3.3.

Costs are on a 1994 basis, assuming a feedstock delivered cost of 50 US$/dt, an availability of 57%, a load factor of 1.0 and a discount rate of 5%.

Table 3.3 BGES performance and cost - Solantausta et al [39]

Where flue gas and steam dryers have been compared (i.e. 30 MW$_e$ CHP schemes), the steam dryer configurations were found to give more heat recovery at increased overall capital cost. The greater heat recovery arose because the moisture evaporated in the steam dryer could be condensed to heat water for a low temperature district heating scheme. No specific information was given on dryer costs.

The second, more recent study to consider BGESs was also carried out within the IEA Bioenergy Agreement, and considered small-scale biomass power and CHP production concepts. Solantausta and Huotari [67] compared a Rankine steam boiler plant system with a BGES and with a diesel engine/fast pyrolysis system. In each case, ASPEN PLUS was used to calculate the performance of the system, with an economic analysis carried out subsequently. No details are given of the models used for each process step. The systems for power production were compared at 2 MW$_e$ output; the systems for CHP were compared at 6 MW$_{th}$ output.

The analysis of the BGES considered two variants. The current technology plant comprised a flue gas dryer, a fluid bed gasifier with fluid bed tar cracker, and a modified natural gas spark ignition gas engine. The future technology plant comprised a silo dryer

64

(presumed hot air), a fixed bed gasifier, "catalytic" gas clean-up (further details not given) and a high-efficiency spark ignition gas engine designed for low heating value gas. The reasons behind the choice of a fixed bed gasifier for the advanced system are not given. Only a single operating point is reported for each configuration, based on a chipped wood feedstock with a moisture content of 80% db delivered and 25% db after drying. Efficiencies are given in Table 3.4.

Table 3.4 BGES efficiencies - Solantausta and Huotari [67]

No information is given on cost analysis methodology, other than to state that "normal practices in process and power generation industries" are used. Table 3.5 gives cost of electricity (1999 prices) obtained for a range of feedstock costs. The plant capacity factor is 0.8, and the heat is sold to a district heating network. Unfortunately the assumed price paid for heat is not made clear.

Table 3.5 BGES costs of electricity - Solantausta and Huotari [67]

The large improvement in cost of electricity for CHP schemes over power-only schemes is due much more to the scale of the plant (about 5 MW_e compared to 2 MW_e) than to the price received for the heat.

3.2.7 University of Ulster

The Centre for Energy Research at the University of Ulster has developed its own process flowsheeting package, ECLIPSE, for technical and economic evaluations of chemical and related processes. This has been applied by McIlveen-Wright et al [51,68] to a techno-economic evaluation of various systems for the production of electricity from wood.

The systems considered in detail were combustion with steam cycle, BIGCC, gasification with simple cycle gas turbine, gasification with steam-injected gas turbine and gasification with IC engine (BGES). Simulations of natural gas combustion in simple and combined cycle gas turbine systems was also carried out for comparison.

Eclipse contains capital cost functions for standard items, but costs for non-standard items have to be estimated based on data from external sources. A total plant cost basis is used including equipment cost, installation, civil works and "indirect" costs. No attempt is made to consider learning factors; "best available" cost estimates are used throughout.

In the case of the BGES simulations, a fixed-bed air-blown downdraft gasifier is assumed, but no information is given on how the gasification process is represented in the model. A dryer using engine exhaust gases has been included in the simulation but no further details are given as to representation. The IC engine is represented as a spark ignition gas engine using data supplied by the Caterpillar company. The engine is simulated initially in stand-alone mode with natural gas as a fuel to calibrate the engine model against supplied data, and then with product gas at the same mixture volumetric flowrate. Details of the engine model are not given.

A total of eight BGES cases were run corresponding to eight engine types of different scale. There is no report of any operating parameter being varied other than biomass input flow rate. Results are given in Table 3.6. All costs are 1992 values. Data for cost of

electricity assume a delivered feedstock cost of £20/dt. The wood is delivered chipped, with a pre-dryer moisture content of 100% db, but post-dryer moisture content is not given.

Table 3.6 BGES performance and cost - McIlveen-Wright [51,68]

Power output (MW$_e$)	Engine Type	Overall efficiency (LHV) %	Capital cost £/kW$_e$	Cost of electricity p/kWh
0.17	Caterpillar 3408NA	22.6	1862	7.21
0.30	Caterpillar 3516NA	22.8	1872	4.90
0.15	Caterpillar 3408TA	26.6	1208	6.93
0.54	Caterpillar 3516TA	29.7	1606	6.46
0.83	Caterpillar 3606TA	24.2	1563	6.25
1.10	Caterpillar 3608TA	24.6	1625	6.39
1.66	Caterpillar 3612TA	25.0	1566	6.19
2.27	Caterpillar 3616TA	25.4	1520	6.04

Reasons are not given why the system based on the 3516NA engine exhibits such a low cost of electricity compared to the other seven systems, but this appears erroneous.

3.2.8 *Utrecht University and Netherlands Energy Research Foundation (ECN)*

The University of Utrecht in collaboration with the Netherlands Energy Research Foundation (ECN) has conducted a number of studies of biomass gasification systems using ASPEN PLUS for process simulation.

As part of a European Commission Joule II programme, Faaij et al [69,70] carried out a techno-economic study of a BIGCC system of about 30 MW$_e$, supplying electricity only and featuring an atmospheric air-blown fluid bed gasifier. ASPEN PLUS was used for process simulation, and this aspect of the work is reported in greater detail by Van Ree et al [45]. The economic analysis was carried out separately.

Three system configurations were considered: a base configuration with rotary dryer and low temperature product gas clean up; the base configuration modified to have a pneumatic conveying steam dryer (Appendix 1 Section A1.7.6.1); and the base configuration modified to have high temperature product gas clean up. The three systems were modelled with poplar wood as the feedstock (moisture 100% db). The base configuration was also modelled with four other feedstocks: verge grass (moisture 150% db), organic domestic waste (moisture 117% db), demolition wood (moisture 25% db) and an 80:20 mixture of demolition wood and sewage sludge (moisture 25% db).

In each modelling case, only a single design point was calculated with no attempt to vary operating conditions. The gasification process was not modelled; all the required parameters (including product gas compositions for the different feedstocks) were based on a manufacturer's calculations. For both dryer types, a fixed final biomass moisture content of 17.6% db was used for all feedstocks. In the case of the rotary dryer, the flue gas temperature was specified to meet the drying requirement. In the case of the steam dryer, the flue gas temperature was set to it's minimum practical value, and the steam requirement for the dryer was drawn from the steam turbine at the appropriate conditions.

Overall efficiency of the base configuration for the five feedstocks was found to range from 34.3% to 39.1% (LHV basis). Use of a steam dryer was found to reduce overall efficiency from 38.2% to 37.7% (LHV basis), due to the rotary dryer's utilisation of low grade heat which is rejected in the case of the steam dryer.

In the economic analysis, the scope of the capital costs presented is not clearly defined, but includes equipment cost, civil works, control systems and engineering costs. Actual costs from manufacturers or from comparable projects are used where possible. It is intended that the final costs should be for a mature (n^{th}) plant, so costs for the gasifier and tar cracker (assumed 1st plant) have been reduced to compensate for the high engineering and development element associated with 1st plants. All other obtained costs are assumed n^{th} plant.

Assumed feed costs were 42.9-50 €/dt (1995) for chipped poplar wood (forestry thinnings), before transport. The corresponding cost of electricity was calculated at 0.062-0.085 €/kWh.

3.3 Novelty

In light of the preceding review, the principal aspects of novelty in the present work are summarised here.

Firstly, there are few examples in the literature of system performance/cost modelling being applied to a BGES, or to any biomass gasification system at below 5 MW$_e$. The only broadly comparable analysis found which focuses exclusively on BGESs (1-5 MW$_e$) was that of Heaton [59]; however Heaton does not predict product gas composition in his model, and cannot therefore consider the effect of different moisture contents or the effect of oxygen enrichment on gasifier performance. The remaining examples where BGESs have been modelled are studies where a number of systems are being compared (primarily economically), and only a very small number of alternative configurations have been run [39,40,51]; again, in none of these is the gasification process modelled in sufficient detail to predict product gas compositions. The issue of energy integration within a BGES (particularly w.r.t. the choice of dryer technology and the trade-off between drying and the supply of heat in a CHP scheme) has therefore not been considered.

Only one modelling study has been found that considers the effect of different levels of moisture in the gasifier feed on the overall performance of a biomass gasification system [63], and that study was limited to efficiency and power output calculations for a large combined-cycle power plant with a pressurised fluid bed gasifier. Cost aspects were not considered.

No studies have been found that consider quantitatively the effect of different levels of gasifier air oxygen enrichment on the overall performance of a biomass gasification system.

No studies have been found that consider biomass gasification systems incorporating a gasifier operating under slagging conditions with air pre-heat, or evaluate comparatively the performance of slagging and non-slagging biomass gasifiers.

No studies of any kind have been found that consider the operation of IC engines fuelled with biomass gasifier product gas and oxygen-enriched air.

Finally, no comprehensive studies have been found on the selection of drying technologies for biomass gasification systems. While there have been reviews of biomass drying technologies, these have tended either to be of limited depth as part of a broader review of bio-energy technologies, or to be restricted to specific scales or applications.

4 DRYER

This chapter deals with the biomass drying module of the BGES (see Figure 2.1). The drying module receives wet biomass from the reception, storage and screening module (Section 7.1) and passes dry biomass to the gasifier module (Chapter 5).

4.1 Summary of Dryer Options for a Biomass Gasification System

A review of dryers for biomass gasification systems can be found in Appendix 1. Six categories of dryer were identified as being suitable for biomass gasification systems, and a summary is presented in Table 4.1 giving the six categories, together with specific dryer types within each category and some of their key characteristics. For each type, a reference is given to the relevant section and figure in Appendix 1.

All of the dryer types listed in Table 4.1 have been used successfully in the past either for biomass gasification system feedstocks or for materials sufficiently closely related for the extrapolation to be made. All have particular advantages and disadvantages, and their respective suitability will depend on the particular feedstock and various other features of the bio-energy system in question, not least the scale.

4.2 Dryers for a Biomass Gasifier-Engine System

The two relevant features of a BGES for the identification of suitable drying technologies within the general context of biomass gasification systems are its biomass throughput range, and its biomass size requirement.

The scale range of interest here corresponds to a material throughput range of about 0.5-2 dt/h (Section 1.1). Taking the largest likely drying duty to be from 120% db to 10% db moisture content, and the smallest from 40% db to 25% db, this gives a possible range of moisture removal requirements of 0.06-2.2 dt/h, or more generally < 3 dt/h. The gasifiers under consideration are of the fixed bed type, and as such will require feeds with particle dimensions broadly in the range 10-100 mm (see Section 5.1.1).

71

Table 4.1 Summary of dryer types for biomass gasification system feedstocks

Dryer Category	Dryer Type	Comments re use with biomass gasification system feedstocks
Batch through-circulation	Perforated floor bin (Section A1.7.1, Figure A1.10)	Low capital cost. Low emissions. Uses low-grade heat, but wide variations in final moisture content. Extent of drying limited. Batch system. Attractive at small scales.
Continuous through-circulation	Band conveyor (Section A1.7.2.1, Figure A1.12)	Moderate capital cost. Highly controllable. Emissions moderate to low. Can use low-grade heat. Well suited to fragile materials.
	Rotary louvre (Section A1.7.2.2, Figure A1.15)	Moderate to high capital cost. High heat transfer rates. Emissions moderate. High specific throughput. Best suited to fragile materials.
Direct rotary	Rotary cascade (Section A1.7.3, Figure A1.17)	Moderate capital cost. Uses large quantities of drying medium. Potentially high emissions. Well understood, low risk. Widely used at medium to large scales
Indirect rotary	Rotary steam-tube (Section A1.7.4, Figure A1.19)	Moderate to high capital cost. Moderate to low emissions. Best suited to materials which cannot be directly exposed to hot gases.
Fluid bed	Conventional once-through (Section A1.7.5, Figure A1.20)	Low capital cost. Efficient heat transfer. Potentially high emissions. Prone to bed instability problems, especially where particle size distribution wide. Suited to small particles of uniform size.
	Pressurised recycled steam (Section A1.7.5.1, Figure A1.21)	Purpose designed for integrated biomass systems. High capital cost. Could be economical at larger scales if recovered energy can be utilised. Very low emissions.
Pneumatic conveying	Pressurised recycled steam (Section A1.7.6.1, Figure A1.24)	Purpose designed for integrated biomass systems. High capital cost. Could be economical at larger scales if recovered energy can be utilised. Well suited to vapour recompression techniques. Very low emissions.

Of the dryer options listed in Table 4.1, the two pressurised steam dryer systems (the Niro and Stork "Exergy" processes) can be ruled out on the grounds of scale. Both of these processes are designed for much larger throughputs of 10 dt/h or more and would be uneconomic at such a relatively small scale. Also, relatively small CHP systems incorporating a reciprocating engine as the prime mover would export heat either as hot water, or as very low pressure steam unsuitable for use in a dryer [24], so there would not be a source of steam already available which could be tapped for drying. This therefore makes any of the smaller-scale systems using steam as a heating medium unattractive (the rotary steam tube dryer and the steam-heated band conveyor dryer). Finally, it is likely that fluid bed dryers, while relatively cheap, would prove difficult to operate with feed sizes in the range anticipated; 10 mm is often considered an upper limit.

The dryer types best suited to a BGES are therefore the following:

- Rotary cascade dryer (using either engine exhaust gas or combustion products from a dedicated biomass burner) - Appendix 1 Figure A1.17

- Band conveyor dryer (using either externally-heated air, engine exhaust gas or combustion products from a dedicated biomass burner) - Appendix 1 Figure A1.12

- Perforated floor bin dryer (using either ambient or low-temperature externally-heated air) - Appendix 1 Figure A1.10

A rotary cascade and a band conveyor dryer have been selected for the system modelling study (Chapters 8 and 9). These are usually abbreviated in this study to *rotary dryer* and *band dryer*.

The rotary dryer has already been used widely in biomass gasification and combustion systems. It provides a drying option which can utilise as an energy source both the thermal energy in the hot combustion products from the IC engine, and the chemical energy in the surplus biomass via a dedicated burner (see the discussion of energy utilisation routes in Section 2.1, and Table 2.1).

73

The band dryer is a high residence time design using low-temperature air as the drying medium (Appendix 1 Section A1.7.2.1), a type that has been recommended for biomass gasification systems in a recent study [71]. This is effectively a continuous perforated floor bin dryer. It provides a drying option which can utilise the relatively low temperature IC engine coolant as an energy source (see again Section 2.1 and Table 2.1).

For both dryer types, performance and cost data have been gathered and analysed, and spreadsheet-based models constructed for the "standard" biomass, as described in the following sections.

4.3 Dryer Modelling

4.3.1 Rotary Dryer

4.3.1.1 Modelling Approach

Much detailed work has been carried out on the modelling of drying in rotary dryers [72,73,74,75,76], often with the intention of resolving in detail the processes taking place within the dryer. In the present study however, it is only necessary to resolve these processes sufficiently to be able to determine the module inputs and outputs; information relating to conditions within the dryer is not required.

The model will be used in scenarios where the biomass and gas conditions at inlet and outlet are specified along with the desired biomass input. The required information is the flow rate of gas, the electrical power demand and the delivered capital cost ("equipment cost") of the dryer. The calculation of the gas flow rate requires only an energy and mass balance (with an assumption for heat loss from the dryer walls). Electrical power demand and capital cost however require an estimation.

Dryer equipment cost EC_3 might reasonably be expected to be related to dryer size (i.e. volume) for a given dryer type:

$$EC_3 = f(V_3) \qquad (4.1)$$

74

where V_3 is dryer volume and f is a function to be determined. Dryer volume must then be related to the available dryer performance parameters. This can be done using the concept of an overall volumetric heat transfer coefficient. This approach has been often used for rotary dryers and other types over the years [77], particularly by manufacturers who have acquired large amounts of operational data on specific dryer designs. The approach assumes that for a given dryer geometry, the dryer volumetric heat transfer coefficient U_{v3} is a constant, defined as:

$$U_{v3} = \frac{Q_{B3}}{V_3(T_{G3} - T_{B3})} \tag{4.2}$$

where T_{B3} is the mean temperature of the biomass, T_{G3} is the mean temperature of the hot gas, and Q_{B3} is the heat flow to the drying biomass.

The concept works well for fixed dryer geometry; however, if geometry changes with scale the volumetric heat transfer coefficient also changes. Some studies have attempted to relate U_{v3} to design features such as number of flights or bulk gas velocity for a range of dryer designs, with varying degrees of success [77]. Here, the model is to apply to a single fixed design of dryer where only the scale will vary, and these concerns do not therefore arise.

However, for biomass drying U_{v3} can also be expected to vary with the absolute moisture content of the drying material, because drying takes place entirely in the falling rate regime (see Appendix 1 Sections A1.3.2 and A1.5.2). At a lower mean moisture content over the drying operation, the mean drying rate will be lower, and the overall heat transfer coefficient will likewise be lower, leading to a larger volume requirement. Therefore, in Equation 4.2 U_{v3} is assumed to be a function of X_{B3}, the mean biomass moisture content during drying.

The relationships for capital cost and volumetric heat transfer coefficient may then be combined, putting $1/U_{v3} = g(X_{B3})$:

$$EC_3 = g\left\{\frac{Q_{B3}\,f(X_{B3})}{T_{G3} - T_{B3}}\right\} \qquad (4.3)$$

The functions f and g must be determined from data from operating dryers.

It is reasonable to assume that electrical demand will be a function of dryer size, as the main power demand is dryer rotation. As capital cost has been assumed to be a function of dryer size (Equation 4.1), the electrical demand can be expressed in the model as a function of capital cost. The function must again be derived from empirical data.

4.3.1.2 Acquisition of Performance and Cost Data

For all system components except the gasifier, the present study considers plant available commercially today. A number of manufacturers of rotary dryers were therefore approached with a request for performance and cost data against a set of scenarios covering the scale range of interest. The "standard" biomass was specified (Table 2.3) - i.e. poplar wood chips with a dry bulk density of 135 kg/m^3 and a volumetric mean diameter of 30mm. The scenarios covered different moisture levels and throughputs.

The responses were evaluated, and a single respondent selected who was able to demonstrate substantial experience of biomass drying, whose equipment costs were typical and who had supplied the full range of data requested. This was the M.E.C. Company of Kansas, USA, who have extensive experience in the supply of hog fuel dryers. The principal data provided by M.E.C. are given in Table 4.2, including delivered capital cost (equipment cost) for a dryer with and without an integral burner.

The system with integral burner (Figure 4.1) includes a post-dryer cyclone for the separation of entrained fines, a post-dryer screen for separation of unentrained undersize particles, a small grinder, a buffer store, a metering bin and a suspension burner, the exhaust gases from which are then mixed with quench air as necessary before either being supplied to the dryer inlet or exported to some other point in the system.

Table 4.2 Data for rotary dryer (M.E.C.) [78]

Aston University

Illustration removed for copyright restrictions

Aston University

Illustration removed for copyright restrictions

Figure 4.1 M.E.C. rotary dryer system with integral wood burner [78]

4.3.1.3 Description of Model

The model operates in two modes: without integral burner, and with integral burner.

1. <u>System without integral burner</u>

    In order to minimise drying costs, energy requirements and potential emissions problems, only the biomass size fraction suitable for gasification is dried (>10 mm mean diameter, see Section 5.3.1). The undersize fraction must therefore be removed (15% by weight, see Table 2.3), so this mode of operation has a pre-screening stage (Section 7.1).

    For power-only cases (flow diagrams Figures 2.4, 2.6), the model calculates the flow rate of engine exhaust gas at the engine outlet temperature, and the flow rate of ambient quench air, such that the specified dryer duty is met and the dryer inlet temperature does not exceed an upper limit of 300°C. This limit is necessary to minimise the risk of fire or explosion, and has been set based on operators' experience (see Appendix 1 Section A1.5.4). If the flow rate of engine exhaust gas exceeds that available, an error message is returned.

    For CHP cases (flow diagrams Figures 2.3, 2.5), the model calculates the gas temperature from the engine exhaust gas water heater (Section 7.3.2.1) at the full engine exhaust gas flow rate, and the flow rate of ambient quench air, again such that the dryer duty is met and the dryer inlet temperature does not exceed the specified upper limit of 300°C. If the engine exhaust gas water heater outlet temperature exceeds the engine exhaust gas water heater inlet temperature, an error message is returned.

    This system is referred to in this study as *rotary dryer without burner*.

2. <u>System with integral burner</u>

    The biomass flow supplying the burner is taken from the dryer output stream, and comprises all or part of the under-10mm size fraction which is too small to be supplied

too the gasifier. Unlike in Mode 1, the undersize fraction passes through the dryer and there is therefore no need for a pre-screening stage.

The under-10mm size fraction of unentrained dried biomass is separated by a post-dryer screen and mixed with the cyclone fines. The fraction of this required by the burner is then ground and supplied to the suspension burner; the remainder is disposed of. In power-only cases (flow diagrams Figures 2.8, 2.10), this fraction is calculated as the minimum necessary to meet drying requirements; the remainder is disposed of. In CHP cases (flow diagrams Figures 2.7, 2.9), all of the separated biomass goes to the burner, and the burner exhaust gases are then supplied first to the engine exhaust gas water heater to increase hot water production directly before the combined burner and engine exhaust flows pass to the dryer (see Section 7.3.2.1).

The model calculations proceed in the same way as for the system without integral burner, except that in the power-only case the model also calculates the required burner exhaust flow rate to the dryer, subject to the condition that the dryer size (i.e. equipment cost) is minimised.

This system is usually referred to in this study as *rotary dryer with burner*.

In both modes there are three main parts to the calculation procedure, performed simultaneously. The first part comprises specification or calculation of the gas conditions at entry to the dryer. The model obtains the engine exhaust gas composition, flow rate and maximum temperature from the engine model, and if the dryer is operating in Mode 2 a combustion calculation is performed. The second part comprises an energy/mass balance over the dryer, to give the required gas flow rates and/or temperatures. In the third part, capital cost, utility requirements and labour requirements are calculated. In both modes, a proprietary solver is employed to carry out the calculation.

Combustion Calculation

For Mode 2 operation (rotary dryer with burner) where supplementary biomass firing in an integral combustor is required, a combustion calculation is performed. Complete combustion of the biomass is assumed, at a fixed air-fuel equivalence ratio of 1.8

calculated from data supplied by M.E.C. for their dryer suspension burner [78]. The temperature of the exhaust gases is calculated from the following relationship:

$$m_{B5}\Delta H + (T_{G6} - 15)\sum(m_{G6}c_{G6}) = 0 \qquad (4.4)$$

where m_{G6} and c_{G6} are the mass flow and specific heat capacity of the various components of the exhaust gas (with c_{G6} evaluated at the mean of the exhaust gas temperature and the reference temperature of 15°C), T_{G6} is the exhaust gas temperature (°C), m_{B5} is the biomass flow rate to the burner and ΔH is the enthalpy of combustion at the reference temperature. The quantity $-\Delta H$ is taken as equal to the lower heating value of the biomass (lower heating value is conveniently quoted at a reference temperature of 15°C).

Energy/Mass Balance

Figure 4.2 shows the various quantities influencing the energy and mass balances, where m denotes mass flow, H enthalpy, Y absolute humidity, X moisture content, and subscripts G gas, B biomass, V water (vapour), W water (liquid). Q_{L3} denotes the heat loss due to radiation and convection from the dryer walls.
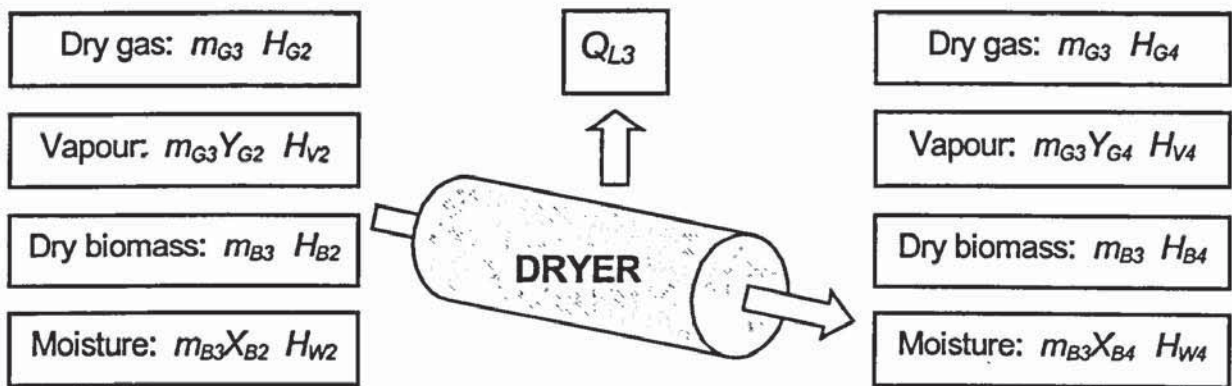
Figure 4.2 Rotary dryer energy/mass balance parameters

The mass balance may then be written:

$$m_{G3}(Y_{G4} - Y_{G2}) = m_{B3}(X_{B4} - X_{B2}) \qquad (4.5)$$

and the energy balance:

$$m_{G3}(H_{G2} + Y_{G2}H_{V2}) + m_{B3}(H_{B2} + X_{B2}H_{W2}) =$$

$$m_{G3}(H_{G4} - Y_{G4}H_{V4}) + m_{B3}(H_{B4} + X_{B4}H_{W4}) + Q_{L3} \qquad (4.6)$$

Gas and liquid enthalpies may be calculated as ΣcT, where c for gases is evaluated preferably at the mean of the inlet and outlet gas temperatures, or alternatively at the mean of the gas temperature and a reference temperature of 0°C. Vapour enthalpies are taken from the steam tables at 1 bar (also referenced to 0°C).

Equations 4.5 and 4.6 may be combined to give an expression for m_{G3} in terms of data input by the model user. Heat loss is specified as a fraction of total enthalpy in. Values of 6-10% were quoted by suppliers [78,79]; a fixed value of 8% has been set for all calculations.

Both gas and biomass enthalpy (i.e. temperature) at dryer outlet must be specified in the energy/mass balance. Companies providing data for the drying of wood chips in rotary dryers gave biomass exit temperatures in the range 65-85°C and gas exit temperatures in the range 100-120°C [78,79]. Values of 75°C and 110°C respectively have been adopted for all study calculations. A gas exit temperature of over 100°C implies no limitation in the vapour carrying capacity of the gas, so that drying medium saturation does not need to be considered in the model.

Capital Cost

The form of the function to be used for deriving equipment cost was discussed earlier (Section 4.3.1.1, Equation 4.3). From the equipment cost data in Table 4.2 and the application of regression analysis, the following functions for equipment cost (EC_3) were derived for the dryer without integral burner:

$$EC_3 = f(X_{B3}) \frac{Q_{B3}}{T_{G3} - T_{B3}} + 93.2 \qquad (4.7)$$

and for the rotary dryer with burner:

$$EC_3 = f(X_{B3})\frac{Q_{B3}}{T_{G3} - T_{B3}} + 288.6 \qquad (4.8)$$

where:

$$f(X_{B3}) = 0.971X_{B3}^{-2} - 0.479X_{B3}^{-1} + 11.0 \qquad (4.9)$$

Equipment cost is expressed in £'000 (1998), heat supplied in kW and temperatures in °C.

The form of the function f is reasonable, implying a heat transfer coefficient that falls with falling mean moisture content, and at an increasing rate as mean moisture content reduces. Figures 4.3 and 4.4 shows plots of equipment cost against $Q_{B3}/(T_{G3}-T_{B3})$ and $f(X_{B3})Q_{B3}/(T_{G3}-T_{B3})$ respectively. The functions of Equations 4.7 and 4.8 are included in Figure 4.4.
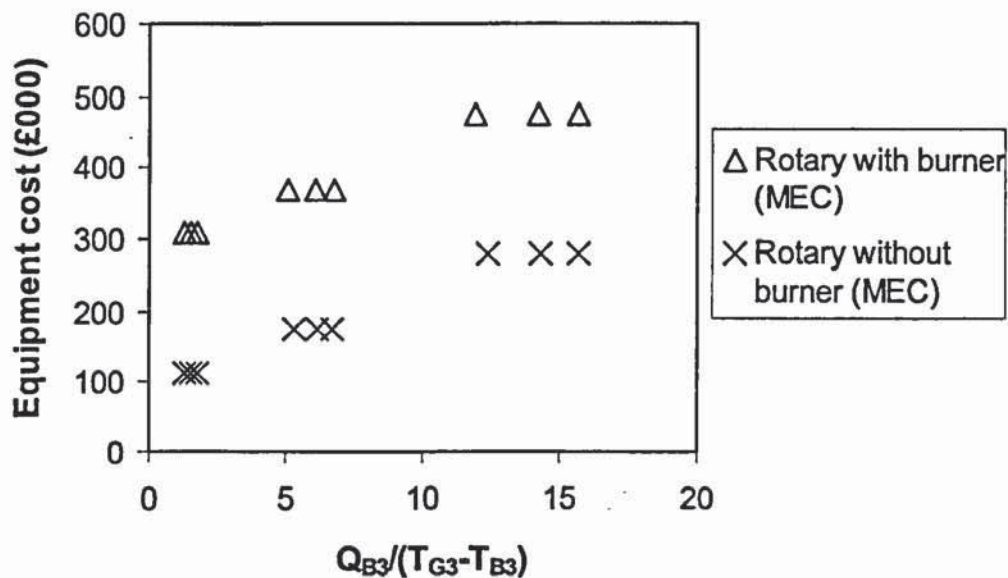
Figure 4.3 Cost vs. size for rotary dryer (without moisture function)

The average error in the calculated equipment cost using the functions of Equations 4.7 and 4.8 is just 0.7% for all cases.
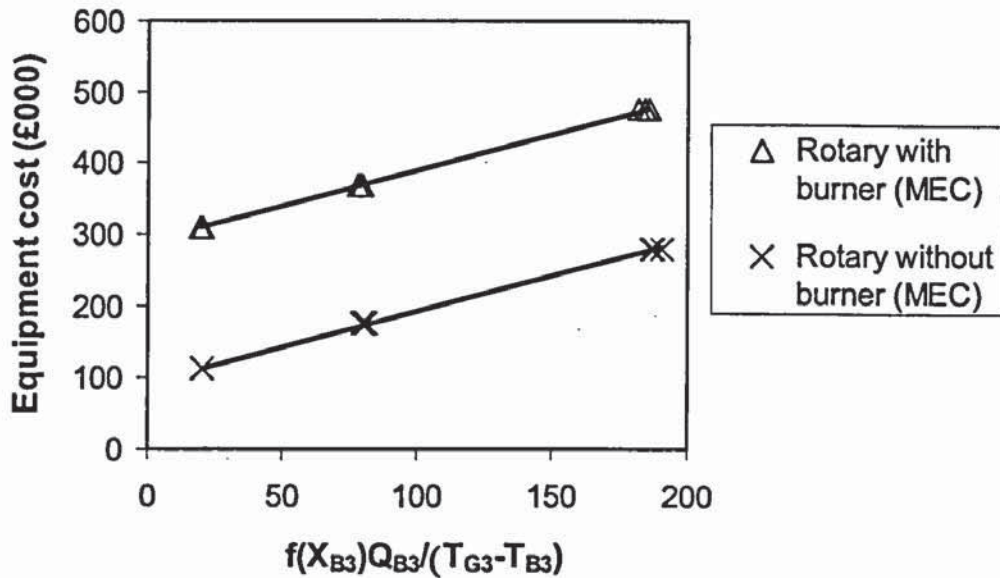
Figure 4.4 Cost vs. size for rotary dryer (with moisture function)

Finally the element of total plant cost attributable to the dryer module (TPC_3, £'000 1998) is calculated using the following function derived as described in Section 2.5.1 using Tables 2.4 and 2.5:

$$TPC_3 = 6.78 EC_3^{0.863} \tag{4.10}$$

Electrical Power Demand

Based on the data in Table 4.2, relationships for electrical power demand P_3 as a function of equipment cost EC_3 were derived using regression analysis. For the dryer without integral burner:

$$P_3 = 0.00179 EC_3^2 - 0.158 EC_3 + 17.6 \tag{4.11}$$

and for the rotary dryer with burner:

$$P_3 = 0.0015 EC_3^2 - 0.633 EC_3 + 75.2 \tag{4.12}$$

Capital cost is again expressed in £'000 (1998), and electrical power demand in kW.

<u>Labour</u>

The labour requirement for a rotary dryer has been estimated at 0.5 persons per shift for a single unit [80]. This figure has been used here, for dryers both with and without an integral burner.

The worksheet for the rotary dryer is shown in Appendix 2 Section A2.2.

4.3.2 Band Dryer

4.3.2.1 Modelling Approach

For this dryer, as for the rotary dryer without burner, the undersize fraction of the delivered biomass unsuitable for the gasifier is screened out prior to the dryer and rejected. Unlike that of the rotary dryer however, the performance of the band dryer operating on low temperature air is highly sensitive to the gas exit temperature from the dryer because the air is well below 100°C and may reach saturation. The gas exit temperature from the dryer cannot therefore simply be estimated or assumed constant if not known, and a simple mass-energy balance is thus insufficient to define the performance of the system. An alternative approach was instead adopted which involved the modelling of through-circulation drying of a static layer of wood chips under a range of conditions.

The modelling work was carried out by the Silsoe Research Institute (SRI) in Bedfordshire, UK. Work at SRI had been reported by Nellist (see Appendix 1 Section A1.7.1) in which a fully-validated grain drying model, XBATCH, was modified for the drying of wood chips and applied to heated air batch drying of beds of various depths [35]. The work was however limited to relatively low temperature air (25°C of heating above ambient), and was also based on spruce and birch chips, for which detailed drying data were available at the time. Since then data of a similar quality have become available for SRC poplar chips. SRI were therefore asked to carry out a similar modelling exercise, only using poplar data and a modified set of boundary conditions involving the use of air inlet temperatures up to 100°C [81]. The model is equally applicable to band systems provided the residence time

of the wood chips is large compared with that of the air, as is the case here (hours versus seconds). The work was funded by ETSU on behalf of the UK Department of Trade and Industry, and results are presented in Section 4.3.2.3.

4.3.2.2 Acquisition of Cost Data

It was not possible to find a commercial manufacturer willing to supply performance data for drying biomass gasification system feedstocks using low-temperature air and long residence times. A dryer of this type is currently being developed by Wood Processing, a subsidiary of Border Biofuels Ltd, a UK bio-energy project developer. However, this dryer is close to commercialisation and the company were unwilling to release performance (or cost) data.

A number of manufacturers offer relatively short residence time thin-layer band dryers for wood, and these were approached instead with a request for capital cost data against the same set of scenarios used for the rotary dryer (see Section 4.3.1.2). The use of these data is justified on the grounds that capital cost would primarily be a function of band area, with only second order influences for residence time and layer depth.

As for the rotary dryer, the responses were evaluated and a single respondent selected who was able to demonstrate substantial experience of biomass drying, whose equipment costs were typical, and who had supplied the full range of data requested (including in particular band area). This was Wolverine Proctor Schwartz of the UK, who supplied data for a single stage single pass dryer using heated air, as illustrated in Appendix 1 Figure A1.12. The data are given in Table 4.3.

4.3.2.3 XBATCH Modelling Exercise

The XBATCH program simulates one-dimensional through-circulation drying of a bed of material of specified depth. The sub-models within the program include the relationship of air-flow through the bed to pressure drop across the bed (and therefore fan power requirement), heat transfer to and mass transfer from the particles, and equilibrium moisture content. The model calculates the drying process in time steps until the specified moisture content (averaged across the full bed depth) is achieved.

Table 4.3 Data for band dryer (Wolverine, Proctor, Schwartz) [82]

"Standard" poplar chips were specified (Table 2.3) with an initial moisture content of 100% db, along with the following boundary conditions:

- Fan pressure (i.e. pressure across the bed):   500 Pa, 1000 Pa

- Bed depth: 0.5 m, 1.0 m

- Air inlet temperature: 50°C, 75°C, 100°C

- Final mean moisture content: 17.6% db, 42.9% db

Results for the 500 Pa fan pressure cases are given in Tables 4.4 (0.5 m bed depth) and 4.5 (1.0 m bed depth). In each case the total floor area and fan power is given for an installation corresponding to approximately 2.1 MW_e, assuming zero loading and unloading time. The results for a fan pressure of 1000 Pa 1.0 m bed depth gave reduced floor area requirements and drying times, but higher energy consumption and much larger fan power requirements.

In all cases, there is a large variation in final moisture across the bed, with the chips at air inlet dried to equilibrium levels and the chips at outlet often not dried at all. Thorough

mixing of the chips after drying would therefore be required and this would require provision of suitable intermediate handling and storage facilities.

Table 4.4 XBATCH results – 500 Pa fan pressure, 0.5 m bed depth

Air inlet temperature (°C)	50	50	75	75	100	100
Final mean moisture (% db)	17.6	42.9	17.6	42.9	17.6	42.9
Final max. moisture (% db)	44.9	99.6	54.3	102.4	61.6	103.3
Final min. moisture (% db)	5.9	11.2	3.2	7.5	1.9	6.2
Drying time (h)	2.03	1.27	1.22	0.80	0.90	0.60
Air mass flow ($kgs^{-1}m^{-2}$)	0.917	0.917	0.852	0.852	0.793	0.793
Heat input (kWm^{-2})	32.3	32.3	51.4	51.4	67.9	67.9
Evaporation rate ($gs^{-1}m^{-2}$)	8.44	9.40	14.1	14.9	19.1	19.8
Energy consumption (MJ/kg_{ME})	3.82	3.43	3.65	3.46	3.56	3.42
Total floor area (m^2) - 2 MW_e	40.7	36.5	24.3	23.0	18.0	17.3
Total fan power (kW) - 2 MW_e	34.1	30.6	20.4	19.3	15.1	14.5

Table 4.5 XBATCH results – 500 Pa fan pressure, 1.0 m bed depth

Air inlet temperature (°C)	50	50	75	75	100	100
Final moisture content (% db)	17.6	42.9	17.6	42.9	17.6	42.9
Final max. moisture (% db)	98.0	101.6	102.4	102.4	103.3	103.3
Final min. moisture (% db)	3.4	3.7	1.4	1.6	0.7	0.7
Drying time (h)	5.07	3.55	3.17	2.23	2.38	1.68
Air mass flow ($kgs^{-1}m^{-2}$)	0.650	0.650	0.603	0.603	0.563	0.563
Heat input (kWm^{-2})	22.9	22.9	36.4	36.4	48.2	48.2
Evaporation rate ($gs^{-1}m^{-2}$)	6.77	6.71	10.8	10.7	14.4	14.1
Energy consumption (MJ/kg_{ME})	3.38	3.41	3.36	3.42	3.35	3.41
Total floor area (m^2) - 2 MW_e	50.6	51.1	31.7	32.2	23.8	24.3
Total fan power (kW) - 2 MW_e	30.1	30.4	18.8	19.1	14.2	14.4

Energy consumption per unit of moisture evaporated varies between 3.82 and 3.35 MJ/kg$_{ME}$, corresponding to thermal efficiency range of about of about 65-74% which compares well with rotary dryers. Thermal efficiency improves and fan power and floor area requirements reduce as air temperature is increased.

4.3.2.4 Description of Model

In order to minimise drying costs and energy requirements, only the biomass size fraction suitable for gasification is dried (>10 mm mean diameter), so this mode of operation requires a pre-screening stage (Section 7.1).

The model assumes heated air drying at a fixed inlet temperature, where the air has been heated by heat exchange with the IC engine cooling water in a radiator. The radiator is modelled separately (Section 7.3.3); the function of the dryer model is limited to calculating the air flow requirement for a specified drying duty, and the capital cost, labour requirements and utility requirements associated with the dryer itself. The model does not require input from any other module sub-model.

The data for a fan pressure of 500 Pa and a bed depth of 0.5 m (Table 4.4) were used to construct the model. The smaller bed depth was arbitrarily chosen because of the smaller energy consumption and fan size.

Drying Time

The XBATCH program predicts that for a given chip type, bed depth and fan power, the drying time t_d (hours) is a function of the reduction in average moisture content X_{B2}-X_{B4} (% db) and the air temperature T_{A2} (°C). At a given temperature, the results of Table 4.4 show that drying time closely approximates a quadratic function of moisture removal (remembering that (0,0) is a third data point for each temperature):

$$t_d = A(X_{B2} - X_{B4})^2 + B(X_{B2} - X_{B4})$$ (4.13)

where A and B are functions of T_{A2}.

From regression analysis, the following function is obtained:

$$t_d = 1.75T_{A2}^{-2.51}(X_{B2} - X_{B4})^2 + 0.399T_{A2}^{-0.810}(X_{B2} - X_{B4}) \qquad (4.14)$$

Figure 4.5 shows t_d plotted against the RHS of Equation 4.14 for the two modelled drying duties, 100% db to 42.9% db and 100% db to 17.6% db. The relationship is linear with unity gradient.
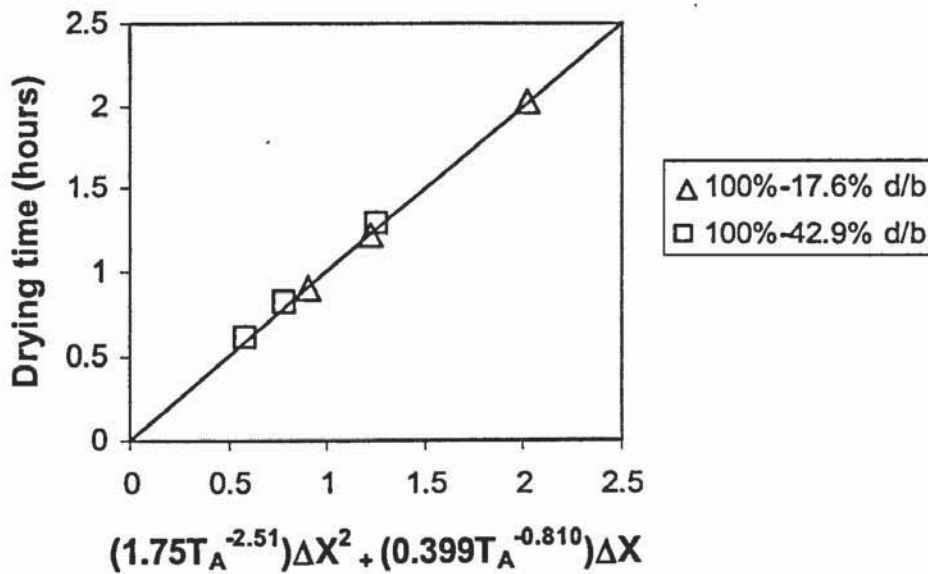
Figure 4.5 Drying time function

When used to predict the drying times calculated by XBATCH, the expression gives an average error of 0.25%. It is however valid only at air temperatures of $\leq 100°C$, for the "standard" biomass, and for the "standard" ambient humidity, these being the conditions under which XBATCH was run.

By specifying the air temperature and desired initial and final mean moisture contents, the drying time may thus be calculated. A fixed air temperature of 50°C was specified for all modelling cases; this is dictated by the operating conditions of the engine coolant radiator (Section 7.3.3). This relatively low temperature would present no risk of thermal degradation of the biomass.

Air Flow Rate, Fan Power, Capital Cost

With the drying time, the biomass throughput and the desired final moisture, the band area may then be calculated. At a constant fan pressure of 500 Pa and a bed depth of 0.5 m, air velocity onto the bed is constant at 0.84 m/s, and fan power per unit floor area is constant at 839 W/m^2. Thus with floor area, total air flow rate and total fan power are simply calculated.

The power requirement to drive the moving band is unknown, but is expected to be very low (band speed is less than 20 cm per minute) and has therefore been ignored.

The data of Table 4.3 have been used to produce an expression for equipment cost EC_3 (£'000 1998) as a function of band area A_3 (m^2):

$$EC_3 = 2.79A_3 + 52.2 \tag{4.15}$$

The data and the function are shown in Figure 4.6.
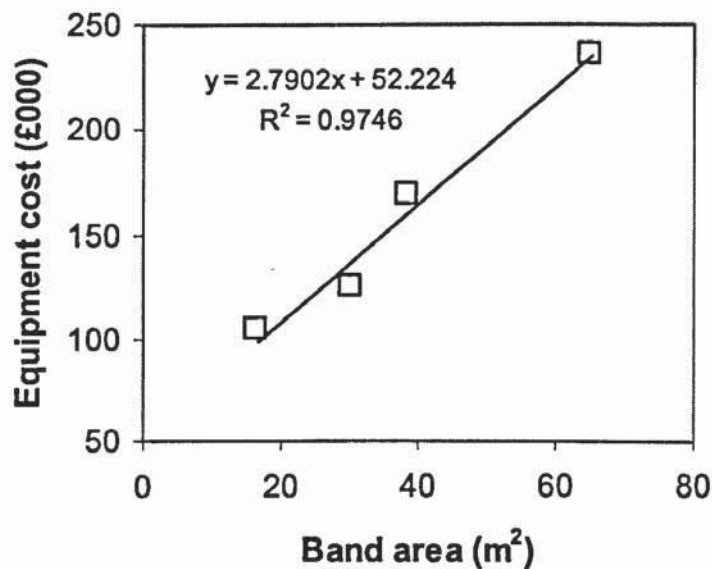
Figure 4.6 Band equipment cost as a function of band area

The element of total plant cost attributable to the dryer module is calculated from equipment cost using the same expression as that used for the rotary dryer (Equation 4.10).

<u>Labour</u>

The labour requirement for a band dryer is assumed to be the same as that for a rotary dryer, at 0.5 persons per shift.

The worksheet for the band dryer is shown in Appendix 2 Section A2.3.

5 GASIFIER

This chapter deals with the gasifier module of the BGES (see Figure 2.1). The module receives dry biomass from the drying module (Chapter 4) and passes product gas to the product gas water heater in CHP systems (Section 7.3), or to the product gas quench in power-only systems (Section 7.4).

5.1 Biomass Gasifier Design

5.1.1 Biomass Gasifier Types

There are two categories of reactor design which are commonly used for the gasification of biomass with air, namely fixed bed and fluid bed. In fixed bed designs, the bed of biomass moves downward under gravity solely as a result of the consumption of solid material in the reactions taking place within the gasifier (hence the alternative term "moving" bed). In fluid bed designs, air is blown through the bed of biomass at sufficient velocity for the bed to become fluidised, resulting in high heat transfer rates and efficient mixing. Different fluid bed types are categorised by the velocity of the fluidising air.

Within these categories there is a wide variety of gasifier types which have been used for the gasification of biomass, and comprehensive reviews of these may be found elsewhere [83,84,85,86,87]. Figure 5.1 shows the configurations of the four main types, and Table 5.1 gives a summary of their characteristics for conventional air-blown operation [7,88].

Other types such as cross-flow or entrained flow gasifiers are rarely used today for the gasification of biomass, although entrained flow reactors have found successful application in the large-scale gasification of coal.

Fixed bed gasifiers are limited in the scale at which they can operate. Updraft gasifiers are normally limited to thermal inputs of below about 30 MW_{th} by the need to achieve a uniform flow of oxidant through the bed [18]. At larger sizes the flow tends to channel (to form high-velocity passages directly through the bed). In the case of downdraft gasifiers the upper limit to scale is much lower, around 3 MW_{th} thermal input, because of the critical nature of the throat dimensions for bed behaviour [18]. A recent development in

downdraft design, the unthroated or "open-core" downdraft gasifier [89,90], offers the possibility of operation at larger scales with a wider particle size range and very low tar levels due to the high uniformity of flow achieved. As yet, however, unthroated downdraft gasifiers have been limited to scales well below 1 MW_{th} [89].
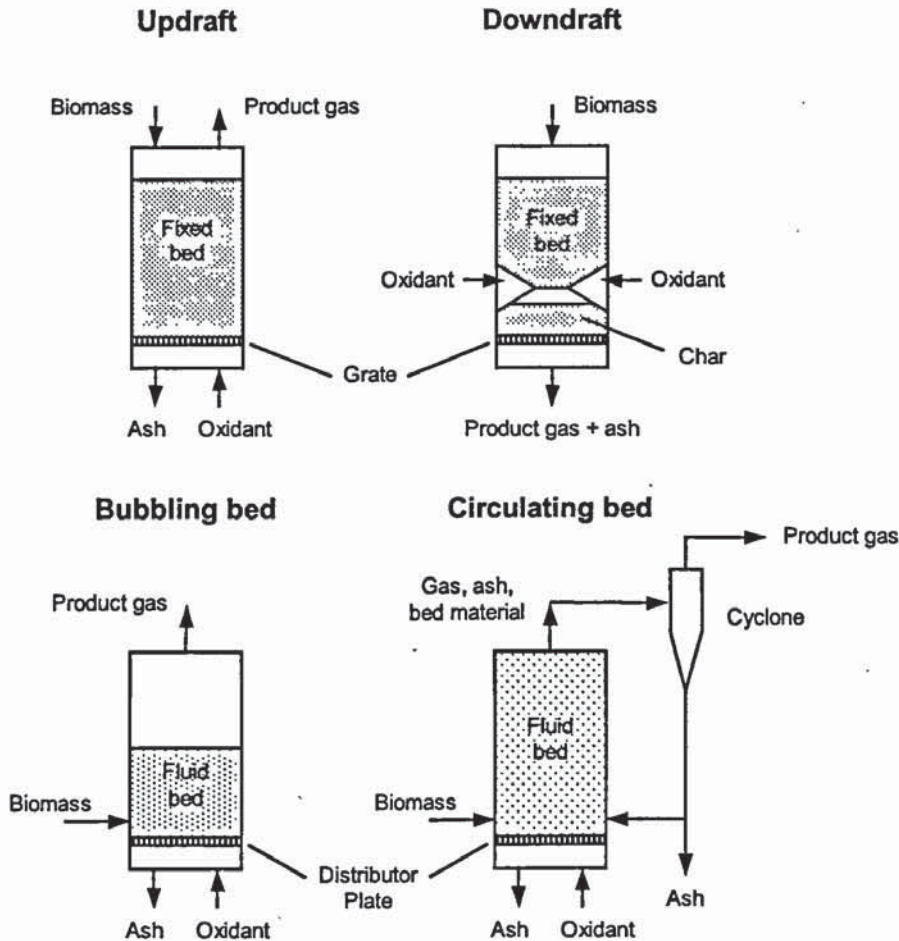
Figure 5.1 Principal biomass gasifier configurations

Fluid bed gasifiers are easy to scale up to very large sizes, the only limiting factor being fuel admission to and subsequent distribution across the bed, which can present difficulties in large diameter vessels. However, due to their increased complexity over fixed bed types, they are usually uneconomic at scales below about 5 MW_{th} thermal input [18].

5.1.2 *Low-tar Gasifier Designs, Biomass Input 0.5-2 dt/h*

Tars (condensable organic vapours) are products of biomass pyrolysis, and may be viewed as an intermediate product in the gasification process. In an ideal gasifier, in which the

gasification reactions proceed fully to equilibrium, these condensable organic vapours would be fully converted to permanent (non-condensable) gases, and the product gas would contain no tars. However, the ideal of equilibrium operation is never reached, and tars are present in the product gas to a level dependent on the design of gasifier and the operating conditions.

Table 5.1 Characteristics of principal biomass gasifier types [18,88,83]

Fixed bed	
Downdraft	Biomass and gas move down (co-current). Biomass particle size 20-80 mm (mean diameter) Biomass moisture content 10-25% db Thermal input <3 MW_{th} (typically 0.5-1 MW_{th})
Updraft	Biomass moves down, gas moves up (counter-current). Biomass particle size 10-200 mm (mean diameter) Biomass moisture content 10-100% db Thermal input 2-30 MW_{th} (typically 5-15 MW_{th})
Fluid Bed	
Bubbling bed	Low velocity gas; bed predominantly inert material; most solid remains in reactor Biomass particle size 3-50 mm (mean diameter) Biomass moisture content 10-100% db Thermal input 5-150 MW_{th} (typically 20-50 MW_{th})
Circulating bed	Medium-velocity gas; bed predominantly inert material; solid is elutriated, separated and returned to reactor. Biomass moisture content 10-40% db Biomass particle size <15 mm (mean diameter) Thermal input 5-250 MW_{th} (typically 20-50 MW_{th})

From Table 5.1, the existing gasifier type most suited to applications in the biomass input range 0.5-2.0 dt/h (thermal input range 2-10 MW_{th}) is the updraft or counter-current.

Unfortunately, this is the type that produces the highest level of tars (condensable organic vapours), with product gas tar levels exceeding 10 g/Nm^3 [21,22]. However, even the product gas tar concentrations from throated downdraft (>500 mg/Nm^3) or fluid bed gasifiers (>1 g/Nm^3) are likely to exceed by a substantial margin the levels demanded by IC engines (<100 mg/Nm^3) [22].

In order to achieve very low levels of tar in the product gas without having to resort to tar removal (which would result in the loss of the fuel energy of the tar as well as a disposal problem), the gasification process must be designed such that two conditions are met. First, there must be sufficient residence time under suitable conditions of temperature and mixing for the gasification reactions to approach equilibrium. Second, all products of pyrolysis must be fully gasified before leaving the system. Of the existing types listed in Table 5.1, the downdraft most closely approaches this ideal, with the gasification zone (the char bed) at the end of the product gas path and higher temperatures and longer residence times than the fluid bed reactor. The updraft is the furthest removed from the ideal, with the gasification zone near the air inlet at the base, and significant pyrolysis taking place downstream of the gasification zone as the product gas passes through the unreacted biomass prior to exit.

One way to approach this ideal is to elevate the temperature of the gasification zone in the gasification reactor, and thus reduce the necessary residence time for reaction completion. This may be achieved through the use of pre-heated air, oxygen-enriched air, or both as the gasifying agent. In downdraft and fluid bed reactor types the product gas is normally at high temperature (>500°C), and this sensible heat may be used to pre-heat the incoming air. The use of oxygen-enriched air incurs a cost penalty associated with providing the oxygen enrichment plant, but results in a product gas of improved heating value (i.e. with less diluting nitrogen) which could be of benefit in improving the performance and reducing the cost of the IC engine (Chapter 6).

Both air pre-heating and oxygen enrichment would result in temperatures exceeding the ash melting point for most biomass feedstocks, at least locally. Ash fusion temperature for biomass feedstocks is in the range 900-1600°C, depending on the feedstock [91]. The gasifier would therefore probably operate in slagging mode (i.e. with the reaction zone at a temperature above that at which the ash contained in the feedstock melts and flows freely

as a "slag"). This adds complexities relating to slag removal, but facilitates the gasification of otherwise difficult high-ash feedstocks with low ash melting points.

Alternatively, one or more secondary reactors may be added downstream of the primary reactor, which accept a tar-laden gas from the primary reactor and further crack the tars to permanent gases [21]. Cracking reactors may be thermal or catalytic. In a thermal cracking reactor a secondary air supply further oxidises the tar-laden gas to give a high temperature environment in which the gasification reactions may proceed towards completion. In a catalytic cracking reactor, the same end is achieved by provision of a catalyst (although the temperature must be sufficient for the catalyst to operate effectively).

If the use of secondary reactors is being considered, there is no necessity to operate at slagging temperatures in the primary gasification reactor. The complexities and hazards of slagging operation can thus be avoided, although any benefits that might accrue from air pre-heat or oxygen enrichment (e.g. improved conversion efficiency, improved heating value gas) would be unavailable.

Two low tar gasifier designs are incorporated in the system model, one a high temperature slagging gasifier and one a non-slagging gasifier incorporating secondary (external) tar cracking. The two designs are described in the following sections. The high-temperature slagging gasifier operates with air pre-heat and oxygen enrichment. The performance of both designs are evaluated and compared as stand-alone units through the use of model calculations (Sections 5.2, 5.3).

5.1.3 The Reverse Flow Slagging Gasifier

Slagging gasification has found widespread application for coals and lignites [92,93,94,95]. Up until now however, experience with the application of slagging gasification to biomass feedstocks has been largely confined to the processing of municipal solid waste and hazardous wastes, both with high ash contents [96,97,98,99,100].

The Reverse Flow Slagging Gasifier (RFSG) [101] is a design intended for the gasification of any biomass, but in particular high ash content low ash melting point energy crop feedstocks such as miscanthus [91]. The target scale for application is 0.5-2.5 MW$_e$, in

either power-only or CHP mode [101]. It is being developed under a European Commission JOULE III project led by the Biomass Technology Group in the Netherlands (JOR3-CT97-0130, "Reverse-Flow Slagging Gasifier"), following successful development of a tar cracker based on a similar principle [102].

The RFSG is illustrated in Figure 5.2. The gasifier consists of a gasification reactor and two regenerative heat exchangers. The gasification reactor is a fixed bed cross-flow concept with biomass feed at the top, slag extraction at the base and gas admission/extraction ports near the base on either side. Packed bed regenerators are positioned on either side of the gasification reactor, through which the gases pass prior to entering and after leaving the gasification reactor.
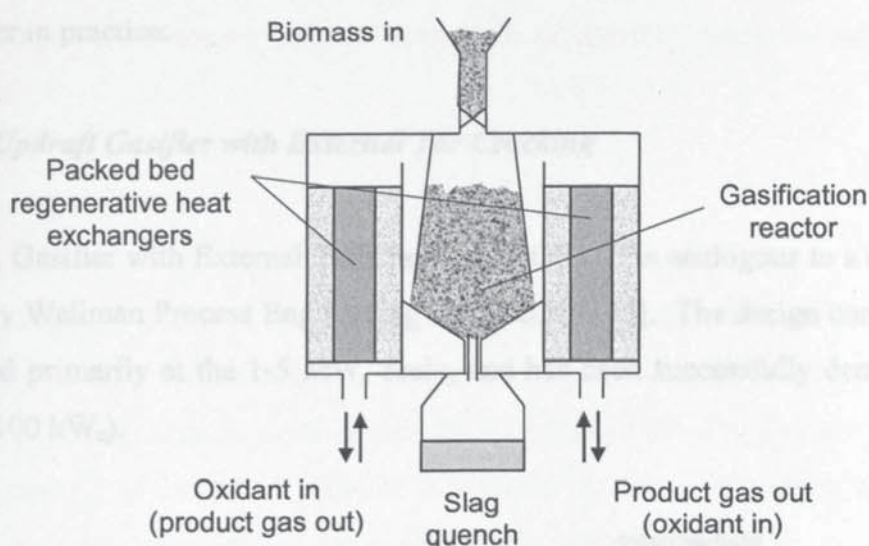
Figure 5.2 Reverse-Flow Slagging Gasifier (RFSG)

The system is symmetrical about its vertical centre-line so that the gas flow through the system can be reversed periodically, enabling regenerative pre-heating of the air. The design envisages oxygen enrichment of the air in order to further increase gasification reactor temperature and improve product gas heating value. However, the designers have specified a maximum oxygen concentration of 60% by volume, in order to minimise the size of air separation plant required and also the potential hazards associated with the use of high oxygen concentrations.

The valving necessary to effect the flow reversal is located beyond the cold end of the regenerators, so that the regenerator/gasification reactor assembly is a self-contained unit with minimal moving parts. The mass flow of product gas from a gasifier is substantially higher than that of the air into it, particularly if oxygen enrichment is used (as there is less inert nitrogen), so the regenerators operate in a high degree of *imbalance* - that is, the product of mass flow and specific heat capacity of the gas being heated is very different from that of the gas being cooled (see Section 5.2.2.1).

Slagging operation will require a relatively dry feedstock in order to help maintain sufficiently high temperatures in the reaction zone. Moisture evaporation consumes heat and therefore reduces bed temperatures. An upper limit for biomass moisture content to the gasifier of 50% db has been arbitrarily assumed in this study, although the upper limit may be lower in practice.

5.1.4 The Updraft Gasifier with External Tar Cracking

The Updraft Gasifier with External Tar Cracking (UGETC) is analogous to a design being developed by Wellman Process Engineering in the U.K [103]. The design concept (Figure 5.3) is aimed primarily at the 1-5 MW_e scale, and has been successfully demonstrated at pilot scale (100 kW_e).
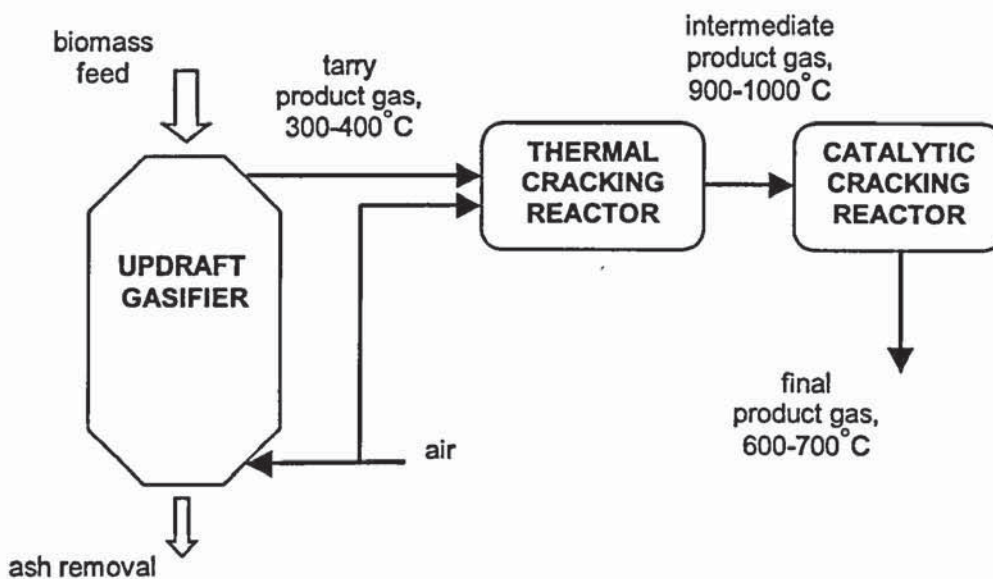
Figure 5.3 Updraft Gasifier with External Tar Cracking (UGETC)

The tar-laden product gas from an updraft gasification reactor is taken to a secondary reactor, the thermal cracking reactor, where it is further oxidised with air at about 900-1000°C. The tar content of the product gas is greatly reduced in the thermal cracking reactor, but some stable phenols remain. To remove these the gas is passed finally through a catalytic cracker to emerge with very low tar levels ($\sim$ 100 mg/Nm^3) at around 600-700° C. The amount of air going to the thermal cracking reactor may be controlled to give the required system temperatures.

Updraft gasification reactors are generally very tolerant of high-moisture feedstocks because of their counter-current operation, in which the upper bed of material is pre-dried by the product gas before reaching the gasification zone. The upper limit of 100% db given in Table 5.1 for biomass moisture content to the UGETC has been assumed in this study.

5.2 Gasifier Model

Both the RFSG and UGETC designs are novel concepts, and little or no satisfactory experimental data exist for the empirical prediction of performance. In order to be able to investigate the performance of these concepts and represent them in a system model, it is therefore necessary to construct a theoretical model of the gasifiers which is able to simulate the main processes influencing overall performance.

For both gasifier types the gasification process must be modelled (Section 5.2.1), and in the case of the RFSG it is also necessary to model the regenerative heat exchangers (Section 5.2.2).

5.2.1 Gasification Reactor Model

5.2.1.1 Model Types

Gasification reactors have been modelled using a wide variety of approaches These modelling approaches may be classified as follows [104]:

99

1. *Equilibrium* models, in which the exit gas composition is calculated from either a pre-specified reaction temperature or a pre-specified equivalence ratio (ratio of actual oxidant to that required for complete combustion), and either heterogeneous or homogeneous reaction equilibrium [105,106].

2. *Kinetics free* models in which the gasification reactor is subdivided into different zones. The gas composition in the gasification zone is calculated from equilibrium data whereas the reaction temperature is calculated in each zone by a separate heat balance. This allows for representation of the drying and pyrolysis zones in an updraft gasifier, for example [107].

3. *Steady state* models in which the gasification reactor is divided into a number of segments, and mass and energy balance equations are solved for each assuming homogeneous conditions within the segment, and with the time derivative neglected [108,109].

4. *Semi-transient* models in which transients are calculated using a pseudo-steady-state assumption on the basis of the results of steady state models [110]

5. *Transient* models, in which the gasification reactor is again divided into a number of segments, with the time-dependent mass and energy balance equations fully solved in each [111,112].

Equilibrium and kinetics free models produce easily-solved algebraic equations, and allow prediction of exit gas composition and temperature. They tend to have short run-times, and relatively low data requirements. The accuracy or suitability of an equilibrium model depends very much on the type of gasifier - in particular whether the temperatures in the gasification zone are high enough for long enough to approach equilibrium conditions, and whether the product gas exits the gasification reactor at that point. If the latter condition is not met (as, for example, in an updraft gasifier) a kinetics-free model may be used to represent the pyrolysis and drying stages, but sub-models of those processes will be required.

Steady state models allow profiles to be computed along the gasification reactor axis. The models include rate equations for the heterogeneous and sometimes the homogeneous reactions. In the case of fixed bed gasifiers, these models result in a set of ordinary differential and algebraic equations. In the case of fluid bed gasifiers, the fluid dynamics must be accounted for, and this may be accomplished with varying degrees of sophistication from well-mixed reactor assumptions to full computational solution of the two-phase flow field. Both run times and data requirements are considerably greater than for equilibrium and kinetics-free models.

Semi-transient and transient models introduce a further level of complexity still, the latter introducing partial differential equations.

Steady state, semi-transient and transient models rely increasingly on the availability of good data for accuracy, and often incorporate adjustable parameters for matching predictions to experimental measurement. They represent a far more difficult modelling challenge that equilibrium, kinetics free or steady state models, with substantially greater model construction effort, computational power and computational time required. They do however offer the possibility of greater accuracy and process resolution.

5.2.1.2 Selection of Model Type

It is intended in both the RFSG and UGETC designs that the temperature and residence time characteristics of the gasification system will allow the gasification reactions to approach equilibrium conditions, and that all products of pyrolysis will proceed to be fully gasified before leaving the system (Section 5.1.2). In the case of the UGETC the system includes the two secondary tar cracking reactors.

For the present study, in the absence of experimental data for validation of a more sophisticated approach, a thermodynamic equilibrium model has been chosen. Despite their simplicity, such models have found to be of great value in gasifier design [105]. The model may be applied equally to the RFSG and UGETC concepts by choosing the gasification reactor boundaries appropriately.

In the case of the RFSG the gasification reactor boundary encloses just the reactor vessel itself, i.e. the region between the two regenerative heat exchangers (Figure 5.2). In the case of the UGETC, the gasification reactor boundary encloses the updraft gasification reactor *and* the external thermal and catalytic reactors (Figure 5.3). The use of equilibrium chemistry to model a gasification concept similar to the UGETC where the system comprises physically separated pyrolysis, partial oxidation and char gasification reactors has yielded very good results [113].

5.2.1.3 Description of Model

The equilibrium model used here is a spreadsheet-based model initially developed by Double [114] based on the method of Baron, Porter and Hammond [115], and adapted to include heat losses from the reactor due to radiation/convection and ash removal, improved pre- and post-processing and improved numerical procedures. It has been demonstrated that for a carbon-hydrogen-oxygen system at equilibrium, the only species present in the gas phase in appreciable amounts ($>10^{-4}$ mole %) are H_2, CO, CO_2, CH_4 and H_2O [116]. Where air is involved, the inert nitrogen may be added as a sixth species.

As equivalence ratio is reduced from unity (stoichiometrically correct combustion), a point is reached at which the products cease to be a homogeneous gas mixture because solid carbon has just appeared. This point is known as the "carbon boundary". As equivalence ratio is further reduced, the amount of excess carbon increases. The carbon boundary is an important point, as fixed bed gasifiers will naturally seek to operate at this point to maintain a steady state (see Section 5.3.1).

In order to calculate the equilibrium concentrations of the products, it is only necessary to consider sufficient reactions to include all the species. The following three reactions are considered below the carbon boundary where excess carbon is present:

$C + H_2O$	=	$CO + H_2$	ΔH 131.4 kJ/mol
$CO + H_2O$	=	$CO_2 + H_2$	ΔH -41.2 kJ/mol
$C + 2H_2$	=	CH_4	ΔH -74.9 kJ/mol
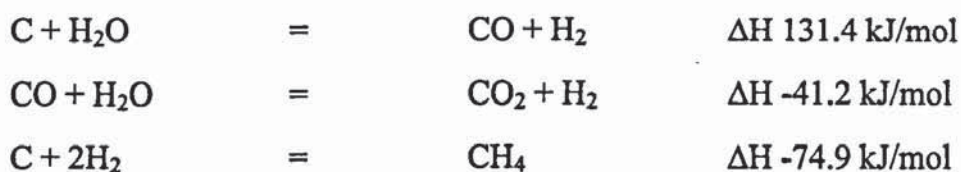
At or above the carbon boundary where no excess carbon is present, only two reactions need to be considered:

$$CO + H_2O \quad = \quad CO_2 + H_2 \qquad \Delta H \text{ -41.2 kJ/mol}$$
$$2H_2 + 2CO \quad = \quad CH_4 + CO_2 \qquad \Delta H \text{ -243.1 kJ/mol}$$
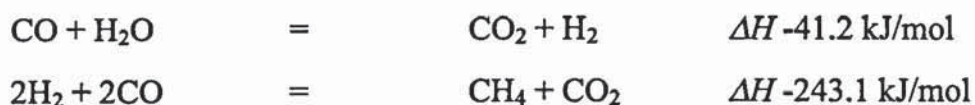
Dry biomass higher heating value can either be entered if known, or calculated from a published correlation. Higher heating value is used in this case, as the latent heat of vaporisation is included in the function used to compute water vapour enthalpy in the product gas. A correlation developed by the Institute of Gas Technology is used here; this has been found to give better agreement for biomass compared with other published correlations [117]:

$$HHV = 34.09[C] + 132.3[H] + 0.069 - 1.53[ash] - 11.99[O + N] \qquad (5.1)$$

where *HHV* is in MJ/kg, and concentrations are mass fractions.

Three modes of operation are possible. In the first two, either equivalence ratio or equilibrium reaction temperature is specified, and an iterative method is employed to perform an energy balance, using thermochemical data in the form of polynomial functions of temperature derived from the Janaf Thermochemical Tables [118]. In the third mode of operation, the carbon boundary is specified and the model calculates the equivalence ratio and equilibrium reaction temperature at the carbon boundary by performing a simultaneous mass and energy balance, again using an iterative method.

In each case, for specified biomass and gasifying agent compositions and temperatures, the model calculates product gas composition, heating value and flow rate, and either equilibrium reaction temperature or equivalence ratio (first two modes) or both (third mode). Gasification reactor heat loss is incorporated as a percentage of enthalpy in, and heat loss with the ash is also calculated. The model has been validated both for composition and reaction temperature against calculations published by Desrosiers [116] for the equilibrium gasification of biomass with composition $CH_{1.4}O_{0.6}$.

Not all the reactions in a gasifier proceed at the same rate, and it is unlikely that the relatively slow heterogeneous reactions will achieve full equilibrium. To describe the degree to which equilibrium is attained, an "equilibrium approach" ΔT_{EA} (°C) may be defined [104]:

$$\Delta T_{EA} = T_{AR} - T_{ER} \qquad (5.2)$$

where T_{AR} is equal to the actual reaction temperature, and T_{ER} is equal to the equilibrium reaction temperature calculated from the reactant streams. A value for ΔT_{EA} of 30-60°C has been suggested for a well-designed fixed bed gasifier [104]; 50°C has been arbitrarily assumed here. In other words, for given biomass and air compositions and temperatures, equivalence ratio and gasification reactor heat loss, the product gas composition calculated by the model is taken to be correct, but the calculated (or specified) equilibrium reaction temperature is taken to be 50°C below the actual reaction temperature.

The meaning of "reaction temperature" and its relationship to product gas exit temperature (T_{G11}) must be understood if this model is to be used to predict the latter. The equilibrium model assumes a conceptual isothermal adiabatic reactor with homogeneous conditions throughout, in which there is a single "reaction temperature". In a real reactor, the reaction temperature can be interpreted as the temperature of the reaction at the point of completion of the gasification reactions [119]. In the absence of excess carbon (i.e. at or above the carbon boundary), this may be taken to be the gas temperature (see also Figure 5.5). If the gasification reactor is designed such that the product gases leave at this point without exchanging heat with the incoming biomass, then their temperature will be equal to the reaction temperature, or

$$T_{G11} = T_{ER} + \Delta T_{EA} \qquad (5.3)$$

This has been assumed for both configurations considered here. In the case of the RFSG, it is assumed that the gasification reactor width will be sized such that there is just room for the gasification zone between the combustion zone and the product gas exit. In the case of the UGETC, it is assumed that the thermal and catalytic cracker temperatures and

residence times have been set to allow the reactions to reach the defined equilibrium approach.

It should be noted that the reaction temperature is *not* either equal to or clearly related to the peak gasification reactor temperature. The latter cannot be calculated without consideration of chemical kinetics and mass transport.

5.2.2 Regenerator Model

5.2.2.1 Selection of Model Type

The RFSG employs regenerative heat exchange between the hot product gases and the cold incoming air, using packed bed heat exchangers. Because the gasification process is continuous, two packed bed heat exchangers are required, each alternately heating cold air ("cold" period) and cooling hot product gas ("hot" period) over a fixed reversal period (see Figure 5.4 and Section 5.1.3). However, steady state operation requires that the amount of heat supplied to the air in each period must equal the amount extracted from the product gas, and this in turn requires the two heat exchangers to have identical thermal capacities - effectively, to be identical. The thermal performance of the two packed bed heat exchangers will therefore be identical over a full heating and cooling cycle, and only one need be modelled.

T_{G15} ⟹ **HOT PERIOD REGENERATOR** ⟹ T_{G13}

T_{G14} ⟸ **COLD PERIOD REGENERATOR** ⟸ T_{G12}
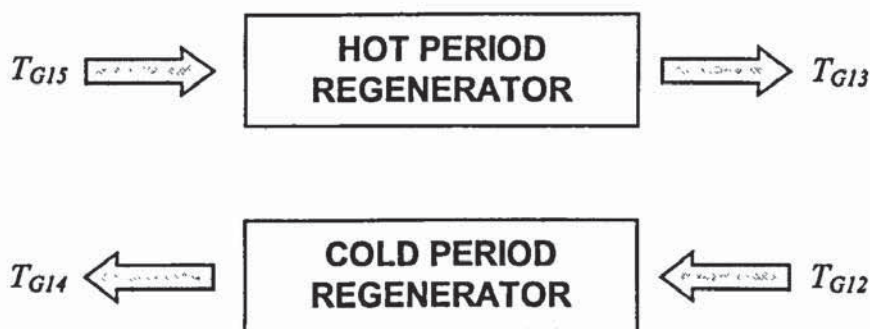
Figure 5.4 Regenerator gas temperatures

The model must be able to calculate the time-varying temperature of both the air and the product gas at regenerator outlet for given regenerator packing characteristics and flow reversal period. A time-dependent rather than time-averaged model is important because

105

of the large temperature excursions that may occur over the reversal period as a result of the heat exchange process. These may affect not only gasifier performance but also that of any downstream equipment for further recovery of heat from the product gas. Therefore a finite-difference iterative model was chosen which calculates steady state temperature conditions for fixed hot and cold period mass flow rates at a selected number of points along the regenerator for a selected number of time intervals throughout each period.

5.2.2.2 Description of Model

After a consideration of possible modelling approaches, a one-dimensional spreadsheet model was developed based on the method of Willmott [25,120]. This method is well suited to the present purpose, and is particularly well documented in the literature. The method involves a numerical solution of the basic equations for heat transfer from gas to solid and solid to gas:

$$UA(T_P - T_G) = m_G c_G Z\left(\frac{\partial T_G}{\partial x} + \frac{1}{v}\frac{\partial T_G}{\partial t}\right) \qquad (5.4)$$

$$UA(T_G - T_P) = M_P c_P \frac{\partial T_P}{\partial t} \qquad (5.5)$$

at a specified number of equi-spaced positions along the regenerator and at a specified number of equal time intervals throughout each period, using an iterative finite difference scheme. In Equations 5.4 and 5.5 subscripts P and G denote packing and gas respectively. The regenerator is non-dimensionalised and the calculation is performed using a "reduced" length (Λ) and period (Π) as suggested by Hausen [121], where:

$$\Lambda = \frac{UA}{m_G c_G} \qquad (5.6)$$

$$\Pi = \frac{UA t_c}{M_P c_P} \qquad (5.7)$$

and t_c is the cycle period. This facilitates the computation.

Ten spatial and time increments were chosen. A larger number was considered unnecessary for the purposes of the study and would add to model size. Fifty iterations were found to give convergence in all cases. The model includes a calculation of the bulk heat transfer coefficient for the case of spherical packing material as a function of sphere diameter [122], and a correction for the ignoring of material temperature variations perpendicular to the flow direction [120].

Willmott's method assumes constant gas mass flow rates and gas inlet temperatures for both hot and cold periods. The IC engine demands constant dry product gas mass flow (see Section 6.1.1.2), and assuming a constant gasifier equivalence ratio over the reversal cycle, gasifier air mass flow will also be constant. The air at inlet to the cold period regenerator is at ambient temperature T_{G12} (Figure 5.4). However, the product gas temperature at inlet to the hot period regenerator (T_{G15}) does not remain constant, but is rather a function of the air temperature at regenerator outlet at the corresponding point during the cold period (T_{G14}) - that is to say, gasification reactor outlet temperature is a function of gasification reactor inlet temperature. This can have an important effect on regenerator performance, and Willmott's algorithm must be modified accordingly.

It would be possible to re-run the gasification reactor model at each time step for each iteration in the regenerator model in order to update the regenerator inlet temperature. Computationally this would be inefficient. However, it is also unnecessary, as application of the gasification reactor model shows the relationship between reactor inlet and outlet temperature over the range of temperatures of interest is approximately linear, and can be established for each case with two additional runs of the gasification reactor model. The following linear relationship is therefore incorporated into the regenerator model:

$$T_{G15} = C_1 T_{G14} + C_2 \qquad (5.8)$$

with the only requirement being the specification of the two constants C_1 and C_2. There is assumed to be no change in air temperature between regenerator outlet and gasification reactor inlet, and likewise in product gas temperature between gasification reactor outlet and regenerator inlet.

5.2.3 Validation

As part of the European Commission JOULE project JOR3-CT97-0130, a pilot RFSG was constructed and operated by the Biomass Technology Group in the Netherlands, at a feed rate of 10 kg/h dry biomass. Numerous experimental difficulties hampered the acquisition of suitable data for validation. However, it was possible shortly before the end of the project to obtain a single set of data averaged over a series of runs which have been used for a limited validation [123].

Because of difficulties experienced in achieving high temperatures within the gasification reactor, the pilot plant incorporated secondary air addition into the zone(s) between the gasification reactor exit and the packed bed inlet, thereby promoting further oxidation and increased temperatures. This resulted in operation at an equivalence ratio well above the carbon boundary (Section 5.2.1.3).

Also, in order to achieve balanced regenerators (equal product of gas mass flow and gas specific heat capacity in each - see Section 5.1.3), a substantial proportion of the product gas was bled from the slag tap so as to bypass the hot period regenerator. The temperature and composition of this gas at the point of extraction was not recorded; the temperature is therefore assumed to be close to the estimated temperature at the centre of the gasification reactor (1200°C), and the composition is assumed to be similar to the product gas entering the packed bed. The product gas temperature in the gasification reactor model is taken to be the mass-weighted mean of the two streams. The streams are reunited downstream of the packed bed, prior to gas analysis.

The biomass utilised in the tests was beech wood. Biomass composition was supplied, but heating value had to be obtained from other sources [124].

Table 5.2 gives data and results for the gasification reactor model; Table 5.3 does the same for the regenerator model. The correct product gas temperature in the gasification reactor model was obtained by varying the gasification reactor heat loss (radiation and convection), data for which were not supplied.

A gasification reactor heat loss of 17.9% of enthalpy in was necessary to achieve the specified product gas temperature. Insufficient data were available to test the accuracy of this result. However, heat loss from downdraft gasifiers has been measured at around 10% for an uninsulated design [125] and estimated at 5% for an insulated design [106]; in both cases the biomass feed rate was about 80 kg/hr. In view of the much smaller scale of the pilot RFSG (10 kg/hr) the figure of 17.9% seems not unreasonable.

Table 5.2 RFSG pilot plant data [123] and model results - gasification reactor

Parameter	Model Inputs	Model Results	Plant Data
Biomass flow rate to gasifier (kg/hr dry basis)	9.0		
Biomass composition: C (%wt d.a.f.)	51.9		
Biomass composition: H (%wt d.a.f.)	6.3		
Biomass composition: O (%wt d.a.f.)	41.8		
Biomass composition: ash (%wt dry basis)	2.0		
Biomass composition: moisture (%wt wet basis)	17.0		
Air flow rate to gasifier (Nm^3/hr dry basis)	20.0		
Air temperature to gasification reactor (°C)	900.0		
Air composition: O_2 (%vol)	21.8		
Air composition: N_2 (%vol)	78.2		
Product gas flow rate from gasifier (Nm^3/hr dry basis)		28.8	29.0
Product gas temperature from gasification reactor (°C)	900.0		
Product gas composition: H_2 (%vol dry basis)		16.0	13.4
Product gas composition: CO (%vol dry basis)		16.7	17.7
Product gas composition: CO_2 (%vol dry basis)		13.0	11.3
Product gas composition: CH_4 (%vol dry basis)		0.0	0.8
Product gas composition: N_2 (%vol dry basis)		54.3	56.9
Product gas lower heating value (MJ/Nm^3 dry basis)		3.84	3.97
Gasification reactor heat loss (% of enthalpy in)		17.9	

The gasification reactor model predicts product gas flow rate and LHV with good accuracy. Product gas composition is also well predicted, with a small under-prediction of

CH_4 and a small over-prediction of H_2, due probably to the non-equilibrium state of the product gas extracted through the slag tap.

The regenerator model results of Table 5.3 shows very close agreement on inlet and exit temperatures.

Table 5.3 RFSG pilot plant data [123] and model results - regenerator

Parameter	Model Inputs	Model Results	Plant Data
Regenerator length (m)	0.6		
Regenerator diameter (m)	0.18		
Packing sphere diameter (mm)	4.8		
Packing sphere density (kg/m^3)	2160		
Packing sphere mean specific heat (J/kgK)	1160		
Packing sphere mean thermal conductivity (W/mK)	11.1		
Flow reversal interval (min)	10.0		
Air flow rate to regenerator (Nm^3/hr)	16.0		
Air temperature at regenerator inlet (°C)	18.0		
Air mean temperature at regenerator outlet (°C)		903.2	900.0
Product gas flow rate to regenerator (Nm^3/hr)	16.0		
Product gas mean temperature at regenerator inlet (°C)		901.8	900.0
Product gas mean temperature at regenerator outlet (°C)		112.8	115.0

This is a very limited validation because of the lack of data: nevertheless, it gives confidence in the general applicability of the models and in the assumptions made.

5.3 Use of the Model to Evaluate Gasifier Performance

In this evaluation the gasification reactor and regenerator models were used to examine the sensitivity of gasifier performance to the principal variables under the control of the operator for a given feedstock, i.e. biomass moisture content (which can be adjusted by drying), and in the case of the RFSG air oxygen concentration. Also examined was the

contribution to the performance of the RFSG of air pre-heat at a given air oxygen concentration.

This work focuses on the gasification systems in isolation, with no other components of the BGES modelled.

5.3.1 Fixed Boundary Conditions

As discussed in Section 5.2.3, it has been assumed that for both the RFSG and UGETC configurations there is sufficient residence time to achieve an equilibrium "approach" of 50°C, and also that no transfer of sensible heat from the product gas to the incoming feed occurs after the completion of the gasification reactions - that is to say the gasification reactor operates with the product gas exiting immediately after the final gasification zone, as in a downdraft gasifier.

The RFSG must be operating at the carbon boundary equivalence ratio if steady state conditions exist with no accumulation or elutriation of carbon and a constant level of feed in the bed [126], and provided no secondary air supply is added downstream of the bed. This self-regulation is a key feature of all continuously fed fixed bed gasifiers, and arises because gravity feeding ensures that the feed is supplied to the reaction zone at the maximum rate at which it can be consumed – i.e. the minimum equivalence ratio such that all the feed is consumed [126]. This is the carbon boundary. The consumption rate may only be adjusted by varying the rate of supply of oxidant. The provision of secondary air which was necessary in the RFSG pilot plant (Section 5.2.4) is assumed to be unnecessary for a full scale unit.

With the UGETC, the equivalence ratio of the *overall* gasification system (including the secondary reactors) is not constrained to the carbon boundary value. The equivalence ratio of the updraft gasifier itself remains fixed at its own carbon boundary value for the same reasons as those given for the RFSG; however this is the carbon boundary relating only to the material passing into the gasification zone in the lower section of the gasification reactor, i.e. excluding the volatile material and moisture removed from the biomass above the gasification zone by the passage of the hot product gas. Secondary air may however be

111

added to the thermal cracking reactor at a rate independent of the biomass feed rate, to achieve the desired operating temperatures in the cracking reactors.

The UGETC could, therefore, be modelled with the reaction temperature set to the exit temperature of the catalytic cracker, given as 600-700°C, less the equilibrium approach. However, as will be seen (Table 5.6), this range corresponds closely to the carbon boundary reaction temperature for the overall gasifier, and the UGETC is therefore modelled at the overall carbon boundary as with the RFSG.

For the purposes of the evaluation, a gasifier biomass input of 1.5 dt/h is arbitrarily assumed (ash free basis), equivalent to a thermal input of about 7.6 MW_{th} (LHV basis) or an electrical output of close to 2.0 MW_e at 25% overall electrical efficiency. The feed is the "standard" biomass, chipped whole-tree short rotation coppice poplar as defined in Table 2.3 [33]. Both gasifiers are assumed to have a minimum acceptable biomass size requirement of 10 mm mean diameter, so that all chips below this size (15% of the total) have been removed by either pre-dryer or post-dryer screening.

Feed moisture content to the gasifier is varied between 5% db and 50% db, achieved through drying using waste process heat from an initial value of 100% db. In the case of the RFSG, the upper value of 50% is justified by the need to maintain very high temperatures in the reaction zone. As the purpose here is to compare the two gasifiers, the same upper value is used for the UGETC; however, the UGETC would be able to accept feed moisture contents of up to 100% db (see Section 5.1.1). In the system modelling study (Chapters 8 and 9) higher feed moisture contents to the UGETC are considered.

In the case of the RFSG, the oxygen content of the enriched air is varied between 21% by volume (normal air) and 100% by volume, although the RFSG is designed specifically for a maximum air oxygen concentration of 60% for cost and safety reasons.

For the RFSG under steady state operation, the mean temperature of the pre-heated air emerging from the cold period regenerator (T_{GI4}) is fundamentally constrained to be less than that of the product gas entering the hot period regenerator (T_{GI5}). However, the purpose of the regenerators in this concept is to achieve as much pre-heating as possible. It

was found through application of the regenerator model that, as a result of the fluctuating nature of the process and the need to keep the regenerator masses within sensible limits, a reasonable mean value of $(T_{G15}-T_{G14})$ is about 70K. This value was specified as a target for the regenerator model in those cases with regenerative air pre-heat, to be achieved if possible within the following constraints:

Regenerator packing mass (M_P)	≤ 10 tonnes
Cycle time (t_r)	≥ 20 minutes
Product gas outlet temperature fluctuation (ΔT_{G16})	≤ 100 K

The upper limit of packing mass is stipulated to avoid the long thermal stabilisation times at start-up which would be associated with very large packing masses. The lower limit of cycle time is stipulated so that the frequency of the short-duration perturbations in gas quality associated with flow reversal do not become too great. The temperature fluctuation limit is stipulated to keep variations in water temperature from the product gas water heater to a minimum.

For both configurations the gasifier is assumed to operate at atmospheric pressure, with heat loss from walls due to radiation and convection equal to 5% of total enthalpy entering the gasification reactor [106]. This value is based on measurements from smaller gasifiers and could probably be reduced for a larger, well-designed gasifier. However, a small overestimation in gasification reactor heat loss provides compensation for the distortion to the energy balance caused by the addition of 50°C to product gas temperature, to allow for non-equilibrium conditions (Section 5.2.1.3).

5.3.2 Modelling Cases

A total of 32 gasification reactor model cases were run for the RFSG, 16 with air pre-heat and 16 without air pre-heat, and four for the UGETC, as defined by the gasification reactor model input parameters given in Table 5.4. Biomass properties are given in Table 2.3.

The variable parameters are shown in Table 5.4 in bold type; all other input parameters remained constant throughout.

The RFSG cases with no air pre-heat were run simply to measure the benefits of air pre-heat, which is an integral part of the RFSG design.

Because of the modelling assumptions, the four RFSG cases with no air pre-heat and no oxygen enrichment are identical to the UGETC cases.

Table 5.4 Principal input parameters, gasification reactor model

Gasifier type	RFSG	UGETC
Product gas temperature T_{G11} (°C)	carbon boundary value	
Biomass dry flow rate m_B (kgs^{-1})	0.417	
Air O$_2$ concentration $[O_2]_{G11}$ (%)	21, 40, 60, 100	21
Air temperature T_{A9} (°C)	$(T_{G15}$-70), 15	15
Biomass moisture content X_{B9} (% db)	5.3, 17.6, 33.3, 50.0	

The regenerator model was run for all RFSG cases with air pre-heat. The regenerators were assumed to be packed beds of fireclay spheres with a constant bed porosity of 0.38. Properties for fireclay were taken from Perry [127].

The sphere diameter may be varied in the model to achieve different bulk heat transfer coefficients (Section 5.2.2.2). Here, sphere diameter was adjusted to give a final product gas temperature fluctuation of 100K (see Section 5.3.1). To achieve a smaller product gas temperature fluctuation would require larger sphere diameters, resulting in greater total packing mass requirement [128].

The regenerator towers were assumed to be cylinders of length equal to four diameters - typical of other similar applications [98]. Finally the minimum flow reversal period of 20

minutes was specified for all cases, as the shorter the reversal period, the smaller the final product gas temperature fluctuation (see Section 5.3.1).

5.3.3 Results: Gasification Reactor Model

Results for the 16 gasification reactor model cases corresponding to the RFSG with air pre-heat are given in Table 5.5, and for the four cases corresponding to the UGETC in Table 5.6. Included are the air inlet and product gas outlet temperatures, the product gas flow rate and lower (or net) heating value (LHV), and the cold gas efficiency (product gas chemical energy output expressed as a percentage of biomass thermal input). Product gas flow rate and LHV are expressed on a dry basis.

Table 5.5 Principal gasification reactor model results: RFSG

Case No.	R1	R2	R3	R4	R5	R6	R7	R8
Feed moisture (% db)	5.3	5.3	5.3	5.3	17.6	17.6	17.6	17.6
Air oxygen conc. (% vol)	21	40	60	100	21	40	60	100
Air temp. in (°C)	668	682	688	693	633	645	650	655
Product gas temp. out (°C)	738	752	758	763	703	715	720	725
Product gas flow (Nm^3/s)	1.09	0.82	0.72	0.64	1.12	0.84	0.74	0.66
Product gas LHV (MJ/Nm^3)	6.12	8.17	9.32	10.5	5.82	7.76	8.83	9.92
Cold gas efficiency (%)	86.1	86.2	86.2	86.2	83.9	84.0	84.0	84.1
Case No.	R9	R10	R11	R12	R13	R14	R15	R16
Feed moisture (% db)	33.3	33.3	33.3	33.3	50	50	50	50
Air oxygen conc. (% vol)	21	40	60	100	21	40	60	100
Air temp. in (°C)	595	606	610	614	556	565	569	572
Product gas temp. out (°C)	665	676	680	684	626	635	639	642
Product gas flow (Nm^3/s)	1.14	0.86	0.75	0.67	1.13	0.85	0.75	0.66
Product gas LHV (MJ/Nm^3)	5.55	7.39	8.40	9.44	5.42	7.21	8.21	9.22
Cold gas efficiency (%)	81.3	81.4	81.4	81.4	78.7	78.8	78.8	78.8

5.3.3.1 Gasification Temperature

A fundamental result for the RFSG design is that regardless of feed moisture content, air oxygen concentration or regenerative air pre-heat, the product gas temperature at gasification reactor exit remains within the range 600-750°C (Table 5.5). Very little reliable data on gasification reactor temperatures has been obtained from the RFSG pilot plant, but the data available suggest that exit temperatures are indeed in this range or a little above, while peak temperatures near the air inlet can reach 1500°C [123].

Table 5.6 Principal gasification reactor model results: UGETC

Case No.	U1	U2	U3	U4
Feed moisture (% db)	5.3	17.6	33.3	50
Air temp. in (°C)	15.0	15.0	15.0	15.0
Product gas temp. out (°C)	713	682	647	609
Product gas flow (Nm^3/s)	1.16	1.18	1.19	1.17
Product gas LHV (MJ/Nm^3)	5.34	5.12	4.94	4.89
Cold gas efficiency (%)	79.5	77.6	75.5	73.5

The temperature distribution within the gasification reactor cannot be predicted with the model employed here; however, it is probable that with such a product gas exit temperature range, a substantial part of the gasification zone of the RFSG will be at temperatures below 1000°C, and the zone near the exit will be below 800°C.

Biomass ash fusion temperatures vary according to biomass type. At one end of the scale, ash fusion temperatures for barley straw have been measured at 750°C for initial deformation and 1050°C for fluid flow (oxidising atmosphere) [91]. At the other, ash fusion temperatures for spruce bark have been measured at 1565°C for initial deformation and 1650°C for fluid flow (reducing atmosphere) [91]. For a typical wood chip, the corresponding temperatures are around 1220°C and 1280°C (either atmosphere) [91]. Hence the RFSG will face considerable design difficulties if it is to operate as a slagging gasifier, as only part of the cross-section of the gasification reactor will achieve slagging

temperatures for most biomass feedstocks. As a consequence, ash will melt and re-freeze at locations along the gas path, eventually blocking the gasifier. Up to now, slagging gasifiers operating with biomass feedstocks (mostly MSW or other wastes) have all been updraft in design [98,100,129]; this is because an updraft gasifier approximates plug flow with the point of air entry (the hottest region) coincident with the point of ash/slag removal.

In addition to anticipated problems with slagging operation, it is likely that with much of the gasification zone of the RFSG at temperatures not greatly above those in a non-slagging design, the hoped-for reduction in tar production may be difficult to realise.

This situation arises because of the composition of the feed, and the constraint with gasifiers of this type to operate at the carbon boundary, which implies a typical stoichiometric ratio of between 0.25 and 0.35 [126,130]. While oxygen enrichment and air pre-heat will certainly result in much-elevated temperatures in the initial part of the gas path where exothermic oxidation reactions dominate, the endothermic reduction reactions which dominate further along the gas path cause the temperature to drop rapidly initially, and then more slowly as residence time continues to increase. The temperature asymptotically approaches the equilibrium reaction temperature. A typical profile through the oxidation and reduction zones of a gasifier is shown in Figure 5.5 [119].
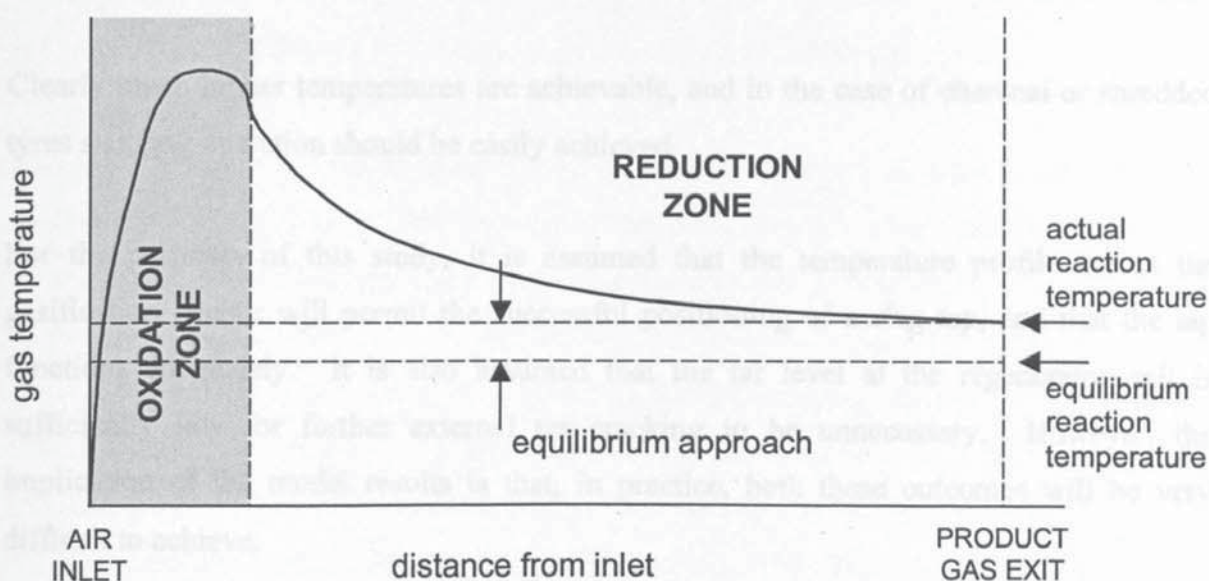
Figure 5.5 Temperature profile through the oxidation and reduction zones of a gasifier

117

Further runs of the gasification reactor model have confirmed that this situation would be the same for any biomass feedstock which has not been chemically upgraded, including MSW. For most such feedstocks the ultimate analysis is more or less constant, and in all cases the H:C and O:C molar ratios are never less than 0.5 and 1.2 respectively. Under these circumstances the endothermic gasification reactions play a powerful role, limiting the reaction temperature. Solid feedstocks with much lower H:C and O:C molar ratios, such as charcoal, give very different results. Table 5.7 shows results for product gas temperature from the gasification reactor model for an RFSG operating with un-enriched air, for various feedstocks.

Table 5.7 Predicted product gas temperatures from the RFSG for various feedstocks

Feedstock	H:C Molar Ratio	O:C Molar Ratio	Moisture Content (% db)	Ash Content (% db)	LHV (MJ/kg dry)	Prod. Gas Temp. (°C)
wood chips	1.53	0.66	17.6	2.3	18.6	703
coal	0.82	0.08	13.6	10.3	34.1	1190
charcoal	0.53	0.22	3.0	4.1	26.5	1559
shredded tyres	1.07	0.03	2.45	6.3	38.5	2026

Clearly much higher temperatures are achievable, and in the case of charcoal or shredded tyres slagging operation should be easily achieved.

For the purposes of this study, it is assumed that the temperature profile across the gasification reactor will permit the successful positioning of a slag tap, and that the tap functions adequately. It is also assumed that the tar level at the regenerator exit is sufficiently low for further external tar cracking to be unnecessary. However, the implication of the model results is that, in practice, both these outcomes will be very difficult to achieve.

The product gas exit temperatures for the four UGETC cases all fall within the range 600-720°C, confirming that the modelling assumption of carbon boundary operation gives the exit temperature values observed in practice (see Sections 5.1.4, 5.3.1).

5.3.3.2 Product Gas Heating Value and Cold Gas Efficiency

Figure 5.6 shows product gas LHV plotted against feed moisture content. The five curves correspond to the RFSG at four air oxygen concentrations, and the UGETC. Figure 5.7 shows a similar plot for cold gas efficiency.
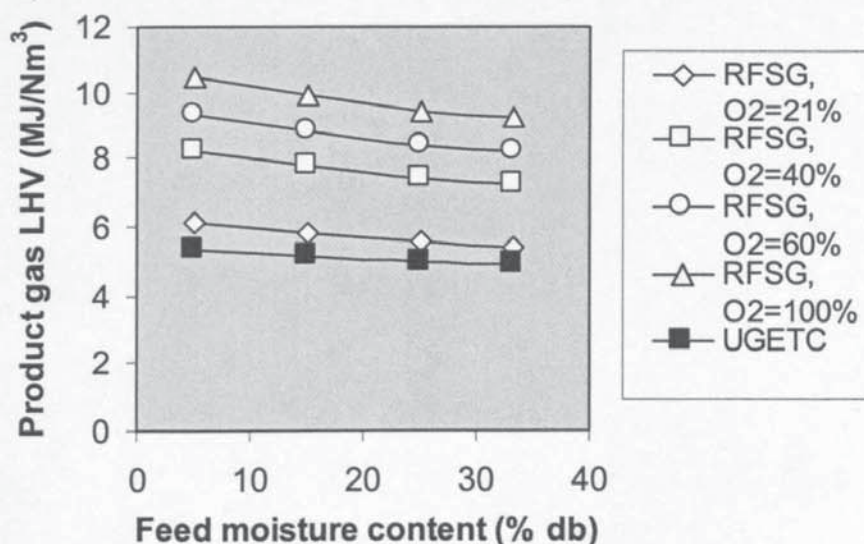
Figure 5.6 Effect of feed moisture on product gas LHV

The superiority of the RFSG over the UGETC both in terms of product gas LHV and particularly cold gas efficiency is apparent in these charts. The observed increase in product gas LHV with increasing air oxygen concentration for the RFSG is to be expected, as the amount of diluting nitrogen is reducing; however the superiority of the RFSG over the UGETC at 21% oxygen is as a result of air pre-heating. In the case of cold gas efficiency there is virtually no effect of air oxygen concentration in the RFSG, with the increasing LHV being almost exactly counterbalanced by the falling product gas flow rate. Without air pre-heat, cold gas efficiency would rise with increasing air oxygen concentration because of the reduced amount of sensible heat leaving with the inert nitrogen. However, when air pre-heat is employed, this benefit is lost as there is less

sensible heat in the product gas available for recovery to heat the air. Values for RFSG cold gas efficiency are however a clear 5% above those for the UGETC at all feed moistures, again as a result of air pre-heating.
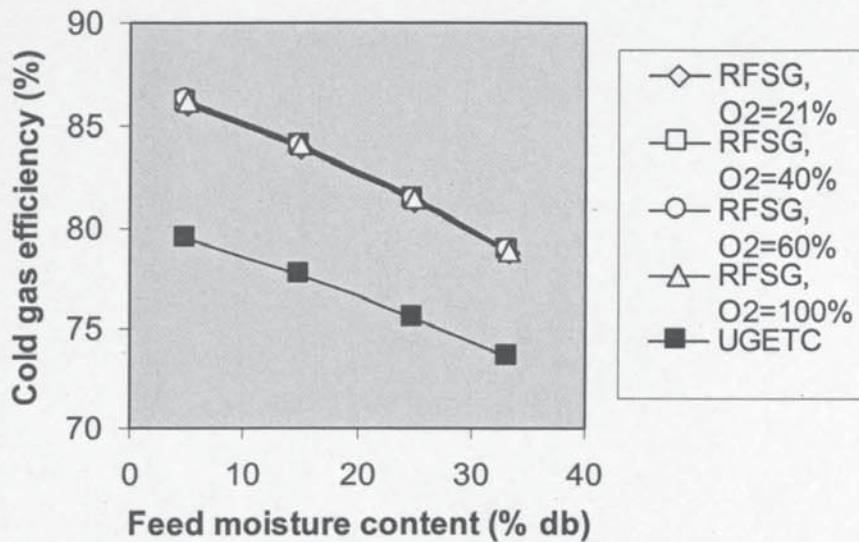
Figure 5.7 Effect of feed moisture on cold gas efficiency

Product gas LHV exhibits only a shallow decline with increasing feed moisture for both gasifier types at all oxygen concentrations, although LHV is expressed on a dry basis and the decline would be more marked if LHV were expressed on a wet basis (product gas moisture content will rise with feed moisture content). A factor of six increase in moisture (5.3-33.3% db) results in an average decrease in dry product gas LHV of just 10%. Similarly, the decline in cold gas efficiency with increasing moisture is only modest, with the factor of six increase in moisture resulting in an average decrease in cold gas efficiency of just 10%. The maximum attainable cold gas efficiency appears to be around 87% for the RFSG, and around 80% for the UGETC.

5.3.3.3 Regenerative Air Pre-heat (RFSG)

Figures 5.8 and 5.9 show the effect of regenerative air pre-heat on product gas LHV and cold gas efficiency for the RFSG. In each case the percentage improvement or increase with pre-heated air compared with zero pre-heat is plotted against air oxygen concentration for the four feed moisture contents.
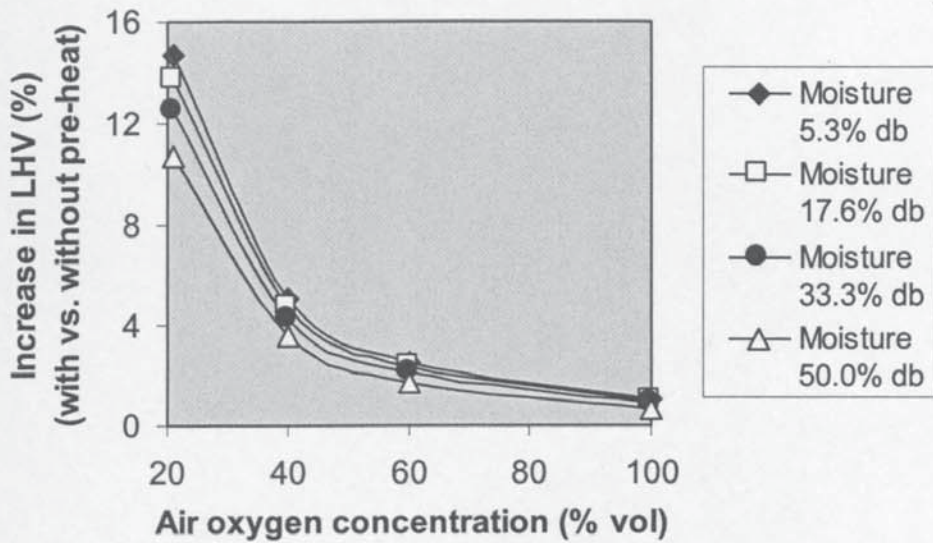
Figure 5.8 Effect of regenerative air pre-heat on RFSG product gas heating value
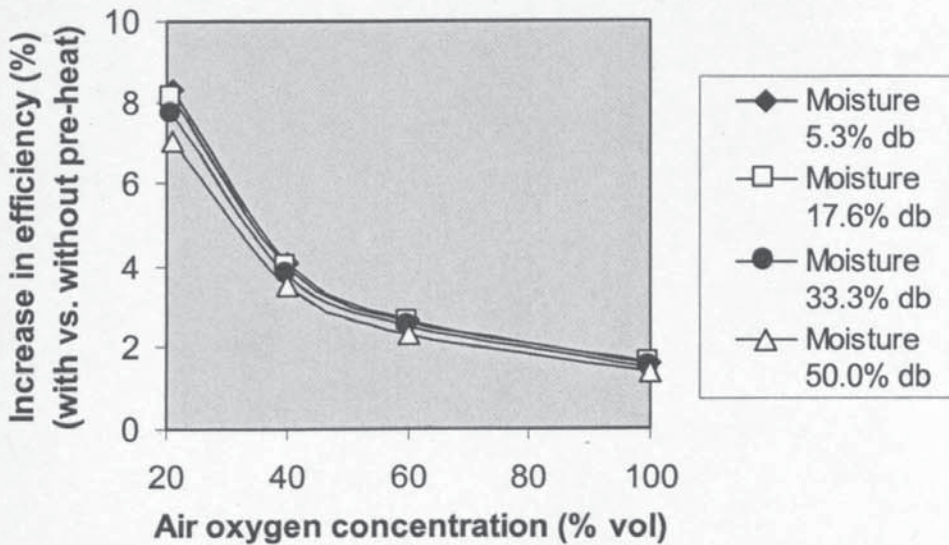
Figure 5.9 Effect of regenerative air pre-heat on RFSG cold gas efficiency

The improvements with air pre-heat are most pronounced at zero oxygen enrichment (10-15% for LHV, 7-9% for cold gas efficiency), but diminish rapidly as enrichment level increases. At 40% oxygen concentration the benefit for both parameters has fallen to 4-6%. This is because as enrichment level increases, the air flow rate falls sharply, and the amount of sensible heat that can be supplied to the gasification reactor via the air falls likewise. In those cases with regenerative air pre-heating, the air flow rate with no oxygen

enrichment is nearly twice that for an oxygen concentration of 40%. Air oxygen enrichment therefore acts to reduce the benefits of regenerative air pre-heating. This result supports operation at relatively low levels of air oxygen enrichment on the grounds of cost, and in the system modelling study (Chapters 8 and 9) the maximum air oxygen concentration is limited to the design value of 60%. The optimum level of oxygen enrichment can only be determined by application of the system model.

5.3.3.4 Product Gas Composition

Tables 5.8 and 5.9 give product gas compositions for the RFSG (with air pre-heat) and the UGETC respectively, on a volume fraction basis.

Table 5.8 Product gas compositions: RFSG

Case No.	R1	R2	R3	R4	R5	R6	R7	R8
Feed moisture (% db)	5.3	5.3	5.3	5.3	17.6	17.6	17.6	17.6
Air O_2 conc. (% vol)	21	40	60	100	21	40	60	100
$[H_2]_{GII}$	0.225	0.292	0.328	0.364	0.233	0.297	0.331	0.365
$[CO]_{GII}$	0.250	0.328	0.371	0.414	0.196	0.255	0.287	0.318
$[CO_2]_{GII}$	0.082	0.106	0.118	0.131	0.114	0.146	0.163	0.180
$[CH_4]_{GII}$	0.008	0.011	0.013	0.015	0.012	0.018	0.020	0.023
$[N_2]_{GII}$	0.392	0.204	0.102	0.000	0.378	0.194	0.097	0.000
$[H_2O]_{GII}$	0.043	0.058	0.067	0.075	0.067	0.089	0.101	0.114
Case No.	**R9**	**R10**	**R11**	**R12**	**R13**	**R14**	**R15**	**R16**
Feed moisture (% db)	33.3	33.3	33.3	33.3	50	50	50	50
Air O_2 conc. (% vol)	21	40	60	100	21	40	60	100
$[H_2]_{GII}$	0.233	0.293	0.323	0.353	0.221	0.273	0.299	0.324
$[CO]_{GII}$	0.139	0.178	0.199	0.220	0.088	0.112	0.124	0.136
$[CO_2]_{GII}$	0.147	0.187	0.207	0.227	0.174	0.218	0.241	0.263
$[CH_4]_{GII}$	0.020	0.028	0.032	0.036	0.032	0.043	0.049	0.054
$[N_2]_{GII}$	0.360	0.183	0.090	0.000	0.343	0.172	0.084	0.000
$[H_2O]_{GII}$	0.100	0.131	0.148	0.164	0.142	0.182	0.203	0.223

In all cases, reducing the moisture content of the feed has the effect of increasing CO but reducing CH_4 and H_2O, with H_2 showing only weak sensitivity.

For the RFSG, the effect of regenerative air pre-heat is always to shift the equilibrium to the production of more CO and H_2 and less CO_2 and H_2O, with CH_4 virtually unaffected. If the effect of air oxygen enrichment on product gas composition is considered on a nitrogen-free basis, no effect is seen with pre-heated air (as there is no requirement to heat the inert nitrogen), whereas without air pre-heat the effect of increased oxygen enrichment is again to raise CO and H_2 production, and reduce CO_2 and H_2O production.

Table 5.9 Product gas compositions: UGETC

Case No.	U1	U2	U3	U4
Feed moisture (% db)	5.3	17.6	33.3	50
$[H_2]_{G11}$	0.199	0.207	0.208	0.196
$[CO]_{G11}$	0.208	0.162	0.113	0.070
$[CO_2]_{G11}$	0.102	0.130	0.158	0.180
$[CH_4]_{G11}$	0.008	0.013	0.021	0.033
$[N_2]_{G11}$	0.432	0.415	0.394	0.373
$[H_2O]_{G11}$	0.051	0.074	0.107	0.148

5.3.4 Results: Regenerator Model (RFSG)

Results from the regenerator model for the RFSG cases with air pre-heat are shown in Table 5.10. Packing sphere diameter was in the range 129-165 mm, and regenerator diameter 0.54-1.2 m, giving total packing masses of 0.65-6.5 t. The large sphere size would result in relatively low pressure drops, with the regenerators resembling the checkerwork brick designs found in the metallurgical or glass industries rather more than the small packed bed columns associated with, for example, solar energy storage.

Temperature deltas refer to the difference between gas temperature at the start and at the finish of a period. In all cases the fluctuation in air temperature entering the gasification

123

reactor is less than 85°C, and this results in a fluctuation in product gas temperature leaving the gasification reactor of less than 2°C. The corresponding fluctuation in product gas LHV or any of the component concentrations is always below ±0.5%. It is therefore a reasonable approximation for the purposes of overall system modelling to take final product gas composition and heating value as being constant with time.

Table 5.10 Principal regenerator model results

Case No.	R1	R2	R3	R4	R5	R6	R7	R8
Feed moisture (% db)	5.3	5.3	5.3	5.3	17.6	17.6	17.6	17.6
Air O_2 conc. (% vol)	21	40	60	100	21	40	60	100
T_{G14} into gas. reactor (°C)	669	683	687	697	633	646	648	651
ΔT_{G14} into gas. reactor (°C)	35.5	40.1	47.5	52.8	38.3	44.0	52.4	64.2
T_{G15} from gas. reactor (°C)	738	752	758	763	703	715	720	725
ΔT_{G15} from gas. reactor (°C)	1.4	0.8	0.6	0.4	1.2	0.7	0.6	0.4
T_{G16} from regenerator (°C)	450	552	606	659	448	541	590	637
Packing mass M_P (tonnes)	7.15	3.39	2.00	1111	6.50	3.03	1.78	922
Case No.	**R9**	**R10**	**R11**	**R12**	**R13**	**R14**	**R15**	**R16**
Feed moisture (% db)	33.3	33.3	33.3	33.3	50	50	50	50
Air O_2 conc. (% vol)	21	40	60	100	21	40	60	100
T_{G14} into gas. reactor (°C)	596	604	612	613	555	565	569	567
ΔT_{G14} into gas. reactor (°C)	41.3	49.9	55.7	69.9	45.6	54.8	64.6	81.8
T_{G15} from gas. reactor (°C)	665	676	680	684	626	635	639	642
ΔT_{G15} from gas. reactor (°C)	1.2	0.7	0.5	0.4	1.4	0.8	0.7	0.5
T_{G16} from regenerator (°C)	444	529	570	611	437	511	548	582
Packing mass M_P (kg)	5.81	2.62	1.58	802	5.03	2.24	1.29	649

The IC engine is a constant speed device and will demand a constant mixture volume flow rate. This therefore implies that given a constant product gas composition, the product gas mass flow rate will also be constant with time, as will the air flow rate to the gasifier. The model cannot predict any transient effects on gas quality in the period immediately following flow reversal; these are therefore neglected.

The product gas stream emerges at a mean temperature of between about 430°C and 610°C depending on the level of air oxygen enrichment and the biomass moisture content; higher oxygen enrichment levels and lower moistures resulting in higher temperatures.

Figure 5.10 shows temperature profiles through the regenerator for Case R5. The form of the profiles was very similar for all cases. The temperature difference between gas and packing is much greater near the outer boundaries than near the gasification reactor, indicating that most heat transfer takes place near the outer boundaries. Figure 5.11 shows the variation in gas temperatures with time for the same case. Each of the profiles is linear.
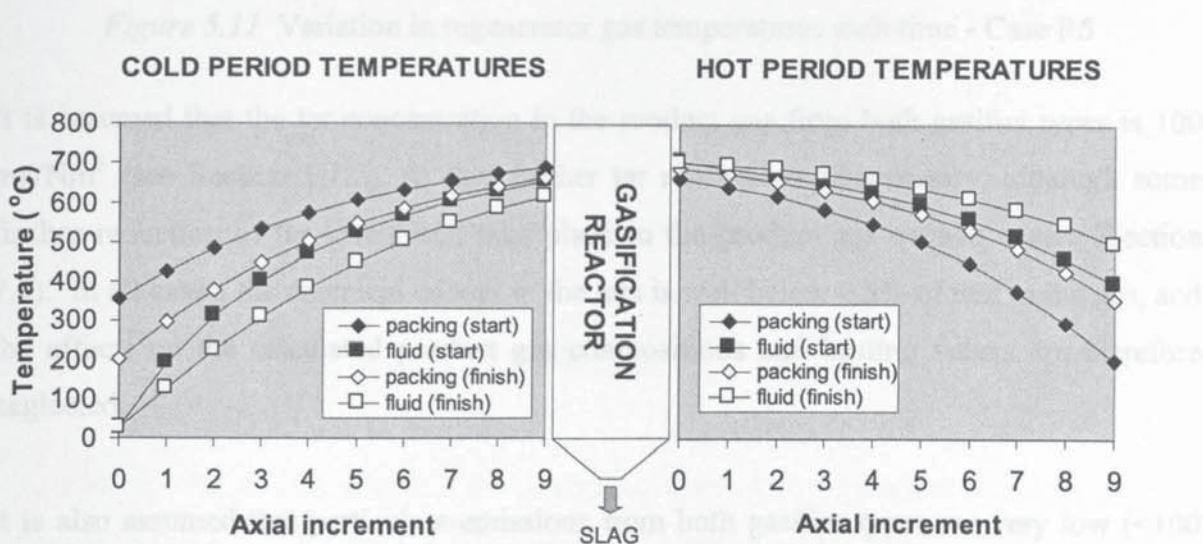
Figure 5.10 Regenerator temperature profiles - Case R5

For all cases, the model achieved convergence after a maximum of 20 iterations.

5.4   Reduced Representation for Incorporation in System Model

The gasification reactor and regenerator models are not well suited to direct incorporation in the system model due to their size and complexity. A reduced performance/cost model of the RFSG (with pre-heat) and the UGETC has therefore been constructed, based on regression analysis of the results presented in Sections 5.3.3 and 5.3.4 supplemented with some additional cases for the UGETC to extend the feed moisture content range up to 100% db.
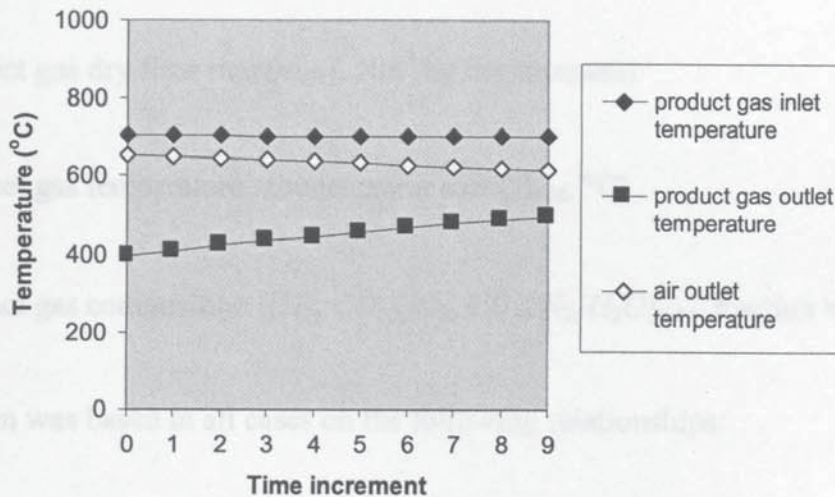
Figure 5.11 Variation in regenerator gas temperatures with time - Case R5

It is assumed that the tar concentration in the product gas from both gasifier types is 100 mg/Nm^3 (see Section 5.1.2), so that further tar removal is unnecessary, although some further reduction of tar levels will take place in the product gas quench cooler (Section 7.4). In all cases, the chemical energy in the tars is well below 0.5% of that in the gas, and the effects on the calculated product gas compositions and heating values are therefore neglected.

It is also assumed that particulate emissions from both gasifier types are very low (<100 mg/Nm^3); the updraft gasifier has inherently low particulate emissions [88], and the RFSG has a packed bed regenerator after the gasification reactor outlet which will provide self-cleaning filtration (with the retained solids removed as slag).

The reduced gasifier model is effectively the starting point of the system model, and receives no input from other module sub-models.

5.4.1 Performance Calculations

The reduced model needs to be able to supply the following performance information to other system module sub-models, given biomass moisture content (X_{B9}, % db) and air oxygen concentration ($[O_2]_{A9}$, fraction by volume):

- Air flow rate (m_{A9}, Nm³/kg dry biomass)

- Product gas dry flow rate (m_{G11}, Nm³/kg dry biomass)

- Product gas temperature at regenerator exit (T_{G16}, °C)

- Product gas composition ([H_2, CO, CO_2, CH_4, N_2, H_2O]$_{G11}$, fraction by volume)

The regression was based in all cases on the following relationships:

$$f(X_{B9}, [O_2]_{A9}) = f'([O_2]_{A9})X_{B9} + f''([O_2]_{A9}) \qquad (5.9)$$

where:

$$f'([O_2]_{A9}) = C_1[O_2]_{A9}{}^m + C_2[O_2]_{A9}{}^n + C_3 \qquad (5.10)$$

$$f''([O_2]_{A9}) = C_4[O_2]_{A9}{}^r + C_5[O_2]_{A9}{}^s + C_6 \qquad (5.11)$$

where m, $r = \pm 2$ and n, $s = \pm 1$. A number of alternative regressions were tested, but Equations 5.9-5.11 gave good results (see below) with a relatively simple form.

Values for the constants C_{1-6} and exponents m, n, r and s are given in Table 5.11 for the RFSG model, and in Table 5.12 for the UGETC model. Note that for the UGETC, air oxygen concentration is constant at the ambient value of 0.21, and therefore the constants $C_{1,2,4,5}$ are zero. Over all model cases and all parameters except [CH_4]$_{G11}$, the average error introduced by regression expressed as a percentage of true value was 1.7%, and maximum error (associated with [CO]$_{G11}$) was 7.1%. Values for [CH_4]$_{G11}$ were exact to three decimal places in all cases, but in some cases the values were very small and to include these errors in the above average would have been distorting.

Limits of applicability for the reduced models are 5<X<50 (RFSG), 5<X<100 (UGETC) and 0.2<[O_2]$_{A9}$<0.6.

Table 5.11 Constant values for reduced model - RFSG

$f(X,[O_2])$	C_1	C_2	C_3	m	n	C_4	C_5	C_6	r	s
m_{A9}	0	7.0×10^{-5}	-1.0×10^{-4}		-1	0	0.288	-4.7×10^{-3}		-1
m_{G11}	0	2.0×10^{-4}	1.2×10^{-3}		-1	0	0.29	1.25		-1
T_{G16}	2.63	-4.72	0.577	2	1	-687	969	279	2	1
$[H_2]_{G11}$	0	-1.5×10^{-3}	2.0×10^{-4}		1	-0.459	0.647	0.115	2	1
$[CO]_{G11}$	7.2×10^{-3}	-0.0107	-1.7×10^{-3}	2	1	-0.544	0.769	0.126	2	1
$[CO_2]_{G11}$	-2.8×10^{-3}	3.8×10^{-3}	1.4×10^{-3}	2	1	-0.145	0.207	0.0379	2	1
$[CH_4]_{G11}$	-1.4×10^{-3}	1.9×10^{-3}	2.0×10^{-4}	2	1	-0.0105	0.018	4.0×10^{-4}	2	1
$[N_2]_{G11}$	-1.6×10^{-3}	3.1×10^{-3}	-1.7×10^{-3}	2	1	1.24	-1.75	0.711	2	1
$[H_2O]_{G11}$	-5.5×10^{-3}	6.5×10^{-3}	1.1×10^{-3}	2	1	-0.0723	0.108	0.0104	2	1

Table 5.12 Constant values for reduced model - UGETC

$f(X,[O_2])$	C_1	C_2	C_3	m	n	C_4	C_5	C_6	r	s
m_{A9}	0	0	-1.01×10^{-3}			0	0	1.61		
m_{G11}	0	0	5.89×10^{-4}			0	0	2.8		
T_{G11}	0	0	-2.32			0	0	724		
$[H_2]_{G11}$	0	0	-7.5×10^{-5}			0	0	0.205		
$[CO]_{G11}$	0	0	-3.08×10^{-3}			0	0	0.22		
$[CO_2]_{G11}$	0	0	1.75×10^{-3}			0	0	0.096		
$[CH_4]_{G11}$	0	0	5.5×10^{-4}			0	0	4.02×10^{-3}		
$[N_2]_{G11}$	0	0	-1.31×10^{-3}			0	0	0.438		
$[H_2O]_{G11}$	0	0	2.18×10^{-3}			0	0	0.037		

129

5.4.2 Cost Calculations

5.4.2.1 Capital Cost

Capital costs of atmospheric pressure biomass gasifier modules have been correlated with biomass feed rate by Bridgwater [38], for a range of inputs from 0.1-10 kg/s (dry basis). The module is defined as from prepared feed on the ground to a clean gas. Module costs are on a total plant cost (*TPC*) basis. The correlation has been updated to 1998 values and converted to sterling:

$$TPC_{10} = 7627\, m_{B9}^{0.698} \qquad\qquad (5.12)$$

where m_{B9} is biomass dry feed rate (kg/s) and TPC_{10} is in £'000 (1998).

This cost comprises both the gasification reactor and the product gas scrubber and associated waste water treatment plant, but no additional tar cracker. Bridgwater gives a breakdown of relative capital costs for a system with an atmospheric pressure gasifier of about 6 MW$_e$ output, in which he estimates the element of *TPC* attributable to gas scrubbing and waste water treatment to be 50% of that for the gasification reactor. Toft has similarly estimated the element of *TPC* attributable to the tar cracker to be 50% of that for the gasification reactor [40]. Equation 5.12 can also be taken therefore to represent the capital cost for the gasification reactor with external tar cracker, but without gas clean-up or waste water treatment.

In the absence of firm cost data from Wellman on the UGETC, it has been assumed that the function of Equation 5.12 will give a reasonable approximation for TPC_{10} (as the UGETC is a conventional atmospheric pressure gasifier with external tar cracking). Wellman have given a rule-of-thumb figure of £1000 per kW$_e$ for the installed plant cost (*IPC*) of a gasifier and associated tar crackers for a system in the power output range 2.5-10 MW$_e$ [131]. If *IPC* is calculated using Equation 5.12 and Table 2.5 assuming an overall system efficiency of 28% (bearing in mind the larger system size), values are obtained of £1115 per kW$_e$ at 5 MW$_e$ and £904 per kW$_e$ at 10 MW$_e$, giving confidence that Equation 5.12 provides a good approximation.

A function for the gasifier equipment cost (EC_{10}) will be necessary in the calculation of the RFSG module total plant cost (see below); this may be estimated using Tables 2.4 and 2.5:

$$EC_{10} = 3451 m_{B9}^{0.773}$$ (5.13)

with EC_{10} in £'000 (1998). Equations 5.12 and 5.13 have been used in the reduced model to give TPC_{10} and EC_{10} for the UGETC module.

Costs for the RFSG module are more difficult to estimate, as there are no comparable designs for which cost data are available. Slagging operation will introduce additional costs over and above non-slagging operation, such as more expensive materials of construction, the requirement for a heated slag tap and quench, and more elaborate safety measures (particularly if oxygen-enriched air is used). Also, two packed-bed regenerator columns are required, and the reversing flow operation will require the necessary valving and associated control systems. On the other hand, no external tar cracking reactors are required, and these can be expensive items. It is assumed that the RFSG equipment cost $(EC_{10})_{RFSG}$ is related to the UGETC equipment cost by a simple constant factor F:

$$(EC_{10})_{RFSG} = 3451 F m_{B9}^{0.773}$$ (5.14)

Values of F of 1.0 and 1.5 are considered in the study. The manufacturer of the pilot-scale RFSG used in the JOULE project to which this study is linked has estimated that the value for F could be close to 1.0. However, anecdotal evidence based on industrial experience at a range of scales indicates that slagging gasifiers usually cost significantly more than non-slagging gasifiers [132]. The values of 1.0 and 1.5 are therefore considered to correspond to optimistic and pessimistic scenarios.

The equipment cost of the RFSG at a given biomass input might be expected to vary to a limited degree with the air oxygen concentration, as the volumetric flows of gas can change significantly at certain locations. However, this variation is difficult to estimate, and has therefore been ignored.

For both the RFSG and the UGETC modules, the equipment cost is taken to include any fan requirements for the air supply to the gasifier. Power supply to the fans will form part of the estimated 5% overall parasitic power demand (Section 2.5.3.3).

It is assumed that all direct costs additional to the equipment cost will be identical for the RFSG and UGETC modules at a given biomass input, so that the element of total plant cost attributable to the RFSG module $(TPC_{10})_{RFSG}$ is given by:

$$(TPC_{10})_{RFSG} = (TPC_{10})_{UGETC} + (EC_{10})_{RFSG} - (EC_{10})_{UGETC} \qquad (5.15)$$

or:

$$(TPC_{10})_{RFSG} = 7627\, m_{B9}^{0.698} + 3451(F-1)m_{B9}^{0.773} \qquad (5.16)$$

This has been assumed on the grounds that both systems are in effect three reactors of comparable size with comparable electrical, instrumentation and civil requirements, and it would be unfair to allocate indirect costs at a different level in each case.

5.4.2.2 Labour

The labour requirement per shift L_{10} for both gasifiers is taken from Toft [40]:

$$L_{10} = 1.91 m_{B9}^{0.475} \qquad (5.17)$$

where m_{B9} is biomass dry flow rate (kg/s).

The worksheet for the RFSG is shown in Appendix 2 Section A2.4, and that for the UGETC in Appendix 2 Section A2.5.

6 IC ENGINE

This chapter deals with the IC engine module of the BGES (see Figure 2.1). The module receives product gas from the product gas quench (Section 7.3), and generates electricity.

6.1 IC Engines on Low Heating Value Gas for Power Generation

6.1.1 Engine Design and Performance

At capacities of less than 5 MW$_e$, the high capital cost of gas turbine combined cycle options renders them uneconomic for power generation [12]. The conventional Rankine cycle with steam turbine also suffers from high capital cost at small scale, as well as low overall efficiency (<20%) in power-only mode [10]. The gas turbine in simple cycle, while having lower capital cost, is also relatively inefficient at these scales (<25% thermal efficiency) as well as being highly intolerant of impurities in the fuel gas [133,134].

Reciprocating internal combustion (IC) engines on the other hand combine low capital cost with high efficiency at small scale. Modern designs can deliver overall electrical efficiencies of 40% or more. As a result the IC engine is widely held to be the preferred prime mover for biomass gasification systems at scales of less than 5 MW$_e$ [7,12,13].

The design aspects of IC engines have been extensively dealt with elsewhere [135,136,137], and attention will only here be drawn to those features of relevance to low heating value gas operation.

6.1.1.1 Main Engine Types

There are two main types of IC engine suitable for fuelling with low heating value gases. In spark ignition (SI) types (Figure 6.1) the charge is ignited by a high-voltage spark. SI engines may operate on 100% gaseous fuel without any requirement for a pilot fuel, at relatively low compression ratios (<12). In compression-ignition (CI) types (Figure 6.1) the charge ignites spontaneously due to the high temperatures achieved in the compression process. Accordingly CI engines operate at higher compression ratios (>12), and with

gaseous fuel it is necessary to admit a pilot charge of diesel oil to the cylinder to provide the combustion source; the engine is therefore "dual-fuel".

Both of these main types have been used successfully with low heating value gases of various kinds, including biomass gasifier product gas [138,139,140,141,142,143]. However, most installations operating on biomass gasifier product gas have suffered to an unacceptable degree from the problem of condensable tars in the product gas, which result in the build-up of damaging deposits on valves and other surfaces [21,144]. IC engines operating on product gas require tar levels of 100 mg/Nm^3 or less for these problems to be tolerable in magnitude [22], levels rarely achieved by existing gasifiers (see Section 5.1.2).
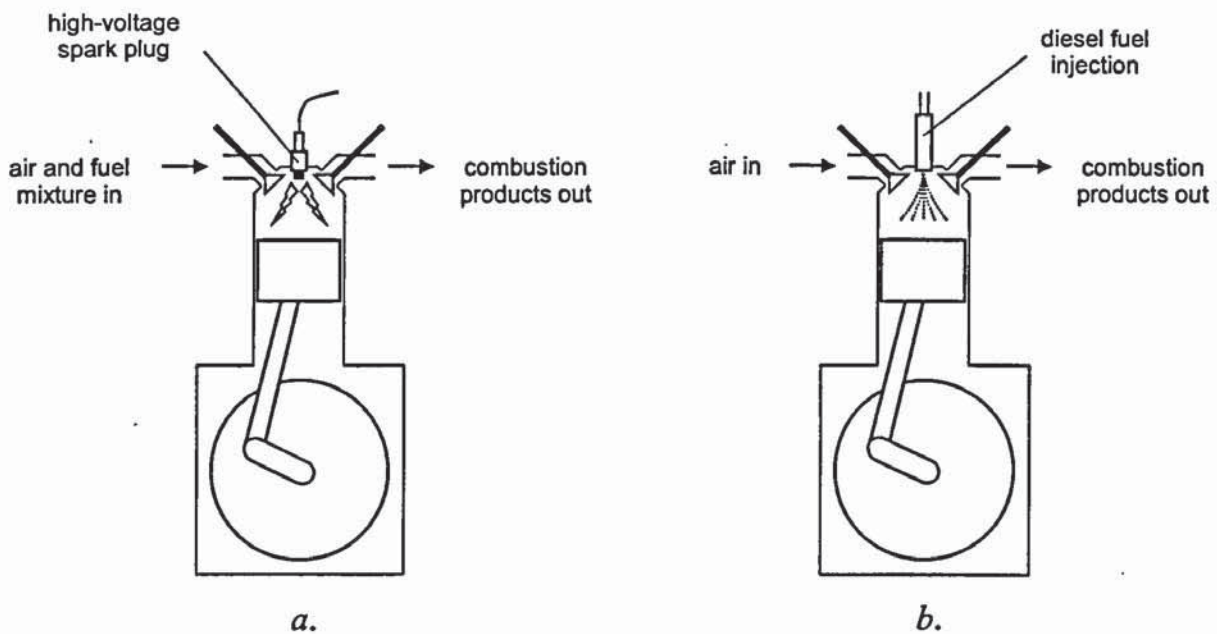
Figure 6.1 IC engine types - *a.* spark ignition, *b.* compression ignition

From the modelling results presented in Table 5.5 and discussed in Section 5.3, product gas LHVs in the present application fall in the range 3.5-10 MJ/Nm^3, depending principally on the level of oxygen enrichment of the gasifying air. This compares with around 35 MJ/Nm^3 for natural gas, 18 MJ/Nm^3 for landfill gas and 23 MJ/Nm^3 for biogas (from anaerobic digestion).

In both SI and dual-fuel CI engines running on gas, the gas is mixed with the required amount of combustion air. Mixing can take place at a single point, before or after a turbocharger if present (a turbocharger is a small turbine/compressor combination for

extracting energy from the engine exhaust gas to raise the pressure of the incoming gas before admission to the cylinder). Alternatively mixing can take place at multiple points just upstream of each cylinder inlet valve. Multiple point injection is usually associated with larger engines (>1 MW$_e$) [145].

The ratio of air to fuel may be varied to suit the particular engine or operation. A traditional SI engine will operate at an air-fuel equivalence ratio λ (ratio of actual oxidant to the stoichiometrically correct amount, or that required for complete combustion) close to 1.0. More modern "lean-burn" designs may operate at λs of about 1.7-2.0 in order to reduce peak temperatures and thus reduce formation of NOx (a strong function of temperature - see Section 6.1.1.3), often with pre-chamber ignition to improve combustion (particularly at sizes >1 MW$_e$) [145].

CI engines commonly operate at a λ of about 1.7 at full load to ensure complete combustion and avoid "detonation" (see below), but have higher NOx emissions than SI engines because of the higher combustion temperatures involved.

Hydrogen as a fuel gas is highly prone to detonation, or pre-ignition of the gas in the cylinder in front of the advancing flame as a result of the elevated temperatures and pressures being generated by the combustion process. Detonation can cause serious damage to cylinder components; hence the presence of significant quantities of hydrogen in the fuel gas can give rise to problems. These are exacerbated by high compression ratios which increase temperatures, but reduced by high λs which reduce temperatures. Problems would be most likely to be encountered therefore in high-compression-ratio CI engines, or in conventional SI engines operating at $\lambda\sim1$.

In biomass gasifier product gas, hydrogen content is typically 10-20% by volume (or 1-2% by weight). Fortuitously, however, the other main constituent of product gas, CO, has excellent detonation resistance, and this offsets to some extent the effects of H$_2$. The net effect is that the detonation tendency of biomass gasifier product gas is usually not significantly worse than methane, the design fuel for most gas-fueled engines [146].

135

6.1.1.2 Efficiency and Power

In stationary power applications, dual-fuel CI designs have generally been able to achieve overall (brake thermal) efficiencies up to 10% above SI engines as a result of their higher compression ratio. In modern designs employing turbocharging and intercooling, the gap has narrowed as a result of the greater potential for efficiency improvement by these methods in the SI engine. Both SI and CI engines are now able to achieve overall efficiencies to electricity in excess of 40% on natural gas for the power range of interest here [147,148,149]. When lower heating value gases are used, this efficiency tends to fall, although only by a small amount (~2-5%) in modern well-designed engines [15].

More importantly the use of a lower heating value gas tends to result in a fall in the engine power output at a given speed (a de-rating). The fall in power results directly from the use of the lower heating value gas, or more importantly the lower heating value *mixture*. If it is assumed that overall efficiency is unchanged, shaft power delivered is then proportional to the energy supplied in the charge. Volumetric input of the charge is unchanged, as speed is constant and volumetric efficiency - actual mass induced per cylinder divided by theoretical maximum mass based on cylinder volume at standard temperature and pressure - is also constant. Shaft power delivered is therefore proportional to the mixture heating value expressed in MJ/Nm^3. This mixture heating value falls as the fuel gas heating value falls, resulting in a fall in power which can be as large as 40%, the actual amount being dependent on the gas composition and the equivalence ratio (see Section 6.2.3 and 6.2.4).

The fall in efficiency results from the increased significance of mechanical losses. Brake thermal efficiency η_B may be expressed as:

$$\eta_B = \frac{P_I - P_L}{Q} = \eta_I - \frac{P_L}{Q} \qquad (6.1)$$

where P_I is indicated power (rate of work delivered to the piston), P_L is the loss in power due to mechanical friction, Q the thermal input and η_I the indicated efficiency [135]. Mechanical losses are a function of the engine dimensions, design and speed only, so that P_L remains virtually constant for a given engine and speed if mixture heating value falls. Also, the rate of work delivered to the piston can be taken to be proportional to the rate of

heat release from the fuel - that is, η_I remains constant if mixture heating value falls (in fact, η_I will tend to fall slightly as combustion duration increases with the poorer-quality fuel) [145]. However, Q falls with falling mixture heating value for a given engine and speed. Hence brake thermal efficiency falls. The degree to which it falls is a function of the size of the mechanical loss in relation to the indicated power, and this is a function of engine design.

Another factor affecting power output is gas temperature. When running on product gas in close coupling with a gasifier, the gas temperature may be above ambient, and the higher this temperature the lower the mass of gas induced per stroke, i.e. the lower the volumetric efficiency and hence the lower the power generated. The gas should therefore be cooled as much as practically possible before entering the engine. One manufacturer of gas engines for operation on wood gasifier product gas suggests a gas temperature of 40°C at a relative humidity of 80% as suitable [143]; this has been assumed as a fixed value in the present study.

The falls in power due to fuel gas composition and temperature may be compensated to some extent by the use of air with an enriched oxygen content, if facilities are available to provide this. The provision of air separation plant for this purpose alone would probably be unjustified economically; however, in a BGES already incorporating an air separation plant for the supply of oxygen-enriched air to the gasifier, an increase in output to supply the engine as well may merit consideration. The use of oxygen-enriched air improves the *mixture* heating value and hence the power delivered. However, it is reasonable to place an upper limit on the level of enrichment equivalent to that required to fully restore the design shaft power of the engine. This level will clearly be dependent on the amount of derating. Exceeding this value will result in overloading of the engine, with consequent reduced life and additional maintenance.

6.1.1.3 Emissions

The issue of emissions has become increasingly important, and has resulted in a trend towards lean-burn SI engines for these types of application.

Most nitrogen-bearing compounds in the product gas (e.g. NH_3, HCN) will have been removed by wet scrubbing in an atmospheric-pressure system such as is being considered here [50], and NOx emissions arising from any nitrogen in the biomass feedstock ("fuel" NOx) are not normally therefore of concern.

"Thermal" NOx emissions on the other hand arise from the reaction of air-borne nitrogen and oxygen, and are a strong function both of temperature and of excess oxygen. At a given excess oxygen level, thermal NOx emissions from biomass gasifier product gas might be expected to be rather lower than from natural gas, gasoline or diesel because of the lower peak flame temperatures involved; nevertheless, levels can still be high enough to present a problem, particularly if oxygen-enriched air is used as the oxidant leading to higher temperatures. In lean-burn SI designs which operate at high excess air levels (high λ), the peak temperatures in the combustion chamber are much reduced, and this effect far outweighs the increased availability of oxygen leading to large reductions in thermal NOx emissions.

Dual-fuel diesels operate at high excess air levels already, for reasons given in Section 6.1.1.1, but also operate at higher temperatures than traditional SI engines due to the higher compression ratio. Furthermore, the use of a diesel pilot fuel accounting for typically 10-15% of thermal input [141] gives rise to emissions of SOx and particularly NOx associated with the sulphur and nitrogen in the diesel fuel, and clean-up equipment may be required. Diesel is in addition a fossil fuel, and would therefore give rise to net emissions of carbon dioxide. Dual-fuel engines have hitherto been regarded as attractive for gasifier systems because of their ability to continue operation if the supply of product gas is interrupted, by reverting to 100% diesel operation. However the stringency of emissions legislation is only likely to increase in the future, and the advantages of lean-burn SI engines in this regard will become more compelling.

Emissions of CO are another concern with IC engines operating on biomass gasifier product gas. Some CO arises from incomplete combustion in the cylinder, but the far greater contribution comes from the fuel gas which bypasses the combustion process due to overlap between the inlet and exhaust valve cycles. This can reach 1-2% of the total fuel input in high-speed SI engines, leading to levels of exhaust CO in the range 0.2-0.3% by volume [143,146]. The magnitude of this potential problem depends very much on the

gas composition and on the specific design of the engine, but the problem does not lend itself easily to solutions within the engine and a back-end oxidation catalyst may be required [146].

6.1.1.4 Combined Heat and Power

IC engines are suitable for CHP applications, with heat recovery possible both from the exhaust gases and from the engine cooling system to raise steam or hot water for an external demand. Typical energy flows in a modern high-efficiency IC engine are given in Table 6.1. As can be seen, nearly 30% of the energy leaves the engine as sensible heat in the exhaust gases, and about the same as sensible heat in the engine cooling water. In theory, therefore, up to 60% of the energy in the fuel is available for recovery as sensible heat.

However, full recovery is not realised in practice, for two important reasons. Firstly, heat exchanger or boiler design will place a lower limit on the exit temperature of the exhaust gases, which will depend on the required temperature of the water or steam. Secondly, the engine coolant maximum temperature is usually less than 120°C [136], and this is therefore a low-grade heat source only suitable for hot water or very low pressure steam production. If the external demand is for high grade heat in the form of steam at more than, say, 2 bar, this source cannot be used.

Table 6.1 Typical energy flows in a modern IC engine [136]

ENERGY FORM	IN	OUT
Chemical energy in fuel	100%	
Shaft power		35%
Sensible heat in exhaust gas		30%
Sensible heat in cooling water		30%
Radiative and convective losses		5%

In practice, therefore, the maximum achievable ratio of useful heat to electrical power will usually fall in the range 0.5-1.0 for steam production, and 1.0-2.0 for hot water production.

For this reason, CHP schemes using IC engines are used almost exclusively for hot water applications rather than steam, particularly at the scale range of interest here [23] (see Section 2.4). Even heat-to-power ratios of 1.0-2.0 are low in comparison with those of conventional steam turbine CHP systems which may reach 3.0 or more [150]. This need not be a problem as electricity is a much higher-value product than heat. However, a typical heat-to-power demand ratio in industry is about 3.0 [151]. In order therefore to be viable, a CHP system based on an IC engine will probably be grid-connected, with suitable commercial arrangements available for export of power to the grid.

6.1.2 Operational History - Major Installations

Although there has been much work done at research level on the operation of IC engines on low heating value gas, there have been relatively few BGESs which have achieved a substantial number of operational hours, and very few that have done so on a commercial basis. Most installations have been at scales of below 100 kW$_e$, and detailed information regarding performance and operational experience is hard to obtain. There have been many ambitious proposals (particularly during the 1980s) which have not resulted in operational installations for various reasons, and also many installations which have been commissioned but which have had very short lives owing to technical or economic difficulties.

Of the successful installations above 100 kW$_e$ which have achieved over 3000 hrs operation, one of the most notable has been that at Loma Plata in Paraguay [17,152]. Two Imbert downdraft gasifiers producing 1800 Nm^3/h each of product gas from wood chips supplied three Waukesha modified SI gas engines, each producing 465 kW$_e$. The system, supplying electricity for a local private agricultural co-operative, operated for in excess of 72,000 hours between 1983 and the early 1990s, when it was decommissioned due to the installation of a national grid. The product gas, with an average net heating value of 5.1 MJ/Nm^3, passed through a dust separator, a washer and an electrostatic filter before entering the engines. The high availability of the system (>90%) attests both to the success of these measures, and to the relative initial cleanliness of the product gas.

Three French-owned projects are worthy of mention. The SEBI sawmill on the Ivory Coast has a Touillet downdraft gasifier coupled to a Mercedes SI gas engine which delivers

200 kW$_e$. The gasifier takes chipped wood waste from the mill, and fulfils the mill's electricity requirements. The system has operated since late 1989, and had achieved over 15,000 hours of operation by 1996 [18]. An almost identical system has operated at the Briollet woodworks in France, this time in CHP mode. Again, more than 15,000 operating hours had been achieved in 1996 [18]. The third project is at Bora-Bora in Tahiti, where an Entropie "external recycling" gasifier gasifies coconut husks, and the product gas fuels a Duvant dual fuel diesel engine delivering 190 kW$_e$. Over 4000 operating hours have been achieved here, but the current status is unknown [18].

There are a few large pilot plants which have operated intermittently, including the Daneco plant at Villasantina, Italy where RDF and wood chips have been gasified in a 3 MW$_{th}$ thermal input updraft gasifier coupled to a 620 kW$_e$ dual fuel diesel engine [18], and the Studsvik plant in Sweden where a 2 MW$_{th}$ thermal input circulating fluid bed gasifer and tar cracker have been coupled to a 500 kW$_e$ dual fuel diesel engine [13].

A number of systems of interest are either under construction or have only recently been commissioned; these include that at Harboore in Denmark, where two Jenbacher 0.7 MW$_e$ gas engines have recently been coupled to a 6 MW$_{th}$ thermal input Volund updraft wood chip gasifier, and that at Espenhain in Germany where an 850 kW$_e$ gas engine will be supplied by a 4 MW$_{th}$ thermal input HTV downdraft gasifier operating on demolition and waste wood.

An illustration of the difficult history of BGESs is provided by the Degrad des Cannes system in French Guyana, owned by EdF of France [153]. This was to have been a very large unsubsidised operation comprising three 6.7 MW$_e$ modules, each with a BIODEV fluidised bed gasifier feeding a large Pielstick dual fuel diesel engine. The gasifiers were to take wood chips, obtained largely from clearing the virgin tropical forest. In the event, one module was built in 1987, but the gasifier was never coupled to the engine. Initial trials with the gasifier revealed problems of wood preparation and feeding, slagging due to the high silica content of the wood, excessive phenol and naphthalene content in the gas, and major difficulties in gas cleaning. The developer pulled out, leaving the dual-fuel engine untested.

6.1.3 Selection of Engine Type

For the present study, it was decided to incorporate a modern SI gas engine in lean-burn configuration. Technical reasons for this choice related to NOx emissions are given in Section 6.1.1. In addition, SI engines are less prone to detonation problems, which could be highly relevant in view of the high hydrogen content of biomass gasifier product gas. Lastly, some manufacturers are beginning to offer this type of engine on a commercial basis specifically for low heating value gases, partly as an evolution from their successful application in landfill schemes. It is therefore becoming possible to obtain good estimates of costs and performance. In contrast, the activity with dual-fuel diesel wood gas engines that was evident in the 1980s seems to have largely ceased, with the major manufacturers that were active at the time no longer prepared to offer suitable designs.

6.2 Engine modelling

6.2.1 Modelling Approach

The engine model has to be able to accept product gas composition and flow rate as variable inputs, and from them calculate the following (note that product gas temperature is fixed - see Section 6.1.1.2):

- generator electrical output

- oxygen-enriched air flow rate, if used

- exhaust gas flow rate, composition and temperature

- cooling water flow rate (given inlet and outlet temperatures)

- engine/generator capital cost.

Capital cost is based on actual data and related to some calculated feature of engine design. However, three options are available for remaining calculations. A fully theoretical

approach could calculate the required quantities from considerations of fluid dynamics, heat transfer, combustion theory and mechanical forces. This is however a complex undertaking, requiring many assumptions and the availability of a large amount of physical and chemical data, as well as extensive computing resources. A wholly empirical approach could also be used, based on data from real engines operating on a range of product gas compositions under a wide range of operating conditions. However, suitable data is not available from the literature, and a dedicated experimental programme would therefore be required which is beyond the means of the present study. A semi-empirical approach has therefore been adopted, in which calculations of stoichiometry are combined with estimations of efficiency and heat flux based on manufacturers' data.

Note that gas clean-up and quench prior to the IC engine is covered in Section 7.4.

6.2.2 Acquisition of Performance and Cost Data

A number of manufacturers of SI gas engines with experience of operation on low heating value gases were approached. The most complete response was from Jenbacher Energie of Austria, who manufacture integrated engine/generator sets for stationary power and CHP applications covering the scale range of interest in the present study [147]. Jenbacher have operational experience with a wide range of gaseous fuels including natural gas, biogas from anaerobic digesters, landfill gas, coke gas, and product gas from both wood and MSW gasification. They are the market leaders in this area, and are likely to become involved in a large proportion of new bio-energy installations of this type, particularly in Europe. Their data have therefore been used in the empirical parts of the engine model, supported where possible by other sources.

The data extracted from performance sheets supplied by Jenbacher for use in the engine model comprised the following [154]:

- Overall thermal efficiency (LHV basis) for a range of models operating at full load on natural gas (36 MJ/Nm^3)

- Energy balance between shaft power, exhaust sensible heat, cooling water sensible heat and losses for one engine model operating at full load on biogas (23 MJ/Nm^3)

143

- Engine cooling water temperature at inlet and outlet

- Generator efficiency (virtually constant for all models and fuels)

- Capital cost for a range of engine/generator models, skid-mounted and delivered in gen-set configuration (not including heat recovery equipment, i.e. cooling water heat exchanger or exhaust gas heat exchanger)

The Jenbacher range of engines are lean-burn designs, for low NOx operation. They operate at an air-fuel equivalence ratio (λ) of about 1.7 for a range of gas types, including natural gas, propane gas, biogas and gasifier product gas [155]. All models are turbocharged and intercooled, and operate at a fixed nominal speed of 1500 rpm for 50 Hz applications.

The cooling water circuit collects waste heat from a number of systems including the water jacket, engine oil and intercoolers. All models in standard configuration are designed to accept cooling water at between 40°C and 70°C (intercooler inlet temperature) and reject it at 90°C. It is possible to operate at higher cooling water temperatures, but at the cost of further derating.

The energy balance data (referenced to ambient conditions) for a model 320 engine running on biogas were [154]:

- Shaft power   37.8 %

- Exhaust sensible heat   26.9 %

- Cooling water sensible heat   31.0 %

- Unrecoverable losses   4.3 %

144

Values reported for Waukesha gas engines running on product gas from Imbert wood chip gasifiers were 29-30 % shaft power, 30 % exhaust, 32% cooling water and 8-10% losses [156]; however, these were stoichiometric engines without turbocharging or intercooling, and as such had a lower efficiency and a hotter exhaust.

The generator efficiency was within the range 97 ± 1 % for all models and fuel types.

The remainder of the data are presented in Table 6.2.

Table 6.2 Engine performance and cost data from Jenbacher Energie [154]

6.2.3 Description of Model

The IC engine model receives product gas composition and flow rate data from the gasifier model, and calculates electrical power output, exhaust gas composition, temperature and flow rate, and engine coolant flow rate. If operation with oxygen enriched air has been specified, it also calculates the oxygen demand.

It is assumed that the product gas scrubber upstream of the engine inlet (Section 7.4) is designed so that the product gas leaves the scrubber at 35°C and saturated with water vapour, and is then re-heated using some source of surplus low-grade heat to 40°C (Section 6.1.1.2) and about 80% relative humidity [143]. The re-heating is necessary to avoid

145

condensation in the turbocharger inlet. The heat required is less than 0.01 MW in all cases, and the process has not been explicitly modelled.

If figures for air are used [157], moisture concentrations at engine inlet would range from about 0.046 to 0.056 by volume for the spread of product gas compositions encountered. Saturation humidities for product gas are not thought to differ greatly from air (they do not for a typical flue gas, for example); however, in the absence of data for product gas, a constant moisture concentration of 0.05 by volume has been assumed throughout.

6.2.3.1 Performance Calculations

The spreadsheet-based model begins with a calculation of product gas thermal input, air-fuel ratio, exhaust gas composition and exhaust gas flow rate, based on product gas composition and flow rate. The air-fuel equivalence ratio, λ, is set to a fixed value of 1.7 for all calculations (Section 6.2.2). In the absence of data indicating otherwise, a combustion efficiency of 100% is assumed; that is to say there is sufficient residence time in the cylinders for the combustion reactions to proceed fully to completion.

Product gas lower heating value LHV is calculated using the following formula [158]:

$$LHV = 10768[H_2]_{G21} + 12696[CO]_{G21} + 35866[CH_4]_{G21} \qquad (6.2)$$

where gas concentrations are expressed as volume fractions, and LHV in kJ/Nm^3.

The total fuel-air mixture volume flow rate W_{22} (m^3/s) is then calculated; this is assumed to be constant for a fixed engine type operating at a fixed speed (see Section 6.1.1.2).

The thermal input of the same engine running at the same speed on natural gas may then be calculated. This is necessary as the ratio of thermal input on natural gas to thermal input on product gas is used to calculate the brake thermal efficiency. If the engine is running on oxygen-enriched air, an iteration is performed at this point to calculate the level of enrichment necessary to restore the thermal input on product gas to be equal to that on natural gas - that is, to remove the derating.

Brake thermal efficiency is calculated semi-empirically in the following manner. Indicated efficiency η_I is assumed constant for a given engine and speed regardless of mixture heating value (see Section 6.1.1.2), so Equation 6.1 may be re-expressed as:

$$\eta_B = C_1 - \frac{C_2}{Q} \qquad (6.3)$$

where $C_{1,2}$ are constants for a given engine and speed. Denoting natural gas and gasifier product gas by NG and PG respectively:

$$(\eta_B)_{PG} = C_1 - \{C_1 - (\eta_B)_{NG}\}\frac{(Q)_{NG}}{(Q)_{PG}} \qquad (6.4)$$

The efficiency data presented in Table 6.2 show a clear distinction between the large 600 series engines and the smaller models. However, for the purposes of this study which is generic in nature, a function for brake thermal efficiency based on linear regression with mixture volume flow rate was derived:

$$(\eta_B)_{NG} = 1.65\frac{W_{22}}{N_{22}} + 38.27 \qquad (6.5)$$

where N_{22} is the number of engines in the installation. This is assumed to be three in all cases. Three units is the minimum number of units likely to be acceptable for reasons of security of energy supply and gas utilisation [159].

As efficiency varies with engine size, the constant C_1 will be a function of efficiency. To derive this function it is necessary to obtain an estimate of the ratio of thermal efficiency with product gas to that with natural gas. Jenkins and Goss [160] obtained a figure of 0.76 for the ratio of efficiency on product gas to that on gasoline, using a small SI engine operating at an equivalence ratio of 1.0, connected to a conventional downdraft gasifier operating on wood chips. Reed and Das [126] propose a range of 0.6-0.85 for the same parameter. However, Jenbacher, in tests using product gas from gasified wood on one of their 200 series engines, obtained a ratio of efficiency on product gas to efficiency on

147

natural gas of 0.95 [15]. The gas contained (on average) 23% CO, 9% H_2 and 2% CH_4. The much higher ratio obtained by Jenbacher may be explained by the engine technology improvements (in particular turbocharging/intercooling and operating in lean-burn mode) which have taken place since the earlier studies. The Jenbacher figure has been used here.

From the air-fuel mixture compositions of natural gas and the product gas used in the Jenbacher tests, it was calculated assuming the same volumetric flow rate that:

$$\frac{(Q)_{NG}}{(Q)_{PG}} = 1.225 \tag{6.6}$$

and from Equations 6.4, 6.6 and the efficiency ratio of 0.95:

$$C_1 = 1.222(\eta_B)_{NG} \tag{6.7}$$

$$(\eta_B)_{PG} = 1.222(\eta_B)_{NG} - 0.222(\eta_B)_{NG}\frac{(Q)_{NG}}{(Q)_{PG}} \tag{6.8}$$

With brake thermal efficiency, the model then calculates overall thermal efficiency and finally electrical output. Electrical output on natural gas is also calculated, as this is used in a correlation to derive capital cost (see below).

In addition, brake thermal efficiency is used to calculate the fraction of thermal input leaving as sensible heat in the cooling water and the exhaust gases. It is assumed that the ratio of exhaust to cooling water heats given in Section 6.2.2 is fixed, and that the unrecoverable losses fraction of 4.3% is also fixed. Exhaust gas temperature and cooling water flow rate may then be calculated, with the assumption that the gas specific heat is evaluated at the mean of actual gas temperature and 0°C.

Cooling water inlet and exit temperatures of 60°C and 90°C respectively have been chosen, reflecting typical values for Jenbacher engines [147,154].

6.2.3.2   Cost Calculations

Capital Cost

The delivered capital cost or equipment cost (EC_{22}), expressed in £'000 (1998), can be correlated with the engine power output on natural gas ($P_{23})_{NG}$ using data from Table 6.2:

$$EC_{22} = N_{22}\left(0.21\frac{(P_{23})_{NG}}{N_{22}} + 74.4\right) \qquad (6.9)$$

where the regression coefficient R^2 is 0.987 (Figure 6.2). The number of units N_{22} is 3 (see Section 6.2.3.1). A 1982 study by ENFOR produced data leading to a very similar correlation for natural gas spark ignition gen-sets (updated to £'000 1998) [161]:

$$EC = 0.215(P)_{NG} + 23.1 \qquad (6.10)$$

with the more modern data differing only by an increased fixed cost, probably related to features such as more sophisticated control systems (see also Figure 6.2).

Equipment cost is then related to the element of total plant cost attributable to the IC engine module (TPC_{22}) by the following function derived as described in Section 2.5.1 using Tables 2.4 and 2.5 (the factors C_3 (Table 2.4) were assigned low values in this case to reflect the fact that the IC engine is a factory-assembled, skid-mounted unit requiring relatively little installation):

$$TPC_{22} = 4.60\,EC_{22}^{0.904} \qquad (6.11)$$

with TPC_{22} in £'000 (1998).

Figure 6.2 IC engine equipment cost [154,161]

Each skid-mounted gen-set will be fitted with an air-cooled radiator of finned-tube design for the cooling water circuit, regardless of whether it is for a power-only or a CHP installation, and this is accounted for in the total plant cost of Equation 6.11. In the case of a CHP installation, the radiator would be used to cool any surplus flow not going to the CHP circuit, or to dump heat in the event of a CHP system failure. If a band dryer is being used, the heated air from the radiator is used as the drying medium.

Labour

The labour requirement per shift L for the engine and generator is taken from Toft [40]:

$$L_{22} = 0.485\, P_{23}^{\,0.483} \tag{6.12}$$

where P is the net electrical power exported from the generator (MW_e).

The worksheet for the IC engine is shown in Appendix 2 Section A2.6.

6.2.4 Effects of Gas Properties

This section reports the use of model described in the previous section to examine the effect of product gas composition, LHV and temperature on engine design point

performance. This work was a deliverable to JOULE project JOR3-CT97-0130 (see Section 1.4). Although the results are not used in any way in the system model, they nevertheless help an understanding of the system model results presented in Chapter 9.

The use of oxygen-enriched air in the engine is not considered, as it was not an option addressed by the JOULE project. Neither is transient behaviour considered; it is assumed that the system will be capable of true steady-state operation and that significant random fluctuations in product gas quality will be absent. Systematic variations in gas quality with time due to the regenerative air pre-heating cycle are predicted to be small (Section 5.3.4).

Results from the gasifier performance evaluation (Tables 5.8 and 5.9) have been used to define the range of gas compositions and LHVs of interest. The H_2O concentration in the product gas entering the engine was assumed to be constant at 0.07. The engine equivalence ratio was fixed at 1.7 (Section 6.2.2).

6.2.4.1 Product Gas LHV

In these calculations, dry LHV was varied between 4.5 and 9.5 MJ/Nm^3 at a constant thermal input to the engine of 10 MW_{th}. This was achieved by allowing the combined concentrations of H_2, CO and CH_4 to vary while keeping the relative volumetric proportions constant at the average values of Tables 5.8 and 5.9 - roughly $[H_2]:[CO]:[CH_4]$ = 23:21:1. The ratio of $[CO_2]$ to $[N_2]$ was also fixed at the average value of 0.7. Product gas inlet temperature was 40°C. Results are shown in Figure 6.3, as a plot of electrical efficiency, derating from natural gas operation and capital cost per kilowatt against LHV.

As LHV increases, the imposed derating from natural gas operation reduces sharply, such that at a LHV of around 9 MJ/Nm^3 no derating at all occurs, despite natural gas having a LHV of 36 MJ/Nm^3. This is because the stoichiometric air requirement for combustion of CO or H_2 is a quarter (by volume) of that for CH_4. As derating reduces, efficiency increases slightly and capital cost per kilowatt falls, particularly at the lower end of the LHV range. If the LHV can be increased from 4.5 to 6.5 MJ/Nm^3, capital cost per kilowatt will fall by around 14%. There are therefore stong marginal benefits from increasing LHV (by O_2 enrichment to the gasifier), particularly at the lower end of the LHV range.
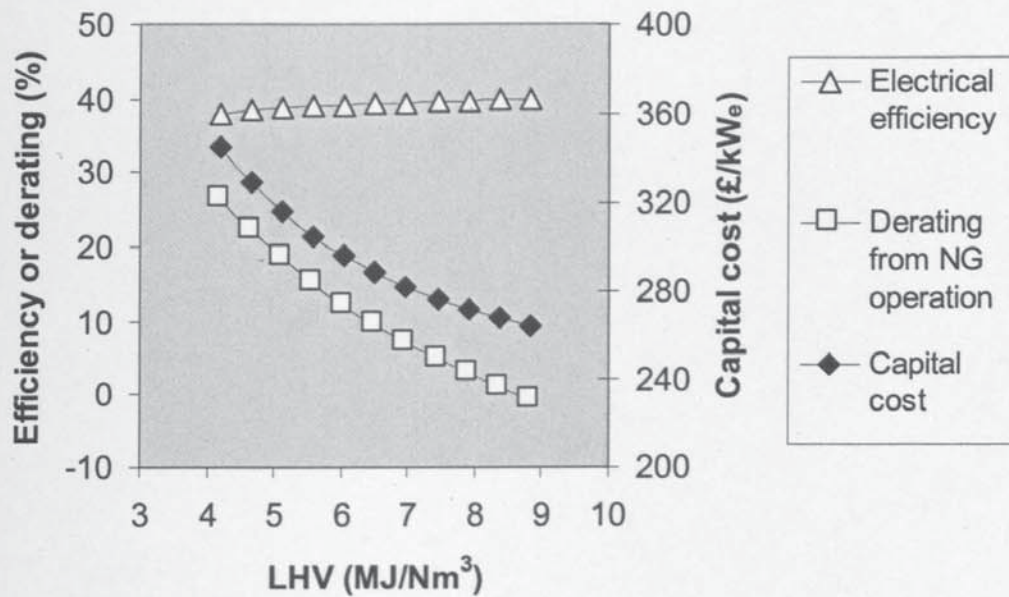
Figure 6.3 Effect of product gas LHV on engine performance

6.2.4.2 Product Gas Composition

At a given LHV, the only significant variation in product gas composition to occur is that in the ratio of H_2 to CO (CH_4 only ever being present in very small quantities). The ratio $[H_2]/[CO]$ is typically around 1, but ranges from 0.7-1.7. In the model calculations, $[H_2]/[CO]$ was allowed to vary across this range, while the thermal input was again fixed at 10 MW_{th} and the dry gas LHV at 7.0 MJ/Nm^3. The ratio $[CO_2]/[N_2]$ was fixed at its average value of 0.7, and $[CH_4]$ was set to zero. Product gas inlet temperature was again 40°C. Results are shown in Figure 6.4, with the same parameters as in Figure 6.3 plotted this time against $[H_2]/[CO]$. The vertical scales are the same as in Figure 6.3.

The higher the $[H_2]/[CO]$ ratio at a fixed LHV, the more derating from natural gas operation is imposed, although the relationship is weak. This occurs because at higher ratios, the combined H_2 and CO flow is greater (H_2 has a lower LHV than CO) so the air requirement is greater. Electrical efficiency falls marginally, and capital cost per kilowatt rises marginally. The strongest influence on $[H_2]/[CO]$ ratio is biomass moisture content - the higher the moisture, the higher the ratio. These results therefore present a weak argument in favour of more drying, but the effects are minor.
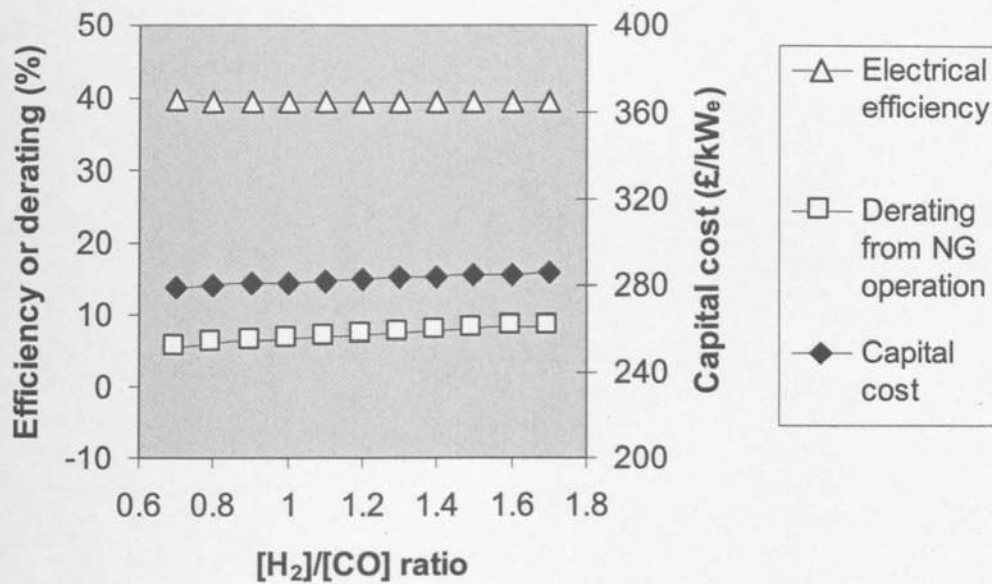
Figure 6.4 Effect of product gas $[H_2]/[CO]$ ratio on engine performance

6.2.4.3 Product Gas Inlet Temperature

The effect of product gas inlet temperature was investigated for a single typical gas composition (dry LHV 7.0 MJ/Nm^3), at a thermal input of 10 MW$_{th}$. Results are shown in Figure 6.5, with the same parameters as in the previous figures (at the same scales) plotted this time against gas inlet temperature.
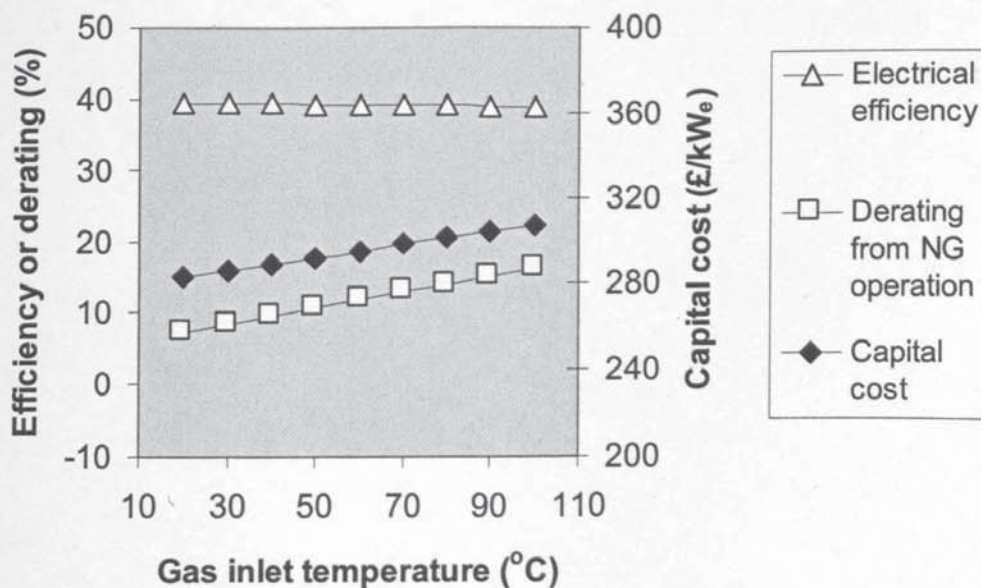
Figure 6.5 Effect of product gas inlet temperature on engine performance

As gas inlet temperature increases, derating increases because of decreasing volumetric efficiency. Electrical efficiency falls slightly, and hence electrical output. Engine size increases because of increased volumetric flow, resulting in an increase in capital cost per kilowatt. Clearly product gas inlet temperature should be minimised within practical constraints, although the benefits are not large in magnitude; reducing gas inlet temperature from 80°C to 40°C gives an increase in electrical output of about 0.7% and a reduction in capital cost per kilowatt of about 4%.

7 OTHER SYSTEM MODULES

7.1 Reception, Storage and Screening

This single module accepts wet biomass as delivered by lorry to the plant gate, and supplies the biomass to the drying module (Figure 2.1). It incorporates reception (i.e. acceptance of the feed from the delivery lorry and transfer to storage using a frond-end loader), storage and screening of the biomass prior to drying, and buffer storage between the drying and gasification steps. These process stages are assumed not to change the biomass in any way (other than in terms of size distribution). In reality, there may be small effects of drying (or wetting), degradation and spillage, but these are difficult to estimate and have been ignored.

The screening stage removes all chips with a mean diameter less than 10 mm for systems with the rotary dryer without burner and the band dryer. This is equivalent to 15% of the delivered biomass (Section 2.4). It may be possible to sell this rejected feed to an external customer; otherwise there will be a disposal cost incurred. No firm economic information was available on either option, however, and these financial streams are therefore not represented in the model. In the case of systems incorporating the rotary dryer with burner, the <10 mm biomass fraction is used as an energy source (Section 2.1). The full biomass size range is dried, with no pre-screening stage necessary (Section 4.3.1.3, Figure 4.1).

At scales of less than about 30 MW_{th} thermal input, the feedstock handling requirements can be met by a single front-end loader [40]. These consume approximately 30 litres per hour of diesel [162]. Assuming an average daily utilisation of 4 hours and a European average diesel price of £0.48/litre [163], this gives an annual fixed utility charge for diesel of £21,000 for all systems. Average daily utilisation may vary with system scale, but such detail is considered beyond the scope of the present work.

In order to avoid a lengthy data collection exercise, functions for the element of total plant cost attributable to the reception, storage and screening systems (TPC_1) has been derived from the model of Toft, who carried out such an exercise in an earlier study [40]. Application of Toft's model for gasifier engine systems in the range 1-5 MW_e results in the

155

following expression for total plant cost attributable to the reception, storage and screening systems:

$$TPC_1 = 679.6\, m_{B1}^{0.338} \qquad (7.1)$$

and excluding a screening stage:

$$TPC_1 = 552.2\, m_{B1}^{0.336} \qquad (7.2)$$

with TPC_1 in £'000. TPC_1 as a proportion of the UGETC capital cost (TPC_{10}) falls in the range 11-18% with screening and 9-15% without screening, for the range of inputs of interest. Labour requirements are also taken from Toft [40], who gives a fixed value of 0.2 persons per shift for each of reception (including handling), storage and screening at scales of below about 30 MW_{th} thermal input, giving a total of 0.6 persons per shift.

The reception, storage and screening model is part of the Other System Modules worksheet, which is shown in Appendix 2 Section A2.11.

7.2 Air Oxygen Enrichment Plant

The air oxygen enrichment plant module takes atmospheric air and delivers oxygen-enriched air to the gasifier module (Chapter 5) and in some cases to the IC engine module (Chapter 6) - see Figure 2.1.

7.2.1 Plant Types

The most widely used method of separating oxygen from air is the cryogenic process, where air is compressed, cooled, partly condensed and fed to a distillation column where the separation takes place. This process delivers very pure oxygen. However, it is only appropriate for applications requiring over 100 tons of oxygen per day, far in excess of the present application, because of its high capital cost and energy requirement [164].

156

Non-cryogenic methods with much lower costs have evolved for smaller applications, and those and less demanding of high purity levels. These include pressure and vacuum swing adsorption (PSA, VSA) techniques and membrane techniques.

PSA and VSA plants use a zeolite molecular-sieve adsorbent to remove nitrogen, carbon dioxide and water from a stream of compressed air. When after a period the sieve becomes saturated, it is regenerated by reducing the pressure. This is done at above-atmospheric pressure in a PSA plant, and under vacuum in a VSA plant. Two parallel sieves are employed, so that a continuous stream of oxygen is produced.

Vacuum operation delivers higher efficiency but at a higher capital cost, and VSA systems tend to be used at higher output requirements. The British Oxygen Company (BOC) recommend PSA systems for oxygen demands below about 15-20 tonnes/day of pure oxygen, and VSA systems for oxygen demands above this, up to a maximum of about 100 tonnes/day [164]. In both systems, oxygen is delivered with an actual purity in the range 90-95%.

Membrane separation, as the name suggests, involves the use of a membrane (hollow-fibre or other) to separate a stream of compressed air into its components as it passes through. As nitrogen will pass the membrane more easily than oxygen, these systems are used primarily to produce a pure nitrogen stream (up to 99.5%); the residual stream is oxygen-enriched, but only up to a maximum of around 40% concentration [165].

The attraction of membrane systems for the production of oxygen-enriched air lies in their simplicity and relatively low cost. However, they are only available commercially at demands of up to about 1250 Nm^3/h of nitrogen [164]. At a nitrogen purity of 95% and a residual stream oxygen concentration of 40% this equates to 420 Nm^3/h of pure oxygen delivered in the residual stream, or about 14.4 tonnes/day.

The anticipated range of demands from the air separation plant in the present study is from about 3 to about 30 tonnes/day of pure oxygen. In view of the inability of membranes to supply above about 14 tonnes/day, or above an oxygen concentration of 40%, it was decided to specify a PSA system for oxygen demands below 15 tonnes/day of pure oxygen, and a VSA system for demands above 15 tonnes/day. Each would supply oxygen at the

minimum purity level of 90%. As the maximum design air oxygen concentration for the RFSG is 60% by volume (Section 5.1.3), there is no need to specify greater than this minimum purity level; to do so would represent increased equipment cost and increased electrical power requirement.

Cost and power consumption data were obtained from BOC for both PSA and VSA types, and these are presented in Table 7.1. Both types would be leased, with the lease fee including installation, commissioning and maintenance but excluding civils and electrical cabling. The lease fee also includes water cooling (PSA) and water treatment (VSA) systems.

Table 7.1 Air separation plant data (BOC)

Generator Type	Generator Output (90% O_2 by vol.) (tonnes/day)	Annual Lease Fee (£/annum, 1999)	Power Consumption (kW)
PSA	3	31,000	50
PSA	10	57,000	175
PSA	20	90,000	350
PSA	30	117,000	525
VSA	20	110,000	245
VSA	30	144,000	306
VSA	40	173,000	408
VSA	58	221,000	590

7.2.2 Performance Calculations

In the performance calculations, the oxygen demands from the gasifier and engine modules are simply added. Each is calculated in a similar way, assuming that the air separation plant delivers oxygen at a purity of 90% by volume which is subsequently mixed with ambient air to achieve the desired oxygen concentration.

By performing a mass balance on the oxygen and nitrogen components, the flow rate of pure oxygen from the air separation unit m_O required by either the gasifier or the engine can be obtained from the following expressions:

$$m_{O8} = m_{A9,21}(1.304[O_2]_{A9,21} - 0.274) \qquad (7.3)$$

$$m_{O8} = m_{A9,21}(1.304[O_2]_{A9,21} - 0.274) \qquad (7.4)$$

where m_{A9} and $[O_2]_{A9}$ are the enriched air flow and concentration to the gasifier, and m_{A21} and $[O_2]_{A21}$ are the enriched air flow and concentration to the engine. Mass flows are expressed in Nm^3/s.

Best-fit correlations for electrical power consumption are derived from Table 7.1, for the PSA system:

$$P_7 = 2470\,m_{O8}^{1.02} \qquad (7.5)$$

and for the VSA system:

$$P_7 = 1153\,m_{O8}^{0.835} \qquad (7.6)$$

where P is electrical power demand in kW. The correlation coefficient R^2 is greater than 0.97 in both cases.

7.2.3 Cost Calculations

Relationships for the lease charge for each system are derived from Table 7.1. For the PSA system:

$$LC_7 = 0.744\left(262.4\,m_{O8}^{0.576}\right) \qquad (7.7)$$

and for the VSA system:

159

$$LC_7 = 0.744\left(373.5\,m_{O8}^{0.654}\right) \qquad (7.8)$$

where LC_7 is lease charge per annum in £'000 (1998). The factor 0.744 is included to adjust the annual payments to real terms, over a project lifetime of 20 years with an inflation rate of 3% (Equation 2.7, Section 2.5.3.1). In both cases, the correlation coefficient R^2 exceeds 0.99.

In addition to the annual lease cost, there will be an initial capital outlay to cover civil work and electrical cabling. From the method described in Section 2.5.1 using Tables 2.4 and 2.5, the capital cost on a total plant cost basis of the civil work and electrical cabling *only* (denoted *ADD*) may be related to that of the entire module *excluding* the civil work and electrical cabling (denoted *EXC*) by the expression:

$$(TPC_7)_{ADD} = 0.822\,(TPC_7)_{EXC}^{0.856} \qquad (7.9)$$

with total plant cost in £'000 (1998). TPC_{EXC} is the capital cost that is avoided by leasing the plant instead, and may be estimated by assuming that the lease fee is equal to the fixed charge on a capital loan of TPC_{EXC}. This fixed charge is calculated to be $0.134 TPC_{EXC}$, assuming a 20 year project life and a discount rate of 12% (Equation 2.6, Section 2.5.3.1). Thus:

$$(TPC_7)_{ADD} = 0.822\left(\frac{LC}{0.134}\right)^{0.856} \qquad (7.10)$$

PSA systems require a substantial flow of water for compressor cooling. The cooling system is recirculating, with a small cooling tower. The make-up water requirement calculated from:

$$m_{C7} = 0.04\left(\frac{P_7}{10}\right) \qquad (7.11)$$

where m_{C7} is expressed in tonnes/hour, and P_7 is compressor power in kW [166]. VSA systems do not require water for cooling, but have a small water requirement for sealing of about 0.7 tonnes/hour independent of size [166]. This water requires treatment on-site prior to use.

The charge for metered water is taken as £0.785/m^3 after correction to 1998 values [43]. It is assumed that the water would be sufficiently uncontaminated and within the required temperature limits for discharge to the drain rather than the foul sewer; charges for this are small, and may be ignored.

There are no maintenance or labour charges to be included.

The air oxygen enrichment plant model is part of the Other System Modules worksheet, which is shown in Appendix 2 Section A2.11.

7.3 Heat Recovery Plant

This module comprises a maximum of four separate heat recovery operations, three of which are associated with CHP systems and the other with hot air drying (see Figure 2.1):

- hot water production from the engine coolant circuits in a CHP system (the engine coolant water heater) - see Chapter 6

- hot water production from the hot product gas in a CHP system (the product gas water heater) - see Chapter 5

- hot water production from the engine exhaust gas in a CHP system (the engine exhaust gas water heater) - see Chapter 6

- hot air production from the engine coolant circuits for use in a band dryer (the engine coolant radiator) - see Chapters 4, 6

For CHP systems, the hot water heat recovery circuit is illustrated in Figure 7.x.

161
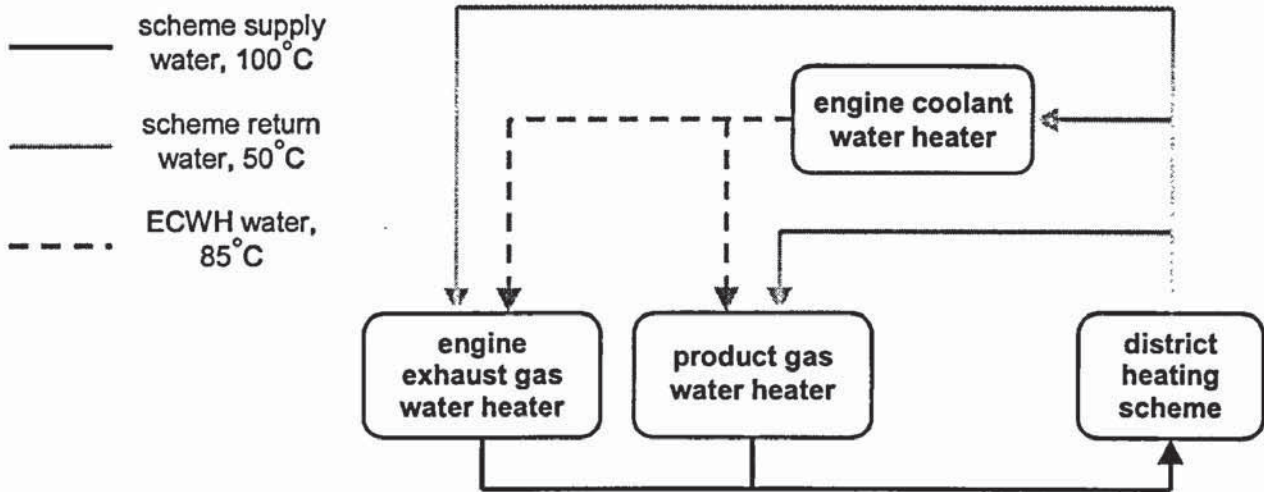
Figure 7.1 CHP heat recovery circuit

For each of these operations, a particular type of heat recovery device has been selected and a model constructed. In the case of hot air production from the engine coolant circuits, the heat recovery device is the radiator supplied with the IC engine (Section 6.2.3.2), and all costs for the radiator are incorporated in the functions for the IC engine. Otherwise, a labour requirement of 0.1 persons per shift has been allocated to each of the CHP system devices, as recommended by Ulrich [167].

7.3.1 Engine Coolant Water Heater

Some 30% of the thermal input to the IC engine is removed by the engine coolant circuits, appearing as a flow of hot water at 90°C which must be cooled externally to 60°C before returning to the engine (Section 6.2.2, Section 6.2.3.1). This is done either by a radiator, or in the case of a CHP system by a parallel combination of a radiator and a heat exchanger heating water for the CHP heat circuit – the engine coolant water heater (Figure 7.1). The radiator in a CHP system may be required if heated air is required for drying, if the maximum flow of hot water attainable exceeds the amount that can be further heated to process conditions in boilers or secondary heaters (unlikely in hot water CHP systems such as this), or if the CHP system fails for some reason.

Liquid-to-liquid heat exchange is most commonly accomplished in industry with shell-and-tube heat exchangers [168], and this has been assumed here. Shell and tube heat

162

exchangers are relatively compact and give high heat transfer coefficients. A typical design is shown in Figure 7.2.
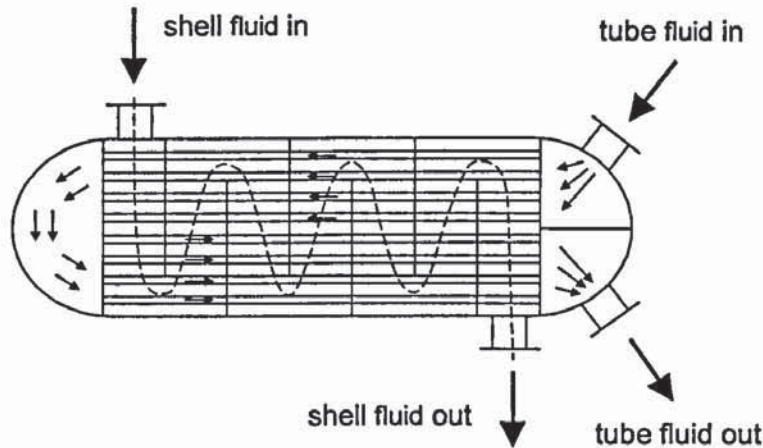
Figure 7.2 Shell-and-tube heat exchanger

7.3.1.1 Performance Calculations

The performance calculation for the engine coolant water heater is a simple energy balance to find the quantity of heated process water, as all other parameters are supplied to the model. The process water mass flow is given by:

$$m_{W28} = m_{C28} \frac{(T_{C27} - T_{C29})}{(T_{W29} - T_{W27})} \qquad (7.12)$$

where m is mass flow, T temperature, and subscripts W and C denote CHP and cooling water respectively. Heat loss from the heat exchanger casing is ignored; in a well-designed example this should be no higher than 1-2% [169]. The cooling water inlet and outlet temperatures are fixed at 90°C and 60°C (Section 6.2.3.1). The process water inlet temperature is the return temperature from the heat customer, and is fixed at 50°C (see Section 2.4 and Figure 7.1).

The heat exchanger pass arrangement is assumed to provide pure counter-flow, so that the minimum temperature difference (the "pinch" temperature) occurs at the point at which the process water leaves and the cooling water enters: this is set at 5°C, to give a fixed process

163

water outlet temperature of 85°C. The cooling water mass flow is therefore the single variable input; this is equal to the total cooling water flow (supplied from the IC engine sub-model) less any flow to the radiator to provide drying air. Equation 7.12 can therefore be reduced to:

$$m_{W28} = 1.2 \, m_{C28} \qquad (7.13)$$

7.3.1.2 Cost Calculations

Equipment cost (EC_{28}) for shell-and-tube heat exchangers is taken from Garrett [170], suitably modified for units and time-base:

$$EC_{28} = 0.898 \, A_{28}^{0.68} \qquad (7.14)$$

where A_{28} is heat transfer area in m^2, and cost is in £'000 (1998). Heat transfer area is calculated from:

$$A_{28} = \frac{Q_{28}}{U_{28} F_C (\Delta T_{28})_{LM}} \qquad (7.15)$$

where Q_{28} is heat transferred (calculated either from the cooling or CHP water streams), U_{28} is an area-based overall heat transfer coefficient, F_C is a counter-flow factor indicating the approximation to pure counterflow (set arbitrarily to 0.9) and ΔT_{28} is the temperature difference with LM denoting log-mean [171]. A value of 938 W/m^{2}K has been used for U_{28} [172].

The element of total plant cost attributable to the engine coolant water heater (TPC_{28}) is then related to equipment cost by the following expression derived as described in Section 2.5.1 using Tables 2.4 and 2.5:

$$TPC_{28} = 9.76 \, EC_{28}^{0.798} \qquad (7.16)$$

with costs again in £'000 (1998).

The worksheet for the ECWH is shown in Appendix 2 Section A2.8.

7.3.2 Product Gas and Engine Exhaust Gas Water Heaters

Recovery of the sensible heat in hot gases to heat water in a small-scale CHP system is usually carried out in a fire-tube "boiler" (Figure 7.3), so known as these devices can also be fired directly, and/or used to raise steam [171,173,174].

Figure 7.3 Firetube boiler (fired type)

Fire-tube boilers are effectively shell-and-tube heat exchangers in which the water is the shell fluid while the tubes carry the hot gases. Two of these devices are required in a BGES for CHP (Figure 7.1). The first recovers heat from the gasifier product gas, and is referred to as the product gas water heater. The second recovers heat from the engine exhaust gas, and is referred to as the engine exhaust gas water heater.

Figure 2.3 shows the locations of the product gas water heater and engine exhaust gas water heater in a typical BGES flowsheet.

7.3.2.1 Performance Calculations

As with the engine coolant water heater, the performance calculation is an energy balance to find the quantity of hot water produced, all other parameters being supplied to the model. The hot water mass flow is given by the expressions:

$$m_{W18} = \frac{m_{G18} \, c_{G18} \, (T_{G17} - T_{G19})}{(H_{W19} - H_{W17})} \qquad (7.17)$$

$$m_{W31} = \frac{m_{G31} \, c_{G31} \, (T_{G30} - T_{G32})}{(H_{W32} - H_{W30})} \qquad (7.18)$$

where c is specific heat evaluated at the mean temperature, H enthalpy, and subscript G denotes gas. Equation 7.17 refers to the product gas water heater, Equation 7.18 to the engine exhaust gas water heater. Heat loss from the heat exchanger casing is again ignored; data for this type of boiler under these conditions could not be obtained, but losses are expected to be small given the relatively low operating temperatures.

All the input parameters in this case are variables supplied from other module sub-models. In the case of the product gas water heater, gas composition, flow rate and temperature are supplied by the gasifier model. In the case of the engine exhaust gas water heater, the same parameters are supplied by the engine model. If the rotary dryer with burner has been selected, similar parameters are supplied by that sub-model for the burner exhaust gases (see Section 4.3.1.3); the two flows are then mixed (Figures 2.7, 2.9).

The minimum gas outlet temperature is assumed to be 20°C above the hot water outlet temperature, or in this case 120°C (see Section 2.4); the differential of 20°C is a typical minimum figure for gas-air heat exchangers in applications such as this, representing a sensible compromise between efficiency and cost [23].

In the case of the product gas water heater, this minimum value is always set (see below). In the case of the engine exhaust gas water heater, the minimum value is set only if a rotary dryer with burner is being used (Section 4.3.1.3, Figures 2.7, 2.9), or if the minimum

temperature exceeds that required by the dryer. Otherwise, the gas outlet temperature is defined by the dryer model (or in the case of the band dryer, the associated heat exchanger model - see Section 7.3.3 and Figures 2.11, 2.13).

Feed water comes from the engine coolant water heater at 85°C, with any deficit made up directly from the CHP return at 50°C (see Figure 7.1). The product gas water heater is assumed to have first call on the feed water from the engine coolant water heater, with any remainder going to the engine exhaust gas water heater. If the feed water to either of the heaters is a mixture of engine coolant water heater water and return water, an iteration is necessary to calculate the actual mix, as the feed water inlet temperature and total flow rate are functions of each other.

It is assumed that there are no contaminants in either gas which would cause corrosion or fouling problems in the water heaters. Corrosion from H_2S has caused problems in syn-gas coolers on coal-fired IGCC systems [175], and chlorine-based corrosion is a well-known problem in boilers firing high-chlorine fuels [176]. However, sulphur and chlorine are present only at very low levels in woody biomass [91]. It is therefore assumed necessary only to maintain gas temperature above the water dew point, which cannot exceed 100°C at atmospheric pressure.

7.3.2.2 Cost Calculations

Equations 7.14 and 7.15 for shell-and-tube heat exchangers are again used to calculate equipment cost. The counter-flow factor is again taken as 0.9, but the area-based overall heat transfer coefficient set to a much lower value of 50 W/m^2K [174,177] because of the poor heat transfer on the gas side.

The element of total plant cost attributable to the product gas water heater and the engine exhaust gas water heater (TPC_{18} and TPC_{31} respectively) is again calculated in each case using Equation 7.16.

The worksheet for the product gas water heater is shown in Appendix 2 Section A2.9, and that for the engine exhaust gas water heater in Appendix 2 Section A2.10.

7.3.3 Engine Coolant Radiator

The engine coolant radiator is supplied with the IC engine, and is assumed to be of the usual air-blown finned-tube design [128]. The hot air is either vented to atmosphere, or ducted to a band dryer (in which case the radiator fan is assumed to be sufficiently sized).

7.3.3.1 Performance Calculations

A performance calculation is only necessary if a band dryer is selected, when it is necessary to calculate the amount of cooling water needed to supply the required drying air flow. In power-only cases, this is simply a check to ensure that enough heat is available. In CHP cases, the amount of cooling water needed is subtracted from the amount supplied by the engine, to give the flow to the engine coolant water heater.

The performance calculation is again a straightforward energy balance to find the quantity of hot water required given the hot air demand. The hot water mass flow is given by:

$$m_{C25} = \frac{m_{A25}\, c_{A25}\, (T_{A26} - T_{A24})}{(H_{C24} - H_{C26})} \qquad (7.19)$$

Heat loss from the engine coolant radiator outer casing is ignored. The engine coolant radiator is assumed to have a cross-flow type arrangement of relatively low effectiveness, with the air assumed to leave the heat exchanger at a temperature 10°C below the water outlet temperature.

The worksheet for the engine coolant radiator is shown in Appendix 2 Section A2.7.

7.4 Product Gas Quench and Waste Water Treatment

The product gas quench scrubber receives hot product gas either directly from the gasifier (Chapter 5) or from the product gas water heater in CHP systems (Section 7.3.2), and supplies cool product gas to the IC engine (Chapter 6).

There has been much effort devoted to technologies for the removal of tars from biomass gasifier product gases [22,178]. In the present study it is assumed that such equipment is unnecessary, as for both gasifier types the tar content of the product gas leaving the gasifier is assumed to be only 100 mg/Nm^3 (Section 5.4), an acceptable level for an IC engine (Section 6.1.1.1). However, in a CHP system the product gas will leave the product gas water heater with a temperature of at least 100°C, and in a power-only system without water heaters the temperature will be around 400°C. The IC engine requires the product gas temperature to be a maximum of 40°C at 75% relative humidity (Section 6.2.3). It is therefore necessary to provide a water quench to achieve the necessary cooling.

The product gas is assumed to leave the quench saturated at 35°C, with a moisture content taken as that for saturated air at 35°C, i.e. about 5% by volume (Section 6.2.3). The quench is a recirculating scrubber with a cooler. The environmental issues surrounding condensates from biomass product gases can present problems for on-site treatment [179]; however it is assumed here that the excess water condensing from the product gas is discharged to the foul sewer for treatment at the local water works (see below). The quench scrubber also serves to provide a final stage of gas clean-up.

Garrett [170] gives correlations for the equipment cost (EC_{20}) of a quench scrubber as a function of volumetric gas throughput. This is assumed to include a cooler, recirculation pump etc. For the range of interest here the equipment cost is virtually constant at £11,100 after adjustment to 1998 values.

The element of total plant cost attributable to the product gas quench module (TPC_{20}) is related to equipment cost by the following expression derived as described in Section 2.5.1 using Tables 2.4 and 2.5:

$$TPC_{20} = 4.57\,EC_{20}^{0.889} \qquad (7.20)$$

with costs in £'000 (1998).

The following fixed rates are taken to apply for industrial water consumption and effluent discharge to the sewerage system (Yorkshire Water data, corrected to 1998 values [43]):

169

Water use:	£0.785/m^3
Effluent conveyance to treatment plant:	£0.229/m^3
Effluent primary treatment:	£0.226/m^3

An additional charge is then made for effluent secondary treatment based on chemical oxygen demand (*COD*) and settleable solids (*StS*), both expressed as mg/l:

$$\left(\frac{COD}{905} \times £0.222\right) + \left(\frac{StS}{314} \times £0.126\right) \qquad (7.21)$$

These rates multiplied by the relevant annual consumption or discharge rates gives the total cost per annum paid to the water company.

The effectiveness of the quench scrubber in removing any remaining tars or particulates is not likely to be high. Tar and particulate levels reaching the scrubber are 100 mg/Nm^3 in each case (Section 5.4). It is assumed that 50 mg/Nm^3 of tars in the product gas are removed (50% efficiency of removal), and in addition an arbitrary 50 mg/Nm^3 of particulates are removed. The water discharged is taken to be the water content of the product gas into the scrubber less the water content of the product gas out of the scrubber - i.e. the system is fully recirculating and only the condensate is discharged. The chemical oxygen demand of tars is taken as 2 kg$_{O2}$/kg$_{TAR}$, based on a typical tar analysis [180].

No specific labour allocation is made for the quench scrubber.

The product gas quench and waste water treatment model is part of the Other System Modules worksheet, which is shown in Appendix 2 Section A2.11.

7.5 Grid Connection

The grid connection module takes the net electrical output from the generator coupled to the IC engine (Chapter 6), and exports it to the grid.

The element of total plant cost attributable to the grid connection module (TPC_{34}) is taken from Toft [40]:

$$TPC_{34} = 234.4 \, P_{33}^{0.537} \qquad (7.22)$$

where P is power exported to the grid, and TPC_{34} is expressed in £'000 (1998). There are no labour costs associated with grid connection.

The grid connection model is part of the Other System Modules worksheet, which is shown in Appendix 2 Section A2.11.

8 SYSTEM MODEL

8.1 Modelling Approach

The modelling task being undertaken here is the development of a steady-state representation of an entire power/CHP system from biomass delivery to power/heat export. The purpose is to predict a number of key overall performance and economic parameters in response to a set of fixed and variable inputs, to enable consistent comparisons and technical and economic optimisation. The accuracy and detail demanded is equivalent to that of a scoping or pre-feasibility study for a new project, in which initial technology choices are to be made, order-of-magnitude costs estimated, operational characteristics investigated and certain key design point values fixed. Detailed design of individual components leading to accurate performance and cost data is not the intention here, nor would it be practical without an actual site and a firm proposal in mind (and the project finance necessary for such an undertaking).

The review of Chapter 3 revealed two main approaches to system studies of this kind. In one, process flow software is used, usually to resolve complex configurations. This generally requires a process flow software package to be already available - few studies of this kind would have the time and resources to develop its own. In the other, spreadsheets (or simple dedicated codes which would nowadays be constructed on spreadsheets) are used.

Process flow software packages are generally expensive, and are intended primarily for the modelling of processes with a large number of components, streams and interconnections whose optimisation is complex. They do not generally give costs. The packages mostly operate in a similar way. There are a number of well-known commercially available general-purpose software packages for the process industries, with a very wide range of functional capabilities, property databases and component sub-models; examples would include ASPEN PLUS [181] and HYSIS [182]. Some of these will have power-plant component sub-models in their libraries (combustors, boilers, steam turbines etc.), but all allow the addition of user-defined sub-models as required.

ASPEN PLUS has been used quite extensively for modelling of large power systems, including biomass gasification combined cycle systems [44,45,46,64] (see Section 3.2). In addition, many companies and institutions have developed their own process flow software packages dedicated to their particular application, and there are a number of these specific to power systems, some of which are available commercially [e.g. 183].

Process flow software is probably essential for the modelling of large scale power systems with complex steam or combined cycles. However, to use such codes to model the small-scale, relatively simple power system under consideration here is not considered justified. Even if a package were already freely available, the task would utilise only a tiny part of the package's capabilities, while still requiring the creation of a number of user-defined sub-models. The setting up of each configuration can be time-consuming, and the initial familiarisation period with the software can be lengthy.

The alternative approach is to construct a spreadsheet model using one of the widely available office packages such as Microsoft Excel or Lotus 1-2-3. The usual practice is to allocate a worksheet to each system component to be modelled in detail, and then to pass key variables between worksheets [40,51]. The modeller usually has to start from a clean sheet with such an approach, as pre-prepared models or sub-models are rarely available in the right format if at all. However, this can be an advantage, as the level of detail to which each system component model is represented can be kept to the minimum necessary for the purposes of the study, and the overall model can be designed specifically to meet the requirements of the study.

Spreadsheet models tend to be easy to reconfigure and fast to run, provided the system being modelled is relatively simple. They are also more directly accessible to the non-expert or unfamiliar user.

The spreadsheet approach is adopted here, using the Microsoft Excel package. The package allows user programming with the Visual Basic code, so that routines can be created for such tasks as multi-variable iterative procedures and rapid calculation of multiple cases. This facility makes such packages well suited to studies such as the present one in which a large number of configurations and design point options are to be tested.

8.2 Model Structure

The model is structured as a series of worksheets. These comprise an initial inputs worksheet, followed by a set of worksheets containing the module sub-models, and ending with a results worksheet. The various module sub-models have been described in the preceding chapters. The Inputs and Results worksheets are described in the following sections.

8.2.1 Inputs Worksheet

The Inputs worksheet is shown in Appendix 2 Section A2.1, and is reproduced here as Figure 8.1. It contains the principal variables the user is able to manipulate to form a standard "case", although there are numerous other constants throughout the model (Section 8.4) which may be modified by the expert user in light of new or better information.

The principal variables are grouped into three categories:

- configuration variables select the gasifier type, the dryer type, the output type (power-only or CHP) and whether or not the IC engine is fed with oxygen-enriched air (RFSG only);

- condition variables specify the biomass cost, the biomass dry flow rate to the gasifier, the biomass moisture content to and from the dryer and the air oxygen concentration to the gasifier (RFSG only);

- cost calculation variables specify the discount rate (the "cost of money"), the project life, the plant number and the RFSG capital cost factor (Section 5.4.2.1).

The model is capable of calculating either a single or multiple sets of the five condition variables. In the case of multiple sets, each condition variable is specified as a list of up to ten values, and the model calculates all permitted combinations of the listed variables.

CONFIGURATION

Gasifier type	1	1	RFSG
		2	UGETC
Dryer type	1	1	rotary cascade
		2	rotary cascade (integral burner)
		3	band conveyor
Engine type	1	1	ambient air
		2	oxygen-enriched air
Output type	2	1	power only
		2	CHP

CONDITIONS - SINGLE RUN

Biomass cost at plant gate	80	£/dt	range 20 - 120
Biomass dry flow rate to gasifier	0.556	kg/s	range 0.1 - 0.6
Biomass moisture at dryer inlet	100	% db	range 40 - 120
Biomass moisture at dryer outlet	50	% db	range 10 - 50
Air oxygen concentration to gasifier	0.60	frac. by vol	range 0.21 - 0.6

Single Run

CONDITIONS - MULTIPLE RUNS
(all combinations calculated)

New Table   Add to Table

Biomass cost at plant gate £/dt	Biomass dry flow rate to gasifier kg/s	Biomass moisture at dryer inlet % db	Biomass moisture at dryer outlet % db	Air oxygen conc. to gasifier frac. by vol
80	0.556	50	10	0.21
		75	20	0.28
		100	35	0.4
			50	0.6

COST CALCULATION PARAMETERS

Discount rate *I*	12	%
Project life *L*	20	yrs
Plant number *n* (i.e. *n*th plant)	10	
Annuity factor *AF*	0.0996	
Learning ratio *LR*	0.476	
Electricity price	0.0369	£/kWh
RFSG capital cost factor (F)	1	

Figure 8.1 Inputs worksheet

The worksheet checks to see whether entered data are within the range of model applicability, and also that the biomass moisture content from the dryer does not exceed that to it. The biomass moisture contents to and from the dryer may be equal, in which case no drying stage is included in the system.

8.2.2 Results Worksheet

The Results worksheet is shown in Appendix 2 Section A2.12, and is reproduced here as Figure 8.2. Results are tabulated with the variables in rows and the cases in columns.

The condition variables from the Inputs worksheet are summarised in the first rows. Thermal input to the gasifier is also calculated, on an LHV basis (it is necessary to reduce the biomass dry LHV at zero moisture by the latent heat of evaporation of the actual post-dryer moisture). Following this the key results from each system module worksheet are summarised. Finally overall system parameters are calculated. These include:

- *Net electrical output*

    The output from the IC engine generator multiplied by a factor of 0.95 to represent an assumed parasitic consumption of 5% for all components excluding the dryer and the air oxygen enrichment plant [40], less the specific calculated electrical consumption of the dryer and the air oxygen enrichment plant (if present).

- *Hot water production*

    The total production from the product gas and engine exhaust gas water heaters.

- *Overall efficiency*

    The net electrical output in MW, plus the net heat output in MW (CHP cases), divided by the thermal input to the system in MW, including the undersize biomass fraction. Again, the biomass dry LHV at zero moisture (Table 2.3) must be reduced by the latent heat of evaporation of the actual pre-dryer moisture.

176

CONFIGURATION: RFSG (F=1), rotary cascade dryer, ambient air engine, CHP

All quantities dry basis u p s.		CURRENT CASE	RESULTS TABLE							
Biomass cost at plant gate	£/t	80	80	80	80	80	80	80	80	80
Biomass flow rate to gasifier	kg/s	0.556	0.556	0.556	0.556	0.556	0.556	0.556	0.556	0.556
Biomass thermal input to gasifier	MW	9.45	9.99	9.99	9.99	9.99	9.85	9.85	9.85	9.85
Biomass moisture at dryer inlet	% db	100	50	50	50	50	50	50	50	50
Biomass moisture at dryer outlet	% db	50	10	10	10	10	20	20	20	20
Air oxygen concentration to gasifier	frac. by vol	0.6	0.21	0.28	0.4	0.6	0.21	0.28	0.4	0.6
Status		OK	OK	OK	OK	OK	OK	OK	OK	OK

MAJOR SYSTEM ELEMENTS

Reception, Storage, Screening

TPC	£000	266	266	266	266	266	266	266	266	266
Annual cost of capital	£000 p.a.	26.4	26.4	26.4	26.4	26.4	26.4	26.4	26.4	26.4
Other operating costs	£000 p.a.	123.2	123.2	123.2	123.2	123.2	123.2	123.2	123.2	123.2

Dryer

Electrical power	kW	34.6	46.9	45.9	45.3	44.7	37.8	37.2	36.9	36.5
Dryer TPC	£000	245	285	282	280	278	257	255	254	252
Dryer annual cost of capital	£000 p.a	24.4	28.4	28.1	27.9	27.7	25.6	25.4	25.2	25.1
Dryer other operating costs	£000 p.a.	69.6	72.8	72.6	72.4	72.3	70.5	70.4	70.3	70.2

Air Oxygen Enrichment Plant

Electrical power	kW	211.9		118.1	227.0	211.6		118.3	227.2	211.7
TPC (additional capital)	£000	86.9		46.0	63.0	86.8		46.0	63.1	86.8
Annual cost of additional capital	£000 p.a	8.6		4.6	6.3	8.6		4.6	6.3	8.6
Lease cost	£000 p.a.	73.7		35.1	50.7	73.7		35.1	50.7	73.7
Other operating costs	£000 p.a.	7.8		4.4	7.5	7.8		4.4	7.5	7.8

Gasifier

Cold gas efficiency (LHV basis)	%	78.8	85.3	84.6	85.7	85.6	83.7	83.2	84.4	84.2
TPC	£000	2412	2412	2412	2412	2412	2412	2412	2412	2412
Annual cost of capital	£000 p.a	240.2	240.2	240.2	240.2	240.2	240.2	240.2	240.2	240.2
Other operating costs	£000 p.a.	337.5	337.5	337.5	337.5	337.5	337.5	337.5	337.5	337.5

Gas Quench & Waste Water Treatment

TPC	£000	19	19	19	19	19	19	19	19	19
Annual cost of capital	£000 p.a	1.8	1.8	1.8	1.8	1.8	1.8	1.8	1.8	1.8
Other operating costs	£000 p.a.	9.0	5.2	5.0	4.8	4.7	6.2	6.0	5.8	5.7

Engine

Engine electrical output	MW	3.09	3.33	3.33	3.40	3.41	3.25	3.25	3.33	3.35
Overall efficiency	%	38.7	38.6	38.9	39.2	39.5	38.4	38.7	39.1	39.3
TPC	£000	1092	1185	1138	1108	1079	1187	1141	1112	1083
Annual cost of capital	£000 p.a	109	118	113	110	107	118	114	111	108
Other operating costs	£000 p.a.	171	181	178	176	174	181	177	176	174

CHP

ECWH TPC	£000	46	48	48	48	48	48	48	48	48
ECWH annual cost of capital	£000 p.a.	4.6	4.8	4.8	4.8	4.8	4.8	4.7	4.7	4.7
ECWH other operating costs	£000 p.a.	13.7	13.9	13.8	13.8	13.8	13.8	13.8	13.8	13.8
PGWH hot water production	kg/s	13.55	11.36	11.36	11.65	11.77	11.81	11.82	12.12	12.20
PGWH TPC	£000	57	56	54	52	50	58	55	54	52
PGWH annual cost of capital	£000 p.a	5.6	5.6	5.4	5.2	5.0	5.7	5.5	5.3	5.2
PGWH other operating costs	£000 p.a.	14.5	14.5	14.3	14.2	14.0	14.6	14.4	14.3	14.1
EEGWH hot water production	kg/s	4.29	8.56	8.37	8.37	8.26	8.56	8.40	8.41	8.33
EEGWH TPC	£000	33	48	47	47	46	53	52	52	52
EEGWH annual cost of capital	£000 p.a.	3.3	4.8	4.7	4.7	4.6	5.3	5.2	5.2	5.1
EEGWH other operating costs	£000 p.a.	12.6	13.8	13.8	13.7	13.7	14.3	14.2	14.2	14.1
Total hot water production	kg/s	17.84	19.92	19.74	20.02	20.03	20.37	20.21	20.53	20.54
TPC	£000	135	153	149	147	144	159	155	153	151
Annual cost of capital	£000 p.a.	13.5	15.2	14.8	14.6	14.4	15.8	15.5	15.3	15.0
Other operating costs	£000 p.a.	40.8	42.2	41.9	41.8	41.6	42.7	42.4	42.3	42.1

Grid Connection

TPC	£000	191	206	202	200	201	203	199	198	199
Annual cost of capital	£000 p.a.	19.0	20.5	20.1	19.9	20.1	20.3	19.9	19.7	19.9
Other operating costs	£000 p.a.	15.2	16.5	16.1	16.0	16.1	16.3	16.0	15.9	16.0

WHOLE SYSTEM

Net electrical output	MW	2.70	3.12	3.00	2.97	3.00	3.05	2.94	2.91	2.94
Hot water production	kg/s	17.84	19.92	19.74	20.02	20.03	20.37	20.21	20.53	20.54
Hot water production	MW	3.74	4.17	4.13	4.19	4.20	4.27	4.23	4.30	4.30
Overall electrical efficiency	%	26.2	28.1	27.0	26.7	27.0	27.5	26.5	26.2	26.5
Overall combined efficiency	%	62.5	65.6	64.2	64.4	64.7	65.9	64.6	64.9	65.2
Total plant cost	£000	4446	4524	4513	4495	4486	4502	4493	4476	4468
Total plant cost	£/kW	690	620	632	628	624	615	626	621	617
Biomass cost	£000 p.a	1320	1320	1320	1320	1320	1320	1320	1320	1320
Annual cost of capital	£000 p.a	443	451	449	448	447	448	447	446	445
Other operating costs	£000 p.a	848	779	814	830	851	777	812	829	850
Total operating costs	£000 p.a.	2611	2550	2583	2598	2618	2546	2580	2595	2615
Revenue from heat sales	£000 p.a	290	320	318	322	322	327	325	329	329
Total sales revenue	£000 p.a	990	1127	1095	1089	1097	1117	1086	1082	1091
Cost of electricity (CHP)	£/kWh	0.122	0.102	0.108	0.109	0.109	0.104	0.109	0.111	0.111

Figure 8.2 Results worksheet

177

- *Total plant cost*

  The sum of all the system module costs (on a total plant cost basis), expressed both in absolute terms and as a cost per installed kW (of electricity for power-only cases, electricity plus heat for CHP cases).

- *Biomass cost*

  The annual cost of biomass, found from the cost per tonne and the flow rate to the gasifier, taking account of the biomass undersize fraction and the system annual capacity factor (Section 2.4).

- *Total production costs*

  The sum of all system module annual operating costs and annual costs of capital, plus the biomass cost.

- *Revenue from heat sales*

  It is assumed that the district heat scheme can take all the heat offered by the CHP plant, but will only purchase from the CHP plant if it is clearly the cheapest way of obtaining the heat. It is also assumed that no price support mechanism or other means of subsidy operates for heat sales.

  Thus the price of the heat is calculated as that equivalent to the cost of meeting the same heat load by installing a new natural gas boiler (capital plus operating costs), less the cost of installing any piping infrastructure to bring the heat from the CHP plant to the district heating scheme, less an arbitrary discount of 10% included to provide a clear price incentive for selection of the CHP option.

  The 1998 European Union average natural gas price to industry of 0.89 p/kWh is used [184]. The boiler thermal efficiency is taken as 0.9 [150], and arbitrary values

are chosen for water mean pipe velocity (0.5 m/s) and distance from CHP plant to district heating scheme connection point (500m). The installed cost for insulated piping is taken from Garrett [170]. The factors of Table 2.5 are used to convert to a total plant cost basis.

From these data the following best-fit correlation is obtained for price of heat *HP* (£/kWh):

$$HP = (70.0 + 8.70 \ln Q)^{-1} \qquad (8.1)$$

where Q is heat exported in MW_{th}. For a typical heat flow of 3 MW_{th}, the heat price is 0.013 £/kWh, or about 30% of the average price paid for electricity by industry in Europe in 1998 [184].

- *Cost of electricity*

Total production cost, less revenue from heat sales (CHP cases), divided by the annual electrical output in kWh ((taking account of capacity factor).

8.2.3 Data Flows

Tables A2.1-A2.16 in Appendix 2 give all parameters passed in to and out of each sub-model. For each parameter, the sending or receiving sub-model is also given.

8.3 Model Operation

The model operates by automatic formula calculation within the spreadsheets, supplemented by Visual Basic routines for overall management and certain more complex calculation procedures.

On completing a set of entries in the Inputs worksheet (Appendix 2 Section A2.1), the user launches the model by clicking one of three buttons on the worksheet; *single run, new*

table or *add to table*. These, combined with the configuration variable selections, initiate the appropriate Visual Basic routines.

For *single run* operation the model calculates only the case defined by the condition variables specified in the "Conditions – Single Run" sector of the worksheet. Any pre-existing data on the Results worksheet (Appendix 2 Section A2.12) are deleted. For *new table* operation the model calculates all the cases defined by the condition variables specified in the "Conditions – Multiple Runs" sector of the worksheet, entering the results for each case on the Results worksheet as a series of columns, having first deleted any pre-existing data. *Add to table* operation is similar, except that the model does not delete pre-existing data, instead adding the new data from the first free column.

For each case calculated, if there is insufficient heat available to meet the specified drying duty, an error message is returned and no data are written to the Results worksheet.

There are two Visual Basic calculation routines, for power-only and for CHP cases involving the rotary dryer (with or without an integral burner). These invoke a proprietary solver within Excel to perform the design point calculation, which in one case involves an optimisation (Section 4.3.1.3).

The overall calculation for power-only cases is a linear process. For CHP cases however, the inter-linkage of the principal fuel path and the heat recovery circuit adds complexity. The logic of the calculation procedure is designed to maximise hot water production in each case. The inlet and outlet gas temperatures of the various heat recovery devices and the flow rates through them are either fixed, or calculated in the upstream and downstream module sub-models. The heat recovery circuit is illustrated in Figure 8.3.

The hot water temperature delivered by the engine coolant water heater is below that required for the district heating scheme, and this water is therefore supplied to the product gas water heater and engine exhaust gas water heater as feed water (Figure 8.3). Hot water production from the engine coolant water heater is independent of both the product gas water heater which has a fixed gas exit temperature, and the engine exhaust gas water heater which is downstream. If there is insufficient water supply from the engine coolant water heater to meet the combined capacities of the product gas water heater and engine

exhaust gas water heater, then district heating scheme return water is added (Figure 8.3). If on the other hand the calculated hot water supply from the engine coolant water heater exceeds the combined capacities of the product gas water heater and engine exhaust gas water heater, the surplus engine coolant is in fact diverted from the engine coolant water heater to the radiator.
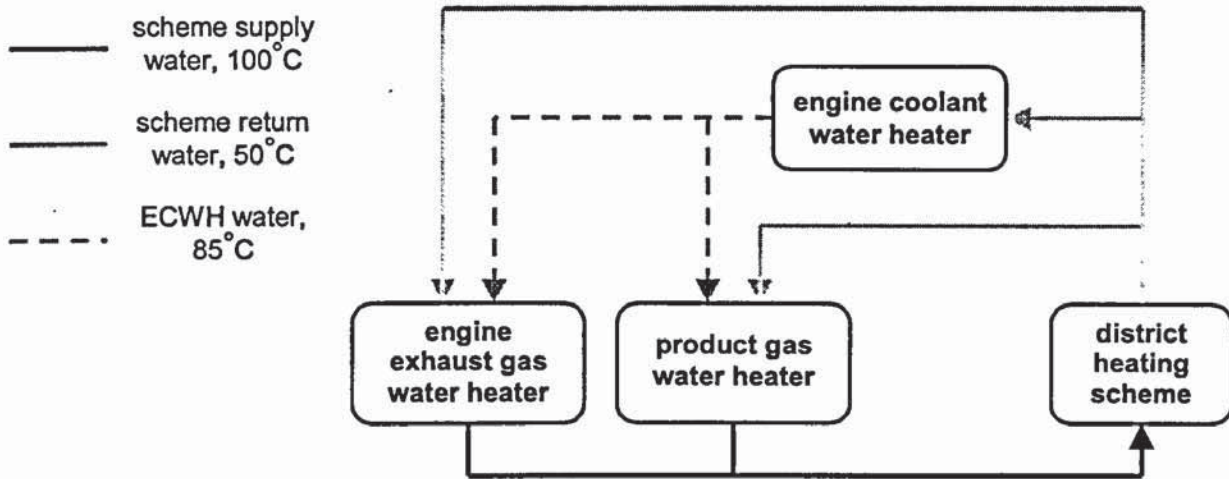
Figure 8.3 CHP heat recovery circuit

The model calculates product gas water heater hot water production first, allowing it to consume as much feed water from the engine coolant water heater as it can. Engine exhaust gas water heater hot water production is then calculated using any remaining feed water from the engine coolant water heater.

It is assumed throughout that the demand of the district heating scheme exceeds the capacity of the CHP system at all times, as the aim is to compare system performance. In any real application, it is likely that the CHP system would have to be selected and designed to meet a fixed heat demand profile in the most efficient manner, taking into account probable variations in demand on an hourly, daily, weekly or seasonal basis [150].

8.4 Fixed Parameters

The principal fixed parameters used within the various modules of the system model and the values ascribed to them have all been defined in the relevant sections of the main text. They are summarised here in Table 8.1, together with a section reference.

181

Table 8.1 Fixed parameter values - system model

Parameter	Unit	Value	Section
Biomass mean specific heat (dry) c_B	kJ/kgK	1.4	2.4
Biomass lower heating value (dry ash free) LHV_B	MJ/kg	18.64	2.4
Ambient temperature T_0	°C	15	2.4
Engine coolant temperature at ECR/ECWH inlet $T_{C24,27}$	°C	90	6.2.3.1
Engine coolant temperature at ECWH/ECR outlet $T_{C26,29}$	°C	60	6.2.3.1
Water temperature at ECWH inlet T_{W27}	°C	50	2.4
Water temperature at ECWH outlet T_{W29}	°C	85	7.3.1.1
ECR air outlet temperature T_{A26}	°C	50	7.3.2.1
PGWH and EEGWH min. gas outlet temperature $T_{G19,32}$	°C	120	7.3.2.1
PGWH and EEGWH water outlet temperature $T_{W19,32}$	°C	100	2.4
Parasitic power requirement (non-specific)	%	5	2.5.3.3
Plant replication number		10	2.5.2
Overall annual capacity factor		0.8	2.4
Overall annual availability	%	90	2.4
Ambient pressure	kPa	101.3	2.4
Ambient relative humidity	%	80	2.4
Ambient air oxygen concentration $[O_2]_0$	by vol.	0.21	2.4
Specific heat of water $c_{C,W}$	kJ/kgK	4.188	2.4
Rotary dryer biomass temperature out T_{B4}	°C	75	4.3.1.3
Rotary dryer gas temperature out T_{G4}	°C	110	4.3.1.3
Rotary dryer wall heat loss Q_{L3}	%	8	4.3.1.3
Rotary dryer maximum gas temperature in T_{G2}	°C	300	4.3.1.3
Biomass burner air-fuel equivalence ratio λ_5		1.8	4.3.1.3
Band dryer air temperature in T_{A2}	°C	50	4.3.2.4
Band dryer specific fan power P_3	W/m^2	839	4.3.2.4
Band dryer air velocity onto bed	m/s	0.840	4.3.2.4
Product gas temperature at engine inlet T_{G21}	°C	40	6.2.3
Product gas moisture conc. at engine inlet $[H_2O]_{G21}$	by vol.	0.05	6.2.3

Table 8.1 (contd.)

Parameter	Unit	Value	Section
Number of engines per plant N_{22}		3	6.2.3.1
Engine air-fuel equivalence ratio λ_{21}		1.7	6.2.3.1
Generator electrical efficiency	%	97	6.2.2

8.5 System Evaluation

8.5.1 Structure

The approach taken in the application of the model for system evaluation is to calculate a comprehensive matrix of cases (Section 8.5.2), and then to extract and analyse certain data so as to meet the primary study objective of analysing performance and cost characteristics (Section 1.4), while also evaluating the energy utilisation options presented in Section 2.1. The study is divided into two parts, power-only systems and CHP systems, for which results are presented separately. In each case, results are presented in sections corresponding to the principal study variables:

- the effect of air oxygen enrichment (RFSG only)
    - air supply to gasifier
    - air supply to IC engine

- the effect of gasifier type

- the effect of dryer type

- the effect of biomass moisture content
    - moisture content before drying
    - moisture content after drying
    - omission of drying stage (UGETC only)

- the effect of biomass feed rate (system scale)

- the effect of biomass cost

The issue of whether to combust the surplus biomass (representing the fraction too small to be gasified) in order to provide additional heat for drying or hot water generation is considered under the effect of dryer type, where one of the options incorporates a burner and associated preparation equipment for this purpose (see Section 4.3.1.2).

Some of the variable input parameters are likely to be pre-defined and therefore beyond the control of the system designer in a real application. These are biomass feed rate (i.e. system scale), biomass cost, pre-dryer biomass moisture content, and RFSG capital cost factor. Baseline values have been assigned to each of these, which are used throughout the presentation of results unless the effect of that specific parameter is being considered:

Biomass feed rate:	1.5 dt/h (~7 MW_{th})
Biomass cost:	£20/dt
Pre-dryer biomass moisture content:	75% db
RFSG capital cost factor:	1.0

These baseline values are assumed when reporting the optimum power-only and CHP configurations in Sections 9.1.1 and 9.2.1. The cases having these input parameters are referred to henceforth as the *baseline cases*.

The parameters used in this study to perform comparisons are:

- Cost of electricity (*COE*), expressed in p/kWh

- System overall efficiency (η_{OV}), expressed as a percentage

- System total plant cost per kilowatt (electrical) installed (*TPC*), expressed in £/kW_e

- System heat-to-power ratio (*HPR*), defined as MW$_{th}$ exported divided by MW$_e$ exported (for CHP only)

The most important of these is *COE*, which takes into account both η_{OV} and *TPC* and is the main determinant of a project's economic viability.

To reflect the uncertainties inherent in the derivations of these parameters, the study considers values of *COE* to the nearest 0.1 p/kWh, η_{OV} to the nearest 0.1%, *TPC* to the nearest £10/kW$_e$ and *HPR* to the nearest 0.01.

8.5.2 Definition of Cases

The system model was run for a total of over 15,000 cases, defined by the matrix presented in Table 8.2. The parameter values have been selected to cover the ranges of interest defined and justified in Section 2.4.

Table 8.2 Definition of system modelling cases (values for baseline cases in bold)

output type	power-only, CHP	
biomass input, dt/h	0.5, 1.0, **1.5**, 2.0	
biomass cost at plant gate, £/dt	**20**, 50, 80	
biomass moisture before drying, % db	50, **75**, 100	
dryer type	band, rotary without burner, rotary with burner	
gasifier type	RFSG	UGETC
IC engine configuration	ambient air, oxygen-enriched air	ambient air
biomass moisture after drying, % db	10, 20, 35, 50	10, 20, 35, 50, 75, 100
air oxygen concentration, % vol.	21, 28, 40, 60	21
RFSG capital cost factor	**1.0**, 1.5	n/a

9 RESULTS

9.1 Power Only

9.1.1 Optimum Design (Baseline Cases)

The set of baseline cases was defined in Section 8.5.1 as those having a biomass feed rate of 1.5 dt/h, a biomass cost of £20/dt, a pre-dryer biomass moisture content of 75% db and an RFSG capital cost factor (if applicable) of 1.0. For power-only systems this corresponds to 111 cases.

The optimum system design from this set (corresponding to that with the lowest cost of electricity) is one comprising an RFSG operating without air oxygen enrichment, and a band dryer drying the biomass to a final moisture content of 10% db. The main overall performance and cost parameters for this case are given in Table 9.1 together with the defining input data. A breakdown of total plant cost by system module in absolute terms is given in Table 9.2, and a breakdown of production cost by cost type is given in Table 9.3.

Table 9.1 Overall parameters for optimum design (baseline cases) - power-only

	INPUTS	OUTPUTS
Gasifier type	RFSG	
Dryer type	band	
Biomass feed rate	1.5 dt/h	
Biomass cost	£20/dt	
Air oxygen concentration	21% by vol.	
Biomass moisture content (before drying)	75% db	
Biomass moisture content (after drying)	10% db	
RFSG capital cost factor	1.0	
Power exported		2.31 MW$_e$
Overall efficiency		28.8%
Cost of electricity		7.7 p/kWh
Total plant cost		£1560/kW$_e$

Table 9.2 Total plant cost for optimum design (baseline cases) - power-only

System Module	Total Plant Cost £000
Reception, Storage, Screening	241
Dryer	245
Gasifier	1973
Gas Quench and Waste Water Treatment	19
IC Engine	961
Grid Connection	175
TOTAL	3614

Table 9.3 Production cost for optimum design (baseline cases) - power-only

Production Cost Type	Proportion
Annual cost of capital	28.7%
Feedstock	19.8%
Utilities	3.6%
Labour	24.8%
Overheads	11.5%
Maintenance	11.5%

In Table 9.2, the dominance of the gasifier and IC engine as elements in *TPC* is clear, in particular that of the gasifier. In Table 9.3, the importance of labour cost in a relatively small plant is clear. The other significant elements are annual cost of capital and feedstock. Feedstock will increase in importance as the cost of biomass increases from the relatively low baseline value of £20/dt.

A Sankey diagram showing the path of energy through the system for the optimum design is shown in Figure 9.1. In the diagram, the width of the arrows is proportional to the

wet
biomass
100

SCREENING

hot air from
engine radiator
21

wet
biomass
85

losses
15

DRYER

dry
biomass
85

losses
21

GASIFIER

product
gas
82

losses
3

GAS CLEAN-UP

product
gas
74

losses
8

IC ENGINE

hot air
to dryer
21

losses
29

exported
power
24
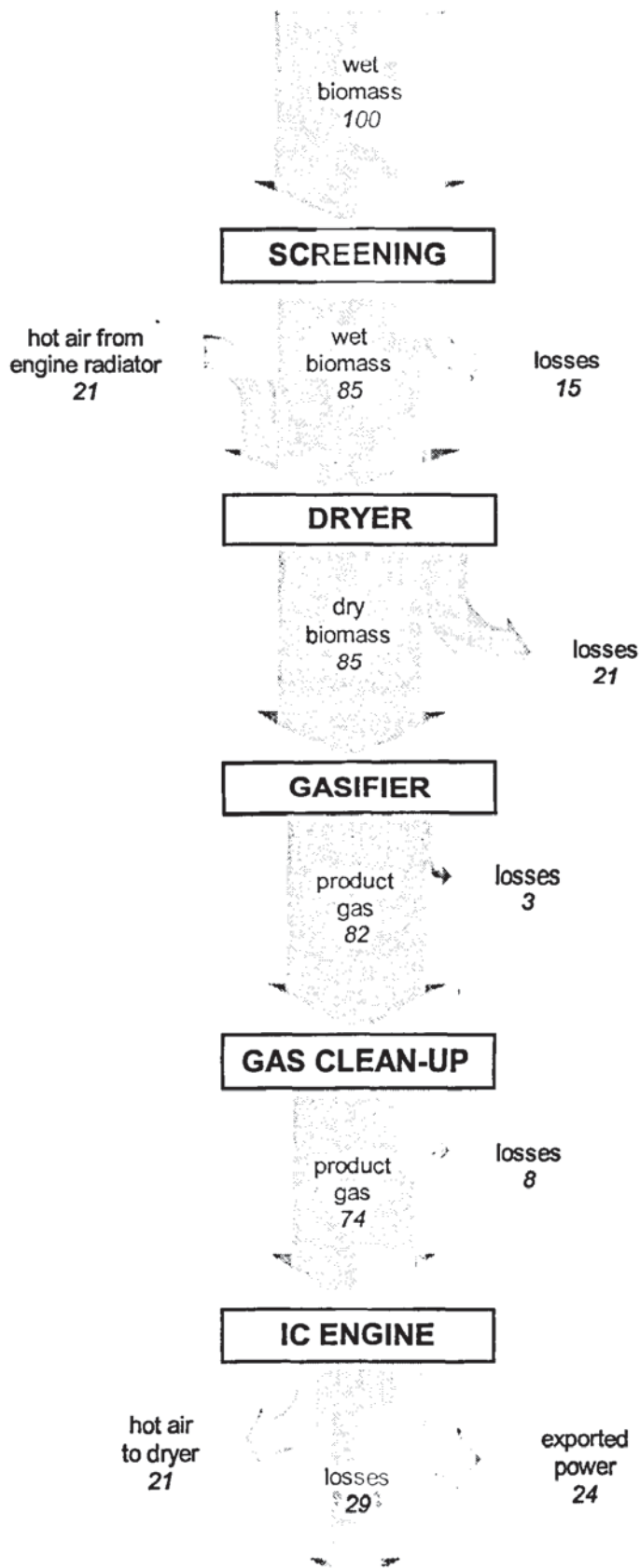
Figure 9.1 Sankey diagram, optimum design, power-only

energy flow. Values for energy flow are also given, normalised to a system energy input of 100 in the form of wet biomass. Unlike elsewhere in this chapter where lower heating values are used, the energy flows in the Sankey diagram are calculated on a higher heating value basis, i.e. the energy content of water vapour includes the latent heat of evaporation. This is greatly facilitates energy accounting. Hence the apparent difference between the efficiency of 28.8% in Table 9.1 and the apparent value of 24% in Figure 9.1.

9.1.2 Validation

Where appropriate, the performance predictions of the various module sub-models have been validated in the relevant chapters (for example, the gasifier in 5.2.3). The cost predictions of the various module sub-models are based either on established correlations of manufacturers' data or on newly-obtained manufacturers' data, and are therefore effectively already validated. The present section deals with validation of the predictions of overall system performance and economic parameters made by the full system model.

The results from the optimum case are compared in Table 9.4 with others for BGESs taken from the limited number of comparable studies in the literature (Section 3.2). All cost data have been updated to a 1998 base. Also included in Table 9.4 are the ranges covering all the baseline cases without air oxygen enrichment in the present study (none of the comparable studies considered air oxygen enrichment).

Table 9.4 Comparison with data for BGESs from other studies - power-only

Study	Plant number	Power exported MW$_e$	Overall efficiency %	Cost of electricity p/kWh	Total plant cost £/kW$_e$
Present (optimum)	10th	2.3	28.8	7.7	1570
Present (range)	10th	1.9-2.3	23.6-28.8	7.7-9.6	1570-1980
Toft [40]	10th	5.0	25.2	10.0	2300
Solantausta [39]	1st	4.9	33.9	9.5	3210
Solantausta [67]	unspecified	2.0	23.9	8.7	2600
Heaton [59]	unspecified	2.5	21.2	10.2	1280

Data from the present study compare well with those from the other studies, particularly when plant number is taken into consideration. The optimum *COE* is lower than all other studies, but it is reasonable to expect this given the degree of optimisation undertaken in the present study. If the range is considered instead, the central value of 8.7 p/kWh is closer to the average of the other studies of 9.6 p/kWh. The values for *TPC* obtained by the other studies show a much wider variation than those for *COE*, with the values of the present study lower than all but one of the other studies. The annual cost of capital typically represents only 30% of *COE*, so it is quite possible for *TPC* to show wide variations while *COE* does not. *TPC* is subject to great uncertainty; for example, the level of contingency can vary from 0% to 50% [39] and is almost arbitrary. Also, the particular equipment types chosen in the studies of Table 9.4 vary widely. Unfortunately there are numerous potential differences of assumption behind each of these sets of data, many of which are hidden, and the level of detail available for comparison of precise methodologies is limited.

The 1995 study by Toft [40] (Section 3.2.1) obtained a *COE* just above upper end of the range of the present study, for a system exporting 5.0 MW$_e$ with a fluid bed gasifier with cracker and a dual fuel diesel engine. The overall efficiency obtained of 25.2% is quite close to the centre of the range of the present study (26.2%), but the *TPC* is well above the upper end of the range. The high *TPC* is partly responsible for the relatively high *COE*; the other responsible factor is feedstock cost, where Toft has assumed £27/dt (1998 prices) before transport, compared with the present study's £20/dt delivered. Toft's was the only study to report the consideration of learning factor, and express costs on a tenth plant basis as in the present study.

The first of Solantausta's two studies [39] (Section 3.2.6) obtained a *COE* close to the upper end of the range of the present study, for a system exporting 5.0 MW$_e$ with a fluid bed gasifier with cracker and a dual fuel diesel engine. In this case however, efficiency was very high at 33.9%; this should have led to a very low *COE*, other things being equal. *COE* was high for three reasons: first, *TPC* was nearly double that of the present study (1st plant costs are assumed); second, capacity factor was 0.57 compared to 0.8 in the present study (again reflecting a first-of-a-kind plant); and third, feedstock cost was £36/dt delivered.

The second of Solantausta's studies [67] (Section 3.2.6) obtained a *COE* very close to the centre of the range of the present study, for a system with a fluid bed gasifier with cracker and a high-efficiency spark ignition engine. The system output was 2.0 MW$_e$ - very close to that in the present study. Efficiency however is towards the bottom end of the range of the present study and *TPC* significantly above the upper end of the range (suggesting 1st plant costs, although this is not specified). Furthermore, feedstock cost was higher than the present study at £26/dt, and capacity factor was the same. This suggests some other element of production cost must be substantially lower than in the present study to result in the relatively low *COE* (e.g. labour, maintenance, overheads, discount rate), but insufficient information is available to enable further investigation.

Heaton's study from 1987 considered a system with a fluid bed gasifier and a dual fuel diesel engine, and an output of 2.5 MW$_e$ - again very close to that of the present study. *COE* was just above the upper end of the range of the present study, despite *TPC* being the lowest of the studies considered. However the high *COE* is accounted for at least in part by the low overall efficiency. No further analysis is possible due to the limited data available in the project report.

The third round of UK Non Fossil Fuel Obligation contracts, awarded in 1995, attracted an average price for projects generating from energy crops, agricultural or forestry wastes of 8.65 p/kWh, with an average project capacity of 13.3 MW$_e$. By the time of the fourth round in 1997, the average price had come down to 5.51 p/kWh with an average project capacity of 9.6 MW$_e$. The optimum value of *COE* of 7.7 p/kWh obtained here is high in comparison with the NFFO prices, but the project capacity is just 2.3 MW$_e$. As will be seen (Section 9.1.7), *COE* falls with increasing scale, and a tentative extrapolation to the NFFO-4 average capacity of 9.6 MW$_e$ would see *COE* falling to around 5.0 p/kWh.

This and the data of Table 9.4 give confidence that the results obtained here are realistic, and therefore that the models and assumptions employed are sound.

The system characteristics which give rise to this optimum case are explored in detail in the following sections.

9.1.3 Air Oxygen Enrichment (RFSG)

9.1.3.1 Air Supply to IC Engine

In the 111 cases calculated, there are 36 (12 for each dryer type) where η_{OV} is higher and *TPC* lower for a system where oxygen-enriched air is supplied to the IC engine, as compared to an otherwise identical system where ambient air is supplied. In only nine cases however (three for each dryer type) is *COE* is lower for the enriched-air system, and in each of these cases the superiority is marginal.

Further analysis of these cases reveals that in each instance moving from ambient to enriched air supply to the engine has resulted in a change in the type of air oxygen enrichment plant used from PSA to VSA (see Section 7.2.1), and it is this change which has led to the superiority of the enriched-air system. For systems where no change occurs, there is never a net benefit in terms of η_{OV}, *TPC* or *COE* in supplying enriched air to the IC engine.

This results because when supplying oxygen-enriched air to the engine, the marginal improvement in engine power output is always much less than the marginal increase in electricity consumption of the oxygen enrichment unit. Also, the marginal increase in lease cost of the oxygen enrichment unit far outweighs the marginal reduction in engine annual cost of capital. By way of illustration, a 30 kW_e improvement in engine output is obtained from an increase in oxygen production of 6 tonnes per day, which requires 115 kW_e. The annual plant lease charge rises by £23,000 whereas the engine annual cost of capital falls by just £3,000.

Supply of oxygen-enriched air to the engine for power-only systems is not therefore justified, and is not considered further.

9.1.3.2 Air Supply to Gasifier

For all dryer types, the lowest *COE* and *TPC* and the highest η_{OV} are always obtained by operating without air oxygen enrichment to the gasifier – i.e. by omitting an air oxygen

enrichment plant altogether. Also, if an air oxygen enrichment plant is employed, then increasing the air oxygen content to the gasifier always results in an increase in *COE* and *TPC* and a decrease in η_{OV} (except for a small number of cases at large scales and high oxygen concentrations which coincide with a change in air oxygen enrichment plant type).

Results are illustrated in Figures 9.2 (*COE*) and 9.3 (η_{OV}) for a system with a band dryer, a moisture content to the dryer of 75% db, a biomass feed rate of 1.5 dt/h and an RFSG capital cost factor of 1.0. The four curves in each chart correspond to different values of biomass moisture content to the gasifier.
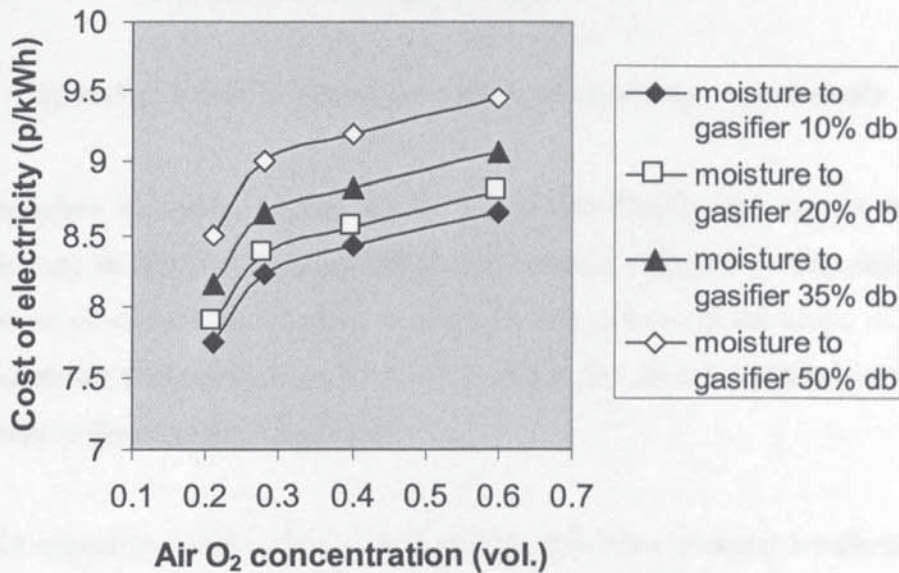
Figure 9.2 Effect of air oxygen concentration on *COE* - power-only

If oxygen enrichment is introduced or increased, the electricity generated increases very slightly due to a marginal improvement in the IC engine efficiency (gasifier cold gas efficiency remains virtually unchanged - see Section 5.3.3.2), but the increase is far outweighed by the increased electricity demand of the oxygen enrichment plant. Also as enrichment level is increased, the higher product gas LHV leads to a small reduction in IC engine derating (Section 6.2.4.1) and a corresponding small reduction in IC engine capital cost; however, this is again far outweighed by the increase in the air oxygen enrichment plant lease charge.
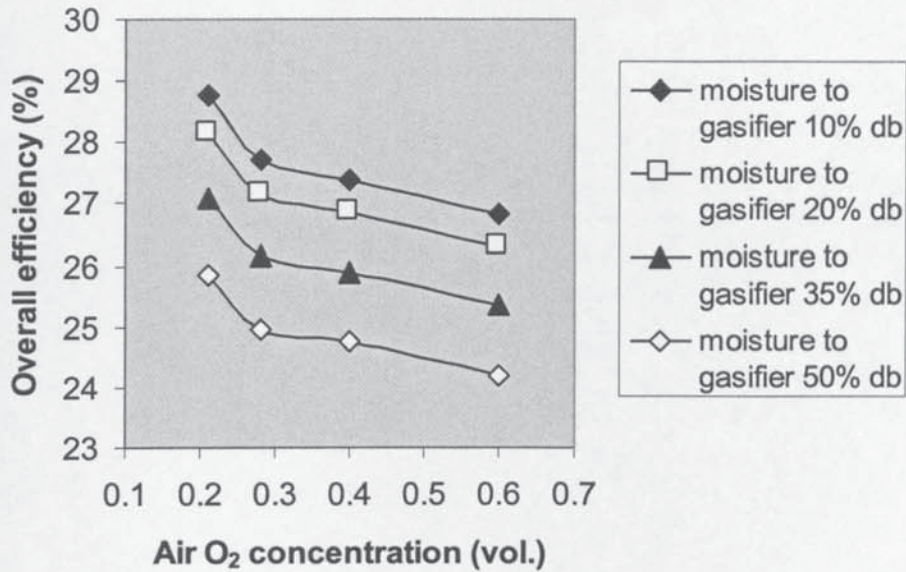
Figure 9.3 Effect of air oxygen concentration on η_{OV} - power-only

It would therefore be recommended not to supply the RFSG with oxygen-enriched air. However, it may be that the RFSG is unable to achieve satisfactory slagging conditions without the use of oxygen enriched air – although this is beyond the scope of the present model to determine (but see Section 5.3.3.1). If this is the case, then oxygen concentration should be kept to the minimum necessary.

There would appear to be little prospect of any modification to these conclusions coming from developments in air separation technology. It would take a 75% reduction in both electricity consumption and lease cost for a system with air oxygen enrichment to deliver a lower *COE* than an equivalent unenriched-air system

9.1.4 Gasifier Type

In all cases, systems with an RFSG have a higher η_{OV} than systems with a UGETC. In cases with an RFSG operating without enriched air, the average difference is 2.3%. Where the RFSG operates with air oxygen concentrations of 28% and 40%, the difference falls to 1.4% and 1.1% respectively. Figure 9.4 shows η_{OV} plotted against biomass moisture to the gasifier for systems with a band dryer, a moisture content to the dryer of 75% db and a

194

biomass feed rate of 1.5 dt/h. The four curves correspond to the RFSG with air oxygen concentrations of 21%, 28% and 40%, and the UGETC.
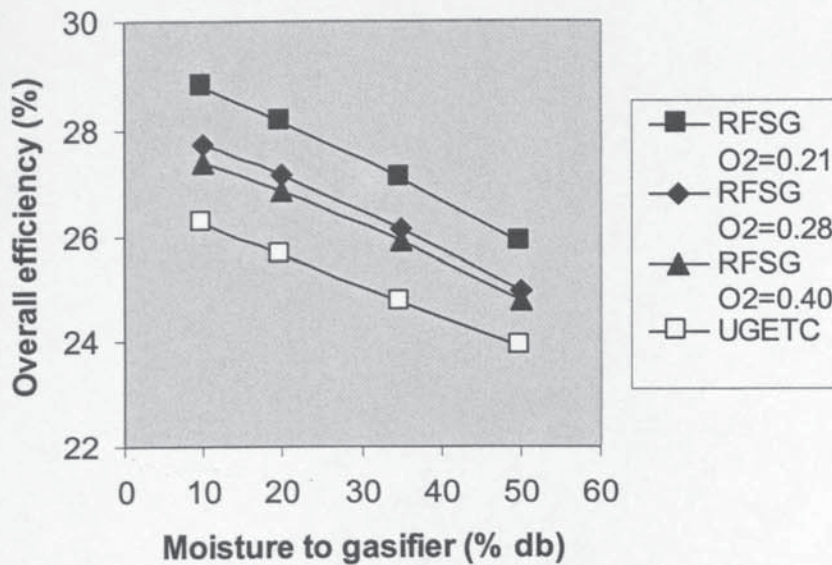
Figure 9.4 Effect of gasifier type on η_{OV} - power-only

The superiority of the RFSG-based systems is due to the higher cold gas efficiency of the RFSG obtained through air pre-heating, and to a lesser extent to an improvement in engine brake thermal efficiency obtained from the higher heating value product gas.

Figure 9.5 shows *COE* plotted against moisture content to the gasifier for systems with the RFSG at various air oxygen concentrations and with the UGETC, for an RFSG capital cost factor of 1.0. In each case, the system has a band dryer, a moisture content to the dryer of 75% db, a biomass feed rate of 1.5 dt/h and a biomass cost of £20/dt. Figure 9.6 shows the same plot for an RFSG capital cost factor of 1.5.

In all cases, systems with an RFSG operating without oxygen-enriched air have a lower *COE* (by an average of 0.8 p/kWh) than equivalent systems with a UGETC. However if the RFSG must operate with an air oxygen concentration of 28%, *COE* is less for RFSG-based systems than for UGETC-based systems at an RFSG capital cost factor of 1.0, but greater at an RFSG capital cost factor of 1.5. At an RFSG air oxygen concentration of 40%, the *COE*s are similar at an RFSG capital cost factor of 1.0.
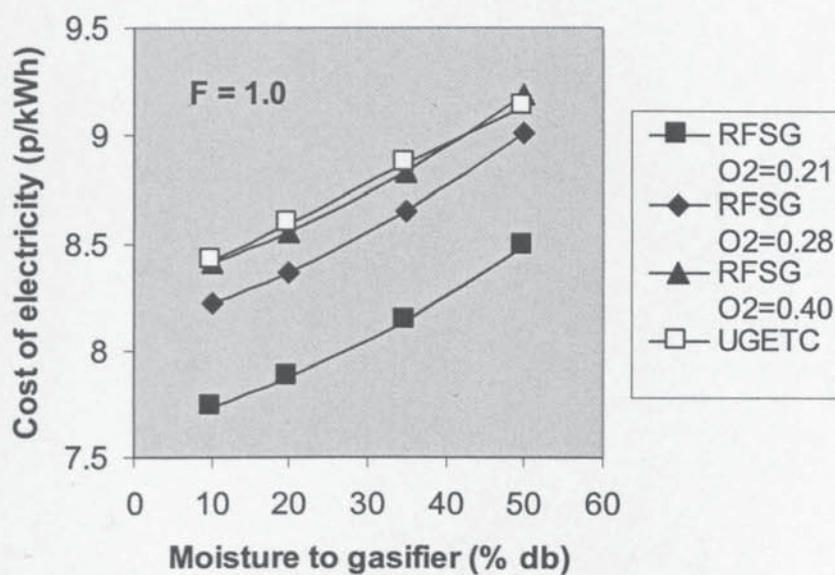
Figure 9.5 Effect of gasifier type on *COE* for *F*=1.0 - power-only
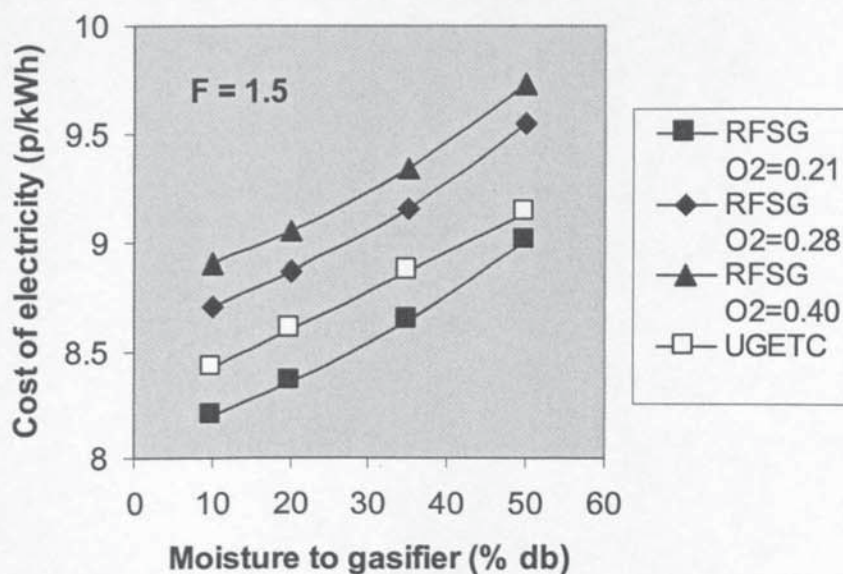
Figure 9.6 Effect of gasifier type on *COE* for *F*=1.5 - power-only

In terms of electricity cost, the increase in electrical output of the RFSG-based system is able to overcome the effect of the increased capital cost of the RFSG (even on a pessimistic view), provided no air oxygen enrichment is not employed. If however oxygen enrichment has to be employed to achieve slagging conditions, the situation in comparison

with UGETC-based systems is less clear-cut and will depend on the actual capital cost of the RFSG and the level of enrichment used. It should be emphasised that the actual equipment capital cost of the RFSG in relation to the UGETC (the factor F) is highly uncertain, due to the novel nature of the RFSG design.

In most cases, RFSG-based systems have a lower TPC than equivalent UGETC-based system for a RFSG capital cost factor of 1.0. On the other hand if the factor rises to 1.5, TPC for the UGETC-based systems is usually the lower.

9.1.5 Dryer Type

In all cases, systems with the band dryer gives a COE and a TPC either equal to or lower than the other two types, and a η_{ov} either equal to or higher than the other two types. The band dryer is able to meet all specified dryer duties; that is to say there is always enough heat available from the engine coolant water heater. The band dryer would always therefore be recommended for power-only systems. The superiority of the band dryer results from its lower electricity requirements, and its usually lower capital cost.

There is insufficient energy in the engine exhaust gases to meet the drying duty with a rotary dryer without burner in just two of the cases calculated - namely where the incoming biomass has a moisture content of 100% db and is to be dried to moisture content of 20% db or less. The rotary dryer with burner could meet these drying duties with ease by utilising a small part of the 15% of undersize biomass. For power-only cases, however, these would be the only circumstances in which it would be employed in favour of the system without an integral burner, because of its much higher capital cost.

9.1.6 Biomass Moisture Content

9.1.6.1 Moisture Content Before Drying

An increased moisture content to the dryer for the same post-dryer moisture content requires a larger dryer, and hence a higher electrical power consumption. The system net power output thus always falls. However, the LHV of the biomass falls by a larger amount (for reasons given in Section 8.2.2), so that η_{ov} always rises with increased moisture to

the dryer. This is shown in Figure 9.7 for an RFSG-based system with unenriched air and a UGETC-based system. In each case the system has a band dryer delivering a final moisture content of 10% at biomass feed rate of 1.5 dt/h.
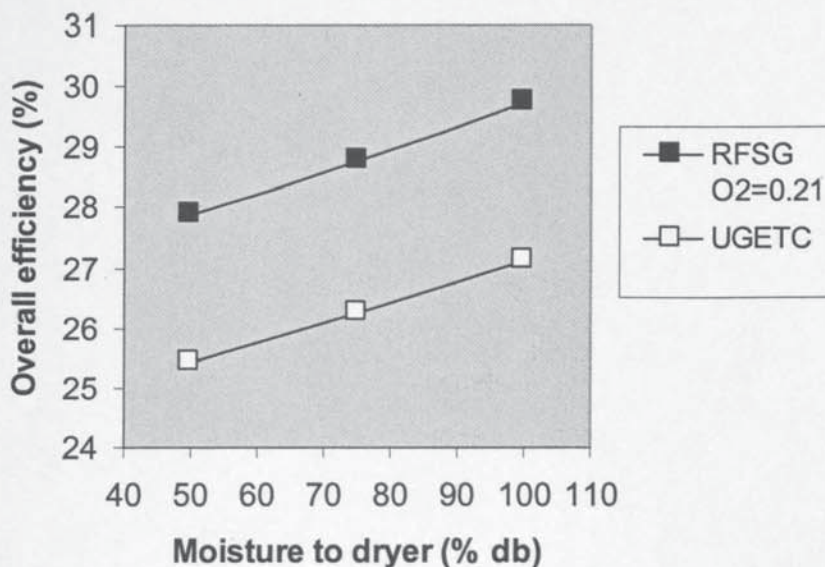
Figure 9.7 Effect of moisture content before drying on η_{OV} - power-only

COE and *TPC* always rise with increased moisture to the dryer, due to the increase in dryer capital cost and the reduction in system net power output. Figure 9.8 shows *COE* for an RFSG-based system with unenriched air and a UGETC-based system. The systems each have a band dryer delivering a final moisture content of 10%, a biomass feed rate of 1.5 dt/h and a biomass cost of £20/dt.

9.1.6.2 Moisture Content After Drying

In all cases, drying to a final moisture of 10% db gives the highest η_{OV} and the lowest *COE* and *TPC*, and any decrease in post-dryer moisture will always give an increased η_{OV} and reduced *COE* and *TPC*. These effects are illustrated in Figures 9.4-9.6. A lower moisture content to the gasifier increases the gasifier cold gas efficiency, and the improved LHV of the product gas results in a higher engine brake thermal efficiency. These give rise to an increase in net system power output which always outweighs the increase in dryer capital cost and electrical power consumption resulting from the larger drying duty. Hence, if a
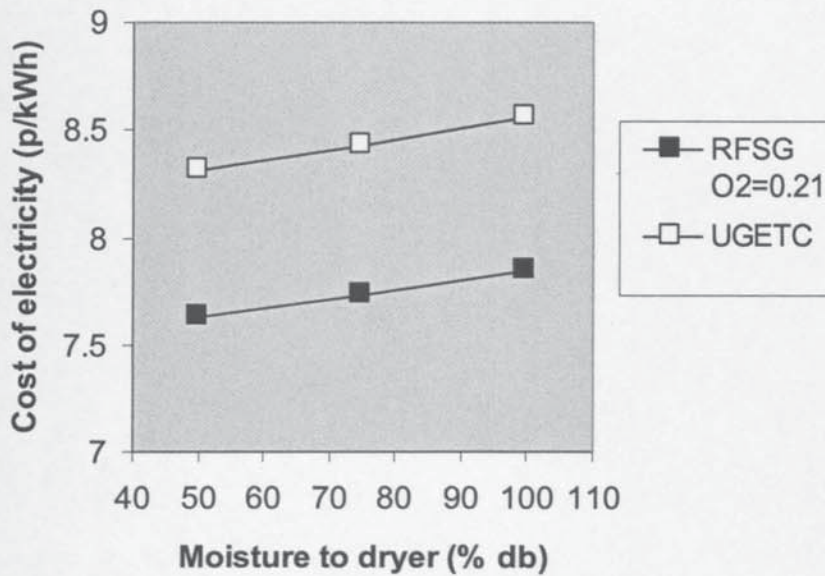
Figure 9.8 Effect of moisture content before drying on *COE* - power-only

drying stage is present, it is always best to dry to the lowest practical moisture content despite the increased dryer size. If the final moisture content is below the ambient air equilibrium moisture content, typically 20% db (Appendix 1 Section A1.3.3), the dried biomass should be stored for as short a time as possible before use to prevent significant re-hydration.

This study only considers post-dryer moisture contents down to 10% db. The dryer size and cost functions within the dryer models are based on data which only extend down to a final moisture content of 17% db. The extrapolation to 10% db is considered reasonable on the basis of other published work which shows reasonably linear behaviour for drying rate down to this level [35,185]. Further economies might be gained by drying further; however, the drying rate may start to decrease increasingly rapidly as these very low moisture contents are approached and the bound moisture in the biomass is increasingly depleted (Appendix 1 Section A1.3.1, [185]). This would imply a rapid increase in dryer volume and cost. Furthermore, the rate of re-hydration during storage is a function of the difference between actual and equilibrium moisture content, and so would initially be greater.

199

9.1.6.3 Omission of Drying Stage (UGETC)

It is never beneficial in terms of η_{OV} to omit the dryer altogether rather than dry to a moisture content of 10% db or 20% db. The benefits from improved gasifier cold gas efficiency far outweigh the small penalty in dryer electric power consumption. Total plant cost expressed in absolute terms clearly falls if the dryer is omitted, although whether *TPC* falls or rises depends on the fall in power output.

The situation regarding *COE* is more interesting. Figures 9.9 and 9.10 show *COE* as a function of biomass moisture before drying for biomass feed rates of 0.5 dt/h and 1.0 dt/h respectively, at a biomass cost of £20/dt for a system with a band dryer. Figures 9.11 and 9.12 show similar charts for a biomass cost of £50/dt. The three bars represent drying to 10% db moisture, drying to 20% db moisture, and omitting the dryer altogether.
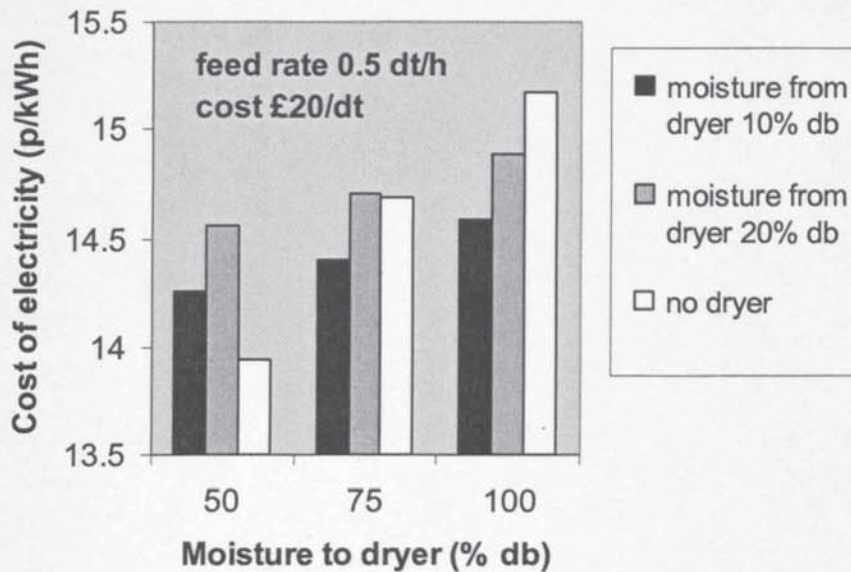
Figure 9.9 Effect of drying on *COE* for feed rate 0.5 dt/h, cost £20/dt - power-only

If drying to 10% db moisture content is a practical option in the circumstances, then it is only advantageous in terms of *COE* to omit a drying stage altogether if the initial moisture content is 50% db and the biomass feed rate 0.5 dt/h, with biomass cost at £50/dt or less. If the characteristics of the biomass limit the minimum moisture content after drying to 20% db, then the domain over which *COE* is lower if the drying stage is omitted widens

somewhat. However, *COE* is never lowest without a drying stage at a biomass cost of £80/dt, or at a biomass feed rate of 1.5 dt/h or more.
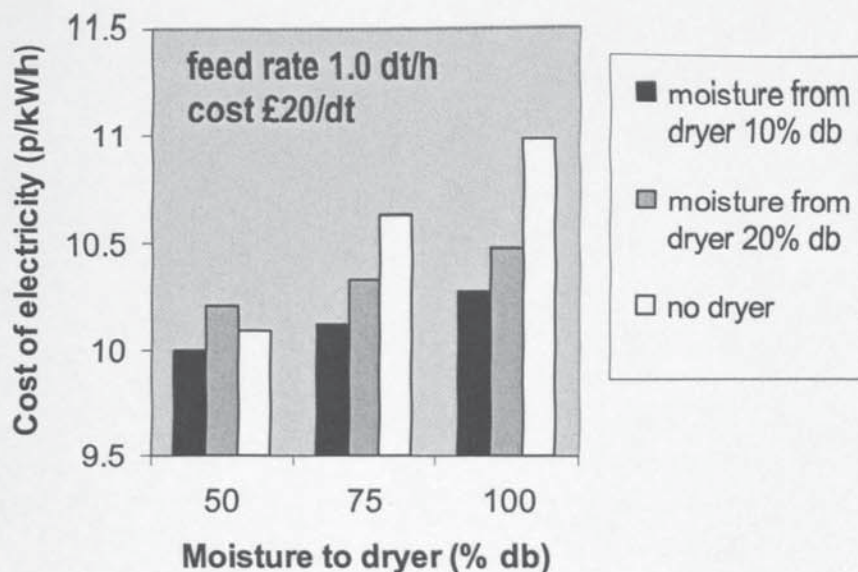
Figure 9.10 Effect of drying on *COE* for feed rate 1.0 dt/h, cost £20/dt - power-only
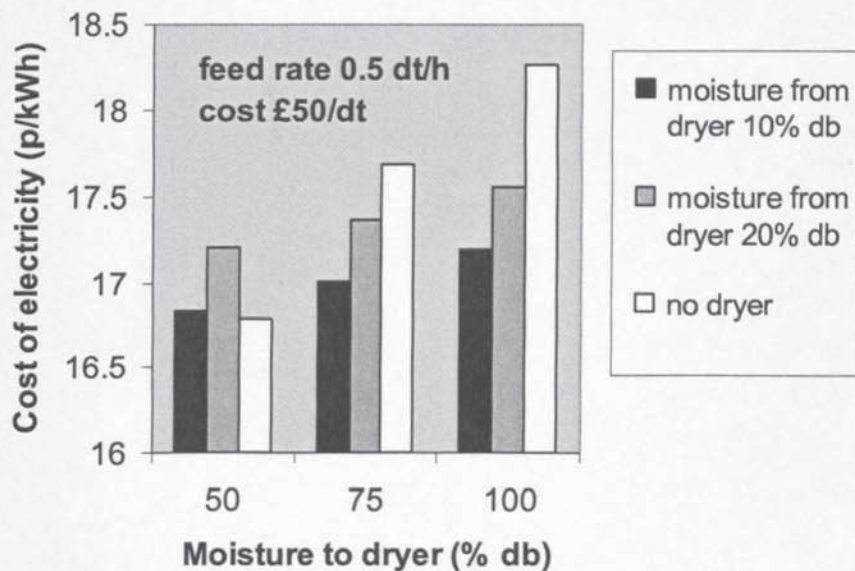
Figure 9.11 Effect of drying on *COE* for feed rate 0.5 dt/h, cost £50/dt - power-only

201
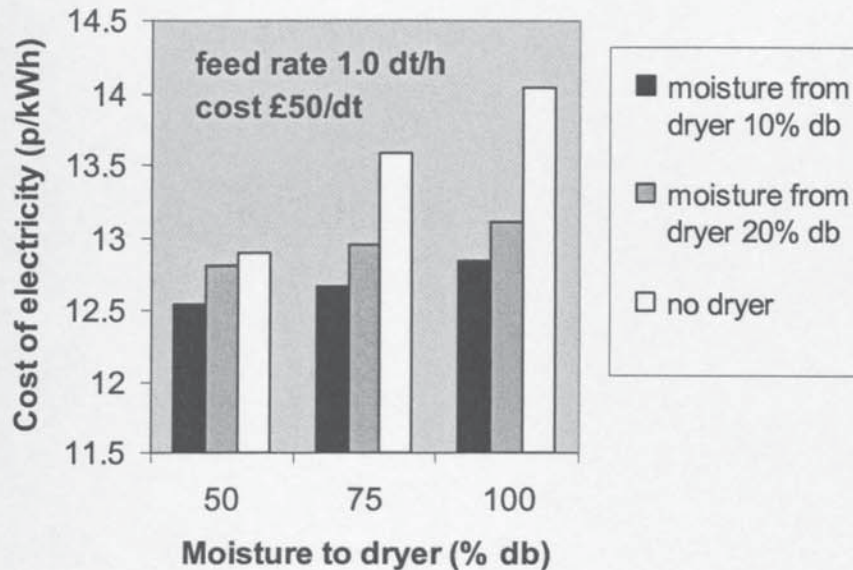
Figure 9.12 Effect of drying on *COE* for feed rate 1.0 dt/h, cost £50/dt - power-only

In general terms, *COE* is lower if the drying stage is omitted at low pre-dryer moistures, low biomass feed rates and low biomass costs. As pre-dryer moisture, biomass feed rate and biomass cost increase however, the gain from omitting the dryer reduces and is soon reversed. This is because at low pre-dryer moistures the deleterious effects on the gasification process of omitting the dryer are least (Section 9.1.6.2), and at low biomass feed rates and costs the dryer capital cost is proportionately more significant. In practice, even if the *COE* without a dryer is slightly higher than with, a developer may still choose to omit the dryer on the grounds of capital cost and plant simplicity.

9.1.7 Biomass Feed Rate (System Scale)

As biomass feed rate rises, η_{OV} always rises, and both *COE* and *TPC* always fall. The rate of change is greatest at low feed rates. These effects are shown in Figures 9.13-9.15 for η_{OV}, *COE* and *TPC* respectively.

In each case the system has a band dryer, biomass moisture contents to and from the dryer of 75% db and 10% db respectively, and a biomass cost of £20/dt. The two curves are for a system with an un-enriched air RFSG (capital cost factor 1.0) and with a UGETC.
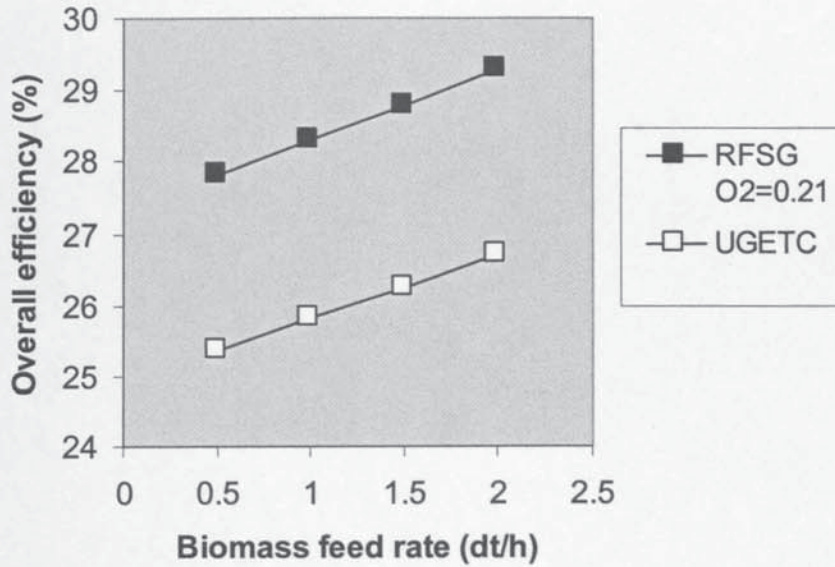
Figure 9.13 Effect of system scale on η_{OV} - power-only
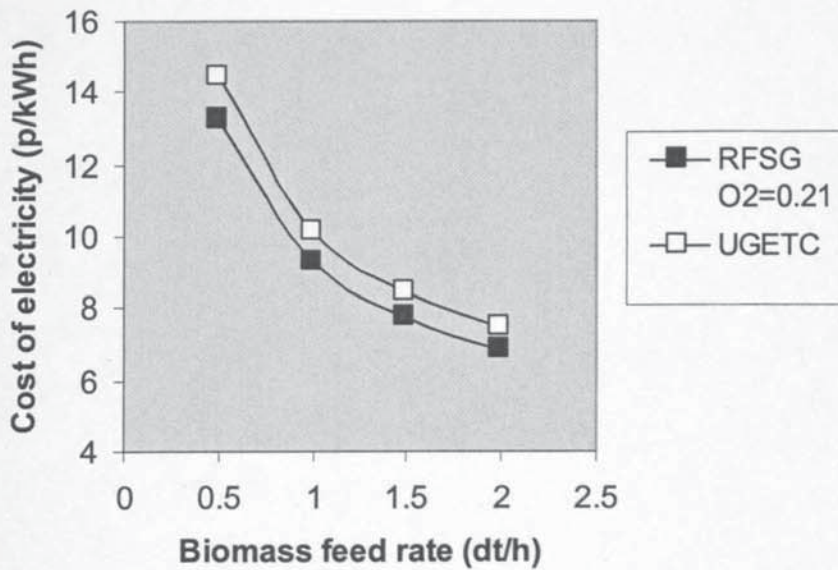
Figure 9.14 Effect of system scale on *COE* - power-only

The increase in efficiency with scale occurs because the IC engine brake thermal efficiency increases with engine size. This is a broadly linear effect over the scale range of interest here. The improved η_{OV} is partly responsible for the falls in *COE* and *TPC*, but there are also capital cost economies of scale accruing for nearly all system modules. The *COE* exponent is approximately -0.46.
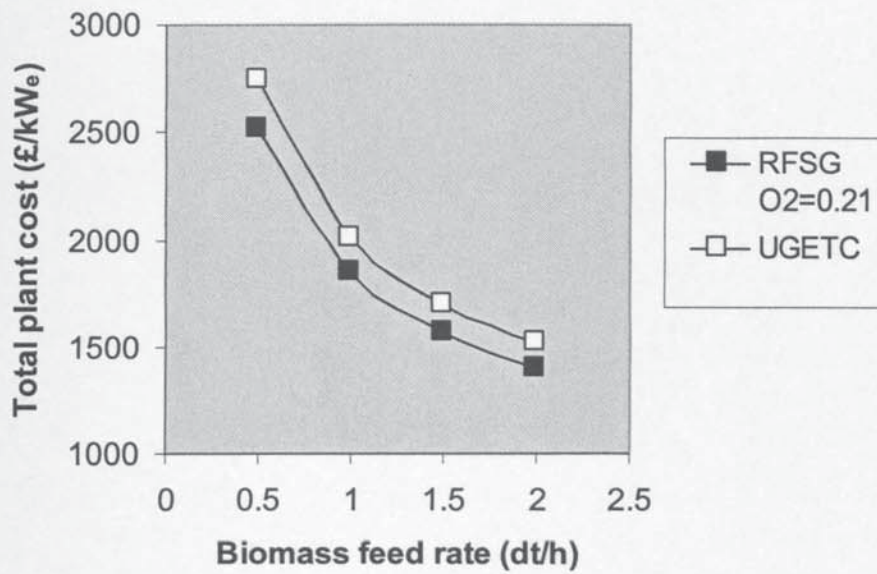
Figure 9.15 Effect of system scale on *TPC* - power-only

Table 9.5 shows a breakdown of total plant cost in absolute terms for a system with a UGETC and a band dryer with inlet and outlet biomass moisture contents of 75% db and 10% db respectively, for biomass feed rates of 1.0 and 2.0 dt/h.

Table 9.5 Total plant cost breakdown, UGETC-based system - power-only

System Module	Total Plant Cost, £000	
	Biomass feed rate 1.0 dt/h	Biomass feed rate 2.0 dt/h
Reception, Storage, Screening	210	266
Dryer	201	288
Gasifier	1487	2412
Gas Quench and Waste Water Treatment	19	19
IC Engine	729	1164
Grid Connection	133	196
TOTAL	2779	4344

The costs for the 2.0 dt/h case are in all cases less the twice those for the 1.0 dt/h case, reflecting the economies of scale operating. These economies of scale are greatest in modules such as the dryer and reception, storage and screening, although the final total is dominated by two modules where the economies of scale are less dramatic, that is the gasifier and the IC engine.

Given the constraints of any specific application (e.g. biomass availability), the benefits of building a BGES for power-only operation at as large a scale as possible are clear.

9.1.8 Biomass Cost

Not surprisingly an increase in biomass cost produces an increase in *COE*. Figure 9.16 shows this for systems with an un-enriched air RFSG (capital cost factor 1.0) and with a UGETC. In each case the system has a band dryer with biomass moisture contents to and from the dryer of 75% db and 10% db respectively, and a biomass feed rate of 1.5 dt/h.
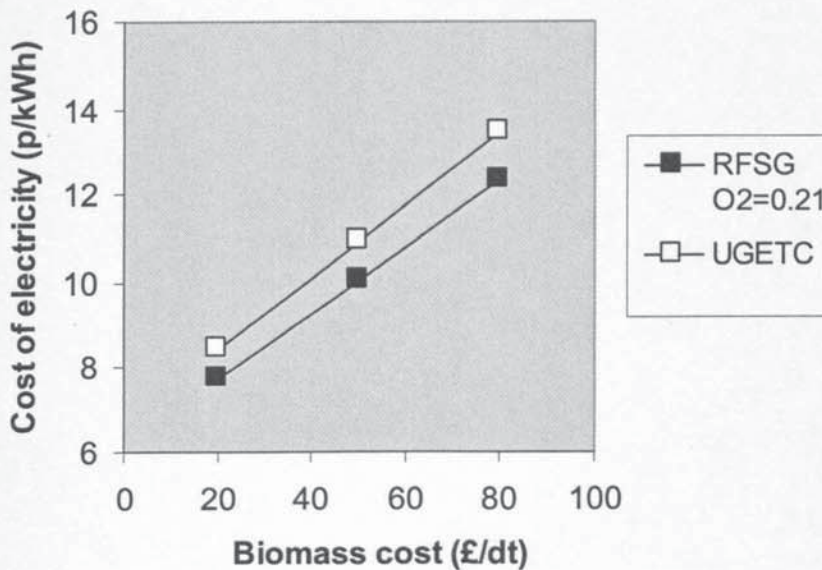
Figure 9.16 Effect of biomass feed cost on *COE* - power-only

Over all cases with the unenriched air RFSG, *COE* rises at an average rate of about 0.8 p/kWh for every £10/dt rise in biomass cost. The equivalent figure for systems with the UGETC is slightly higher at about 0.9 p/kWh.

205

9.2 Combined Heat and Power

9.2.1 Optimum Design (Baseline Cases)

The set of baseline cases was defined in Section 8.5.1 as those having a biomass feed rate of 1.5 dt/h, a biomass cost of £20/dt, a pre-dryer biomass moisture content of 75% db and an RFSG capital cost factor (if applicable) of 1.0. For CHP systems this corresponds to 111 cases.

The optimum system design from this set (corresponding to that with the lowest cost of electricity) comprises an RFSG operating without air oxygen enrichment, and a rotary dryer with burner drying the biomass to a final moisture content of 10% db. The main overall performance and cost parameters for this case are given in Table 9.6 together with the defining input data. A breakdown of total plant cost in absolute terms by system module is given in Table 9.7, and of production cost by cost type in Table 9.8.

Table 9.6 Overall parameters for optimum design (baseline cases) - CHP

Gasifier type	RFSG
Dryer type	rotary with burner
Biomass feed rate	1.5 dt/h
Biomass cost	£20/dt
Air oxygen concentration	21% by vol.
Biomass moisture content (before drying)	75% db
Biomass moisture content (after drying)	10% db
RFSG capital cost factor	1.0
Power exported	2.29 MW$_e$
Heat exported	3.91 MW$_{th}$
Heat to power ratio	1.71
Electrical efficiency	28.5%
Overall efficiency	77.2%
Cost of electricity	6.5 p/kWh
Total plant cost	£1743/kW$_e$

Table 9.7 Total plant cost for optimum design (baseline cases) - CHP

System Module	Total Plant Cost £000
Reception, Storage, Screening	196
Dryer	526
Gasifier	2391
Gas Quench and Waste Water Treatment	19
IC Engine	961
Heat Recovery System	161
Grid Connection	174
TOTAL	4429

Table 9.8 Production cost for optimum design (baseline cases) - CHP

Production Cost Type	Proportion
Annual cost of capital	29.5%
Feedstock	18.3%
Utilities	3.3%
Labour	25.4%
Overheads	11.8%
Maintenance	11.8%

The optimum design *COE* of 6.5 p/kWh is significantly below the power-only value of 7.7 p/kWh, showing that CHP operation is economically beneficial for the operator even when the price obtained for the heat is an undistorted market price.

From Table 9.7, where the dominance of the gasifier and IC engine in *TPC* is again clear. The additional cost of heat recovery is relatively low, reflecting the well-established, low-technology nature of such equipment, particularly in the context of a system containing

such items as an advanced biomass gasifier and a high-efficiency IC engine. This is an important contributory factor to the improved *COE* for CHP systems as compared to power-only systems referred to above. Table 9.8 shows a very similar pattern to that for power only systems (Section 9.1.1, Table 9.3).

A Sankey diagram showing the path of energy through the system for the optimum design is shown in Figure 9.17. As in Figure 9.1, the width of the arrows is proportional to the energy flow, and the values given for energy flow are normalised to a system energy input of 100 in the form of wet biomass. Again, energy flows are calculated on a higher heating value basis, i.e. the energy content of water vapour includes the latent heat of evaporation (see remarks in Section 9.1.1).

9.2.2 Validation

Only one study was found in the literature which looked at a BGES operating in CHP mode, that of Solantausta and Huotari [67]. They obtained a *COE* in the range 4.9-6.1 p/kWh, rather lower than the optimum value from the present study. Very little data is available in the report to analyse the reasons for this (the work concentrated on power only systems); however, the system scale was rather larger at 5.0 MW$_e$, and if the results obtained in the present work were extrapolated accordingly the resulting *COE* would be comparable (see Figure 9.33 later).

The system characteristics which give rise to this optimum case are explored in detail in the following sections.

9.2.3 Air Oxygen Enrichment (RFSG)

9.2.3.1 Air Supply to IC Engine

The situation here is very similar to that for power-only systems. This time, there are only 12 cases in total where η_{OV} is higher and *TPC* lower for a system where oxygen-enriched air is supplied to the IC engine, as compared to an otherwise identical system where ambient air is supplied instead, and no cases at all where *COE* is lower. The reasons are the same as given in Section 9.1.3.1 for power-only systems.

exhaust
gases from
heat recovery
26

wet
biomass
100

DRYER

burner exhaust
gases to heat
recovery
15

dry
biomass
85

losses
26

GASIFIER

product
gas
82

losses
3

HEAT REC.

product
gas
76

hot water to
district heating
6

GAS CLEAN-UP

product
gas
74

losses
2

IC ENGINE

losses 4

exported power 24

hot water to
district heating
20

exhaust gases
from dryer burner
15

exhaust
gas
26

HEAT REC.

exhaust gases
to dryer
26

hot water to
district heating
15

Figure 9.17 Sankey diagram, optimum design - CHP

209

Supply of oxygen-enriched air to the engine for CHP systems is not therefore justified, and is not considered further.

9.2.3.2 Air Supply to Gasifier

As for power-only systems, the lowest *COE* and *TPC* and the highest η_{OV} are always obtained by operating without air oxygen enrichment to the gasifier – i.e. by omitting an air oxygen enrichment plant altogether.

If an air oxygen enrichment plant is employed, then increasing the air oxygen content to the gasifier always results in an increase in *COE*.

Results are illustrated in Figures 9.18 (*COE*) and 9.19 (η_{OV}) for a system with a band dryer, a moisture content to the dryer of 75% db, a biomass feed rate of 1.5 dt/h and an RFSG capital cost factor of 1.0. The four curves in each chart correspond to different values of biomass moisture content to the gasifier.
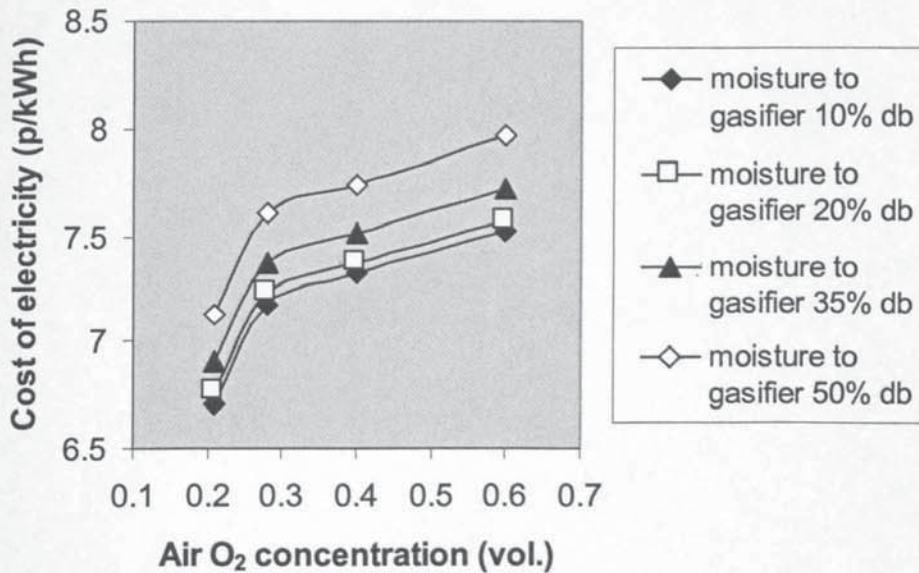
Figure 9.18 Effect of air oxygen concentration on *COE* - CHP
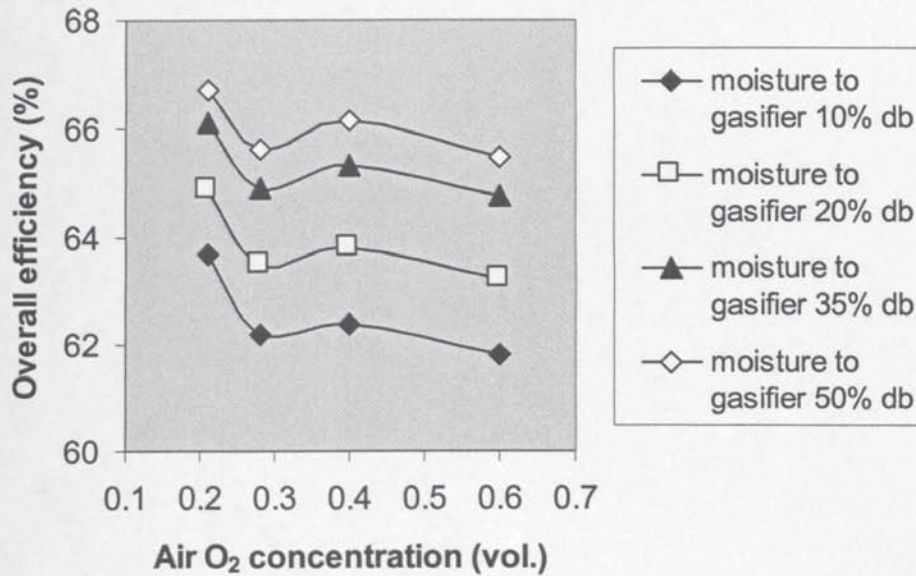
Figure 9.19 Effect of air oxygen concentration on η_{OV} - CHP

Again, for a small number of cases at large scales and high oxygen concentrations which coincide with a change in the air oxygen enrichment plant type, *TPC* can fall and η_{OV} rise with increasing air oxygen content. Also in going from 28% to 40% oxygen, although net electrical output falls, η_{OV} rises slightly because a rise in product gas temperature from the gasifier and in exhaust gas temperature from the IC engine allows more heat to be recovered (Figure 9.19). Otherwise, a rise in air oxygen content results in a rise in *TPC* and a fall in η_{OV}.

The explanation for these characteristics is the same as that given for power-only systems (Section 9.1.3.2), and the comments and conclusions presented there apply equally to CHP systems; principally, it would be recommended to operate without air oxygen enrichment to the gasifier, or alternatively at the minimum practical level if enrichment were necessary for gasifier temperature management.

9.2.4 Gasifier Type

In all cases, systems with an RFSG have a lower η_{OV} than systems with a UGETC, by an average margin of 1.6%. This is the reverse result to power-only systems, and arises from

a larger recovery of heat in UGETC systems which outweighs the reduced net electrical output reported and discussed in Section 9.1.4.

The increased heat recovery is mostly due to a higher product gas temperature in the case of the UGETC. The RFSG aims by design to retain this energy within the gasifier.

Figure 9.20 shows η_{OV} plotted against biomass moisture to the gasifier for systems with a rotary dryer with burner, a moisture content to the dryer of 75% db and a biomass feed rate of 1.5 dt/h. The four curves correspond to the RFSG with air oxygen concentrations of 21%, 28% and 40%, and the UGETC.
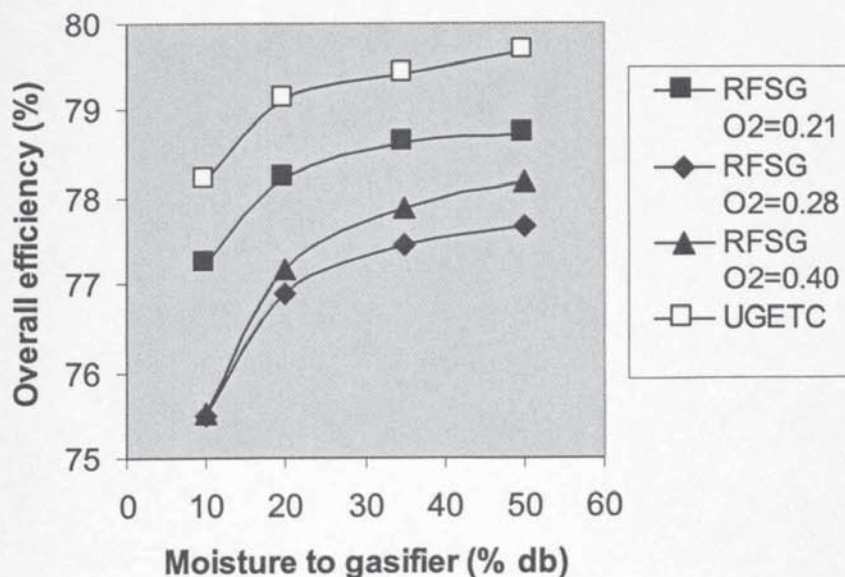
Figure 9.20 Effect of gasifier type on η_{OV} - CHP

Figure 9.21 shows *COE* plotted against moisture content to the gasifier for systems with the RFSG at various air oxygen concentrations and with the UGETC, for an RFSG capital cost factor of 1.0. In each case, the system has a rotary dryer with burner, a moisture content to the dryer of 75% db, a biomass feed rate of 1.5 dt/h and a biomass cost of £20/dt. Figure 9.22 shows the same plot for an RFSG capital cost factor of 1.5.
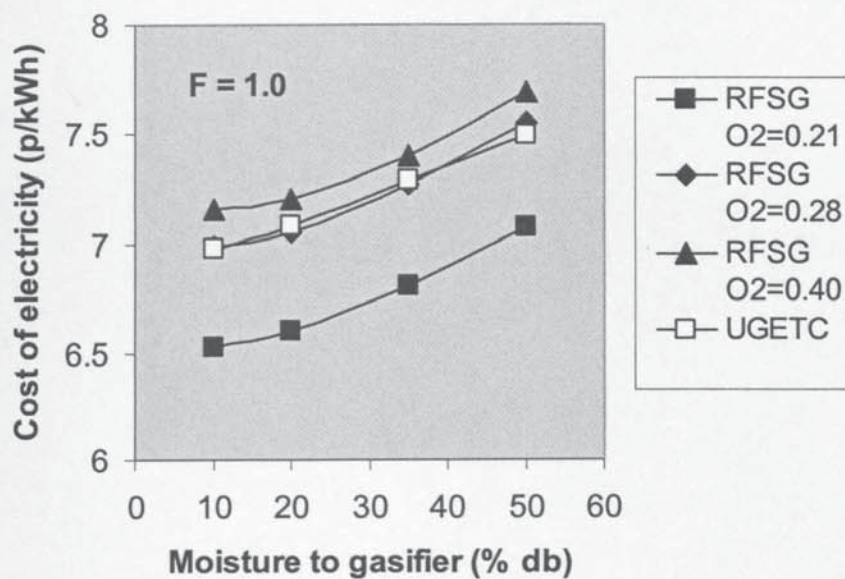
Figure 9.21 Effect of gasifier type on *COE* for *F*=1.0 - CHP
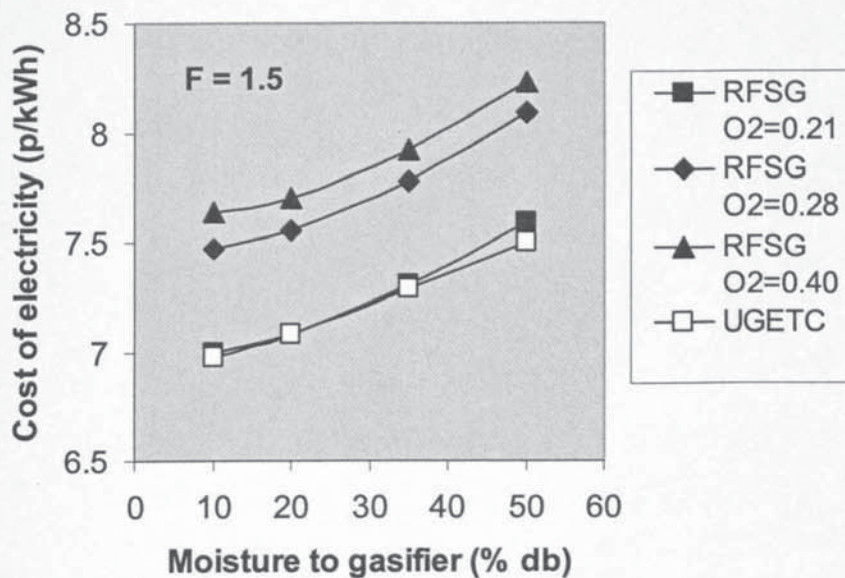
Figure 9.22 Effect of gasifier type on *COE* for *F*=1.5 - CHP

Systems with an unenriched air RFSG have a lower *COE* than equivalent systems with a UGETC for all cases except those with a biomass feed cost of £20/dt and an RFSG capital cost factor of 1.5, where *COE* is similar for the two types at low biomass moisture contents to the gasifier and lower for the UGETC systems at high biomass moisture contents to the

213

gasifier. The average difference in *COE* over all cases is 0.6 p/kWh in favour of the RFSG.

If the RFSG must operate with air oxygen enrichment to achieve slagging conditions, the position of UGETC systems improves. For an air oxygen concentration of 28%, *COE* for RFSG systems is only lower if the RFSG capital cost factor is 1.0, and if the biomass cost is £50/dt or £80/dt. In all other cases, UGETC systems are equal or superior. If the air oxygen concentration rises to 40%, UGETC systems also become cheaper at an RFSG capital cost factor of 1.0 and a biomass cost of £50/dt.

Essentially, as RFSG capital cost falls and biomass cost rises, *COE* from RFSG systems improves relative to that from UGETC systems. If the RFSG can run without oxygen-enriched air, then it will generally give a lower system *COE* than the UGETC. However if capital cost is at the high end of expectation and biomass is relatively cheap, it is likely that the UGETC will be the better option on economic grounds, particularly considering the technical risk associated with the RFSG. If the RFSG has to operate with oxygen enriched air however, it is only likely to give a lower system *COE* than the UGETC if the RFSG capital cost is at the low end of expectation and biomass price is relatively high.

As for power-only operation, RFSG-based systems always have a lower *TPC* than equivalent UGETC-based systems when the RFSG capital cost factor is set to 1.0, but if the factor rises to 1.5, *TPC* for UGETC-based systems is nearly always the lower.

Figure 9.23 shows heat-to-power ratio (*HPR*) plotted against biomass moisture to the gasifier for systems with a rotary dryer with burner, a moisture content to the dryer of 75% db and a biomass feed rate of 1.5 dt/h. Again the four curves correspond to the RFSG with air oxygen concentrations of 21%, 28% and 40%, and the UGETC.

HPR is always highest for systems with the UGETC because of its lower cold gas efficiency, which results in lower net electrical output but higher heat availability.
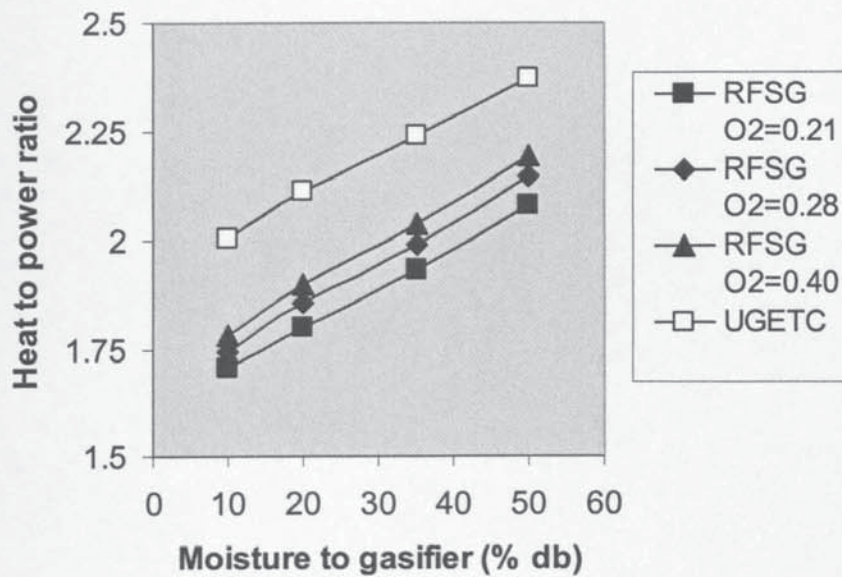
Figure 9.23 Effect of gasifier type on *HPR* - CHP

9.2.5 Dryer Type

The relative performance of the three dryer options is shown in Figures 9.24 and 9.25. Biomass feed rate is found to be the principal determinant of dryer choice. Figure 9.24 shows average η_{OV} over all pre- and post- dryer moisture contents plotted against biomass feed rate for each of the three dryer options. Figure 9.25 shows a similar plot for *COE*, only here *COE* is expressed relative to the average for all dryers at that feed rate - this helps to see relative performance.

Systems with the rotary dryer with burner give a much higher η_{OV} than either of the other two systems in all cases (by about 11% on average), because of the utilisation of the undersize biomass which results in additional heat export.

However the lowest *COE* at biomass feed rates up to about 1.2 dt/h comes from systems with the band dryer. Systems incorporating the rotary dryer with burner only give the lowest system *COE* at feed rates above this level. The rotary dryer without burner never gives the lowest system *COE*. Furthermore, for both the band dryer and the rotary dryer with burner there is sufficient heat available from the system to achieve all specified drying duties, whereas for the rotary dryer without burner there is insufficient heat available

215

where the initial moisture content is 100% db and the desired moisture content is 20% db or less.
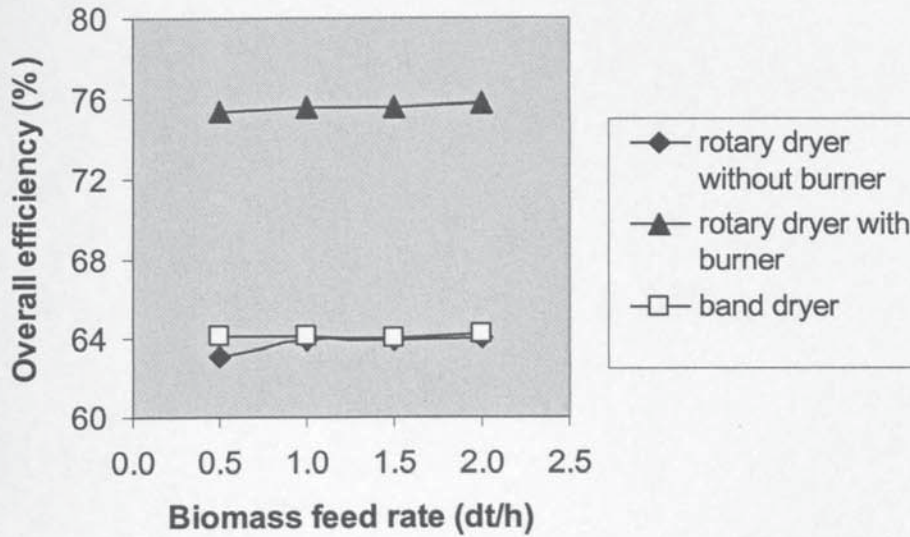
Figure 9.24 η_{OV} for different dryer options - CHP
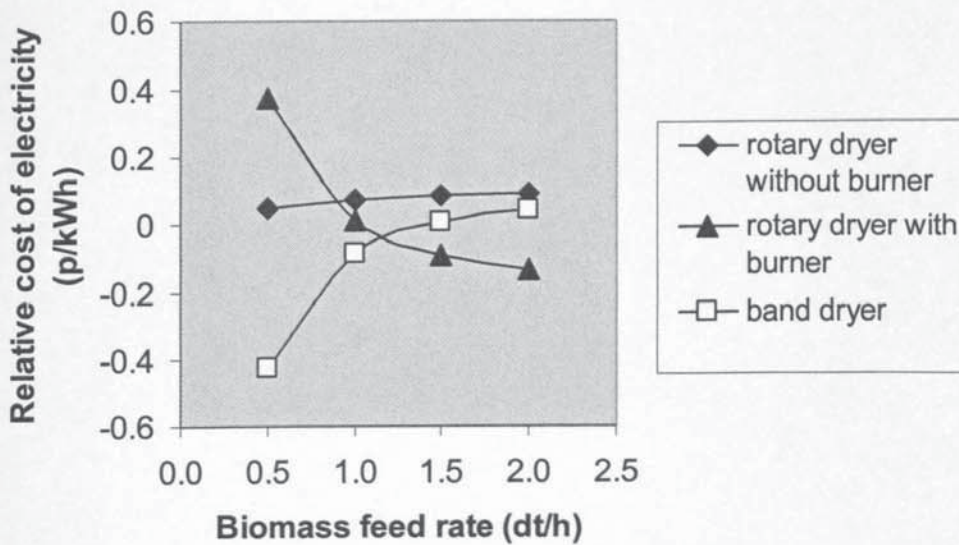
Figure 9.25 COE for different dryer options - CHP

In all cases, the rotary dryer with burner gives the highest system *TPC*, followed by the rotary dryer without burner, with the band dryer giving the lowest.

The band dryer has lower electrical power requirements and lower capital cost, and also utilises lower-grade heat than the rotary dryers. However, the increased revenue from heat

associated with the rotary dryer with burner becomes increasingly important as economies of scale reduce the influence of capital cost. With the assumptions made for heat revenue, it is likely that the added complexity and capital cost of the rotary dryer with burner would result in the band dryer being selected up to at least 1.5 dt/h. However, the relative economics of systems incorporating the rotary dryer with burner would improve if greater revenue could be obtained for the heat, for example through public subsidy.

9.2.6 Biomass Moisture Content

9.2.6.1 Moisture Content Before Drying

An increased moisture to the dryer for the same final moisture content requires a larger dryer, and hence a higher electrical power consumption, so that the system net power output thus always falls. Furthermore the higher the moisture content before drying, the greater the system heat required for the drying process and therefore the lesser the heat exported. Unlike with power-only systems (Section 9.1.6.1) this fall in total energy output always exceeds the fall in dry LHV of the biomass (Section 8.2.2); so that η_{OV} always falls with increased moisture to the dryer. This is shown in Figure 9.26 for an RFSG-based system with unenriched air and a UGETC-based system. In each case the system has a rotary dryer with burner and a biomass feed rate of 1.5 dt/h.
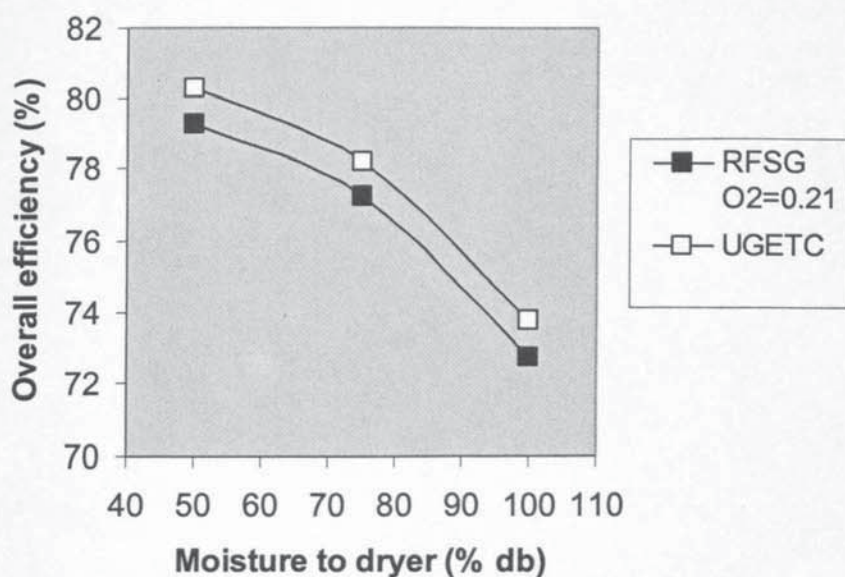
Figure 9.26 Effect of moisture content before drying on η_{OV} - CHP

217

COE and *TPC* always rise with increased moisture to the dryer, due to the increase in dryer capital cost and the reduction in system net energy output. Figure 9.27 shows *COE* for an RFSG-based system with unenriched air and a UGETC-based system. The systems each have a rotary dryer with burner, a biomass feed rate of 1.5 dt/h and a biomass cost of £20/dt.
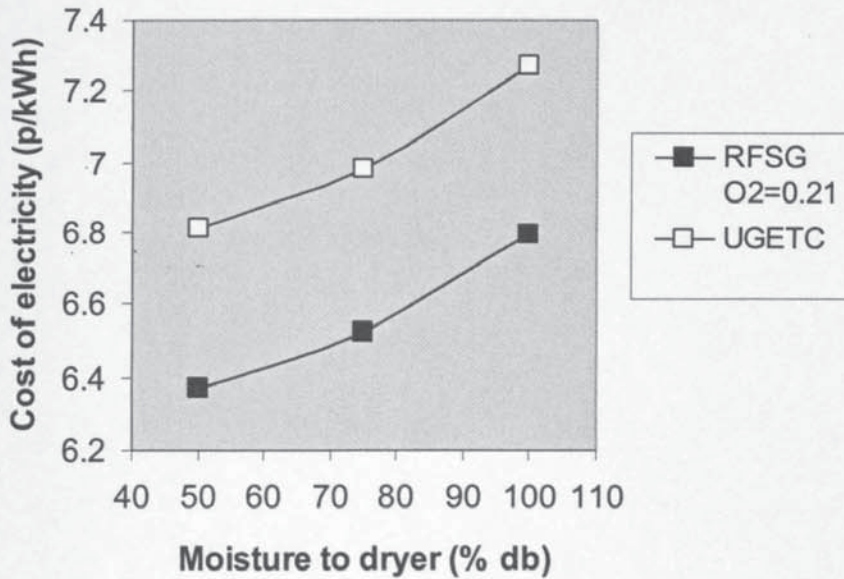
Figure 9.27 Effect of moisture content before drying on *COE* - CHP

9.2.6.2 Moisture Content After Drying

Whereas for power-only systems (Section 9.1.6.2) drying to a final moisture of 10% db gives the highest η_{ov}, in the case of CHP systems drying to a final moisture of 10% db gives the lowest η_{ov}, and η_{ov} nearly always improves the higher the final moisture. This is shown in Figure 9.20. As moisture to the gasifier increases, net electricity output falls (Section 9.1.6.2), but this fall is outweighed by the gain in heat for export which results from less heat being required for drying.

COE still nevertheless always rises with increasing final moisture, with a final moisture of 10% db giving the lowest *COE* (Figures 9.21, 9.22). As with power-only systems, a lower moisture content to the gasifier increases the gasifier cold gas efficiency, and the improved

LHV of the product gas results in a higher engine brake thermal efficiency. These give rise to an increase in net system power output which always outweighs not only the increase in dryer capital cost and electrical power consumption resulting from the larger drying duty, but also now the reduced revenue from the sale of heat. This results because of the much higher value of electricity compared to heat. Whereas over all cases *COE* ranges from 5-25 p/kWh, the price paid for heat ranges from just 1.2-1.5 p/kWh.

TPC also always rises with increasing final moisture as the dryer cost reduces and the net electrical output increases

As with power-only systems, therefore, it is always best to dry to the lowest practical moisture content if a drying stage is present, although the comments made in Section 9.1.6.2 with regard to equilibrium moisture content and drying to ultra-low moisture contents apply equally to CHP systems.

9.2.6.3 Omission of Drying Stage (UGETC)

If the dryer is omitted altogether, η_{OV} is always higher than if the biomass is dried to a moisture content of 10% db or 20% db in either a band dryer or a rotary dryer without burner, as the heat available for export rises by more than the net electricity output falls. If the dryer is a rotary dryer with burner, however, the reverse is true as the extra heat available from the integral burner is lost if the dryer is absent. (Note that the option to have no dryer but a stand-alone biomass burner and associated feed preparation equipment has not been considered here, but may be a viable configuration).

As with power-only systems (Section 9.1.6.3), total plant cost expressed in absolute terms clearly falls if the dryer is omitted, although whether *TPC* falls or rises depends on the fall in power output.

The situation regarding *COE* is similar to that for power-only systems (Section 9.1.6.3) and the same general comments apply. In the case of CHP systems however the range of cases ᐧover which it is economically advantageous to omit the dryer is wider, as a result of the added benefit of extra heat for export. Figures 9.28 and 9.29 show *COE* as a function of biomass moisture before drying for biomass feed rates of 0.5 dt/h and 1.0 dt/h respectively,

219

at a biomass cost of £20/dt for a system with a band dryer. Figures 9.30 and 9.31 show similar charts for a biomass cost of £50/dt. As in Section 9.1.6.3, the three bars represent drying to 10% db moisture, drying to 20% db moisture, and omitting the dryer altogether.
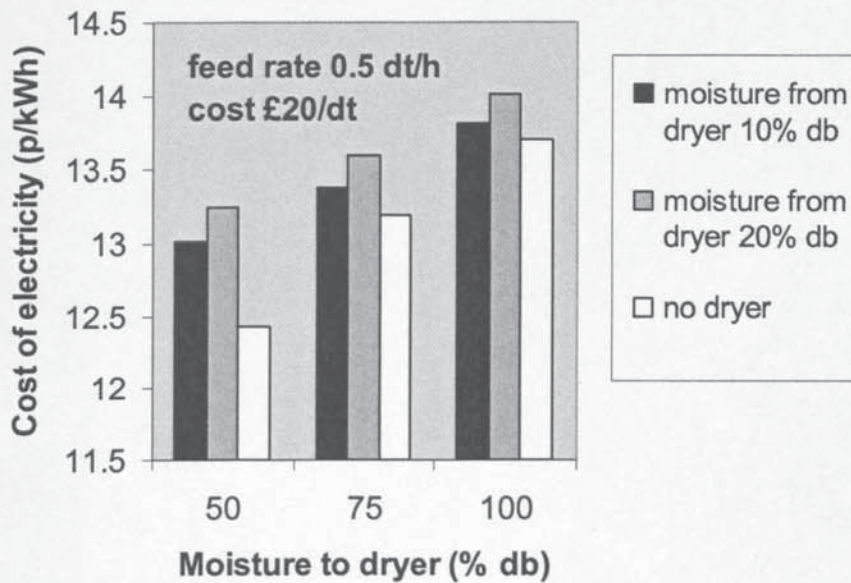
Figure 9.28 Effect of drying on *COE* for feed rate 0.5 dt/h, cost £20/dt - CHP
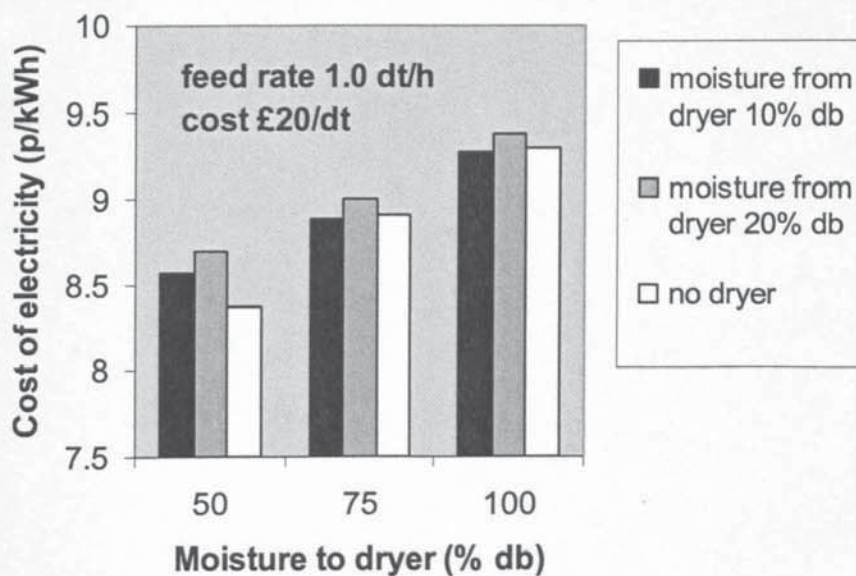
Figure 9.29 Effect of drying on *COE* for feed rate 1.0 dt/h, cost £20/dt - CHP
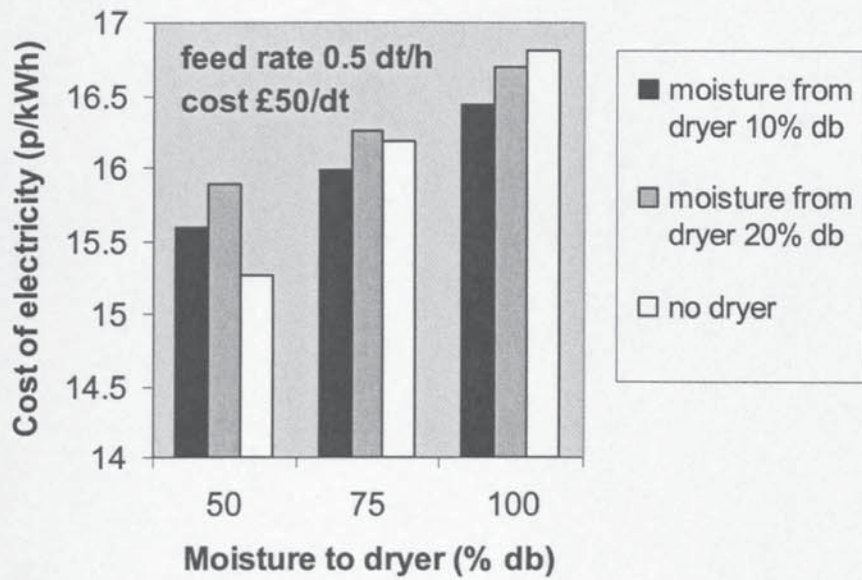
Figure 9.30 Effect of drying on *COE* for feed rate 0.5 dt/h, cost £50/dt - CHP
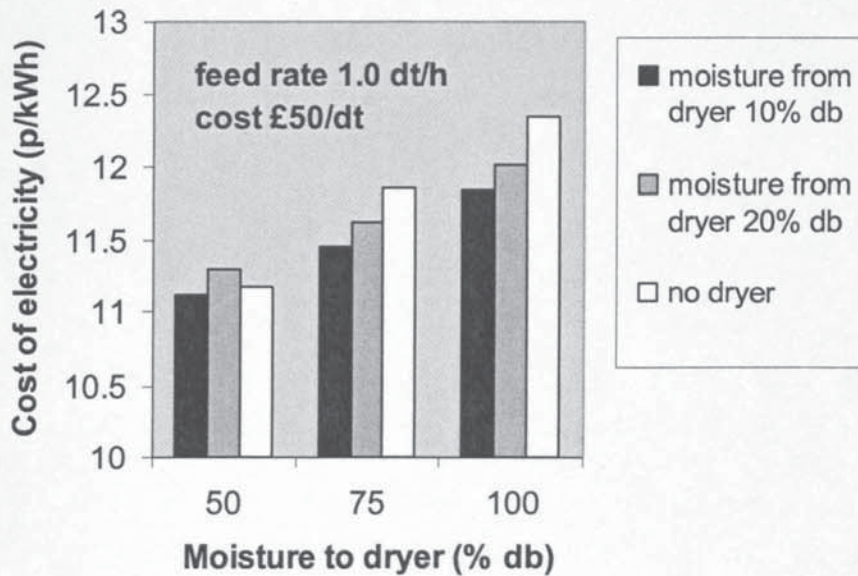
Figure 9.31 Effect of drying on *COE* for feed rate 1.0 dt/h, cost £50/dt - CHP

Comparing Figures 9.28-9.31 with their power-only equivalents (Figures 9.9-9.12), it is clear that the option to omit the dryer (white bars) is superior in many more cases. Nevertheless, the general trends of dryer omission being economically more advantageous at low pre-dryer moistures, low biomass feed rates and low biomass costs remains.

9.2.7 Biomass Feed Rate (System Scale)

The effects of system scale are shown in Figures 9.32-9.35 for η_{OV}, COE, TPC and HPR respectively. The system has a rotary dryer with burner, biomass moisture contents to and from the dryer of 75% db and 10% db respectively, and a biomass cost of £20/dt.
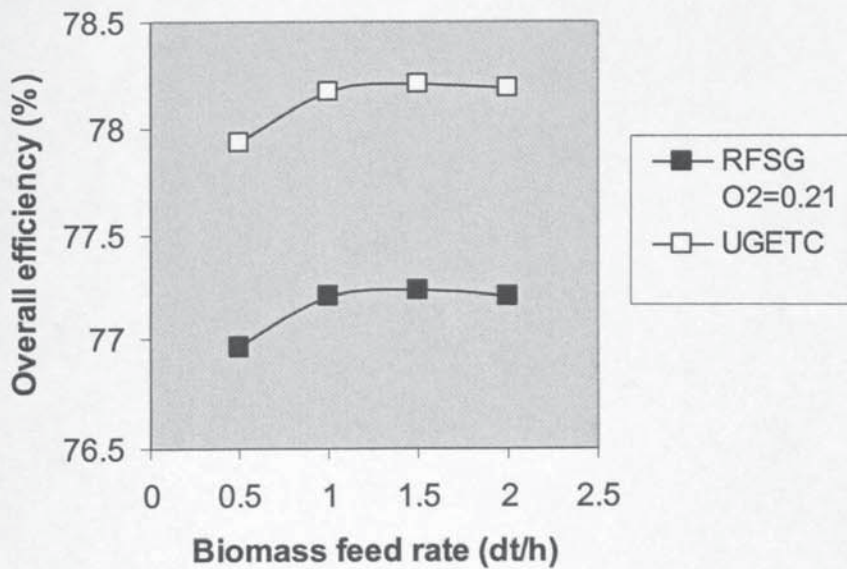
Figure 9.32 Effect of system scale on η_{OV} - CHP
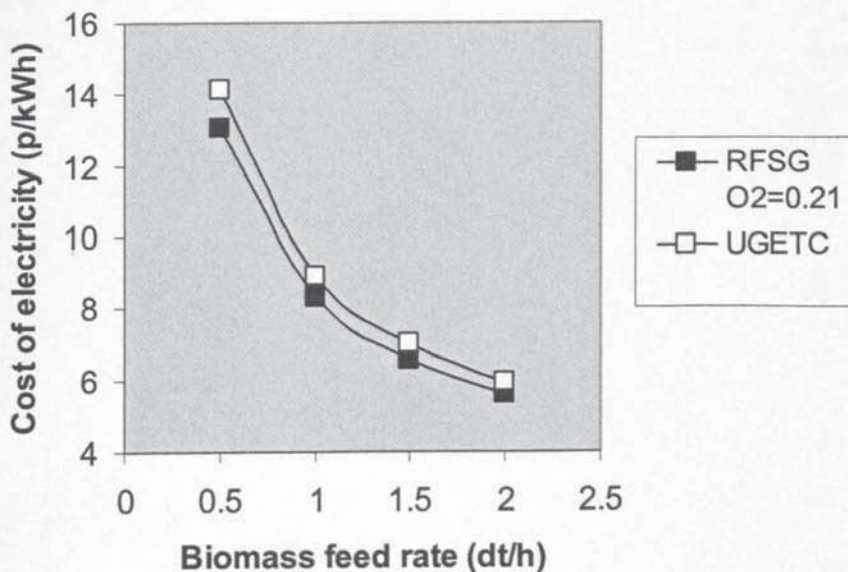
Figure 9.33 Effect of system scale on *COE* - CHP
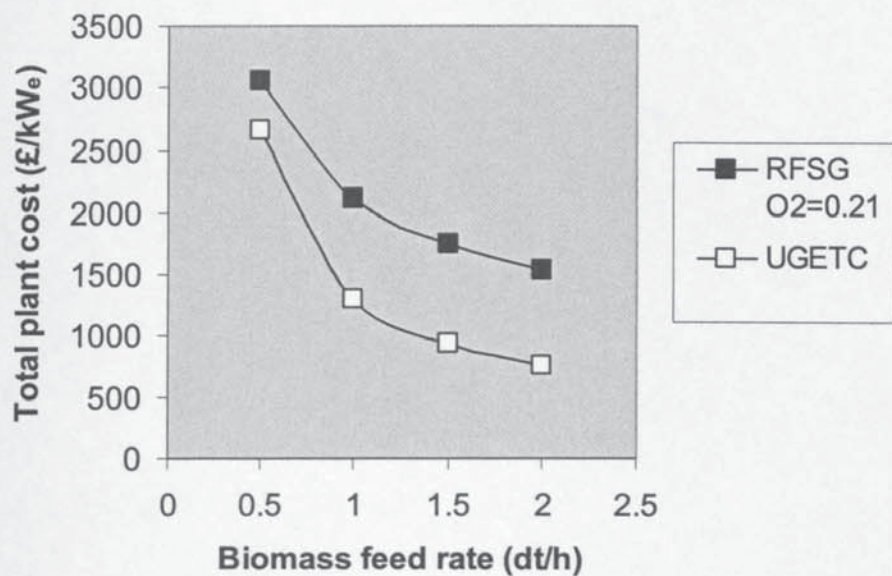
Figure 9.34 Effect of system scale on *TPC* - CHP
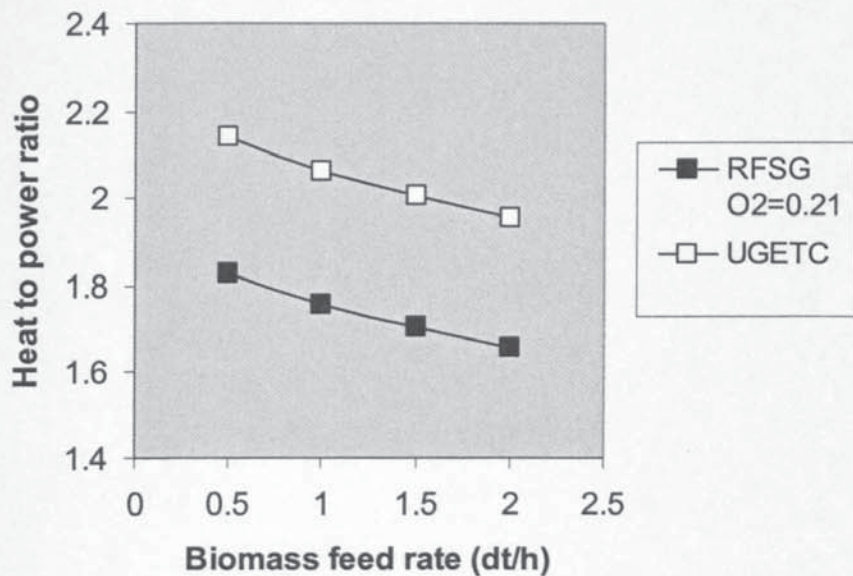
Figure 9.35 Effect of system scale on *HPR* - CHP

The two curves are for a system with an un-enriched air RFSG (capital cost factor 1.0) and a system with a UGETC.

In contrast to power-only systems (Section 9.1.7), η_{OV} is hardly affected by system scale, increasing only very slightly as scale increases. This is because although net electrical output increases due to an increase in IC engine brake thermal efficiency, this energy is taken from the sensible heat in the exhaust gases and cooling circuit which would otherwise go to hot water production. *HPR* falls with increasing scale accordingly.

Both *COE* and *TPC* always fall as scale increases, with. the rate of change greatest at low feed rates. This is due partly to improved electrical efficiency, and partly to capital cost economies of scale accruing for nearly all system modules. The *COE* exponent is approximately -0.63.

Table 9.9 shows a breakdown of total plant cost in absolute terms for a system with a UGETC and a rotary dryer with burner for biomass feed rates of 1.0 and 2.0 dt/h. Dryer inlet and outlet biomass moisture contents are 75% db and 10% db respectively.

Table 9.9 Total plant cost breakdown, UGETC-based system - CHP

System Module	Total Plant Cost, £000	
	Biomass feed rate 1.0 dt/h	Biomass feed rate 2.0 dt/h
Reception, Storage, Screening	171	216
Dryer	493	557
Gasifier	1487	2412
Gas Quench and Waste Water Treatment	19	19
IC Engine	729	1164
Heat Recovery System	122	177
Grid Connection	132	195
TOTAL	3153	4739

As with power-only systems, the benefits of building a BGES for CHP at as large a scale as possible within the constraints of the application are clear.

9.2.8 Biomass Cost

Again not surprisingly, an increase in biomass cost produces an increase in *COE*. Figure 9.36 shows this for systems with an un-enriched air RFSG (capital cost factor 1.0) and with a UGETC. In each case the system has a rotary dryer with burner, biomass moisture contents to and from the dryer of 75% db and 10% db respectively, and a biomass feed rate of 1.5 dt/h.
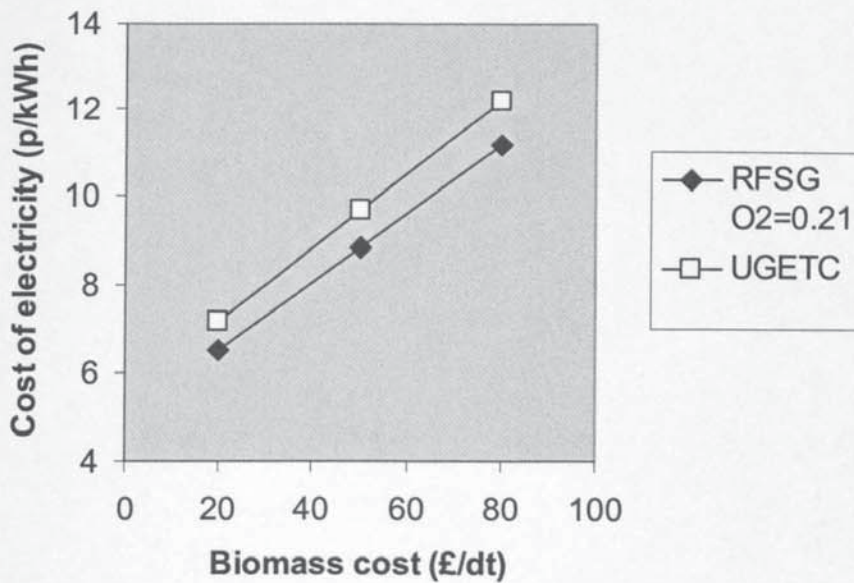
Figure 9.36 Effect of biomass feed cost on *COE* - CHP

Over all cases with the unenriched air RFSG, *COE* rises at an average rate of about 0.8 p/kWh for every £10/dt rise in biomass cost, the same as for power-only systems. The equivalent figure for systems with the UGETC is again the same as for power-only systems at about 0.9 p/kWh.

10 CONCLUSIONS

10.1 System Modelling Study - General (Chapter 9)

1. A spreadsheet-based model of a BGES has been successfully constructed and used to evaluate the performance and economic characteristics of such a system, with particular reference to the integration of heat and the need for biomass drying. No such study has been previously reported in the literature.

2. The spreadsheet approach was vindicated in that over 15,000 cases were run in a relatively short period of time, thus allowing a study of the full operational and design envelope of the BGES. Only a small fraction of the number of cases would have been possible in the time available with flow-sheeting software.

3. The model was validated by comparison to previous studies. The average value for *COE* from the baseline set of cases (biomass feed rate 1.5 dt/h, biomass cost £20/dt and pre-dryer biomass moisture content 75% db, RFSG capital cost factor 1.0 where applicable) was within 10% of the average from the previous studies considered, and discrepancies with specific previous studies could be explained by choice of boundary conditions where these were published.

4. If a drying stage is included, then the lowest cost of electricity is always achieved by drying to the lowest practical moisture content, despite the increased dryer size.

5. For systems with a biomass feed rate, cost and pre-dryer moisture at the lower end of the range of study, cost of electricity can be lower if the drying stage is omitted altogether. This would however only be a practical proposition with a UGETC. As biomass feed rate, cost and pre-dryer moisture increase however, the gain from omitting the dryer reduces and is soon reversed.

6. For systems with an RFSG, the lowest cost of electricity and the highest overall efficiency is always obtained by operating without air oxygen enrichment to the gasifier – i.e. by omitting an air oxygen enrichment plant altogether. If an air oxygen

enrichment plant must be employed, then increasing the air oxygen content to the gasifier always results in an increase in cost of electricity.

7. On average, systems with an RFSG operating without oxygen-enriched air have a lower cost of electricity (by about 0.7 p/kWh or around 10%) than equivalent systems with a UGETC. However if the RFSG must operate with air oxygen enrichment, then the cost of electricity from UGETC systems can often be lower, whether and by how much depending on a number of parameters.

8. Cost of electricity always falls as biomass feed rate (system scale) increases, with exponents of approximately -0.46 for power-only and -0.63 for CHP systems. The rate of fall is greatest at low feed rates. Within the scale range studied here, a BGES should always be built as large as possible within the constraints of feed supply, output demand and finance.

9. For systems with an RFSG operating on un-enriched air, cost of electricity rises at an average rate of about 0.8 p/kWh for every £10/dt rise in biomass cost. The equivalent figure for systems with a UGETC is about 0.9 p/kWh.

10. For systems with an RFSG and an oxygen enrichment plant, supply of oxygen-enriched air to the IC engine to boost output always causes a reduction in overall efficiency and an increase in cost of electricity, and is not therefore justified.

10.2 System Modelling Study - Power-only Systems (Section 9.1)

11. For the baseline cases, the lowest cost of electricity obtained is 7.7 p/kWh, for a system with an RFSG and a band dryer. Overall efficiency is 28.8%.

12. Of the three dryer options, systems with the band dryer always give the lowest cost of electricity - as a result of lower electrical consumption and capital cost.

13. In all cases, systems with an RFSG have a higher overall efficiency than equivalent systems with a UGETC. In cases with an RFSG operating without enriched air, the average difference is 2.3%.

10.3 System Modelling Study - CHP Systems (Section 9.2)

14. For the baseline cases, the lowest cost of electricity obtained is 6.5 p/kWh, for a system with an RFSG and a rotary dryer with burner. Overall efficiency is 77.2% (heat *and* power). In this study therefore, CHP operation gives a lower cost of electricity than power-only operation.

15. Of the three dryer options, systems with a band dryer give the lowest cost of electricity at feed rates below about 1.2 dt/h, and systems incorporating a rotary dryer with burner give the lowest cost of electricity at feed rates above this level.

16. In all cases, systems with a UGETC have a higher overall efficiency than equivalent systems with an RFSG, by an average margin of 1.6%.

10.4 Model Evaluation of Gasifier Performance (Section 5.3)

17. A gasifier model based on equilibrium chemistry has been validated against limited data from a pilot-scale RFSG.

18. Even with air pre-heat and oxygen enrichment, temperatures over large parts of the RFSG gasification reactor are likely to remain much too low for effective slagging operation on most biomass feedstocks. The RFSG could operate in non-slagging mode on biomass feedstocks with very high ash fusion temperatures, such as bark. Much higher temperatures could be achieved using feedstocks with lower oxygen content (and to a lesser extent hydrogen content), such as charcoal or shredded tyres.

19. The UGETC gives a cold gas efficiency of 77.6% and a product gas lower heating value of 5.12 MJ/Nm^3 when fed with biomass with a moisture content of 17.6% db (15% on a wet basis).

20. The cold gas efficiency of the RFSG is about 5% higher than that of the UGETC. This is due entirely to air pre-heat (the UGETC cannot operate with air pre-heat without risk of slagging).

21. The lower heating value of the product gas from the RFSG when operating with unenriched air is about 1 MJ/Nm^3 higher than that of the UGETC. With air oxygen enrichment this differential increases to about 3 MJ/Nm^3 at 40% oxygen, and 5 MJ/Nm^3 at 100% oxygen.

22. For both gasifier types, cold gas efficiency and product gas heating value fall with increasing biomass moisture content. For the RFSG, product gas heating value rises with increasing air oxygen concentration, but cold gas efficiency is unchanged.

23. The benefits of air pre-heating in the RFSG, while significant for unenriched air, are much diminished if oxygen enrichment is employed, as the flow rate and hence thermal capacity of the air is reduced.

10.5 Effects of Gas Properties on Engine Performance (Section 6.2.4)

24. Operation on a typical biomass gasifier product gas with a lower heating value of 4.5 MJ/Nm^3 dry basis gives rise to an engine power derating of about 23% from natural gas operation. As heating value increases through reduction in nitrogen content, derating falls. By a lower heating value of around 9.0 MJ/Nm^3, the derating has fallen to zero.

25. Product gas temperature at inlet should be minimised. Reducing gas inlet temperature from 80°C to 40°C gives an increase in electrical output of about 0.7% and a reduction in capital cost per kilowatt of about 4%.

10.6 Dryers for a Biomass Gasification System (Appendix 1)

26. Dryer types suited to biomass gasification systems in general (not specifically BGESs) are perforated floor bin, band conveyor, rotary louvre, rotary cascade, rotary steam tube, atmospheric fluid bed, pressurised fluid bed and pressurised pneumatic conveying.

27. For biomass gasification systems (not specifically BGESs) below ~ 0.5 MWe the best suited dryer type is either a batch perforated floor bin or a deep bed band conveyor, both using heated air. For systems in the range 0.5-5.0 MWe the best suited type is either a deep bed band conveyor using heated air, or a rotary cascade or thin bed band conveyor using engine exhaust gas. For systems above 5.0 MWe the best suited type is either a rotary cascade using engine exhaust gas, or a pressurised steam dryer.

28. Final choice of dryer will follow careful technical and economic evaluation of the specific system under consideration. Key determinants in the choice of dryer are cost, capacity range, available sources of heat, alternative uses of that heat, avoidance of excessive material temperatures to prevent thermal degradation and emissions, and avoidance of fire or explosion hazards.

10.7 Further Work

The spreadsheet-based system modelling approach has proved successful in investigating the characteristics of biomass gasifier engine systems. As indicated in Section 8.1 however, it was selected on the grounds that it offered certain advantages in the modelling of relatively simple systems such as a BGES, but would be less well suited to larger more complex systems where flow-sheeting packages would be more appropriate. It is not therefore proposed that the model be extended in scope to encompass much larger systems, particularly those incorporating steam power cycles or combined cycles. Nevertheless, there are a number of areas where further work both in model development and application is merited while retaining the focus on BGES modelling.

In Section 5.3.3.1 it was shown that the RFSG faces fundamental problems of a thermodynamic nature in operating in its intended mode. This, combined with its relative complexity, makes it unlikely that the design will proceed to commercialisation. Further development of the model should therefore focus on the more conventional UGETC design. Without the added complexity of the RFSG regenerator modelling, it would be practical to integrate the equilibrium gasification reactor model into the system model without greatly compromising model run time. This would offer the big advantage that alternative feedstock compositions could be tested without the need to generate new relationships for each type.

While not proposing to extend the model to much larger and more complex systems, the BGES scale range of the model should nevertheless be increased to the equivalent of about 5 MW$_e$, a better upper limit for a BGES than the 2.5 MW$_e$ used in the study which derived from the target range of the RFSG (Section 5.1.3) [5,11,12]. This would involve returning to the dryer manufacturers used in the study to obtain cost data for a wider range of models. All other cost data are applicable up to 5 MW$_e$ (excepting oxygen enrichment equipment, but that would not be required for a UGETC).

The option should also be incorporated into the model at certain points to override theoretical predictions of performance with empirical data or correlations if the user so desires. This would allow for more accurate model calculations as experience with these

systems increases, and would be of particular relevance to gasifier product gas composition and energy pathways within the IC engine.

The application of the model should be extended to explore the influence of the size of the rejected biomass fraction on the relative merits of the rotary dryer with burner in CHP systems, as this is a key determinant in the superiority of this dryer at higher feed rates. Also for CHP systems, the model could consider the influence of different heat pricing scenarios on the choice of optimum configuration, and also the influence of different hot water temperatures to the heat customer. It would be relatively simple to add the option for generating low-pressure steam rather than hot water for those scenarios where the customer specifically demands steam. A BGES is usually a poor choice for the supply of steam because in most cases a large part of the available heat is from the engine cooling system at temperatures of 100°C or less; however, some engine manufacturers offer designs where the coolant outlet temperature has been deliberately increased (at the expense of efficiency) to allow low-pressure steam generation [147].

The model could also be extended to look at the possibility of heat recovery from the moist dryer exhaust for district heating schemes in cold climates. This option was rejected for consideration in the present study because of the assumption of temperate ambient conditions typical of Western Europe, in which district heating return temperatures are no lower than 50°C (Section 2.4). However, in much colder environments such as northern Sweden or Finland, return temperatures may be much lower. Furthermore, when ambient air is at temperatures of 0°C or less, it may be economically viable to use the recovered heat to warm ambient air for use in a band dryer, thus releasing some of the energy from the engine coolant circuits which would otherwise be utilised for the purpose but which could instead contribute to the district heating load.

REFERENCES

1. Merriam-Webster Inc. (1998). *Merriam Webster's Collegiate Dictionary, 10th edition.*

2. Klass, D. L. (1998). *Biomass for Renewable Energy, Fuels and Chemicals.* Academic Press.

3. UK Royal Commission on Environmental Protection (2000). *Energy - the Changing Climate.* 22nd Report of the RCEP.

4. European Commission (1997). *Energy for the Future: Renewable Sources of Energy (White Paper for a Community Strategy and Action Plan).* EC document COM(97)599.

5. UK Department of Trade and Industry (1999). *New and Renewable Energy: Prospects for the 21st Century.*

6. US Department of Energy. *DOE Biomass Power Program Strategic Plan 1996-2015.* http://www.eren.doe.gov/biopower/library.

7. Bridgwater, A. V. (1995). *The technical and economic feasibility of biomass gasification for power generation.* Fuel, vol. 74 no. 5, pp. 631-653.

8. North, P., Utriainen, T. (2000). *The use of biomass in power generation and CHP schemes.* Proc. UK Institute of Mechanical Engineers Symposium S717: Power Generation by Renewables, London.

9. Miles, T. R. (1992). *Environmental implications of increased biomass energy use.* National Renewable Energy Laboratory (NREL) report TP-230-4633.

10. Energy Technology Support Unit (1991). *Review of Small Steam Turbines (0.25-10 MW_e).* UK Energy Efficiency Office Best Practice Programme general report 5.

11. Williams, R., Larson, E. (1993). *Advanced gasification-based biomass power generation.* Renewable Energy: Sources for Fuel and Electricity (ed. Johansson, T. B.). Island.

12. Nussbaumer, T., Neuenschwander, P., Jenni, A., Bühler, R. (1998). *Technological and economic assessment of the technologies for the conversion of wood to heat, electricity and synthetic fuels.* Proc. 10th European Conference: Biomass for Energy and Industry, Würzburg, CARMEN, pp. 1142-1146.

13. Blackadder, W., Lundberg, H., Rensfelt, E., Waldheim, L. (1992). *Heat and power production via gasification in the range 5-50 MW_e.* Advances in Thermochemical Biomass Conversion (ed. Bridgwater, A. V.), Blackie A & P, pp. 449-475.

14. Drouin, G., Bechard, L., Du Chouchet, P. (1987). *Electricity generated by a diesel engine running on lean gas produced from a biomass pressurised fluid-bed gasifier.* Energy from Biomass and Wastes X (ed. Klass, D. L.), Institute of Gas Technology, pp. 529-536.

15. Wagner, M. (1997). *Utilisation of producer gas in Jenbacher gas engines.* Proc. International Energy Agency Seminar: IC Engines for LCV Gas from Biomass Gasifiers, Zurich, pp. 81-94.

16. Bridgwater, A. V. (1991). *Review of Thermochemical Biomass Conversion.* Energy Technology Support Unit (ETSU) report B1202.

17. Sonnenberg, R., Zerbin, W. O., Krispin, T. (1985). *1.4 and 4.8 MW wood gas power plants in operation.* Proc. 3rd European Conference: Energy from Biomass, Venice, Elsevier, pp. 1117-1121.

18. Ed. Kaltschmitt, M., Rosch, C., Dinkelbach, L. (1998). *Biomass Gasification in Europe.* European Commission report AIR3-CT-94-2284.

19. Cleland, J., Purvis, C. R. (1997). *Demonstration of a 1 MW$_e$ biomass power plant at USMC base Camp Lejeune.* Proc. 3rd Biomass Conference of the Americas: Making a Business from Biomass in Energy, Environment, Chemicals, Fibers and Materials, Montreal, Pergamon, pp. 551-558.

20. Trezek, G., Glaub, J. C. (1987). *Integrated producer gasifier-diesel engine system for solid waste.* Energy from Biomass and Wastes X (ed. Klass, D. L.), Institute of Gas Technology, pp. 629-641.

21. Milne, T. A., Evans, R. J., Abatzoglou, N. (1997). *Biomass gasifier "tars": their nature, formation, destruction, and tolerance limits in energy conversion devices.* Proc. 3rd Biomass Conference of the Americas: Making a Business from Biomass in Energy, Environment, Chemicals, Fibers and Materials, Montreal, Pergamon, pp. 729-738.

22. Hasler, P., Buehler, R., Nussbaumer, T. (1998). *Evaluation of gas cleaning technologies for biomass.* Proc. 10th European Conference: Biomass for Energy and Industry, Würzburg, CARMEN, pp. 272-275.

23. Nicholson, R. (1999). Private communication, Thermal Developments Ltd.

24. Albisu, F. (1990). *Cogeneration technologies: present and future developments.* Combined Production of Heat and Power (Cogeneration) (ed. Sirchis), Spon, pp. 10-19.

25. Schmidt, F. W., Willmott, A. J. (1981). *Thermal Energy Storage and Regeneration.* Hemisphere.

26. Cassitto, L. (1990). *District heating systems in Europe: a review.* Resources, Conservation and Recycling, vol. 4 no. 4, pp. 271-281.

27. Rakos, C. (1994). *Diffusion of biomass district heating in Austria.* Proc. 8th European Conference: Biomass for Energy, Environment, Agriculture and Industry, Vienna, Pergamon, pp. 886-897.

28. Evald, A., Larsen, M. G. (1996). *Experiences from 61 straw-fired district heating plants in Denmark.* Proc. 9th European Conference: Biomass for Energy and the Environment, Copenhagen, Pergamon, pp. 211-216.

29. Diamant, R. M. E., Kut, D. (1981). *District Heating and Cooling for Energy Conservation.* Wiley.

30. Miles, T. R., Baxter, L. L., Bryers, R. W., Jenkins, B. M., Oden, L. L. (1995). *Alkali Deposits Found in Biomass Power Plants: a Preliminary Investigation of their Extent and Nature.* National Renewable Energy Laboratory (NREL) report TP-433-8142.

31. Kuiper, L. C., Kolster, H. W. (1996). *Twenty years of research on poplar biomass production in the Netherlands.* Proc. 9th European Conference: Biomass for Energy and the Environment, Copenhagen, Pergamon, pp. 96-102.

32. UK Forestry Commission (1991). *Coppiced Trees as Energy Crops.* Energy Technology Support Unit (ETSU) report B 1078.

33. Esteban-Pascual, L. (1998). Private communication, CIEMAT.

34. Skaar, C. (1988). *Wood-water Relations.* Springer-Verlag.

35. Nellist, M. E. (1997). *Storage and Drying of Short Rotation Coppice.* Energy Technology Support Unit (ETSU) report B/W2/00391/REP.

36. Rogers, G. F. C., Mayhew, Y. R. (1987). *Thermodynamic and Transport Properties of Fluids.* Blackwell.

37. Ed. Gerrard, A. M. (2000). *A Guide to Capital Cost Estimating, 4th Edition.* UK Institution of Chemical Engineers.

38. Bridgwater, A. V. (1994). *Capital Cost Estimation Procedures.* Aston University.

39. Solantausta, Y., Bridgwater, A. V., Beckman, D. (1996). *Electricity Production by Advanced Biomass Power Systems.* Technical Research Centre of Finland (VTT) research note 1729.

40. Toft, A. J. (1996). *A Comparison of Integrated Biomass to Electricity Systems.* PhD thesis, Aston University.

41. Taylor, J. H., Craven, P. J. (1979). *Experience curves for chemicals.* Process Economics International, vol. 1 no. 1, pp. 13-28.

42. Elliott, P. (1993). *Biomass energy overview in the context of Brazilian biomass power demonstration.* Bioresource Technology, vol. 46, pp. 13-22.

43. Yorkshire Water Services (1999). *Charges Scheme and Scale of Other Charges 1999/2000.*

44. Craig, K. R., Mann, M. K. (1996). *Cost and Performance Analysis of Three Integrated Biomass Gasification Combined Cycle Power Systems.* National Renewable Energy Laboratory (NREL) report TP-430-21657.

45. van Ree, R., Oudhuis, A. B. J., Faaij, A., Curvers, A. (1995). *Modelling of a Biomass Integrated Gasifier/Combined Cycle (BIG/CC) System with the Flowsheet Simulation Programme AspenPlus.* Netherlands Energy Research Foundation (ECN) report ECN-C-95-041.

46. Solantausta, Y., Makinen, T., McKeough, P., Kurkela, E. (1992). *Performance of cogeneration gasification combined cycle power plants employing biomass as fuel.* Advances in Thermochemical Biomass Conversion (ed. Bridgwater, A. V.), Blackie A & P, pp. 476-494.

47. Consonni, S., Larson, E. D. (1996). *Biomass-gasifier/aeroderivative gas turbine combined cycles: part A - technologies and performance modelling.* Transactions of the American Society of Mechanical Engineers: Journal of Engineering for Gas Turbines and Power, vol. 118, pp. 507-515.

48. Consonni, S., Larson, E. D. (1996). *Biomass-gasifier/aeroderivative gas turbine combined cycles: part B - performance calculations and economic assessment.* Transactions of the American Society of Mechanical Engineers: Journal of Engineering for Gas Turbines and Power, vol. 118, pp. 516-525.

49. Wan, E. I., Fraser, M. D. (1990). *Economic assessment of advanced biomass gasification systems.* Energy from Biomass and Wastes XIII (ed. Klass, D. L.), Institute of Gas Technology, pp. 791-828.

50. Electric Power Research Institute (1993). *Strategic Analysis of Biomass and Waste Fuels for Electric Power Generation.* EPRI report TR-102773.

51. McIlveen-Wright, D. (1995). *Electricity Generation from Wood.* PhD thesis, University of Ulster.

52. Stassen, H. E. M., Stiles, H. N. (1989). *Economic analysis of small-scale biomass conversion systems.* Energy from Biomass and Wastes XII (ed. Klass, D. L.), Institute of Gas Technology, pp. 865-890.

53. Bridgwater, A. V., Cottam, M. L. (1992). *Opportunities for biomass pyrolysis liquids production and upgrading.* Energy and Fuels, vol. 6 no. 2, pp. 113-120.

54. Bridgwater, A. V., Double, J. M. (1991). *Production costs of liquid fuels from biomass*. Fuel, vol. 70, pp. 1209-1224.

55. Mitchell, C. P., Bridgwater, A. V., Stevens, D. J., Toft, A. J., Watters, M. P. (1995). *Technoeconomic assessment of biomass to energy*. Biomass and Bioenergy, vol. 9 nos. 1-5, pp. 205-226.

56. Mitchell, C. P., Bridgwater, A. V., Toft, A. J., Watters, M. P., Stevens, D. J., Aumonier, S., Ellander, R. (1996). *Technoeconomic Assessment of Biomass to Energy - the BEAM Report*. Aberdeen University Forestry Research Paper 1996:1,.

57. McGowin, C. R., Wiltsee, G. A. (1996). *Strategic analysis of biomass and waste fuels for electric power generation*. Biomass and Bioenergy, vol. 10 nos. 2-3, pp. 167-175.

58. Korens, N. (1993). *BIOPOWER: Biomass and Waste-fired Power Plant Performance and Cost Model*. Electric Power Research Institute (EPRI) draft report, Project 3295-02.

59. Heaton, J. (1990). *Modelling and Application of Biomass Gasification Based Power Generation Systems*. European Commission report EUR 11994 EN.

60. Paisley, M., Farris, G., Slack, W., Irving, J. (1997). *Commercial development of the Battelle/FERCO biomass gasification process - initial operation of the McNiel gasifier*. Proc.3rd Biomass Conference of the Americas: Making a Business from Biomass in Energy, Environment, Chemicals, Fibers and Materials, Montreal, Pergamon, pp. 579-588.

61. Mann, M. K., Spath, P. L. (1997). *Life-cycle Assessment of a Biomass Gasification Combined-cycle System*. National Renewable Energy Laboratory (NREL) report TP-430-23076.

62. Consonni, S., Lozza, G., Macchi, E., Chiesa, P., Bombarda, P. (1991). *Gas-turbine-based advanced cycles for power generation: part A - a calculation model*. Proc. 1991 Yokohama International Gas Turbine Congress, Tokyo, pp. 201-210.

63. Hughes, W. E. M., Larson, E. D. (1998). *Effect of fuel moisture content on biomass-IGCC performance*. Transactions of the American Society of Mechanical Engineers: Journal of Engineering for Gas Turbines and Power, vol. 120, pp. 455-459.

64. Solantausta, Y., Makinen, T., Kurkela, E., Sipila, K. (1993). *New Alternatives for Energy Production, Part 4: Performance of Peat-fuelled Air Gasification Combined-cycle Power Plants*. Technical Research Centre of Finland (VTT) research note 1451.

65. Solantausta, Y., Bridgwater, A. V., Beckman, D. (1995). *Feasibility of power production with pyrolysis and gasification systems*. Biomass and Bioenergy, vol. 9 nos. 1-5, pp. 257-269.

66. Solantausta, Y., Bridgwater, A. V., Beckman, D. (1997). *The performance and economics of power from biomass*. Developments in Thermochemical Biomass Conversion (ed. Bridgwater, A. V., Boocock, D. G. B.), pp. 1539-1555.

67. Solantausta, Y., Huotari, J. (2000). *Power Production from Wood - Comparison of the Rankine Cycle to Concepts Using Gasification and Fast Pyrolysis*. IEA Bioenergy Task 22 Final Report, VTT Research Notes 2024.

68. McIlveen-Wright, D., Williams, B. C., McMullan, J. T. (1997). *Electricity generation from wood-fired power plants; the principal technologies reviewed*. Developments in Thermochemical Biomass Conversion (ed. Bridgwater, A. V., Boocock, D. G. B.), Blackie A & P, pp. 1525-1538.

69. Faaij, A., van Ree, R., Oudhuis, A. (1995). *Gasification of Biomass Wastes and Residues for Electricity Production*. University of Utrecht report 95035.

70. Faaij, A., van Wijk, A., van Ree, R., Oudhuis, A., Waldheim, L., Olsson, E., Daey-Ouwens, C., Turkenburg, W. (1997). *Gasification of biomass wastes and residues for electricity production*. Biomass and Bioenergy, vol. 12 no. 6, pp 387-407.

71. Brown, D. A. G. (1994). *Coppice Wood Drying in a Gasification Power Plant*. Energy Technology Support Unit (ETSU) report B/M3/00388/08/REP.

72. Baker, C. G. J. (1983). *Cascading rotary dryers*. Advances in Drying (ed. Mujumdar, A. S.), vol. 2, pp. 1-51.

73. Kiranoulis, C. T., Maroulis, Z. B., Marinos-Kouris, D. (1997). *Modelling and optimization of fluidized bed and rotary dryers*. Drying Technology, vol. 15 no. 3-4, pp. 735-763.

74. Duchesne, C., Thibault, J., Bazin, C. (1996). *Modelling of solids transportation within an industrial rotary dryer: a simple model*. Industrial and Engineering Chemistry Research, vol. 35, pp. 2334-2341.

75. Papadakis, S. E., Langrish, T. A. G., Kemp, I. C., Bahu, R. E. (1994). *Scale-up of cascading rotary dryers*. Drying Technology, vol. 12 no. 1-2, pp. 259-277.

76. Kemp, I. C., Oakley, D. E. (1997). *Simulation and scale-up of pneumatic conveying and cascading rotary dryers*. Drying Technology, vol. 15 no. 6-8, pp. 1699-1710.

77. Toei, R., Okazaki, M., Tamon, H. (1994). *Conventional basic design for convection or conduction dryers*. Drying Technology, vol. 12 no. 1-2, pp. 59-97.

78. Brooks, B. C. (1998). Private communication, MEC Company.

79. Brammer J. G., Bridgwater A. V. (1999). *Drying technologies for an integrated gasification bio-energy plant.* Renewable and Sustainable Energy Reviews, no. 3, pp. 243-289.

80. Peters, M. S., Timmerhaus, K. D. (1980). *Plant Design and Economics for Chemical Engineers.* McGraw Hill.

81. Bruce, D. M., Hamer, P. J. C. (1998). *Simulations of Poplar Wood Chip Drying in Batch with Waste Heat.* Silsoe Research Institute report CR/867/98/1418.

82. Thompson, C. W. (1998). Private communication, Wolverine Proctor & Schwartz.

83. Bridgwater, A. V., Evans, G. D. (1993). *An Assessment of Thermochemical Conversion Systems for Processing Biomass and Refuse.* Energy Technology Support Unit (ETSU) report B/T1/00207/REP.

84. Kaupp, A. (1983). *State of the Art for Small Scale (to 50kW) Gas Producer-engine Systems.* US Department of Agriculture Forest Service final report contract 53-319R-0-141.

85. Biomass Technology Group (1996). *State of Small-scale Biomass Gasification Technology.* Novem report 9622.

86. Beenackers, A. A. C. M., Maniatis, K. (1996). *Gasification technologies for heat and power from biomass.* Proc. 9th European Conference: Biomass for Energy and the Environment, Copenhagen, Pergamon, pp. 228-259.

87. Stassen, H. E. (1995). *Small-scale Biomass Gasifiers for Heat and Power.* World Bank technical paper no. 296 (energy series).

88. Bridgwater, A. V., Maniatis, K., Masson, H. A. (1990). *Gasification technology.* Commercial and Marketing Aspects of Gasifiers (ed. Buekens, A. G., Bridgwater, A. V., Ferrero, G.-L., Maniatis, K.), European Commission, pp. 41-65.

89. Sharan, H. N., Mukunda, H. S., Shrinivasa, U., Dassapa, S., Paul, P. J., Rajan, N. K. S. (1997). *IISc-DASAG biomass gasifiers: development, technology, experience and economics.* Developments in Thermochemical Biomass Conversion (ed. Bridgwater, A. V., Boocock, D. G. B.), Blackie A & P, pp. 1058-1072.

90. Mukunda, H. S., Dasappa, S., Paul, P. J., Rajan, N. K. S., Shrinivista, U., Sridhar, G., Sridhar, H. V. (1997). *Fixed bed gasification for electricity generation.* Biomass Gasification and Pyrolysis: State of the Art and Future Prospects (ed. Kaltschmitt, M., Bridgwater, A. V.), CPL, pp. 105-116.

91. Wilén, C., Moilanen, V., Kurkela, E. (1996). *Biomass Feedstock Analysis.* Technical Research Centre of Finland (VTT) publication 282.

92. Lacey, J. A. (1988). *Gasification: a key to the clean use of coal, part 1.* Energy World, no. 155, pp. 3-9.

93. Thomas, K. M. (1985). *Some scientific aspects of the development of the slagging gasifier.* Proc. North Atlantic Treaty Organisation Conference: Carbon and Coal Gasification - Science and Technology, Port Alvor, pp. 439-453.

94. Weissman, R., Thone, P. (1995). *Gasification of solid, liquid and gaseous feedstocks: commercial portfolio of Texaco technology.* Proc. UK Institution of Chemical Engineers Conference: Gasification - an Alternative to Natural Gas, London.

95. Hauserman, W. B., Willson, W. G. (1984). *Conclusions on slagging, fixed-bed gasification of lignite.* Proc. 12th Biennial Lignite Symposium: Technology and Utilisation of Low-rank Coals, vol. 1, pp. 149-223.

96. Niessen, W. R., Marks, C. H., Sommerlad, R. E. (1997). *Evaluation of Gasification and Novel Thermal Processes for the Treatment of Municipal Solid Wastes.* National Renewable Energy Laboratory (USA) report TP-430-21612.

97. Eberle, D. J., Spencer, J. L., Schultz, H. W. (1985). *Destruction of hazardous organic substances in a slagging gasifier.* Industrial and Engineering Chemistry Process Design and Development, no. 24, pp. 873-877.

98. Robinson, E. K., Easton, R. J. (1976). *Partial oxidation of refuse using the Purox system.* Proc. 1st International Symposium on Materials and Energy from Refuse, Antwerp.

99. Lorson, H., Schingnitz, M., Leipnitz, Y. (1995). *The thermal treatment of wastes and sludges with the Noell entrained flow gasifier.* Proc. UK Institution of Chemical Engineers Conference: Gasification - an Alternative to Natural Gas, London.

100. Davidson, P. E., Lucas, T. W. (1978). *The Andco-Torrax high temperature slagging pyrolysis system.* Proc. 175th National Meeting of the American Chemical Society, Anaheim.

101. Brammer, J. G., van de Beld, L., Bridgwater, A. V., Assink, D. (1999). *Development of a novel reverse-flow slagging gasifier for small-scale cogeneration applications.* Proc. 4th Biomass Conference of the Americas: Biomass - a Growth Opportunity in Green Energy and Value-added Products, Oakland, Pergamon, pp. 1119-1126.

102. van de Beld, L., Wagenaar, B.M., Prins, W. (1996). *Cleaning of hot producer gas in a catalytic reverse-flow reactor.* Developments in Thermochemical Biomass Conversion (ed. Bridgwater, A.V., Boocock, D. G. B.), Blackie A & P, pp. 907-920.

103. McLellan, R. (1997). *Wellman biomass gasification technology*. Proc. 4th International Wood Fuel Conference, ETSU, Kenilworth.

104. Buekens, A. G., Schoeters, J. G. (1982). *Modelling of biomass gasification*. Fundamentals of Thermochemical Biomass Conversion (ed. Overend, R. P.), Elsevier, pp. 619-689.

105. Gibbins, J. R. (1982). *Equilibrium Modelling - a Cheap and Effective Aid to Gasifier Modelling*. Foster Wheeler Power Products report RD 659/TN 17.

106. Chern, S., Walawender, W. P., Fan, L. T. (1989). *Equilibrium modelling of a downdraft biomass gasifier*. Proc. American Institute of Chemical Engineers Spring National Meeting.

107. Reed, T. B., Markson, M. (1983). *A predictive model for stratified downdraft gasification of biomass*. Progress in Biomass Conversion, vol. 4, pp. 217-253.

108. Davies, R. M., Tait, A. R., Yung, B. P. K. (1991). *Modelling of coal gasification reactors*. 18th International Gas Union World Gas Conference, Berlin.

109. van den Aarsen, F. G., Beenackers, A. A. C. M., van Swaaij, W. P. M. (1983). *Modelling of a Fluidised Bed Wood Gasifier*. European Commission report contract ESE-R-029-NL

110. Fernando, W. J. N., Hewitt, G. F. (1995). *A model for fluidised bed gasification of biomass*. Proc. UK Institution of Chemical Engineers Conference: Gasification - an Alternative to Natural Gas, London.

111. di Blasi, C. (2000). *Dynamic behaviour of stratified downdraft gasifiers*. Chemical Engineering Science, vol. 55 no. 15, pp. 2931-2944.

112. Fletcher, D. F., Haynes, B. S., Chen, J., Joseph, S. D. (2000) *A CFD based combustion model of an entrained flow biomass gasifier*. Applied Mathematical Modelling, vol. 22 no. 10, pp. 747-757

113. Gøbel, B., Bentzen, J. D., Henriksen, U., Houbak, N. (1999). *Dynamic modelling of the two-stage gasification process*. Proc. 4th Biomass Conference of the Americas: Biomass - a Growth Opportunity in Green Energy and Value-added Products, Oakland, Pergamon, pp. 1025-1031.

114. Double, J. M. (1988). *The Design, Evaluation and Costing of Biomass Gasifiers*. PhD thesis, Aston University.

115. Baron, R. E., Porter, J. H., Hammond, O. H. (1976). *Chemical Equilibria in Carbon-hydrogen-oxygen Systems*. MIT.

116. Desrosiers, R. (1981). *Thermodynamics of gas-char reactions.* Biomass Gasification: Principles and Technology (ed. Reed, T. B.), Noyes Data Corporation, pp. 119-153.

117. Graboski, M., Bain, R. (1981). *Properties of biomass relevant to gasification.* Biomass Gasification: Principles and Technology (ed. Reed, T. B.), Noyes Data Corporation, pp. 41-69.

118. Ed. Chase, M. W. (1986). *Janaf Thermochemical Tables, 3rd Edition.* American Chemical Society.

119. Gumz, W. (1950). *Gas Producers and Blast Furnaces.* Wiley.

120. Ed. Schlunder, E. U. (1984). *Regeneration and thermal energy storage.* Heat Exchanger Design Handbook (ed. Schlunder, E. U.), Hemisphere.

121. Hausen, H. (1983). *Heat Transfer in Counterflow, Parallel Flow and Cross Flow.* McGraw Hill.

122. Gnielinski, V. (1981). *Equations for the calculation of heat and mass transfer during flow through stationary spherical packings at moderate and high Peclet numbers.* International Chemical Engineering, vol. 21, pp. 378-383.

123. Assink, D. (2000). Private communication, Biomass Technology Group.

124. Ed. Rathbauer J. (1999). *Small Scale Biomass Boilers Guidelines.* European Commission ALTENER programme publication.

125. Chern, S., Fan, L. T., Walawender, W. P. (1989). *Analytical calculation of equilibrium gas composition in a C-H-O-inert system.* American Institute of Chemical Engineers Journal, vol. 35 no. 4, pp. 673-675.

126. Reed, T. B., Das, A. (1988). *Handbook of Biomass Downdraft Gasifier Engine Systems.* Solar Energy Research Institute (SERI) report SP-271-3022.

127. Liley, P. E., Thomson, G. H., Friend, D. G., Daubert, T. E., Buck, E. (1997). *Physical and chemical data.* Perry's Chemical Engineers' Handbook, 7th Edition. McGraw Hill.

128. Kays, W. M., London, A. L. (1984). *Compact Heat Exchangers.* McGraw Hill.

129. Rensfelt, E., Oastman, A. (1996). *Gasification of Waste: Summary and Conclusions of Twenty-five Years of Development.* Termiska Processer (TPS) report TPS-96/19.

130. Walawender, W. P., Chee, C. S., Fan, L. T. (1988). *Operating parameters influencing downdraft gasifier performance.* Energy from wastes and biomass XI (ed. Klass, D. L.), Institute of Gas Technology, pp. 411-446.

131. McLellan, R. (1999). Private communication, Wellman Process Engineering.

132. Reed, T. B. (1997). Private communication, Biomass Energy Foundation.

133. Haselbacher, H. (1997). *Gas turbines fore electricity production from LCV gas.* Biomass Gasification and Pyrolysis: State of the Art and Future Prospects (ed. Kaltschmitt, M., Bridgwater, A. V.), CPL, pp. 291-299.

134. Kaltschmitt, M., Bridgwater, A. V. (1997). *Research, development and demonstration needs for biomass gasification and pyrolysis.* Biomass Gasification and Pyrolysis: State of the Art and Future Prospects (ed. Kaltschmitt, M., Bridgwater, A. V.), CPL, pp. 537-550.

135. Heywood, J. B. (1988). *Internal Combustion Engine Fundamentals.* McGraw-Hill.

136. Taylor, C. F. (1985). *The Internal-combustion Engine in Theory and Practice: Combustion, Fuels, Materials, Design.* MIT.

137. Karim, G. A. (1986). *The dual fuel engine.* Proc. International Symposium on Alternative and Advanced Automotive Engines, Vancouver, pp. 83-104.

138. Daugas, M. (1983). *Pielstick tests on AFB biogas diesels give promising results.* Modern Power Systems, February, pp. 43-45.

139. Boevey, T. M. C. (1983). *Producer gas from trash and bagasse as a viable supplementary fuel for diesel engines.* Proc. S. African Sugar Technologists' Association Meeting.

140. Nolting, E., Leuchs, M. (1985). *The use of gas from biomass in engines - experiences.* Proc. 3rd European Conference: Energy from Biomass, Venice, Elsevier, pp. 1141-1145.

141. van der Weide, J., Buekens, A. G., Maniatis, K. (1990). *Product gas utilisation.* Commercial and Marketing Aspects of Gasifiers (ed. Buekens, A. G., Bridgwater, A. V., Ferrero, G.-L., Maniatis, K.), European Commission, pp. 90-114.

142. Brogan, T. R., Graboski, M. S., Macomber, J. R., Helmich, M. J., Schaub, F. S. (1993). *Operation of a large bore medium speed turbosupercharged dual fuel engine on low BTU wood gas.* American Society of Mechanical Engineers Internal Combustion Engine Division (Publication) ICE, vol. 20, pp. 51-62.

143. Vielhaber, K. (1996). *The use of process gases as sources of heat and power using spark ignition gas engines.* Proc. Insitution of Diesel and Gas Turbine Engineers INPOWER 96 Conference, London.

144. Parikh, P. P., Shashikantha, Kamat, P. P. (1992). *Wear and maintenance of biomass-based producer-gas dual-fuel engines - effect of tars and particulates.* Energy from Biomass and Wastes XVI (ed. Klass, D. L.), Institute of Gas Technology.

145. Tschalamoff, T. (1997). *Wood gas operation of spark ignited gas engines in the power range 100-2000 kW*. Proc. International Energy Agency Seminar: IC Engines for LCV Gas from Biomass Gasifiers, Zurich, pp. 47-65.

146. Barker, S. N. (1998). *Gas Turbines, Reciprocating Engines and Other Conversion Devices in Biomass to Electricity Systems*. AEA Technology report AEAT-4288.

147. Jenbacher Energie (1998). http://www.jenbacher.com.

148. Caterpillar Inc. (1998). http://www.cat.com.

149. S.E.M.T. Pielstick (1998). http://www.pielstick.com.

150. Horlock, J. (1997). *Cogeneration - Combined Heat and Power (CHP)*. Krieger.

151. International Energy Agency (2000). *Energy Statistics of OECD Countries 1997-1998 (2000 Edition)*.

152. Park, W. R., Oliveros, A., Duran, E., Caballero, E. (1987). *Wood Gasifier, Loma Plata, Paraguay*. Organisation of American States report.

153. (1986). *Low-Btu gas from wood to fuel 20-MW diesel CHP power plant*. Cogeneration, September, pp. 18-20.

154. Jeffries, S. (1998). Private communication, Clarke Energy.

155. Wagner, M. (2000). Private communication, Jenbacher AG.

156. Cooke, A. G. (1983). *The Combustion of Low/medium Calorific Value Gas in Gas and Dual Fuel Engines*. Wellman Process Engineering report.

157. Moyers, C. G., Baldwin, G. W. (1997). *Psychrometry, evaporative cooling and solids drying*. Perry's Chemical Engineers' Handbook, 7th Edition. McGraw Hill.

158. Stassen, H. E., Koele, H. J. (1997). *The use of LCV-gas from biomass gasifiers in internal combustion engines*. Biomass Gasification and Pyrolysis: State of the Art and Future Prospects (ed. Kaltschmitt, M., Bridgwater, A. V.), CPL, pp. 269-281.

159. Blowes, J. H. (1999). *Gas Engine Power Generation Costs*. Diesel Consult report.

160. Jenkins, B. M., Goss, J. R. (1988). *Performance of a small spark-ignited internal combustion engine on producer gas from rice hulls*. Research in Thermochemical Biomass Conversion, (ed. Bridgwater, A. V., Kuester, J. L.), Elsevier, pp. 1057-1070.

161. Simons Resource Consultants (1983). *Data book of unit processes for secondary conversion of energy forms*. Enfor Project C-258: A Comparative Assessment of Forest Biomass Conversion to Energy Forms (Phase 1), vol. 8.

162. Biomass Technology Group (1996). *Pretreatment Technologies for Energy Crops*. Novem report 9525.

163. Bio-Energy Research Group (1998). *Energy prices and taxes*. PyNe Newsletter, issue 6.

164. BOC Group (1998). http://www.boc.com/gases/air/air.htm.

165. Bhide, B. D., Stern, S. A. (1991). *A new evaluation of membrane processes for the oxygen enrichment of air*. Journal of Membrane Science, vol. 62, pp. 13-58.

166. Lockyer, D. (1999). Private communication, BOC Group.

167. Ulrich, G. D. (1984). *A Guide to Chemical Engineering Process Design and Economics*. Wiley.

168. Ed. Rohsenow, W. M., Hartnett, J. P., Ganic, E. N. (1985) *Handbook of Heat Transfer Applications*. McGraw Hill.

169. Reay, D. A. (1979). *Heat Recovery Systems*. Spon.

170. Garrett, D. E. (1989). *Chemical Engineering Economics*. Van Nostrand Reinhold.

171. Eastop, T. D., Croft, D. R. (1990). *Energy Efficiency for Engineers and Technologists*. Longman.

172. Saunders, E. A. D. (1988). *Heat Exchangers - Selection, Design and Construction*. Longman.

173. Goldstick, R., Thumann, A. (1986). *Principles of Waste Heat Recovery*. Fairmont.

174. Cleaver Brooks (1998). http://www.cleaver-brooks.com.

175. Kihara, S., Namba, I ., Kuwabara, T, Fujii, N. (1997). *Corrosion of T-11 syngas cooler tubes in IGCC pilot plant*. Materials at High Temperatures, vol. 4 no. 4, pp.429-433.

176. Nielsen, H. P., Frandsen, F. J., Dam-Johansen, K., Baxter, L. L. (2000). *The implications of chlorine-associated corrosion on the operation of biomass-fired boilers*. Progress in Energy and Combustion Science, vol. 26, no. 3, pp. 283-298

177. Shilling, R. L., Bell, K. J., Bernhagen, P. M., Flynn, T. M., Goldschmidt, V. M., Hrnjak, P. S., Standiford, F. C., Timmerhaus, K. D. (1997). *Heat-transfer equipment*. Perry's Chemical Engineers' Handbook, 7th Edition. McGraw Hill.

178. Brown, M. D., Baker, E. G., Mudge, L. K. (1987). *Evaluation of processes for removal of particulates, tars and oils from biomass gasifier product gases*. Energy from Biomass and Wastes X (ed. Klass, D. L.), Institute of Gas Technology, pp. 655-676.

179. Knoef, H. A. M., Stassen, H. E. M., Hovestad, A., Visser, R. (1987). *Environmental aspects of condensates from down-draft biomass gasifiers*. Proc.4th European conference: biomass for energy and industry, Orleans, Elsevier, pp. 1152-1159.

180. Guigon, P., Large, J. F. (1990). *Environmental aspects of gasification.* Commercial and Marketing Aspects of Gasifiers (ed. Buekens, A. G., Bridgwater, A. V., Ferrero, G.-L., Maniatis, K.), European Commission, pp. 115-131.

181. Aspen Technology Inc. (1997). *Aspen Plus Version 10.*

182. AEA Technology - Hyprotech (2000). http://www.hyprotech.com/hysys/process.

183. Green, C. H., Ready, A. B., Chew, P. E., Hartwell, K. (1998). *PROATES^{TM} - whole power plant modelling software package for optimising performance.* Proc. UK Institute of Mechanical Engineers Conference: Optimisation and Development of Existing Steam Plant by Modelling, London.

184. International Energy Agency (1998). *Energy Prices and Taxes, 4th Quarter.*

185. Johansson, A., Rasmuson, A. (1997). *The influence of the drying medium on high temperature convective drying of single wood chips.* Drying Technology, Vol. 15 no. 6-8, pp. 1801-1813.

186. Pierik, J. T. G., Curvers, A. P. W. M. (1995). *Logistics and Pretreatment of Biomass Fuels for Gasification and Combustion.* Netherlands Energy Research Foundation (ECN) report ECN-C-95-038.

187. Simons Resource Consultants (1983). *Data book of unit processes for fuel preparation and handling.* Enfor project C-258: A comparative assessment of forest biomass conversion to energy forms (phase 1), vol. 3.

188. Burnett, D. J., Landry, S. G., McKenna, R. G. (1990). *Hog Fuel Drying: Status of Existing Systems in the Canadian Pulp and Paper Industry.* Report for Canadian Department of Energy, Mines and Resources.

189. Jonkanski, F. (1994). *Miscanthus - the future biomass crop for energy and industry.* Proc. 8th European Conference: Biomass for Energy, Environment, Agriculture and Industry, Vienna, Pergamon, pp. 372-379.

190. Mitchell C. P. (1990). *Biomass treatment for fuel production.* Commercial and Marketing Aspects of Gasifiers (ed. Buekens, A. G., Bridgwater, A. V., Ferrero, G.-L., Maniatis, K.), pp. 30-40.

191. Bloomfield, R. B. (1989). *Wood and wood fuel handling.* Standard Handbook of Power Engineering (ed. Elliot, T. C.), McGraw Hill, pp. 3.73-3.115.

192. Edwards, W., Tam, P. (1989). *Operating parameters for effective mechanical dewatering of wood residues.* Proc. 7th National Research Council of Canada Bioenergy R & D Seminar, Ottowa, pp. 315-320.

193. Strumillo, C., Kudra, T. (1986). *Drying: Principles, Applications and Design.* Gordon and Breach.

194. Keey, R. B. (1978). *Introduction to Industrial Drying Operations*. Pergamon.

195. Ed. Mujumdar, A. S (1995). *Handbook of Industrial Drying, Volume 1*. Marcel Dekker.

196. Keey, R. B. (1991). *Drying of Loose and Particulate Materials*. Hemisphere.

197. Williams-Gardner, A. (1971). *Industrial Drying*. Leonard Hill Books.

198. Potter, O. E., Beeby, C. (1994). *Scale-up of steam drying*. Drying Technology, vol. 12 no. 1-2, pp. 179-215.

199. Wimmerstedt, R., Hager, J. (1996). *Steam drying - modelling and applications*. Drying Technology, vol. 14 no. 5, pp. 1099-1119.

200. Garin, P., Boy-Marcotte, J. L., Roche, A., Danneville, A. (1988). *Superheated steam drying with mechanical steam recompression*. Drying '88 (ed. Mujumdar, A. S.), Hemisphere, pp. 99-103.

201. Gray, R. M. (1982). *Mechanical vapour recompression techniques*. UK Institute of Electrical Engineers Colloquium Digest no. 1982/81, pp. 5/1-2.

202. Benstead, R. (1982). *Steam recompression drying*. Drying '82 (ed. Mujumdar, A. S.), Hemisphere, pp. 274-284.

203. Sayegh, N. N., Azarniouch, M. K. (1982). *Hog fuel drying using vapour recompression*. Proc. 4th National Research Council of Canada Bioenergy R & D Seminar, Ottowa, pp. 207-210.

204. Heaton, A. V. (1984). *Steam recompression drying*. Proc. 2nd British Hydraulics Research Association International Symposium on Large Scale Applications of Heat Pumps, York.

205. Lamond, W. J., Graham, R. (1992). *Thin-layer Drying of Wood Chips*. Scottish Centre of Agricultural Engineering departmental note 49.

206. Kemp, I. C., Bahu, R. E. (1995). *A new algorithm for dryer selection*. Drying Technology, vol. 13 no. 5-7, pp. 1563-1578.

207. Nellist, M. E., Lamond, W. J., Pringle, R. T., Burfoot, D. (1993). *Storage and Drying of Comminuted Forest Residues*. Energy Technology Support Unit (ETSU) report B/W1/00146/REP.

208. Wastney, S. C. (1994). *Emissions from Wood and Biomass Drying: a Literature Review*. New Zealand Forestry Research Institute report no. 94/1.

209. Fagernäs, L., Sipilä, K. (1997). *Emissions of biomass drying*. Developments in Thermochemical Biomass Conversion (ed. Bridgwater, A. V., Boocock, D. G. B.), Blackie A & P, pp. 783-797.

210. Fagernäs, L. (1993). *Investigation of the Formation of Volatile Organics During Biomass Drying*. International Energy Agency report: project ES7.

211. Ed. Mujumdar, A. S. (1995). *Handbook of Industrial Drying, Volume 2*. Marcel Dekker.

212. Rader Companies (1995). *Rader High Efficiency Dryer - Process Applications*.

213. Johansson, T. B., Kelly, H., Reddy, A. K. N., Williams, R. H. (1993). *Renewable fuels and electricity for a growing world economy*. Renewable Energy: Sources for Fuel and Electricity (ed. Johansson, T. B.), Island, pp. 1-71.

214. Frea, W. J. (1984). *Economic analysis of systems to pre-dry forest residues for industrial boiler fuel*. Energy from Biomass and Wastes VIII (ed. Klass, D. L.), Institute of Gas Technology, pp. 307-338.

215. GSI Group (1998). http://www.grainsystems.com/GSI/index.htm.

216. (1998). *Wood-fuelled gasifier opens in Londonderry*. UK Department of Trade and Industry New Review, issue 35.

217. Saxlund A/S (1998). Product literature.

218. Purcell, J. G. (1979). *Practical rotary cascading dryer design*. The Chemical Engineer, no. 346, pp. 496-500.

219. Miller, B. (1987). *Commercial application of wood gasification - two case studies*. Energy from Biomass and Wastes X (ed. Klass, D. L.), Institute of Gas Technology, pp.723-747.

220. Stahl, K. (1996). *Biomass IGCC overview and the Värnamo power plant*. Proc. 9th European Conference: Biomass for Energy and the Environment, Copenhagen, Pergamon, pp. 177-186.

221. R. Simon (Dryers) Ltd (1998). Product literature.

222. Jensen, A. S. (1996). *Pressurised steam drying of biofuels*. Proc. 9th European Conference: Biomass for Energy and the Environment, Copenhagen, Pergamon, pp. 937-941.

223. Hulkkonnen, S., Heilonen, O. (1997). *Bed mixing dryer for high moisture content fuels*. Proc. 3rd Biomass Conference of the Americas: Making a Business from Biomass in Energy, Environment, Chemicals, Fibers and Materials, Montreal, Pergamon, pp. 695-702.

224. Alves-Filho, O., Strommen, I. (1996). *The application of heat pumps in drying of biomaterials*. Drying Technology, vol. 14 no. 9, pp. 2061-2090.

225. Jensen, A. S. (1994). *Industrial steam fluid bed drying under pressure*. Drying '94 (ed. Mujumdar, A. S.), Hemisphere.

248

226. Munter, M. (1996). *Use of dried biomass in Boras - present experiences and future plans*. Proc. 9th European Conference: Biomass for Energy and the Environment, Copenhagen, Pergamon, pp. 923-928.

227. Jensen, A. S. (1995). *Industrial experience in pressurised steam drying of beet pulp, sewage sludge and wood chips*. Drying Technology, vol. 13 no. 5-7, pp. 1377-1393.

228. Mejnert Kristensen, N. (1998). Private communication, Niro A/S.

229. Kemp, I. C., Bahu, R. E. , Palsey, H. S. (1994) *Model development and experimental studies of vertical pneumatic conveying dryers*. Drying Technology, vol. 12 no. 6, pp. 1323-1340.

230. Hulkonnen, S., Heinonen, O., Tiihonen, J. (1994). *Drying of wood biomass at high pressure steam atmosphere: experimental research and application*. Drying Technology, vol. 12 no. 4, pp. 869-887.

231. Fyhr, C., Rasmuson, A. (1997). *Steam drying of wood chips in pneumatic conveying dryers*. Drying Technology, vol. 15 no. 6-8, pp. 1775-1785.

232. Stork Protech UK (1998). Product literature.

APPENDIX 1 DRYING IN BIOMASS GASIFICATION SYSTEMS

A1.1 Introduction

This appendix constitutes a review of dryer technologies for biomass gasification systems. It has been conceived as a stand-alone document for general reference, and has been published in slightly modified form in a scientific journal [79]. It does not focus specifically on selection of drying technologies for a BGES, but contains the information necessary for such a selection to be made (see Section 4.2).

Considering that the dryer can represent the highest capital cost item in the pre-treatment section of biomass gasification system [40], there has been relatively little attention paid in the literature to the selection and performance of the drying process. Reviews that are to be found in the literature are either in the form of relatively limited summaries forming part of a wider review of biomass technologies, or instead are focused on specific large-scale applications.

An example of the former type is a review of pre-treatment of biomass feedstocks for gasification and combustion carried by the Netherlands Energy Research Foundation (ECN) as part of the European Commission JOULE programme [186]. Drying is one of five pre-treatment steps considered, in a 12-page section. In such a short review, detail is inevitably limited. After a very short discussion of theoretical aspects and classification, four types of dryer are described. Rotary cascade and fluid bed dryers are described in general terms with some indicative performance figures. Then two specific steam dryers are described; the Stork "Exergy" dryer and the Niro dryer, again with some indicative performance figures. A section is included on vapour recompression techniques in steam drying. The review focuses on large-scale applications, with no consideration of the particular requirements of small scale systems. There are a number of other similar examples [e.g. 162,187].

An example of the latter type is a review of wood fuel dryers for application in the Canadian pulp and paper industry was carried out some ten years ago for the Canadian government [188]. The review (26 pages plus appendices) evaluates operational experience at five installations, each incorporating a direct-contact flue gas dryer upstream

of a large steam-raising boiler. Three of the installations had rotary cascade dryers, each from different manufacturers; one had a "cascade" dryer (effectively a fluid bed design); and one had a flash (pneumatic) dryer. All were installed in the early 1980s, and throughputs of the individual units ranged from 9-26 t/h. The review devotes most attention to operational and maintenance problems experienced at each of the installations, and how these were overcome. Some performance figures are given. There is no real attempt to compare the dryer types or make recommendations.

In addition to being limited in detail or focused on specific industries, the reviews that have been published tend to consider only those drying technologies which have an established operational history in bio-energy systems, and this is bound to be a restrictive criterion given the early stage of development of the industry. There have been no comprehensive reviews covering the selection of drying technologies for bio-energy systems which consider all available technologies at all scales, or which focus on biomass gasification systems in particular. These are the objectives here.

The review gives a overview of drying theory and evaporative dryer technologies, and then describes and evaluates in detail the technologies available for drying of biomass gasification system feedstocks.

After a consideration of the requirement for drying in a biomass gasification system (Section A1.2), the review goes on to a general consideration of the evaporative drying process (Section A1.3) and dryer classification (Section A1.4) before focusing specifically on the drying of biomass gasification system feedstocks. Section A1.5 considers relevant biomass properties, and Section A1.6 considers relevant system characteristics. Section A1.7 then identifies the dryer technologies suited to a biomass gasification system, and goes on to describe each in detail.

A1.2 The Requirement for Drying

Biomass feedstocks for the types of gasifier under consideration here must be in the form of loose particulate solids, including wood chips from forestry residues or short rotation coppice (SRC) poplar or willow, or herbaceous energy crops such as miscanthus or reed canary grass in the form of chopped stalks. Such material can have moisture contents

ranging from 20% db to 150% db at the point of harvest, depending on the material type, the growing location and the time of year. A value of 100% db is often quoted as typical for woody material at harvest under European or North American conditions [35,50], whereas an herbaceous crop such as miscanthus, which is harvested at the end of the winter, can have a content of 40% db or less under similar conditions [188].

Natural drying of biomass feedstocks can occur during storage, the degree again depending on the material type and location, the form the material is stored in, the initial moisture content and whether the store is in the open or enclosed. In the present case where crops would be harvested annually in the winter but would be required on a continuous basis at the conversion plant, up to a full year's storage may be necessary. At the end of the summer, a woody crop might have dried naturally from a moisture content of up to 120% db down to as low as 40% db [190]. However, during operation in the spring, the storage period will have been far shorter and the moisture content correspondingly higher. The conversion plant might therefore expect to receive feedstock with moisture content in the range 40% db to 120% db in the case of woody material, and 20% db to 70% db in the case of herbaceous material.

Biomass gasification processes require the moisture content of the feed to be in a certain range, depending on the technology (see Section 5.1.1), although sizeable variations in moisture content from particle to particle are not likely to be a problem provided the feed is well mixed. Conventional down-draft gasifiers are limited to moisture contents of 25% db or less, while updraft and fluidised bed gasifiers can tolerate higher levels of moisture [88]. In all gasifier types, however, an increase in the average moisture content of the feed results in a greater energy requirement for evaporation and a correspondingly lower reaction temperature, which in turn results in a poorer quality product gas with increased levels of tar and a lower overall conversion efficiency. This is illustrated in Figure A1.1, from model calculations by the author of an idealised gasifier operating under equilibrium conditions. The moisture content of the product gas will also be greater, presenting an increased waste water treatment burden if this water has to be removed prior to use of the gas in an engine or turbine.

In slagging gasification, the need to maintain the required temperature levels provides further incentive to reduce feed moisture content.
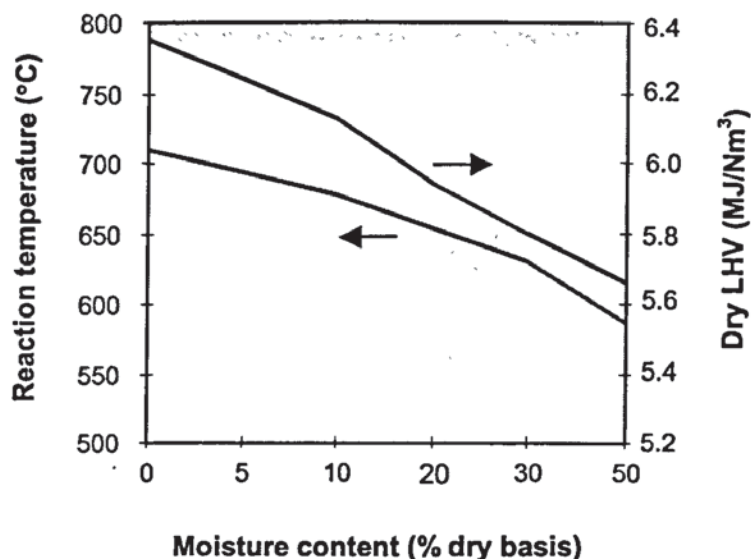
Figure A1.1 Effect of feed moisture content on an idealised gasifier

In a biomass gasification system then, it is usually necessary to dry the feed to some extent at some point between reception and delivery to the gasifier.

Forced or assisted drying often requires a large supply of heat energy, and the provision of suitable equipment which can be expensive. It is therefore in the interests of the system designer to attempt to maximise the efficiency of the drying process (Section A1.3.5) while at the same time minimising the capital outlay, so as to minimise the final cost of electricity. Unfortunately greater efficiency is often associated with greater capital cost. The impact of the drying operation on overall system efficiency can however be reduced by integration, making use of surplus energy streams within the process. If there are competing uses for those energy streams, as is the case in CHP schemes, then a further dimension is added to the task of specifying the extent of drying required and the means to achieve it.

There are many methods of drying available, reflecting the wide range of drying tasks encountered in industry. Often, a number of different technologies would be suited to the drying of a particular material, and the final choice is made after careful consideration of operational and economic factors specific to the application. This is certainly true of biomass gasification system feedstocks.

A4

Here the interest is in drying technologies where water is removed by evaporation, making use as far as possible of available energy sources within the biomass gasification system. Mechanical de-watering techniques (e.g. rams, centrifuges) are available, but are designed for very wet materials such as slurries and pastes which are easily compacted or deformed, and they cannot generally achieve moisture contents below about 120% db [191,192]. Even considering evaporative techniques alone, however, the range of options is vast, and the classification of evaporative dryers (Section A1.4) is a substantial task in itself.

A1.3   The Evaporative Drying Process

This section aims to give an overview of evaporative drying theory pertaining to the drying of any loose particulate solids. Emphasis has been given to aspects which are of relevance in the understanding of why dryers are designed in the way they are, and on what basis they should be selected. For greater detail the reader is referred to the many texts in the literature dealing with the theory of drying [157,193,194,195,196], probably the most relevant of which is that of Keey [196] which deals exclusively with drying of particulate solids, and from which much of the theory presented here is taken.

The evaporative drying process for solids can be thought of as two simultaneous processes, one a heat transfer process in which heat is transferred to the wet solid in order to evaporate the liquid, and the other a mass transfer process in which liquid or vapour moves within the solid and vapour leaves the solid surface (Figure A1.2).

HEAT TRANSFER
CONVECTION
OR
CONDUCTION
CONDUCTION
WITHIN SOLID

MASS TRANSFER
TRANSPORT
SURFACE
EVAPORATION
MOVEMENT
WITHIN
SOLID
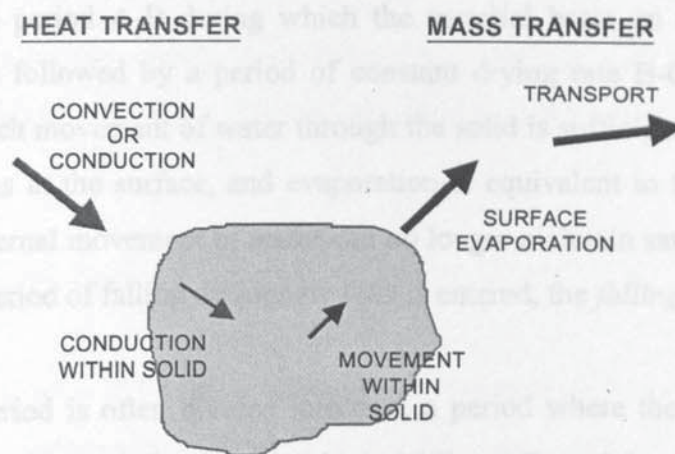
Figure A1.2 Processes involved in evaporative drying

In the technologies considered here, heat transfer occurs predominantly by convection or conduction or a combination of the two, with radiation playing a negligible part. Dryer types can be distinguished according to which of these is the principal mechanism of heat transfer, as will be discussed in Section A1.4. It is clearly important to maximise contact between the drying medium (the gaseous medium surrounding the drying solid as it dries) and the material being dried, and a great deal of attention has been paid to this aspect in the evolution of the wide range of dryer types in existence.

Mass transfer takes place by two general mechanisms; internal movement of liquid or vapour through the wet solid by processes such as capillary flow and diffusion, and external movement of vapour away from the material surface. The former depends on material structure and properties, as well as moisture content; the latter on external temperature and pressure, material surface area, Reynolds Number, and humidity if air or some other inert gas is being used as the transport medium. Both mechanisms can limit the overall drying rate, depending on the stage of the drying process.

A1.3.1. Periods of Drying

If a sample of the material to be dried is exposed to the drying medium at controlled constant conditions, and the rate of moisture loss from the sample is plotted against time, the resultant curve takes the general form shown in Figure A1.3 [197].

There is an initial period A-B during which the material heats up and the drying rate increases. This is followed by a period of constant drying rate B-C, the *constant rate period*, during which movement of water through the solid is sufficiently rapid to maintain saturated conditions at the surface, and evaporation is equivalent to that from a body of water. Finally, internal movement of water can no longer maintain saturated conditions at the surface and a period of falling drying rate C-D is entered, the *falling rate period*.

The falling rate period is often divided into two, a period where the material surface is partially wet and neither mechanism dominates fully, followed by a period where the material surface is completely dry and movement of water through the solid is fully rate limiting. Clearly, drying to low moisture levels implies progressively longer drying time

(and therefore greater dryer capital cost) the lower the final moisture level, and it is most important in these situations to avoid drying beyond the requirements of the subsequent process or use.
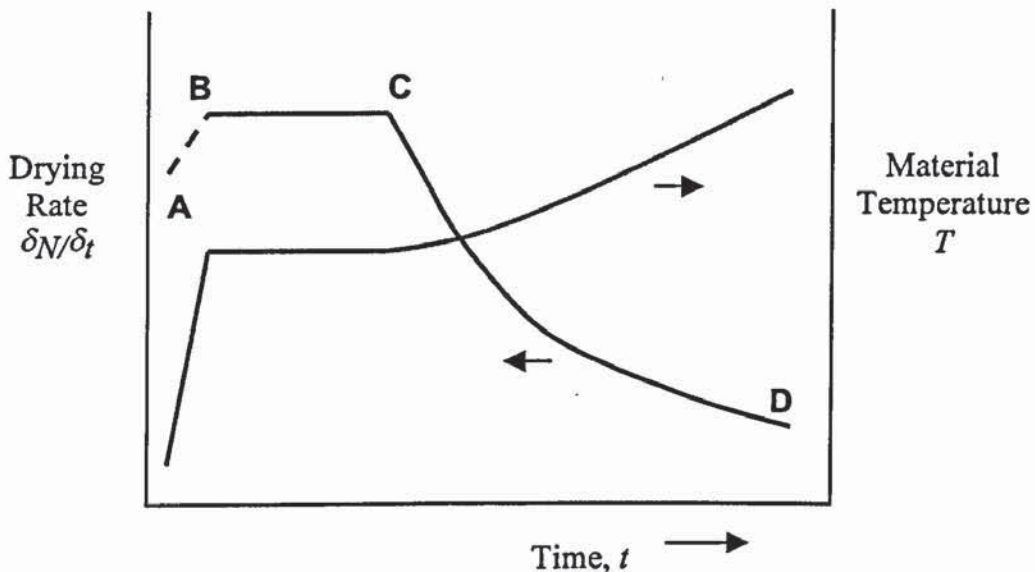
Figure A1.3 The periods of drying

Drying rates are very difficult to predict for a given material, particularly for the falling rate period, and experimental methods under controlled conditions are usually required to determine them. One of the key variables to be determined is the moisture content at which constant rate drying finishes and falling rate drying begins - the so-called critical moisture content. This is a function of many variables, including material structure, material thickness and initial moisture content.

In some materials a constant rate period may not be observed at all except for very high initial moisture contents; in others constant rate drying continues to very low values of moisture content.

A1.3.2 The Drying Medium

The drying medium refers to the gaseous medium surrounding the drying solid as it dries, and can either be a mixture of vapour and a non-condensable gas such as air or combustion products, or pure vapour (in this case steam). In convective systems, the drying medium is

also the source of heat; in conductive systems it represents only the evolved moisture, in some cases combined with a transport gas.

For mixtures of gas and vapour, the principles of psychrometry apply. Properties of air-water mixtures are readily obtained from tabulations, or from a psychrometric chart (an example of which is shown in Figure A1.4). The mixture must be below the saturation point for further evaporation to take place, so the saturation point represents an ultimate limit for a given drying situation if the dry bulb temperature is below the liquid boiling point. If the dry bulb temperature remains above the liquid boiling point, the moisture carrying capacity is infinite. Where the gas is combustion products rather than air, small corrections to the results obtained for air-water mixtures from tables and charts may be necessary to compensate for differences in specific heat capacity.
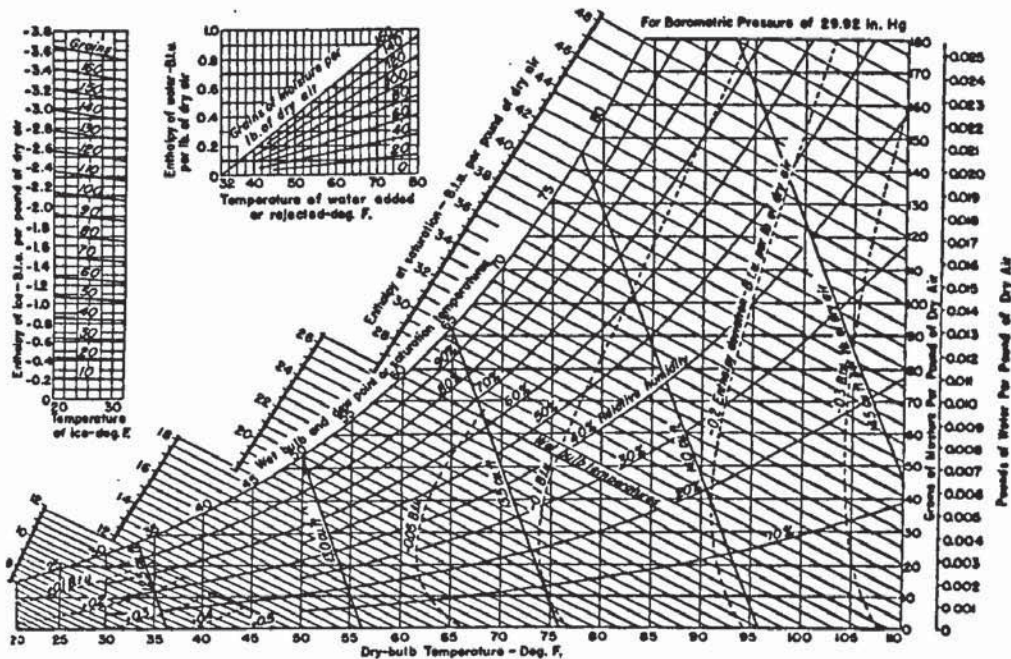
Figure A1.4 Psychrometric chart, medium temperatures

In the case of a pure vapour medium, the medium must be superheated for further drying to take place - otherwise the evaporated moisture would simply re-condense. That is to say, the medium must be at a temperature greater than the boiling point of the moisture at the pressure of the system (see Section A1.3.4). Provided this condition is met, there is no limit to the carrying capacity of the medium. In the case of steam, properties are readily obtained from standard tabulations.

A8

Pure steam drying media are infrequently used compared with gas-steam mixtures. However, an advantage of a pure steam drying medium [198,199] is that the steam product may be utilised, either externally by operating the drying process at elevated pressure and exporting the steam product to the external point of use, or internally by using mechanical vapour recompression (MVR) to return some of the steam enthalpy to the drying process. MVR drying is illustrated in Figure 5, with indicative process conditions [200].

Aston University

Illustration removed for copyright restrictions

Figure A1.5 Mechanical vapour recompression drying [200]

The process involves compressing the extracted vapour in an electrically-driven compressor, and then effecting heat transfer with the drying steam via a condensing heat exchanger so that the latent heat is returned to the process [200,201,202,203]. The process has however to be suitably configured for this to be possible.

MVR is impractical for mixtures of vapour and air or other gases due to excessive compressor costs, and is also highly susceptible to particulate contamination of the vapour which can cause compressor damage. Indeed the viability of MVR for drying has been constrained in the past by the availability of suitable compressor technology [204], although this is improving. Also, recovery of heat from mixtures of vapour and air by condensation would require large and expensive heat exchangers, and can only take place at the dew point temperature of the mixture which would not exceed about 60°C, so that water could only practically be heated to about 50°C at most. Finally, the steam condensate may require costly water treatment prior to disposal.

A1.3.3 Moisture Equilibrium

In an evaporative drying operation, in order to leave the solid the liquid must be heated either to a temperature exceeding the saturation temperature of the liquid at the system pressure (in the case of a pure vapour atmosphere) or to a temperature at which its exerted vapour pressure exceeds the partial pressure of the vapour in the surrounding medium (in the case of gas-vapour mixtures).

Moisture associated with a solid may be freely attached, or bound so that it does not exert its full vapour pressure. Materials whose structure retains bound moisture are known as hygroscopic materials, and biomass materials are generally of this type.

For non-hygroscopic materials, drying will proceed provided the conditions referred to above are met - in other words that the pure vapour medium remains superheated, or that the gas-vapour mixture remains unsaturated (relative humidity < 100%). Under these circumstances such materials could be completely dried.

In the case of hygroscopic materials, however, as the moisture content falls the exerted vapour pressure falls, and an equilibrium moisture content is eventually reached for a given set of drying conditions at which the ratio of the actual to full vapour pressure exerted by the liquid (the *activity*) equals either the ratio of actual to saturation pressure (for pure vapour) or the relative humidity of the drying medium (for gas-vapour mixtures).

Importantly, the equilibrium moisture content increases significantly as relative humidity increases (or degree of superheat falls), and if low final moistures are to be achieved then the transport medium must leave the drying chamber at well below 100% relative humidity (or with substantial superheat).

For hygroscopic materials, the equilibrium moisture content at ambient air conditions will represent the minimum moisture content the material can attain if being dried with ambient air. An important consequence of this is that if material dried to below its ambient air equilibrium moisture content is then stored for a significant period in ambient air, its moisture content will *rise* to the equilibrium value. In the case of woody biomass in a

European country this might vary between 15% db and 35% db depending on season and location [205].

A1.3.4 Material Temperature

The temperature attained by the material during drying can have important consequences for material degradation and dryer emissions (see Section A1.5.3).

The temperature history of the material as it undergoes drying also shows characteristic stages corresponding to the three drying periods defined in Section A1.3.1 (Figure A1.5). Actual temperatures depend also on the type of drying medium and the heat transfer processes involved.

For gas-vapour mixtures during the constant rate period, the evaporating surface of the material will be at the wet bulb temperature of the drying medium for purely convective processes (approximately equal to the adiabatic saturation temperature for air/water mixtures), and provided no heat is lost this temperature will remain constant throughout the period. Where heat transfer is purely by conduction, the material surface temperature will remain at the liquid boiling point. Most real conductive process are at least partially convective, and here the surface will lie between the wet bulb and boiling point temperatures. For pure vapour drying media during the constant rate period, the material surface temperature will remain at the liquid boiling point for both convective and conductive processes.

During the falling rate period, material surface temperature will be somewhere between the constant rate temperature and the actual or dry-bulb temperature of the drying medium. The temperature will rise as drying progresses.

A1.3.5 Thermal Efficiency of Dryers

The thermal efficiency of a dryer is generally taken to be the ratio of the theoretical heat required to evaporate the moisture during drying (i.e. raise its temperature to the evaporation temperature and supply the latent heat of evaporation) divided by the net heat

supplied to the dryer (i.e. the total heat supplied to the dryer from external sources less any heat recovered from the process for external use) [197].

Besides the heat required to evaporate the moisture, the total heat consumption of the dryer will include the heat necessary to raise the temperature of the solids and retained moisture, the heat in the humid exhaust leaving the dryer, and the heat losses from the dryer structure to the surrounding air. The first of these is unavoidable; the second and third can be influenced by dryer design and operation. The theoretical energy consumption for evaporation, assuming an ambient temperature of 15°C, lies in the range 2.48-2.57 GJ/t of water evaporated, depending on the wet bulb temperature [40].

Dryer thermal efficiency can be a misleading parameter in convective dryers, as it is strongly dependent on the initial temperature of the drying medium. For a given dryer, the thermal efficiency will increase with increasing initial temperature. However, in an integrated system the cost in energy terms of providing the higher-temperature drying medium may result in a net loss in overall system efficiency. Convective dryer thermal efficiencies should only be compared at the same drying medium temperature.

A1.4 Dryer Classification

Many different classifications of dryers have been developed in attempts to rationalise what is a complex diversity of technologies, and simplify the process of dryer selection.

Most classifications begin with major criteria which are usually either aspects of the drying process, usually mode of operation (batch or continuous) and mode of feed heating (conductive, convective or other), or the form of the feed (e.g. particle, sheet, block, paste etc.), or both. There may then be further minor criteria such as gas flow pattern, solids transport method or type of drying medium employed before actual dryer types are given. Terminology can often be confusing - for example, conductive and convective dryers are also known as indirect and direct dryers respectively.

Kemp and Bahu [206] have developed a helpful and relatively simple classification system based on three major and five minor criteria:

1. Mode of operation
   - Batch (including semi-batch operation of "continuous" dryers)
   - Continuous (including semi-continuous operation)

2. Form of feed and product
   - Particles (including granules, agglomerates, pellets)
   - Film or sheet
   - Block, slab or artefact
   - Paste, slurry or solution

3. Mode of heating
   - Conduction or contact drying
   - Cross-circulated, through-circulated or dispersion convective drying
   - Radiation; infra-red, solar or flame radiation
   - Dielectric; radio-frequency or microwave radiation
   - Combinations; e.g. conductive/convective, radio-frequency enhancement

4. Operating pressure - vacuum or atmospheric

5. Gas flow pattern - none, cross-flow, co-current, counter-current, complex

6. Solids flow pattern - stationary, well mixed, plug flow, complex

7. Solids transport method - stationary, mechanical, airborne, combined

8. Solids mixing - undisturbed layer, mechanical agitation, rotary, airborne.

The authors give classifications of the principal types of batch and continuous dryers using mode of heating as the primary criterion: these are reproduced as Figures A1.6 and A1.7.

It is not the purpose here to give detailed descriptions of each of the multiplicity of dryer types contained in these classifications; the reader is referred instead to the extensive literature on the subject [157,195,197]. It should be understood, however, that the

categories of Figures A1.6 and A1.7 are by no means all-encompassing and there are numerous hybrid or intermediate types, as well as sub-types within categories.

Figure A1.6 Classification of batch dryers by heat transfer mode [206]

Figure A1.7 Classification of continuous dryers by heat transfer mode [206]

Perry [157] gives a more comprehensive and for present purposes more useful classification based on material to be dried, and this is reproduced with a few modifications as Table A1.1. As the table clearly shows, many dryer types are highly specialised towards the type of material being dried. When materials as different as milk and lumber require drying, this is not surprising.

Table A1.1 Dryer classification based on material to be dried [157]

A13

Page removed for copyright restrictions.

Biomass gasification system feedstocks are in the form of loose particulate solids which, in the context of Table A1.1, are covered by the material type "Granular, crystalline or fibrous solids" (highlighted with a grey background). This sub-section has been taken as the starting point for the more focused selection and description of dryer types suitable for a biomass gasification system (Section A1.7).

A1.5 Biomass Properties Relevant to Drying

Biomass as a feedstock for a biomass gasification system has a number of characteristics which place constraints on the selection of drying technology. These include physical characteristics (size, density and friability), moisture properties, the effects of temperature with regard to emissions and fire risk, and tolerance to different gaseous environments.

A1.5.1 Physical Characteristics

Biomass as a feedstock for a biomass gasification system will be in the form of loose particulate solids of a fibrous nature. The biomass could either be in whole form in the case of, for example, olive pits or almond shells, or in comminuted form (chipped or chopped) as in the case of woody or herbaceous crops (Figure A1.8).

WOOD CHIPS   FOREST RESIDUE   PINE BARK
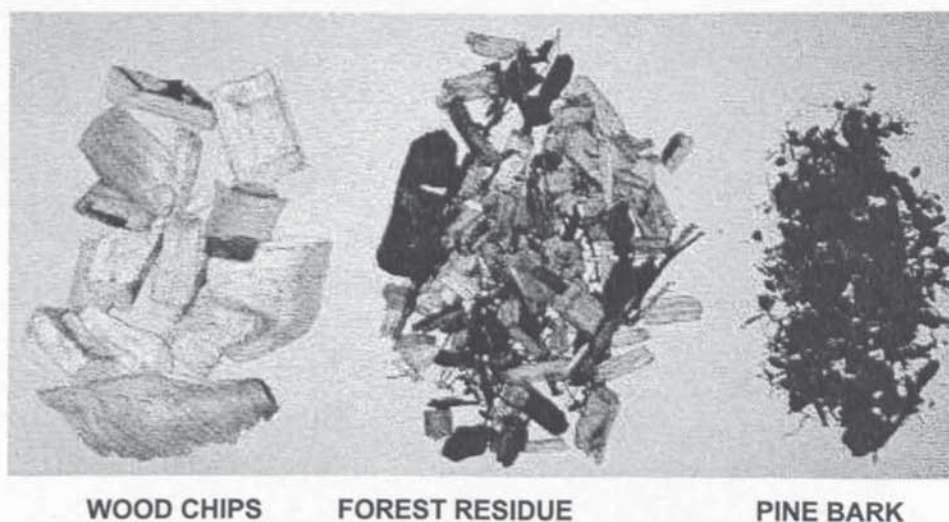
Figure A1.8 Various biomass gasifier feedstocks

A18

Size requirements are dictated largely by the gasification process, with each specific gasifier design having its own particle size range requirement (see Section 5.1.1). A throated downdraft gasifier will require particles of 20-80 mm (longest dimension), whereas an updraft gasifier can accept 10-200 mm and a fluid bed design generally requires particles of <15 mm for fast/circulating types and <50mm for bubbling types [88].

Fluid bed gasifiers are able to accept very small particles; however pre-treatment costs can escalate rapidly if the biomass has to be comminuted and mean particle sizes below those attainable from chippers and choppers are required (~5mm [190]).

Example size distributions from a wood chipper are shown in Figure A1.9. The size range can usually be controlled within certain limits at the comminution stage without greatly affecting costs, in order to meet specific gasifier, dryer or handling requirements. It is assumed here that fines will normally be screened out prior to the drying process (see Section 7.1).

Aston University

Illustration removed for copyright restrictions

Figure A1.9 Wood chip size distributions [35]

In most cases, the material will have a bulk density in the range 50-300 kgm^{-3}, depending on type and moisture content. Usually the bulk material will have only moderate flow properties, but will readily permit through-circulation of the drying medium. The biomass particles are generally not friable under all but the most strongly agitated of processes, and

physical damage or generation of significant amounts of additional dust within the drying process is therefore not normally a problem.

A1.5.2 Moisture Properties

The typical moisture content of biomass feedstocks as received at a biomass gasification plant and as required by the gasification process has been discussed in Section A1.2. The biomass material will be hygroscopic (see Section A1.3.3), with equilibrium moisture content varying from 35% db or more if the drying medium is close to saturation, down to below 1% db where the medium is exceptionally dry [205]. As indicated in Section A1.3.3, under ambient air conditions typical of European locations the equilibrium moisture content of woody biomass will range approximately from 15% db to 35% db. If very low moisture contents are required, then not only will a large supply of energy be required, but careful measures must be taken to prevent re-hydration during post-dryer handling. It has been suggested that drying in a biomass gasification system to below 10% db moisture is impractical [50].

For most agricultural materials the constant rate period during drying is either very short or non-existent [207] (see Section A1.3.1). Falling rate drying commences immediately after the short heating period, which is often ignored in analysis or modelling. In tests on various different types of wood chip carried out by Nellist [35], no constant rate was observed when drying from up to 150% db.

A1.5.3 Emissions

The subject of emissions from the drying of biomass materials has received some attention recently [208,209,210]. Feedstocks for a biomass gasification system have a very high volatile content. Emissions arise either from vaporisation of volatile components in the biomass, or from thermal degradation of the biomass. Vaporised components can be further subdivided into those that remain volatile at ambient conditions, and those that condense. The most volatile vaporised components consist of monoterpenes, which are emitted naturally at ambient temperatures but whose emission rate increases with temperature, particularly above 100°C. They are strong-smelling irritants whose presence

becomes annoying in the long run. The haze visible above a forest on a warm day is due to photochemical reactions involving these species.

Condensable components create more of a problem, being principally responsible for so-called "blue haze", a more localised discoloration of the exhaust plume. The release of the condensable components causing blue haze occurs at material temperatures above about 100°C. The visual nuisance caused by blue haze has to date been the source of greatest concern regarding emissions from dryers, although the phenomenon can also cause odour problems. Legislative limits regarding the production of blue haze are in force in some countries, and are likely to become tighter and more widespread with time.

Thermal degradation products are released at higher wood temperatures still (>200°C for short drying times, rather less for longer drying times), and the rate of loss accelerates rapidly as temperature is increased further.

The release of all these components would ideally occur in the gasifier, and any premature release represents a loss of potentially gasifiable material and is therefore to be minimised. It may also require the provision of clean-up equipment for exhaust gas or condensate streams, as may the excessive release of solid particulate material into the atmosphere.

Solid particulates may usually be dealt with satisfactorily with cyclones or bag filters. Blue haze however is composed largely of sub-micron aerosols, and these are notoriously difficult to remove with conventional gas cleaning techniques such as wet scrubbers, requiring instead more exotic and expensive methods such as wet electrostatic precipitation or electro-filter beds [208]. As a general rule, therefore, material temperatures should be kept below 100°C for all processes [208]. The ability of biomass materials to tolerate temperatures up to these limits with no serious consequences means that drying options specifically designed for heat-sensitive materials, such as vacuum methods, are unnecessary.

The actual emissions (gaseous and particulate) to be expected from a given biomass drying installation depend on a range of factors, and cannot be easily predicted. Many of the factors are in the control of the process designer or operator. Factors may be grouped into

three categories: those related to dryer type; those related to drying medium characteristics; and those related to feedstock characteristics.

Dryer type

Different dryers have widely differing characteristics regarding emissions. However, the key design features of relevance are:

- whether the system is closed or open - i.e. whether the drying medium is reused, or whether it is exhausted to atmosphere

- the degree to which material is agitated and broken up in the drying process

- the residence time of material in the dryer

- whether any emissions abatement equipment is supplied with the dryer.

Drying medium characteristics

Important factors are the temperature of the drying medium, and the velocity of the medium through the dryer. As indicated above, a drying medium inlet temperature sufficiently low to keep the material temperature below 100°C will not cause pre-pyrolysis and thus will avoid blue haze problems. The actual drying medium temperature will depend strongly on feedstock and drying medium mass flow rates, feedstock initial moisture content and dryer design.

High gas velocities will tend to entrain fine particles and some entrainment will always occur. These emissions are however relatively easy to control with physical filtration equipment. Fixed bed dryers (Section A1.7.1, A1.7.2.1) will minimise this problem from the very low superficial gas velocity.

Steam dryers (see Sections A1.7.5.1 and A1.7.6.1), although having no gaseous emissions, pose a special problem of producing a contaminated waste water which requires

A22

conventional water treatment as the chemical oxygen demand will tend to be high. There is so little data or experience with such systems that estimation of cost or performance is not possible.

Feedstock characteristics

Emissions vary very much according to the type of biomass being dried. Even different types of wood can exhibit very different emissions characteristics, including the species evolved and the temperature at which they evolve. Also, feedstock size range is very important. A wide size range may result in the smaller particles being over-dried, causing their temperature to rise excessively with resultant thermal degradation.

The requirement to implement emissions reduction measures at a particular drying installation will depend also on the immediate location of the installation (i.e. is it close to a residential area), and on the local legislative limits applying. These cannot be generalised as they will vary from country to country and sometimes from region to region. Furthermore regulations governing certain emissions of more recent concern, such as volatile organic compounds (VOCs), are still evolving, and requirements governing compliance change regularly.

A1.5.4 Fire or Explosion Risk

A dryer fire or explosion can arise from two causes - ignition of a dust cloud brought about by the presence of a large proportion of fines in the material, and ignition of the combustible gaseous emissions from the drying material. Fines can be screened out prior to the dryer, although this represents an additional cost, is not necessarily 100% efficient, and in certain special cases may be undesirable (see Section A1.7.3, for example). If significant quantities of fines are present, not only is there a risk of dust ignition, but the release of the combustible products of thermal degradation may increase to dangerous levels.

Both types of ignition referred to above require the presence of sufficient oxygen and a sufficiently high temperature. Under conditions found in most dryers, the risk of fire or explosion from flammable vapours becomes significant if O_2 concentration in the drying

A23

medium exceeds a certain level. This level has been given values of 8% [50] and 10% [211] by volume in different studies; the lower will be assumed in the present study.

Actual ignition temperature is a function of local gaseous composition and is difficult to predict in such a heterogeneous environment. Problems have been encountered at inlet temperatures as low as 200°C with wood chips in rotary dryers using combustion products [187], where a temporarily high oxygen concentration has occurred as a result of an air in-leakage. A general upper working limit in the range 250-300°C has been suggested [188]. In those cases where combustion products with an oxygen content below 8% are used as the drying medium, much higher inlet temperatures may be used; one rotary dryer manufacturer quotes up to 1000°C for very wet materials in co-current operation [212]. If high temperatures are used, however, it becomes very important both to minimise the possibility of air in-leakage and to ensure that material temperatures do not exceed the limits discussed in Section A1.5.3.

A1.6 System Characteristics Relevant to Drying

The power or CHP system also has a number of characteristics which influence the choice of dryer. These include the available heat sources, the mode of operation of the system and the system capacity range.

A1.6.1 Sources of Heat

Integration of the drying process into the overall system by making use of sources of thermal energy available at other points in the system is central to this study. This implies that the selected dryer must either be of the conductive or convective type (Section A1.4), or a combination of the two. For a biomass gasification system for power or CHP, suitable sources of heat take the following forms (see also Figure 2.1):

- hot fuel gas which requires cooling (via heat exchange with secondary medium)

- hot combustion products from the engine or turbine (direct or via heat exchange with secondary medium)

- hot products from combustion at the dryer of surplus biomass (e.g. undersize)

- hot air from the air cooler in a steam or combined cycle system (direct or via heat exchange with secondary medium)

- hot water from engine cooling and/or condenser in a steam or combined cycle system (via heat exchange with secondary medium).

The secondary medium referred to will in almost all cases be either air or steam. In the case of CHP systems in which steam is being raised for external use, drying may be a competing demand and a techno-economic optimisation would be necessary.

A1.6.2 Mode of System Operation

The bio-energy system, whether for power or CHP, will be required to run continuously for extended periods. In order to make most efficient use of the heat sources which will therefore be continuously available, the drying technology should also be of the continuous type. Continuous dryers tend to be more expensive capital items than batch dryers which usually involve relatively simple technology, although this is usually offset by the greater operational costs associated with batch systems because of handling requirements. Batch methods may be considered at very small system scales of the order a hundred kilowatts or less where the capital cost of continuous methods may become excessive. They may also be considered where the method permits large batch sizes and long drying times so that the ratio of loading/unloading to drying time (i.e. the period during which the available process heat is not being used) can be minimised.

A1.6.3 Capacity Range

A biomass gasification system for power or CHP may have a thermal capacity ranging from 100 kW_{th} at the smallest farm scale to maybe 100 MW_e for the largest envisaged power generation systems that could be competitive with coal and gas [213]. This corresponds to a range in dry throughput of biomass of less than 20 kg/h to over 50 t/h. This is a very wide range, and most available drying technologies will be suited to some

part of it at least in terms of capacity. At the larger scales it will be reasonable to consider multiple units. It is therefore only possible to rule out drying technologies at the very smallest end of the capacity range on these grounds alone - those designed for laboratory work, for example.

A1.7 Dryers for a Biomass Gasification System

An initial selection of dryer technologies has been made using the classification given in Table A1.1. As discussed in Section A1.4, the material category in Perry's classification corresponding to biomass gasification system feedstocks is "Granular, crystalline or fibrous solids". Small batch technologies, vacuum technologies, those technologies requiring good free-flow characteristics and those technologies not based on conductive or convective heat transfer can be eliminated, for the reasons given in Sections A1.5 and A1.6. Tunnel or cross-flow tray types can be eliminated, as these would always be rejected in favour of through-flow systems if the latter are applicable (as is the case here), due to their superior heat and mass transfer rates. Also, certain specialised technologies may be rejected, such as screw conveyor dryers which are rarely used except when the material has to be conveyed over large distances. The following six categories then remain:

- Batch through-circulation

- Continuous through-circulation

- Direct rotary

- Indirect rotary

- Fluid bed

- Pneumatic conveying.

Each of these categories may contain numerous specific dryer types, only some of which may be suitable for biomass gasification system feedstocks. Those suitable will fall generally into three groups:

- dryers designed specifically for biomass gasification system feedstocks

- dryers designed for a different material or materials but deemed to be suited to biomass gasification system feedstocks (possibly with some adaptation)

- less specialised dryers that can accept a range of material types, but which would be suitable for biomass gasification system feedstocks

In the case of specialised dryer designs, there may in some cases be only a single manufacturer or a very limited number. On the other hand for the less specialised design concepts there may be a multitude of manufacturers each with their own range of subtly different models.

A1.7.1 Batch Through-Circulation

Through-circulation methods are attractive because of the efficient heat and mass transfer involved, and because of the minimal disturbance of the material being dried. In most industrial contexts, batch through-circulation drying implies tray dryers, where the material is placed on a number of trays, usually stacked vertically in two or more columns and enclosed in a cabinet. A range of configurations is possible. The trays will have screen or perforated bases to allow through-circulation of the drying medium, usually air. As indicated in Table A1.1 these are relatively small-capacity devices, and in Section A1.6.2 reasons were given why small-capacity batch methods were inappropriate for biomass gasification system feedstocks.

One group of drying techniques which can be classed as batch through-circulation methods do however provide an option for biomass gasification system feedstocks, because of their low capital cost, high capacities, and particularly their characteristic of low intensity drying which makes them well suited to the use of low grade heat. These are the fixed-bed ventilated-floor methods used widely in the agricultural industry, particularly for air-drying

of grain [211]. Such systems have indeed been found to offer a more economic alternative to high-temperature flue gas drying for *biomass combustion* systems under certain circumstances [214].
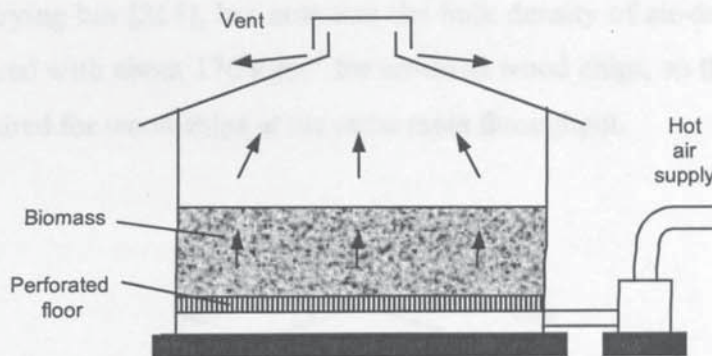
Figure A1.10 Perforated floor bin dryer for grain

The conventional form of system comprises a bin (Figure A1.10) or more simply a room, with a perforated floor through which the hot drying medium, nearly always air, can be made to flow via a plenum by the use of electrically powered fans. The wet material is loaded onto the perforated floor to form a bed, the depth being chosen to give the desired drying characteristics. Drying then takes place, the batch time being anywhere from a few hours to a number of days. At the completion of this period the dried material is removed and deposited in a buffer store and a fresh batch of wet material loaded. Means of heating the drying medium (if required) may be provided at inlet, either electrically or by heat exchange from a secondary carrier such as steam or the combustion products of a small burner. Alternatively an already heated drying medium may be used directly. These are simple systems which would require little adaptation for biomass gasification system feedstocks, although their performance characteristics would differ from grain drying.

A more sophisticated design used in grain drying and of potential application to biomass gasification system feedstocks is the top-drying bin (Figure A1.11), in which the ventilated floor is located near the top of the bin and supports a relatively shallow bed of drying material [211]. Once dry, this material is allowed to fall through doors in the ventilated floor into the lower, much larger region of the bin which acts as a store. The hot drying medium is admitted to this region above the maximum material level. In some designs, the base of this zone is also perforated and a flow of ambient air is circulated up through the

stored dried material to augment the heated flow entering above (as shown in Figure A1.11), thereby reclaiming some of the sensible heat in the dried material at the expense of some fan power. Again provision may be made for heating the primary drying medium if this is required. Table A1.2 shows typical performance figures for corn drying in a commercial top-drying bin [215], but note that the bulk density of air-dried corn is about 700 kgm^{-3} compared with about 170 kgm^{-3} for air-dried wood chips, so that a much larger bin would be required for wood chips at the same mass throughput.
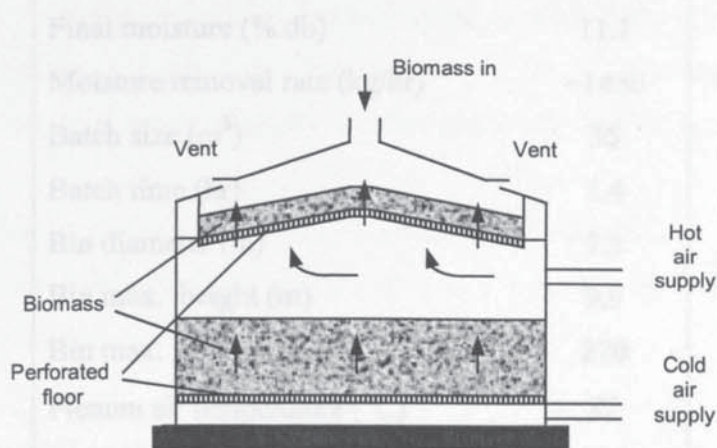
Figure A1.11 Top drying bin

With both conventional and top-drying systems it is possible to automate the material loading and unloading to varying degrees, greater degrees of automation requiring greater capital outlay particularly for large systems, although the poor flow properties of biomass gasification system feedstocks compared with grain may limit the possibilities of direct read-across from grain systems.

Perforated floor bin dryers are not marketed specifically for biomass gasification system feedstocks. They are principally designed for grain, with some manufacturers offering adapted designs for other agricultural produce such as peanuts or rice [215]. There are nevertheless cases where perforated floor bin dryers designed for grain have been used for the drying of biomass gasification system feedstocks in small bio-energy systems [216], in which any necessary adaptation has been carried out by the user. It is important however to bear in mind the large differences in bulk density referred to earlier, particularly for more sophisticated systems. Equipment designed for grain may be purchased at a wide

range of capacities. The use of multiple units at larger system sizes may improve utilisation of handling equipment and fan power, and make better use of available heat.

Table A1.2 Top drying bin performance data (corn) [215]

Illustration removed for copyright restrictions

The choice of depth of the fixed bed in such systems is a key consideration. Fixed-bed through-circulation heated drying of wood chips has been studied by Nellist at Silsoe Research Institute in the UK [35], where models have been developed and validated to describe the process. The issue of bed depth is addressed and recommendations are made. The main recommendation is for relatively shallow depths (0.4-0.6 m), as these minimise fan power requirements and reduce over-drying of the lower layers. However, the shallower the bed, the shorter the drying time to reach a target mean moisture and the greater the frequency of charging and discharging.

Drying performance will also be influenced by drying medium humidity at inlet. The direct use of combustion products is usually not possible, because the combination of relatively high humidity and limits on maximum inlet temperature (see below) would result in very little drying taking place. This is why air is nearly always used as the drying medium, heated from whatever heat source is available by a heat exchanger.

A drawback with fixed bed through-circulation methods is that they invariably produce a large vertical gradient in moisture content of the dried bed. The lower levels of the bed almost always reach the inlet temperature of the drying medium, and this effectively limits the latter to the material temperature limit which for long residence time systems such as this would be 100°C or less (see Section A1.5.3). Importantly, the dried product needs to be thoroughly mixed, and possibly allowed to equilibrate for a period in a buffer store, before being used. If in the process the material is exposed to ambient conditions for any length of time, the moisture content may rise (see Section A1.3.3). In top-drying systems, mixing and equilibration is accomplished to some extent in the integral store [211].

In general, the characteristics of low gas velocity, low temperatures and a static bed associated with these methods mean that there is no need for clean-up of the gaseous exhaust. This adds further to their capital cost advantage.

A1.7.2 Continuous Through-Circulation

Continuous through-circulation methods take one of two basic forms. By far the most widely used is the band or belt conveyor dryer, in which the drying medium is blown through a static layer of material on a moving band. Less common is the rotary louvre dryer, in which material passes along a slowly rotating tube, forming a rolling bed through which drying medium is blown from an outer annulus via louvres. Continuous through-circulation dryers are most often used for materials that require gentle handling.

A1.7.2.1 Band Conveyor Dryers

The band conveyor dryer operates by blowing the hot drying medium vertically through a uniform layer of material carried on a permeable band which moves horizontally through the enclosed drying chamber. Gas flow may be upward or downward. In the single-stage single-pass design (Figure A1.12), a continuous band runs the whole length of the dryer. In the multi-stage single-pass design (Figure A1.13), a number of bands are arranged in series, with the material discharged from the end of one band onto the beginning of the next and in the process exposing new surfaces to the drying medium. In the multi-pass design, a number of bands are installed one above the other, each discharging onto the

A31

band below (Figure A1.14). The same re-exposure benefit is gained, but dryer length is much reduced at the expense of height.
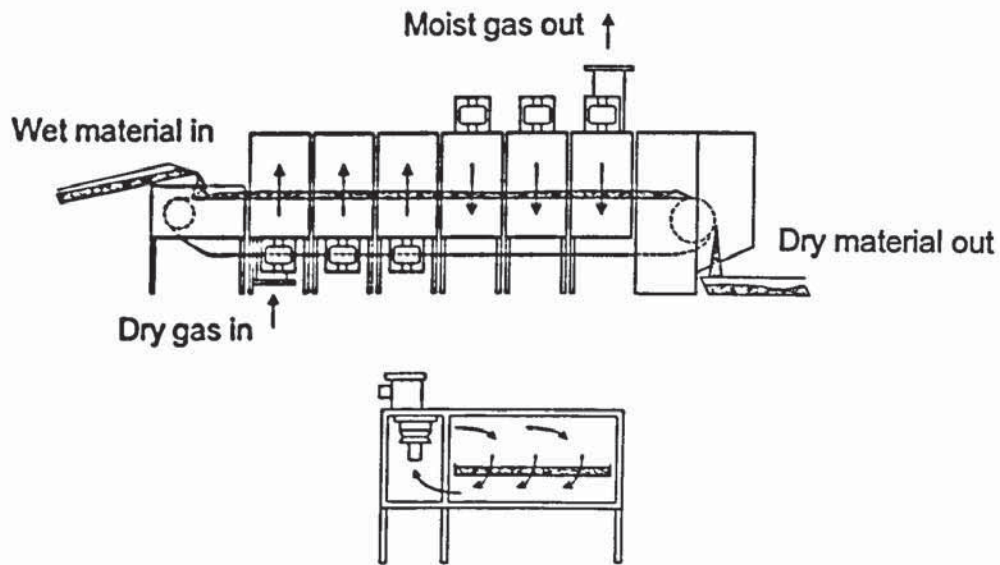
Figure A1.12 Single stage single pass band conveyor dryer
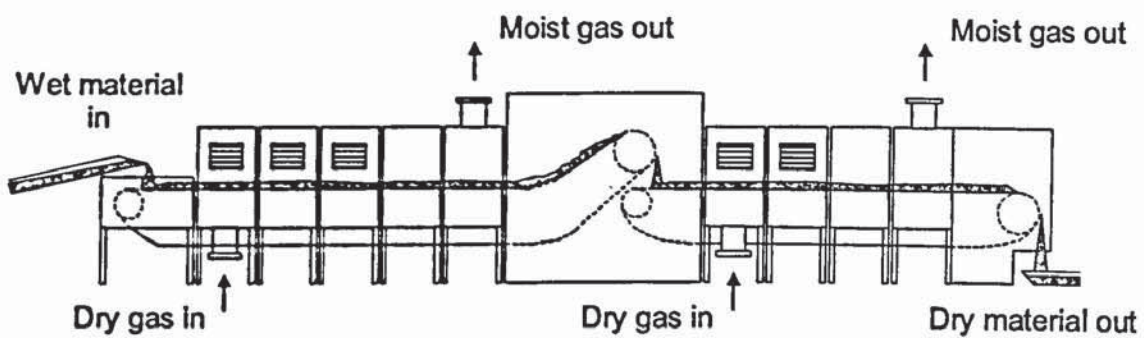
Figure A1.13 Multi-stage single pass band conveyor dryer
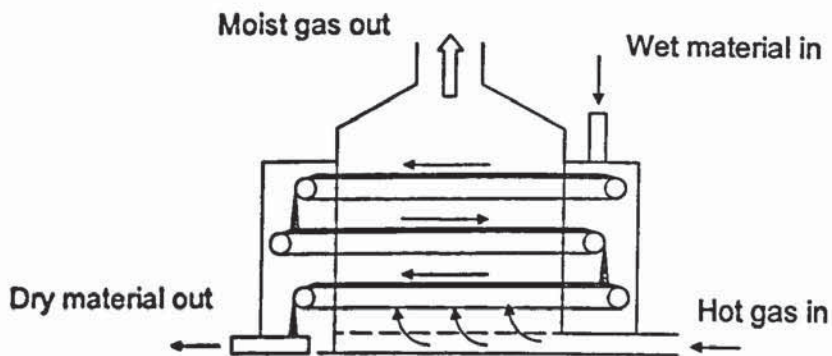
Figure A1.14 Multi-stage multi-pass band conveyor dryer

The drying medium is usually either hot air or combustion products or a mixture of both, and is moved through the dryer by a number of fans. In most modern systems, the dryer is divided up into zones (usually corresponding to the stages in a multi-stage dryer) through which the drying medium progressively passes (as in Figure A1.12). Each zone usually has its own fan. In the case of ambient inlet air systems each zone will have either a steam heater or a gas or oil burner for heating and re-heating of the air. The fans and heaters are often located in a side compartment, as shown in Figure A1.12. In the case of systems using pre-heated air or hot combustion products as the drying medium, there may be ports in each zone for the progressive admixture of fresh gas. The general movement from drying medium inlet to outlet can be either co- or counter-current with respect to the passage of material.

Even spreading of the material over the band at the material inlet and between each stage or pass is very important, and considerable attention is paid to this aspect by designers resulting in many patented designs. In some cases these are material-specific, with at least one commercially available system (made by Saxlund of Norway) having been designed specifically for wood fuel chips [217].

The band conveyor dryer has the advantage that both residence time and, in most designs, temperature can be closely controlled. This is of particular use in drying heat-sensitive materials. Residence time for a given band length is set simply by the speed of the band. Temperature control is achieved either by controlling the steam flow to each steam heater or the fuel flow to each burner, or in hot gas systems where progressive admixture is possible, controlling the flow rate to each hot gas port. Temperature is however limited to around 350°C because of the problems of lubricating the conveyor, chain and roller drives [157].

Most designs have a relatively shallow depth of material on the band (usually in the range 2-15 cm), and the uniformity of drying is very good. There is no reason however why much greater depths and slower band speeds cannot be used for low temperature air drying; the dryer is then like a continuous fixed bed where the residence time in the dryer is similar to the batch time of the fixed bed dryers described in Section A1.7.1. Air temperature must be limited to below 100°C for the same reasons as given in Section

A1.7.1. This configuration is sometimes called a moving floor dryer. The main advantage over the batch approach would be the reduced labour requirement. Also, although this type of dryer would still produce a large vertical gradient in the bed moisture content, the subsequent mixing of the product would happen naturally as the product deposits continuously from the conveyor. The drawbacks in comparison with the batch approach would be the increased capital, power and maintenance costs.

On multi-stage and multi-pass designs, bed depth can be varied through the dryer if desired by adopting different band speeds. Because the material suffers very little agitation during the drying process (particularly for single pass designs), band conveyor dryers are particularly well suited to friable materials, although as pointed out in Section A1.5.1 this would not generally be of advantage to biomass gasification system feedstocks.

Entrainment of fines with this type of dryer should be low due to the low velocities and static material bed. A bag filter may still however be necessary, depending on local regulations. A major advantage of using indirect steam re-heating of air in this context would be the much reduced volume flow of gaseous emissions, so that if clean-up equipment is required it is much smaller and therefore cheaper.

Specific performance data for a band conveyor dryer with biomass gasification system feedstocks may be found in Section 4.3.2.2.

A1.7.2.2 Rotary Louvre Dryers

The rotary louvre dryer (Figure A1.15) may be thought of as a direct rotary dryer; however, unlike more conventional rotary dryers (Section A1.7.3) it uses through-circulation drying, and so is included in the present section. The dryer comprises a long tube inclined at a small angle to the horizontal which rotates slowly. On the inner side of the tube wall are a large number of longitudinal channels, each with a hinged tangential louvre covering it. The louvres overlap, forming an inner cylinder which carries the material being dried. The material forms a slumping bed moving slowly down the tube as it rotates. The drying medium is admitted along the channels and blows through the bed of material via the louvres, exiting at the material outlet. A stationary head plate constrains

the drying medium to enter only those channels which are covered by the material bed (Figure A1.16).
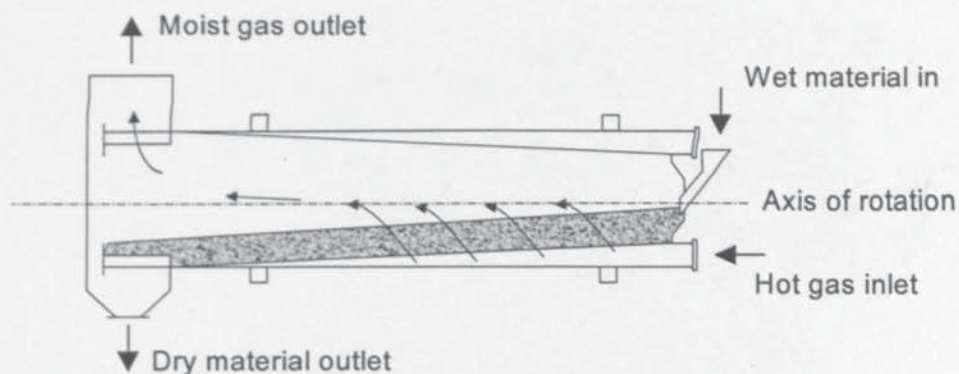
Figure A1.15 Rotary louvre dryer
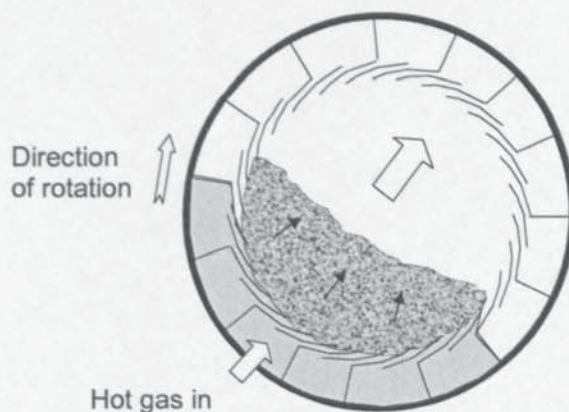
Figure A1.16 Gas flow - rotary louvre dryer

The material depth tends to increase as the outlet is approached. The gas velocity through the bed is therefore at its lowest near the exit where the material is driest, and this tends to reduce entrainment. The depth is controlled by an exit weir over which the material passes to reach the dryer outlet. Drying is highly uniform as the material is constantly rolling in the bed; however, the particle motion is relatively gentle compared with cascading rotary techniques (see Section A1.7.3), and this also leads to low entrainment. Exhaust clean-up equipment is more likely to be required than with band conveyor dryers, however, *if fines* are present in significant quantities, as the material is agitated to some extent. Temperature

along the dryer may be controlled if required by using multiple gas feeds of different temperatures along the dryer.

The drying medium is usually air or hot combustion products. Direct oil or gas burners or indirect steam heaters can be incorporated for the heating of ambient air prior to the drying section inlet. An upper temperature limit of 600°C has been quoted [157].

Heat transfer in the rotary louvre dryer is very efficient as with other through-circulation methods, and dryer volumes are substantially less than for an equivalent cascade rotary dryer (Section A1.7.3). However, this is offset by greater complexity of construction which pushes capital costs up. Pressure drop across the dryer is also higher, necessitating greater fan power. The dryer is best suited to free-flowing materials for obvious reasons; the design is prone to clogging [195], and this could prove a problem with some biomass gasification system feedstocks.

A1.7.3 Direct Rotary

The direct rotary dryer, or rotary cascade dryer, is very widely used in industry for a wide range of materials [72,218]. It is often the dryer of choice on economical grounds where air or combustion products are the drying medium and the material can withstand moderate agitation. The rotary cascade is the type of dryer most often found in the limited number of existing large-scale biomass gasification system projects, as well as in large wood-chip combustion system [219,220]. It is well-understood, empirical design rules exist, and the rotary cascade dryer is thus perceived as a low risk choice.

The dryer (Figure A1.17) consists of a cylindrical shell, inclined at a small degree to the horizontal and rotating at between about 1 and 10 r.p.m. depending on size. The length to diameter ratio of the shell usually lies between 4 and 10, with actual diameter ranging from <1m to >6m depending on throughput. Material is loaded into the shell at the upper end, passes along the shell and exits at the lower end. The drying medium, either heated air or combustion products, may either enter at the upper end (parallel-flow arrangement) or at the lower end (counter-flow arrangement). On the inside of the shell are a number of longitudinal flights (Figure A1.18) which may be continuous or staggered, and which are designed to lift the material around the periphery of the dryer and cascade it in a uniform

curtain through the passing gases. The material thus moves down the dryer by a combination of gravity and, in the case of parallel-flow dryers, entrainment with the drying medium.
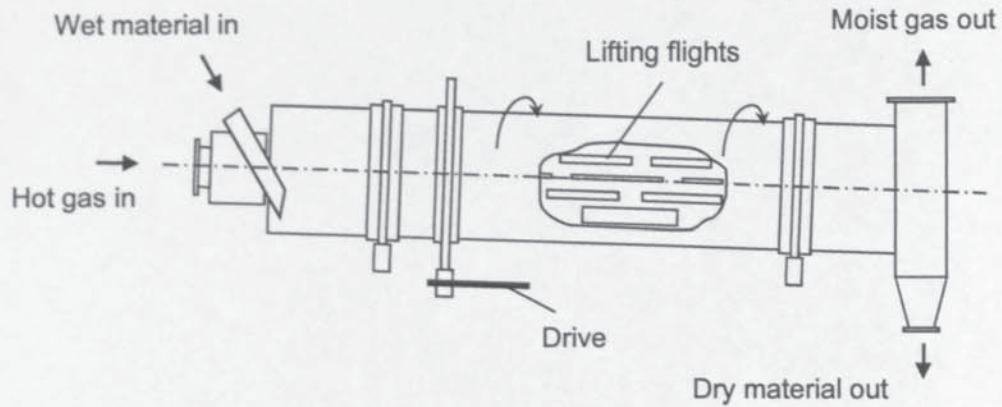
Figure A1.17 Rotary cascade dryer

Figure A1.18 Typical flight arrangement, rotary cascade dryer

Residence time in the dryer is controlled by a *number* of factors including flight design (the amount of hold-up on the flight), number of flights, rotational speed, gas velocity, dryer length and dryer inclination. The overall hold-up bulk volume is usually in the range 3-12% of dryer volume, 7-8% being a common figure [197]. Drying takes place almost totally during the period when the material is falling through the gas stream; drying whilst being lifted by the flights is minimal. In a well designed and operated dryer, there should be no significant bed of material in the base of the shell.

Overall heat transfer is less effective than for through-circulation systems, and higher inlet temperatures are generally used. Heat transfer is generally superior in counter-flow systems; however, in such systems the driest material sees the highest drying medium temperature, and they are generally therefore not suitable for temperature-limited materials including biomass gasification system feedstocks. Inlet temperatures of up to 1000°C are possible with non-heat-*sensitive* materials, or with very wet materials in a parallel-flow configuration (as the drying medium loses temperature rapidly during the *initial drying* stages), although temperatures above about 600°C would require either expensive alloy steels or refractory lining [221]. However in the interests of safety (see Section A1.5.4) inlet temperatures when drying wood chips in commercial installations have often been limited to between 250°C and 300°C [188]. The dryer is usually operated under slight suction with an induced draught fan at the exit, and sealing problems leading to air in-leakage have been a weakness in many installations trying to maintain a low-oxygen environment.

Gas velocities are usually in the range of 0.5-5 ms^{-1} at exit, depending on type of material, flow arrangement and the amount of carry-over of material due to entrainment [157]. A design value of 2-3 ms^{-1} is typical in modern systems. The unavoidable carry-over of entrained material and the relatively large gas volume flow rates make sizeable dust removal equipment usually essential, and this can represent a significant additional capital cost. However, entrainment can also serve to reduce the residence time of the smaller particles and inhibit over-drying.

Exhaust gas recycle is often incorporated in direct rotary dryers to try to reduce the drying medium requirement and the exhaust gas flow rate. This results in more humid conditions in the dryer. Less drying can take place; however, overall thermal efficiency may be improved. In general, thermal efficiency for direct rotary dryers lies in the range 50-75% [197], the highest values being found for counter-current systems with high inlet temperatures.

Many systems are offered with heating equipment at inlet, often in the form of a gas burner. In at least two systems for drying wood chips, fines separated in the exhaust cyclone are used to fire a small combustor to provide additional hot gases for the dryer

[78,212]. In this case fines would not be screened prior to *the dryer, although fire risk and* blue haze emissions may be increased. An alternative would be to divert the combustor feedstock prior to drying; however, this would lead to a lower temperature drying medium with a higher initial humidity, both of which would lead to reduced efficiency.

Specific performance data for direct rotary dryers with biomass gasification system feedstocks may be found in Section 4.3.1.2.

A1.7.4 Indirect Rotary

There are three main reasons for employing indirect (conductive) rather than direct (convective) heating in a rotary dryer:

- The material being dried cannot be exposed to combustion products

- Direct heating will lead to excessive entrainment and carry-over of fines or dust

- A low-cost source of low to medium pressure steam is available

Where the heating medium is combustion products but the material cannot be exposed directly to them, a number of designs exist for bringing the gases into indirect contact with the material, including single-pass concentric outer shells, or double-pass arrangements with an outer shell and an inner tube. As this situation does not arise with biomass gasification system feedstocks, these designs will not be considered further.

It may well be the case, however, that a suitable source of steam may be available, and that benefits of much reduced exhaust gas flow and carry-over make an indirect rotary option attractive. In this case, the most usual form of dryer is known as a steam-tube rotary dryer (Figure A1.19). Steam tubes running the full length of the dryer are arranged in a number of concentric rows moving inwards from the dryer shell. The number of rows will depend on the nature of the feed; Figure A1.19 shows two. The tubes are fixed to the dryer end plates and rotate with it. The dryer shell is usually inclined at a small angle to the horizontal, and the wet material enters the shell at one end and moves down the dryer by gravity, assisted by the ploughing effect as the tubes rotate through the material bed.

Flights may be fitted to improve the motion. The arrangement gives excellent material contact with the conducting surfaces of the tubes. A small flow of air is employed, usually counter-current to the material flow, to effect the removal of the evaporated moisture - the volume flow is very low compared with direct designs. Hold-up within the dryer is usually controlled by a weir plate or similar device at the discharge end, as with the rotary louvre dryer (Section A1.7.2.2).
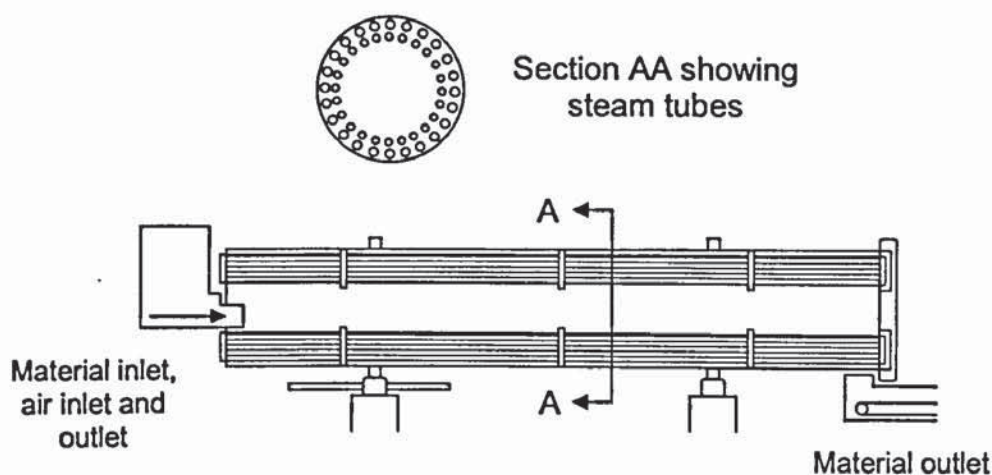
Figure A1.19 Steam-tube rotary dryer

Heat transfer in these devices is by conduction from surfaces at or close to the steam temperature. The material temperature will normally be close to the moisture boiling point at discharge, rather hotter than in direct systems (see Section A1.3.4). Saturated steam is normally used, typically at 10 bar, and the steam passages will be designed to be fully condensing. Thermal efficiency can be very high, in the range 75-90% [197], although this takes no account of the efficiency of steam generation. Capital costs can also be high, however, due to the tubing requirements, rotating seals and so forth. This may be partially offset by the lower cost of back end clean-up due to the low exhaust gas flow volume.

A1.7.5 Fluid Bed

If the gas velocity through the bed of an up-flow through-circulation dryer is steadily increased, a point is reached where the bed becomes fluidised - that is, it behaves like a fluid. Between this point and that where the velocity is sufficient to entrain the typical

particle and carry it out of the bed, lies the fluid or fluidised bed regime. Once entrainment dominates, we enter the regime of pneumatic conveying dryers (Section A1.7.6).

Fluid beds are characterised by very high heat transfer rates and very good mixing; they represent in many respects ideal drying conditions [197]. In fluid bed dryers (Figure A1.20) the fluidising gas is the drying medium, and may be air, combustion products or in special cases steam [222,223] (see Section A1.7.5.1). Usually the source of heat is the sensible heat of the drying medium at entry to the bed, although indirect heating of the medium by in-bed steam tubes has been used in some designs.
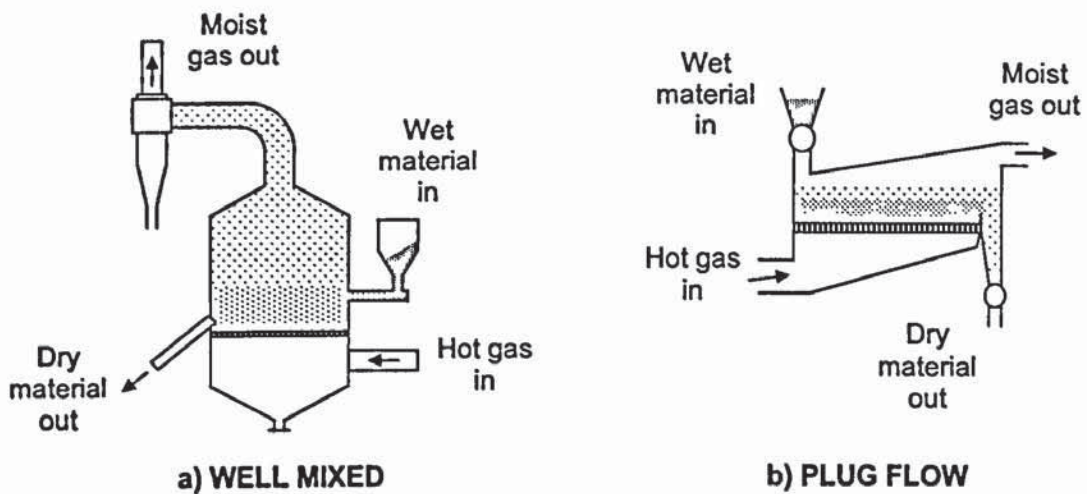
Figure A1.20 Types of fluid bed dryer

Fluid bed drying is well established for both batch and continuous processes. It is generally fast and efficient, and equipment size is relatively small compared with more traditional techniques. In the case of continuous processes, beds are usually either of the well-mixed type or the plug-flow type (Figure A1.20).

Well-mixed types are characterised by large bed depth to width ratios and a large particle residence time distribution because of the highly vigorous mixing. In drying this implies a wide range of moisture contents, and plug flow designs with shallower beds in which the mixing is less vigorous are usually preferred. Material is admitted to one side of the bed and extracted from the other. Two or more bed chambers may be used in series to control the temperature/time history.

Because of the efficient heat transfer and mixing, the bed temperature is very uniform away from the immediate vicinity of the distributor plate through which the fluidising gas is admitted. This has two important consequences. Firstly the temperature of the drying medium drops very rapidly from its inlet value to the bed value, so that high inlet temperatures can be used (up to 750°C with normal materials of construction) without the risk of exposing the material to such temperatures for more than very brief periods. Secondly the temperature of the dried material leaving the bed and that of the exhausting gas is usually very similar.

Material size is an important consideration for fluid bed dryers. The material must be in a suitable form for fluidisation. This generally means *particulate material* of a reasonably small size (dependent to some extent on density) and a reasonably uniform size distribution. Fluid bed dryers have found widest application for particle sizes of less than 10mm (usually significantly less) - often granular or crystalline materials with very uniform size. An *average* particle size of 10mm has been suggested as the upper limit [224].

Larger size materials can be dried successfully, although there are one or two potential problems the seriousness of which will be dependent on the specific material and end use. Higher fluidisation velocities are required for larger particles, and also longer residence times in order to complete the drying. This will increase the tendency to entrainment and carry-over of smaller particles, and as particle size increases the size range tends to increase also, compounding the problem. Fortuitously the particles that become entrained will tend to be the lightest and therefore the driest particles, so that carry-over can be viewed as a self-ejection mechanism which acts to prevent over-drying.

Cyclone separation is nearly always necessary with this type of dryer (certainly for biomass gasification system feedstocks), so the separated dry material could simply be added to the main material outlet stream. Also associated with larger particles is the phenomenon of channelling - the formation of large voids in the bed due to fluid dynamic instabilities. This is very much a function of the precise material and size distribution, and would need to be investigated experimentally.

Emissions such as blue haze would be controlled by selecting an appropriate bed temperature. Particulate emissions are more of a problem, and a second stage of dust removal may well be necessary beyond the cyclone stage (bag filter or scrubber) depending on local legislation.

A1.7.5.1 Pressurised Steam Fluid Bed Dryer

A Danish company, Niro, has recently developed a unique design of pressurised steam fluid bed dryer specifically for moist fibrous particulate materials [222,225,226]. The dryer is shown in Figure A1.21. The dryer was designed primarily for the brewing, food and sugar processing industries, but at least two systems are in operation for the drying of wood chips [227].
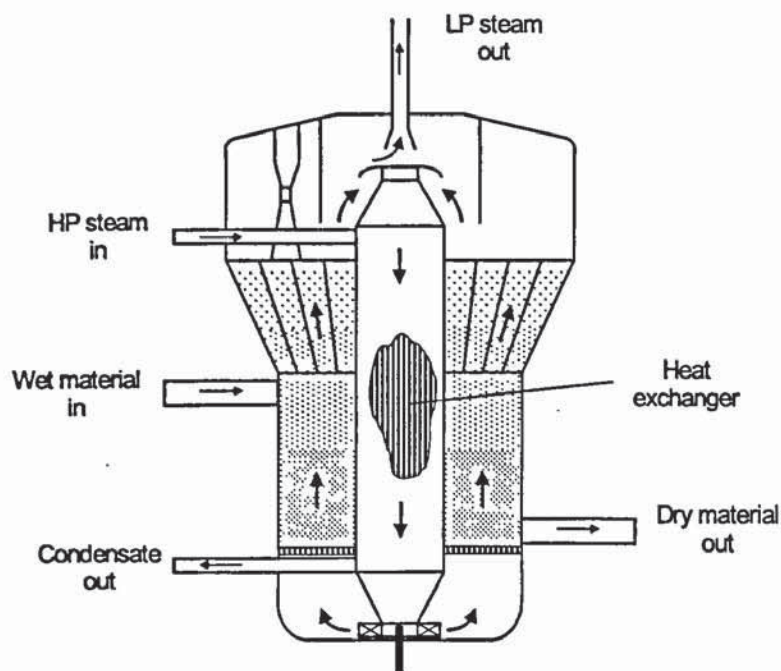
Figure A1.21 Pressurised steam fluid bed dryer (Niro A/S)

Recycled moisture evaporated from the feed forms the low-pressure steam drying and fluidising medium. The bed of material is contained in 16 cells, arranged around a central high-pressure superheated steam heat exchanger. After leaving the cells the low-pressure steam passes through a cyclone for dust separation, after which the excess steam from evaporation is discharged, and the remainder passes down through the heat exchanger to be heated indirectly to about 200°C by the high-pressure steam (max. 25 bar g, 250°C), before returning to the bed distributor plates. The continuously discharged flow of

evaporated steam is at about 2.8 bar g and 150°C, and may therefore be used as process steam elsewhere although it may require cleaning once condensed. The drying material passes through the 16 cells in sequence before being discharged from the last. Fines separated in the cyclone are passed directly to the final cell. Table A1.3 gives typical performance data for the drying of wood chips.

Table A1.3 Pressurised steam fluid bed dryer performance data
(data provided by Niro A/S [228])

Niro claim a very efficient process because of the utilisation of the recovered steam, although a suitable external use must exist, as MVR for internal heat recovery is impractical with this configuration without major modifications. If the energy recovery is ignored, the thermal efficiency is around 70% if the high-pressure condensate is discharged, rising to well over 90% if the condensate is part of a closed high-pressure steam cycle. Almost all of the energy used to dry the material can be recovered.

Niro also claim excellent environmental performance as a result of the system being fully closed with no gaseous emissions to atmosphere.

The minimum size of dryer offered has a capacity at 25 bar steam pressure of 3 tonnes per hour water evaporated, and the largest 40 tonnes per hour. Niro have suggested 5 tonnes per hour as a minimum for a viable installation drying wood chips [228].

Capital cost is high due to complexity of design, and the dryer is likely only to prove attractive for relatively large scale systems and where the full benefit of energy recovery can be realised.

A1.7.6 Pneumatic Conveying

Pneumatic conveying dryers achieve rapid drying with short residence times by fully entraining the material in a high velocity gas flow. The category is usually taken to include dryers where the entraining gas is combustion products or steam as well as air. Most pneumatic conveying dryer types can be dismissed for the present purposes because they require a fine particle size much smaller than would be suitable for most gasifiers or than could be economically prepared for biomass gasification system feedstocks [229]. These include conventional flash dryers (Figure A1.22) - very short residence time single-pass devices for removing relatively small amounts of moisture - and most ring dryers, in which the material is carried in an endless ring duct (Figure A1.23).
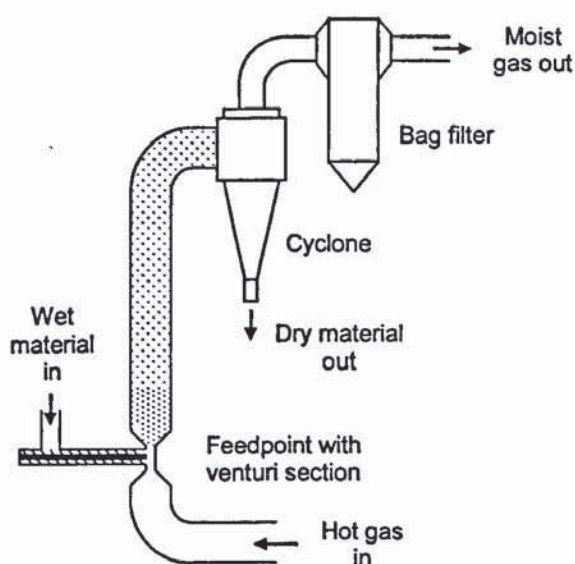
Figure A1.22 Flash dryer

A high-pressure steam flash dryer has been developed for biomass gasification system feedstocks by IVO in Finland [230], but this is specifically intended for a pressurised fluid bed gasifier using very small particles of 2-3 mm diameter. The dryer is intended for use in the IVOSDIG cycle, in which the high pressure steam produced in the dryer is used to boost the mass flow through the gas turbine, thereby offering overall efficiency improvements.
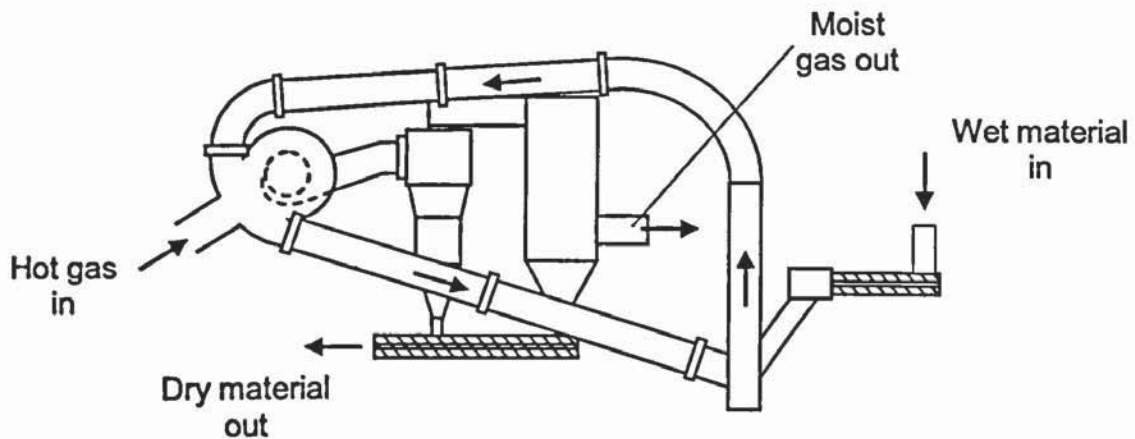
Figure A1.23 Ring dryer

A1.7.6.1 Pneumatic Conveying Pressurised Steam Dryer

One pneumatic conveying design related to the ring dryer has been developed specifically for steam drying of biomass at particle sizes up to 50 mm. The dryer is a closed-loop pneumatic conveying dryer using only indirectly heated steam from the liberated moisture as the conveying and drying medium. It has been developed in Sweden over a number of years by the Chalmers University at Gothenburg, the MoDo-Chemetics company and Stork Friesland Scandinavia [186,187,231]. The technology, which was developed primarily for the wood products industry, is now owned and marketed as the "Exergy" steam dryer by Stork Engineering.

The system layout is depicted in Figure A1.24. The design philosophy has much in common with the Niro steam dryer (Section A1.7.5.1), including a high degree of energy recovery and zero gaseous emissions.

The drying section consists of a sequence of vertically orientated shell-and-tube heat exchangers, through which the material is conveyed and the liberated steam superheated indirectly, usually by high-pressure *saturated steam* although combustion products or thermal oil can also be used. In the case of high-pressure steam, the heat exchangers are designed to be fully condensing. The number of stages depends on the degree of drying required. The dried material is extracted in a cyclone at the end of the heat exchanger train, and the near-saturated steam continues around the loop to a steam extraction point where the excess is continuously bled off at between 2 and 6 bar, available for external use. The remainder of the steam continues to a first stage of superheater before reaching the material inlet point and re-entering the drying section. Typical residence time of material in the dryer is 10-30 seconds, and a high level of uniformity in final moisture content is achieved.
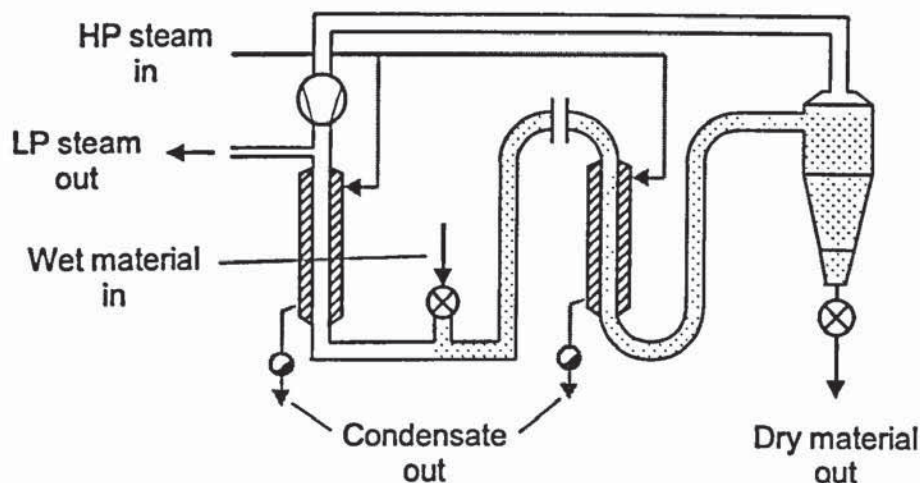
Figure A1.24 "Exergy" steam dryer (Stork Engineering)

Figures given imply a thermal drying efficiency (excluding recovery) of about 75% where the heating steam condensate is discharged, rising to 95% where the condensate is part of a closed steam cycle [232].

Standard units using 10 bar steam as the heating medium are offered at sizes from 0.25-5 tonnes of water evaporated per hour, but these are designed for fine materials such as wood shavings, sawdust, sludge etc. with a high initial moisture content. Much larger units have however been supplied specifically for forestry wastes including wood chips of up to 50mm, with the objective of producing wood fuel pellets.

Process data for two such systems is given in Table A1.4; unfortunately cost information has not been provided.

Table A1.4 "Exergy" steam dryer process data

System	Skellefteå Kraft	Example B
Evaporation capacity (t/h)	22	12.5
Inlet moisture (% db)	122	150-233
Final moisture content (% db)	14.9	5.3-25
HP steam pressure (bar)	26	12
LP steam pressure (bar)	4.2	6.5

The process configuration is well suited to the application of MVR (Figure A1.4), and an MVR option for internal heat recovery *is* offered by Stork for cases where there is no external use for the extracted steam.

APPENDIX 2   SYSTEM MODEL WORKSHEETS

A2.1 Worksheet: Inputs

CONFIGURATION

Gasifier type	`1`	1 RFSG
		2 UGETC
Dryer type	`1`	1 rotary cascade
		2 rotary cascade (integral burner)
		3 band conveyor
Engine type	`1`	1 ambient air
		2 oxygen-enriched air
Output type	`2`	1 power only
		2 CHP

CONDITIONS - SINGLE RUN

Biomass cost at plant gate	`80`	£/dt	range 20 - 120
Biomass dry flow rate to gasifier	`0.556`	kg/s	range 0.1 - 0.6
Biomass moisture at dryer inlet	`100`	% db	range 40 - 120
Biomass moisture at dryer outlet	`50`	% db	range 10 - 50
Air oxygen concentration to gasifier	`0.60`	frac. by vol	range 0.21 - 0.6

`Single Run`

CONDITIONS - MULTIPLE RUNS
(all combinations calculated)

`New Table` `Add to Table`

Biomass cost at plant gate £/dt	Biomass dry flow rate to gasifier kg/s	Biomass moisture at dryer inlet % db	Biomass moisture at dryer outlet % db	Air oxygen conc. to gasifier frac. by vol
80	0.556	50	10	0.21
		75	20	0.28
		100	35	0.4
			50	0.6

COST CALCULATION PARAMETERS

Discount rate i	`12`	%
Project life L	`20`	yrs
Plant number n (i.e. nth plant)	`10`	
Annuity factor AF	0.0996	
Learning ratio LR	0.476	
Electricity price	`0.0369`	£/kWh
RFSG capital cost factor (F)	`1`	

A49

A2.2 Worksheet: Rotary Cascade Dryer

ROTARY CASCADE DRYER (direct, air or flue gas)
Standard fuel (chipped SRC poplar) only

All gas and biomass quantities on dry basis u.o s.
Burner (RCIE) operates at fixed AFR

	Value	Units		Value	Units			
PERFORMANCE								
Required biomass flow rate	8.417	kg/s	Total biomass flow rate	0.491	kg/s			
Biomass moisture in	100	%	Water evaporation rate	0.245	kg/s			
Biomass moisture out	50	%	Water enthalpy in	62.8	kJ/kg			
Biomass temperature out	75	°C	Water enthalpy out	314 1	kJ/kg			
Biomass mean specific heat	1.4	kJ/kgK						
Ambient temperature	15	°C	Ambient air specific heat	1.003	kg/kg			
Ambient humidity	0 00865	kg/kg	Ambient vapour enthalpy	2526.2	kJ/kg	**ITERATIONS**		
Max. burner biomass flow rate (d a f)	0 072	kg/s	Max. burner exhaust gas flow rate	0 807	kg/s			
Fraction of max. burner feed used for drying	0.373		Max. burner exhaust gas CO2 flow rate	0.132	kg/s	Cp CO2	1153 5	
			Max. burner exhaust gas N2 flow rate	0.595	kg/s	Cp N2	1121.2	
			Max. burner exhaust gas O2 flow rate	0.081	kg/s	Cp O2	1047 6	
			Max. burner exhaust gas H2O flow rate	0.084	kg/s	Cp H2O	2138 5	
			Burner exhaust gas humidity	0.104	kg/kg			
			Burner exhaust gas temperature	1222.9	°C	GasTemp	1000 0	
			Burner exhaust gas specific heat	0.980	kJ/kgK			
			Burner exhaust gas vapour enthalpy	4950.8	kJ/kg			
Quench air flow rate	1.937	kg/s	Burner exhaust gas flow rate to dryer	0.301	kg/s			
Engine exhaust wet gas flow rate	1.705	Nm3/s	Engine exhaust wet gas flow rate (PO)	1.705	Nm3/s	GasDel	1.180	
Engine exhaust gas temperature	397.5	°C	Engine exhaust gas temperature (CHP)	296.8	°C	TempDel	0.0	
Engine exhaust [CO2]	0.131	frac. by vol	Engine exhaust gas flow rate	2.009	kg/s			
Engine exhaust [N2]	0.658	frac. by vol	Engine exhaust vapour enthalpy	3272.3	kJ/kg			
Engine exhaust [H2O]	0.142	frac. by vol	Engine exhaust gas humidity	0.097	kg/kg			
Engine exhaust [O2]	0.069	frac. by vol	Engine exhaust gas specific heat	1.022	kJ/kgK			
Target or max. gas temperature in	300.0	°C	Calculated gas temperature in	300 0	°C	TempError	0 000	
Gas temperature out	110	°C	Gas CO2 flow rate	0.487	kg/s			
			Gas N2 flow rate	3.110	kg/s			
			Gas O2 flow rate	0.649	kg/s			
			Gas humidity in	0.057	kg/kg			
			Summed gas flow rate	4.247	kg/s			
			Calculated gas flow rate	4.247	kg/s	FlowError	0.000	
			Gas humidity out	0.115	kg/kg			
			Gas specific heat in	1.016	kJ/kg			
			Gas specific heat out	1.002	kJ/kg			
			Vapour enthalpy in	3072 5	kJ/kg			
			Vapour enthalpy out	2702.1	kJ/kg			
Wall heat loss	8	% heat in	Electrical power	33.3	kW			
			Energy consumption (thermal)	8.320	MJ/kgWE			
			Energy consumption (total)	8 456	MJ/kgWE			
COST								
			Adiabatic saturation temperature	58 3	°C			
			Mean latent heat of vaporisation	2339.6	kJ/kg			
			Heat transferred to solids	676.7	kW			
			Mean temperature difference	160 0	°C			
			Equipment cost	339.7	£000			
			Total plant cost - 1st plant	1036 6	£000			
			Total plant cost - 10th plant	493.8	£000			
			Annual cost of capital	49.2	£000 p a			
			Other operating costs:					
			Labour	50 0	£000 p a			
			Overheads	19.8	£000 p.a.			
			Maintenance	19 8	£000 p a.			
			Total	89.5	£000 p a.			

A50

A2.3 Worksheet: Band Conveyor Dryer

BAND CONVEYOR DRYER (direct, air)

Bed depth 0.5 m, fan pressure 500 Pa, ambient conditions 15°C and 80% relative humidity

All gas and biomass quantities on dry basis u.o.s.

	Value	Units		Value	Units
PERFORMANCE					
Required biomass flow rate	0.556	kg/s			
Biomass moisture in	100	%	Water evaporation rate	0.278	kg/s
Biomass moisture out	50	%			
			Specific water evaporated	37.50	kg/m²
			Specific water evaporation rate	0.00970	kg/s/m²
Ambient humidity	0.00865	kg/kg			
Air temperature in	50	°C			
Specific fan power	839	W/m²			
Air velocity onto bed	0.84	m/s			
			Specific air flow rate	0.840	m³/s/m²
			Air flow rate	0.000	Nm³/s
			Air volume flow rate	24.07	m³/s
			Air specific heat in	1.005	kJ/kgK
			Vapour enthalpy in	2590.3	kJ/kg
			Drying time	1.07	hours
			Total bin floor area	28.66	m²
			Electrical (fan) power	0.00	kW
			Energy consumption (thermal)	6.290	MJ/kg$_{WE}$
			Energy consumption (total)	6.376	MJ/kg$_{WE}$
COST					
			Equipment cost	132.1	£000
			Total plant cost - 1st plant	0.0	£000
			Total plant cost - 10th plant	0.0	£000
			Annual cost of capital	0.0	£000 p.a.
			Other operating costs:		
			Labour	0.0	£000 p.a.
			Overheads	0.0	£000 p.a.
			Maintenance	0.0	£000 p.a.
			Total	0.0	£000 p.a.

A2.4 Worksheet: Reverse Flow Slagging Gasifier

RFSG CONFIGURATION
Air pre-heat and oxygen enrichment

Feedstock:	chipped SRC poplar	
Analysis (dry ash free):	$CH_{1.63}O_{0.66}$	
Ash content (dry):	2.30%	
LHV (dry):	18.2 MJ/kg	

All gas and biomass quantities on d.a.f. basis u.o.s.

Biomass flow rate	0.543	kg/s
Biomass moisture content	50	%
Air oxygen concentration	0.60	frac. by vol
Specific air flow rate (per unit biomass)	0.476	Nm^3/kg
Air flow rate	0.259	Nm^3/s
Specific product gas flow rate (per unit biomass)	1.810	Nm^3/kg
Product gas flow rate	0.983	Nm^3/s
Product gas temperature at regenerator exit	547.7	°C

Product gas composition

$[H_2]$	0.303	frac. by vol
$[CO]$	0.115	frac. by vol
$[CO_2]$	0.244	frac. by vol
$[CH_4]$	0.049	frac. by vol
$[N_2]$	0.087	frac. by vol
$[H_2O]$	0.200	frac. by vol

Product gas LHV	8.114	MJ/Nm^3
Cold gas efficiency (LHV basis)	78.8	%
Gasifier total plant cost - 1st plant	5063.1	£000
Gasifier total plant cost - 10th plant	2412.2	£000
Annual cost of capital	240.2	£000 p.a.
Other operating costs:		
Labour	144.5	£000 p.a.
Overheads	96.5	£000 p.a.
Maintenance	96.5	£000 p.a.
Total	337.5	£000 p.a.

A2.5 Worksheet: Updraft Gasifier with External Tar Cracking

UGETC CONFIGURATION						
No air pre-heat or oxygen enrichment						
Feedstock:	chipped SRC poplar					
Analysis (dry ash free):	$CH_{1.63}O_{0.88}$					
Ash content (dry):	2.30%					
LHV (dry):	18.2 MJ/kg					
All gas and biomass quantities on d.a.f. basis u.o.s.						
Biomass flow rate				0.543	kg/s	
Biomass moisture content				50	%	
Air oxygen concentration				0.21	frac. by vol	
Specific air flow rate (per unit biomass)				1.569	Nm^3/kg	
Air flow rate				0.852	Nm^3/s	
Specific product gas flow rate (per unit biomass)				2.809	Nm^3/kg	
Product gas flow rate				1.526	Nm^3/s	
Product gas temperature at gasifier exit				611.0	°C	
Product gas composition						
$[H_2]$				0.196	frac. by vol	
[CO]				0.070	frac. by vol	
$[CO_2]$				0.179	frac. by vol	
$[CH_4]$				0.031	frac. by vol	
$[N_2]$				0.373	frac. by vol	
$[H_2O]$				0.149	frac. by vol	
Product gas LHV				4.846	MJ/Nm^3	
Cold gas efficiency (LHV basis)				0.0	%	
Gasifier total plant cost - 1st plant				0.0	£'000	
Gasifier total plant cost - 10th plant				0.0	£'000	
Annual cost of capital				0.0	£'000 p.a.	
Other operating costs:						
Labour				0.0	£'000 p.a.	
Overheads				0.0	£'000 p.a.	
Maintenance				0.0	£'000 p.a.	
Total				0.0	£'000 p.a.	

A2.6 Worksheet: IC Engine

SPARK-IGNITION GAS ENGINE

All quantities wet basis u.o.s.

	PRODUCT GAS			NATURAL GAS			
Gasifier exit [H_2]	0.303	frac. by vol					
Gasifier exit [CO]	0.115	frac. by vol					
Gasifier exit [CO_2]	0.244	frac. by vol					
Gasifier exit [CH_4]	0.049	frac. by vol					
Gasifier exit [N_2]	0.087	frac. by vol					
Engine inlet [H_2]	0.361	frac. by vol				No. of engines	3
Engine inlet [CO]	0.137	frac. by vol					
Engine inlet [CO_2]	0.290	frac. by vol					
Engine inlet [CH_4]	0.059	frac. by vol	1.0	by vol			
Engine inlet [N_2]	0.103	frac. by vol					
Engine inlet [H_2O]	0.05	frac. by vol					
						[O_2] ITERATION	**1**
Air oxygen concentration	0.210	frac. by vol	0.21	frac. by vol	Air oxygen concentration	0.210
Air-fuel equivalence ratio	1.7		1.7		Stiochiometric air-fuel ratio	1.744
Stiochiometric air-fuel ratio	1.744	by vol	9.524	by vol	Air-fuel ratio	2.966
Air-fuel ratio	2.966	by vol	16.190	by vol	Air flow rate	3.069
					Mixture total flow rate	4.424
					CH_4 fuel flow rate	0.244
					CH_4 thermal input	8.750
Fuel LHV (dry basis)	8.138	MJ/Nm^3	35.87	MJ/Nm^3	No. of engines	3
					CH_4 brake thermal efficiency	40.703
					CH_4 electrical output	3.455
					Brake thermal efficiency	39.868
Fuel temperature	40	°C	15	°C	Electrical output	3.094
Fuel flow rate (dry basis)	0.983	Nm^3/s	0.244	Nm^3/s	Derating	10.457
Thermal input	8.002	MW	8.750	MW		
Air temperature	15	°C	15	°C		
Air flow rate	3.069	Nm^3/s	3.950	Nm^3/s		
Mixture total flow rate	4.424	m^3/s	4.424	m^3/s		
Brake thermal efficiency	39.86	%	40.70	%		
Generator efficiency	97	%	97	%		
Overall electrical efficiency	38.66	%	39.48	%		
Electrical output	3.094	MW	3.455	MW		
Derating to product gas operation			10.5	%	**TEMP. ITERATION**	**1**
Exhaust gas flowrate	3.846	Nm^3/s				
Exhaust gas temperature	393.7	°C			Exhaust gas temperature	400
Exhaust gas [CO_2]	0.131	frac. by vol				
Exhaust gas [N_2]	0.658	frac. by vol				
Exhaust gas [H_2O]	0.142	frac. by vol				
Exhaust gas [O_2]	0.069	frac. by vol				
Exhaust gas humidity	0.097	kg/kg				
Exhaust gas specific heat	1.105	kJ/kgK			Exhaust gas specific heat	1.106
Cooling water flow rate	19.04	kg/s				
Cooling water inlet temperature	60	°C				
Cooling water outlet temperature	90	°C				
Engine/generator equipment cost	948.7	£000				
Engine/generator total plant cost - 1st plant	2291.1	£000				
Engine/generator total plant cost - 10th plant	1091.5	£000				
Annual cost of capital	108.7	£000 p.a.				
Other operating costs:						
Labour	83.7	£000 p.a.				
Overheads	43.7	£000 p.a.				
Maintenance	43.7	£000 p.a.				
Total	171.0	£000 p.a.				

A2.7 Worksheet: Engine Coolant Radiator

ENGINE COOLANT RADIATOR							
Air blown, finned tube design							
All quantities wet basis u.o.s.							
Hot water inlet temperature	90	°C					
Hot water outlet temperature	60	°C					
Water specific heat	4.188	kJ/kgK					
Max. hot water flow rate	19.04	kg/s	Hot water flow rate to meet drying requirements	0.00	kg/s	FlowDel	19.04
Air inlet temperature	15	°C	Air outlet temperature	50	°C		
ΔT(air outlet to water outlet)	10	°C	Air mean specific heat	1.005	kJ/kgK		
Air flow rate to meet drying requirements	0.00	Nm³/s	Air flow rate to meet drying requirements	0.00	kg/s		
			Heat transferred	0.0	kW		

A2.8 Worksheet: Engine Coolant Water Heater

ENGINE COOLANT WATER HEATER						
Shell-and-tube design, hot water production						
All quantities wet basis u.o.s.						
Hot water inlet temperature	90	°C				
Hot water outlet temperature	60	°C				
Water specific heat	4.188	kJ/kgK				
Hot water flow rate	19.04	kg/s				
Cold water inlet temperature	50	°C	Cold water outlet temperature	85	°C	
ΔT_{PINCH}	5	°C				
			Cold water flow rate	16.32	kg/s	
			Heat transferred	2391.7	kW	
Overall heat transfer coefficient	938	W/m²K	Log mean temperature difference	35.0	°C	
Counter-flow factor	0.9		Heat transfer area (LMTD)	80.84	m²	
			Equipment cost	17.8	£'000	
			Total plant cost - 1st plant	97.1	£'000	
			Total plant cost - 10th plant	46.3	£'000	
			Annual cost of capital	4.6	£'000 p.a.	
			Other operating costs:			
			Labour	10.0	£'000 p.a.	
			Overheads	1.9	£'000 p.a.	
			Maintenance	1.9	£'000 p.a.	
			Total	13.7	£'000 p.a.	

A2.9 Worksheet: Product Gas Water Heater

PRODUCT GAS WATER HEATER								
Firetube design, hot water production			A56					
All quantities wet basis u.o.s.								
Product gas $[H_2]$	0.303	frac. by vol						
Product gas [CO]	0.115	frac. by vol						
Product gas $[CO_2]$	0.244	frac. by vol						
Product gas $[CH_4]$	0.049	frac. by vol						
Product gas $[N_2]$	0.087	frac. by vol						
Product gas $[H_2O]$	0.200	frac. by vol						
Product gas inlet temperature	547.7	°C	Product gas mean temperature	333.8	°C			
Product gas outlet temperature	120	°C						
			Product gas specific heat	1.698	kJ/kgK			
Product gas dry flow rate	0.983	Nm³/s	Product gas flow rate	1.172	kg/s			ITERATIONS
								0.5
Water inlet temperature from EC	85	°C	Actual water inlet temperature	85.0	°C			85
Water inlet temperature from return	50	°C	Water inlet enthalpy	356.0	kJ/kg			356.0
Water outlet temperature	100	°C	Water outlet enthalpy	418.8	kJ/kg			
			Water flow rate	13.55	kg/s			13.547
								-2.769
			Heat transferred	851.1	kW			
Overall heat transfer coefficient	50	W/m²K	Log mean temperature difference	161.9	°C			
Counter-flow factor	0.9		Heat transfer area (LMTD)	116.80	m²			
			Equipment cost	22.9	£'000			
			Total plant cost - 1st plant	118.6	£'000			
			Total plant cost - 10th plant	56.5	£'000			
			Annual cost of capital	5.6	£'000 p.a.			
			Other operating costs:					
			Labour	10.0	£'000 p.a.			
			Overheads	2.3	£'000 p.a.			
			Maintenance	2.3	£'000 p.a.			
			Total	14.5	£'000 p.a.			

A2.10 Worksheet: Engine Exhaust Gas Water Heater

ENGINE EXHAUST GAS WATER HEATER								
Firetube design, hot water production								
All quantities wet basis u.o.s.								
Engine exhaust gas inlet temperature	393.7	°C						
Engine exhaust gas flow rate	3.846	Nm³/s						
Engine exhaust gas [CO_2]	0.131	frac. by vol	Engine exhaust gas CO_2 flow rate	0.988	kg/s			
Engine exhaust gas [N_2]	0.658	frac. by vol	Engine exhaust gas N_2 flow rate	3.164	kg/s			
Engine exhaust gas [H_2O]	0.142	frac. by vol	Engine exhaust gas H_2O flow rate	0.439	kg/s			
Engine exhaust gas [O_2]	0.069	frac. by vol	Engine exhaust gas O_2 flow rate	0.379	kg/s			
Burner exhaust gas inlet temperature	0.0	°C	Burner exhaust gas CO_2 flow rate	0.000	kg/s			
			Burner exhaust gas N_2 flow rate	0.000	kg/s			
			Burner exhaust gas H_2O flow rate	0.000	kg/s		**ITERATIONS**	
			Burner exhaust gas O_2 flow rate	0.000	kg/s			
						m EEG	4.971	
Gas outlet temperature	308.2	°C	Gas CO_2 flow rate	0.988	kg/s	m BEG	0.000	
			Gas N_2 flow rate	3.164	kg/s	m tot	4.971	
			Gas H_2O flow rate	0.439	kg/s	Cp EEG	1.113	
			Gas O_2 flow rate	0.379	kg/s	Cp BEG	0.000	
			Gas flow rate	4.971	kg/s	Cp tot	1.113	
			Gas inlet temperature	393.7	°C	GasTemp	393.7	
			Gas mean temperature	350.9	°C			
			Gas mean specific heat	1.160	kJ/kgK			
							0.5	
Water inlet temperature from EC	85	°C	Actual water inlet temperature	72.6	°C		85	
Water inlet temperature from return	50	°C	Water inlet enthalpy	303.9	kJ/kg		356.0	
Water outlet temperature	100	°C	Water outlet enthalpy	418.8	kJ/kgK			
			Water flow rate	4.293	kg/s		7.850	
							5.081	
			Heat transferred	493.1	kW			
Overall heat transfer coefficient	50	W/m²K	Log mean temperature difference	256.8	°C			
Counter-flow factor	0.9		Heat transfer area (LMTD)	42.67	m²			
			Equipment cost	11.5	£000			
			Total plant cost - 1st plant	68.7	£000			
			Total plant cost - 10th plant	32.7	£000			
			Annual cost of capital	3.3	£000 p.a.			
			Other operating costs:					
			Labour	10.0	£000 p.a.			
			Overheads	1.3	£000 p.a.			
			Maintenance	1.3	£000 p.a.			
			Total	12.6	£000 p.a.			

A2.11 Worksheet: Other System Modules

OTHER SYSTEM MODULES		
Biomass flow rate	0.556	kg/s
Overall power exported	2.70	MW$_e$
RECEPTION, STORAGE, SCREENING		
Capital cost		
TPC (with buffer store) - 1st plant	557.3	£'000
TPC (with buffer store) - 10th plant	265.5	£'000
Annual cost of capital	26.4	£'000 p.a.
Operating costs		
Labour	60.0	£'000 p.a.
Utilities	42.0	£'000 p.a.
Overheads	10.6	£'000 p.a.
Maintenance	10.6	£'000 p.a.
Total	123.2	£'000 p.a.
AIR OXYGEN ENRICHMENT PLANT		
Gasifier air oxygen concentration	0.60	frac. by vol
Gasifier air flow rate	0.259	Nm^3/s
Engine air oxygen concentration	0.210	frac. by vol
Engine air flow rate	3.069	Nm^3/s
Oxygen flow rate from separation unit	0.131	Nm^3/s
Electrical power consumption	211.9	kW
Lease cost	73.7	£'000 p.a.
TPC of additional capital - 1st plant	182.3	£'000
TPC of additional capital - 10th plant	86.9	£'000
Annual cost of additional capital	8.6	£'000 p.a.
Other operating costs		
Utilities (water supply and disposal)	4.3	£'000 p.a.
Overheads	3.5	£'000 p.a.
Maintenance	0.0	£'000 p.a.
Total	7.8	£'000 p.a.
PRODUCT GAS QUENCH AND WASTE WATER TREATMENT		
Product gas wet flow rate	0.983	Nm^3/s
Product gas water content	0.200	frac. by vol.
Waste water flow rate	0.198	kg/s
Capital cost		
Equipment cost	11.1	£'000
TPC - 1st plant	38.8	£'000
TPC - 10th plant	18.5	£'000
Annual cost of capital	1.8	£'000 p.a.
Operating costs		
Utilities (water supply and disposal)	7.6	£'000 p.a.
Overheads	0.7	£'000 p.a.
Maintenance	0.7	£'000 p.a.
Total	9.0	£'000 p.a.
GRID CONNECTION		
Capital cost		
TPC - 1st plant	400.0	£'000
TPC - 10th plant	190.5	£'000
Annual cost of capital	19.0	£'000 p.a.
Operating costs		
Overheads	7.6	£'000 p.a.
Maintenance	7.6	£'000 p.a.
Total	15.2	£'000 p.a.

CONFIGURATION: RFSG (F=1), rotary cascade dryer, ambient air engine, CHP

All quantities dry basis u.o.s		CURRENT CASE	RESULTS TABLE							
Biomass cost at plant gate	£/t	80	80	80	80	80	80	80	80	80
Biomass flow rate to gasifier	kg/s	0.556	0 556	0 556	0 556	0 556	0 556	0 556	0 556	0 556
Biomass thermal input to gasifier	MW	9 45	9 99	9 99	9.99	9 99	9 85	9 85	9 85	9 85
Biomass moisture at dryer inlet	% db	100	50	50	50	50	50	50	50	50
Biomass moisture at dryer outlet	% db	50	10	10	10	10	20	20	20	20
Air oxygen concentration to gasifier	frac. by vol	0.6	0.21	0.28	0 4	0 6	0.21	0.28	0 4	0 6
Status		OK	OK	OK	OK	OK	OK	OK	OK	OK

MAJOR SYSTEM ELEMENTS

Reception, Storage, Screening

TPC	£000	266	266	266	266	266	266	266	266	266
Annual cost of capital	£000 p.a.	26 4	26 4	26 4	26 4	26 4	26 4	26 4	26 4	26 4
Other operating costs	£000 p.a.	123.2	123.2	123.2	123.2	123.2	123.2	123.2	123.2	123.2

Dryer

Electrical power	kW	34.6	46 9	45 9	45.3	44 7	37.8	37.2	36 9	36 5
Dryer TPC	£000	245	285	282	280	278	257	256	254	252
Dryer annual cost of capital	£000 p.a.	24 4	28 4	28 1	27.9	27.7	25 6	25 4	25 2	25 1
Dryer other operating costs	£000 p.a.	69.6	72.8	72.6	72.4	72.3	70.5	70.4	70.3	70.2

Air Oxygen Enrichment Plant

Electrical power	kW	211.9		118.1	227.0	211.6		118.3	227.2	211.7
TPC (additional capital)	£000	86.9		46 0	63 0	86 8		46 0	63.1	86 8
Annual cost of additional capital	£000 p.a.	8 6		4 6	6 3	8 6		4 6	6 3	8 6
Lease cost	£000 p.a.	73 7		35 1	50.7	73.7		35.1	50.7	73.7
Other operating costs	£000 p.a.	7.8		4 4	7.5	7.8		4 4	7 5	7.8

Gasifier

Cold gas efficiency (LHV basis)	%	78 8	85 3	84 6	85.7	85 6	83.7	83.2	84 4	84.2
TPC	£000	2412	2412	2412	2412	2412	2412	2412	2412	2412
Annual cost of capital	£000 p.a.	240 2	240.2	240.2	240.2	240 2	240 2	240.2	240.2	240 2
Other operating costs	£000 p.a.	337.5	337.5	337.5	337.5	337.5	337.5	337.5	337.5	337.5

Gas Quench & Waste Water Treatment

TPC	£000	19	19	19	19	19	19	19	19	19
Annual cost of capital	£000 p.a.	1.8	1 8	1.8	1 8	1.8	1 8	1 8	1 8	1 8
Other operating costs	£000 p.a.	9 0	5 2	5 0	4 8	4 7	6.2	6 0	5 8	5.7

Engine

Engine electrical output	MW	3 09	3.33	3.33	3.40	3.41	3.25	3.25	3.33	3.35
Overall efficiency	%	38.7	38 6	38 9	39.2	39 5	38 4	38 7	39 1	39 3
TPC	£000	1092	1185	1138	1108	1079	1187	1141	1112	1083
Annual cost of capital	£000 p.a.	109	118	113	110	107	118	114	111	108
Other operating costs	£000 p.a.	171	181	178	176	174	181	177	176	174

CHP

ECWH TPC	£000	46	48	48	48	48	48	48	48	48
ECWH annual cost of capital	£000 p.a.	4 6	4 8	4.8	4 8	4 8	4 8	4.7	4.7	4.7
ECWH other operating costs	£000 p.a.	13.7	13 9	13 8	13 8	13 8	13 8	13 8	13 8	13.8
PGWH hot water production	kg/s	13 56	11 36	11 36	11 65	11.77	11 81	11 82	12.12	12 20
PGWH TPC	£000	57	56	54	52	50	58	55	54	52
PGWH annual cost of capital	£000 p.a.	5 6	5 6	5 4	5.2	5 0	5 7	5 5	5 3	5 2
PGWH other operating costs	£000 p.a.	14 5	14 5	14 3	14 2	14 0	14 6	14 4	14 3	14 1
EEGWH hot water production	kg/s	4.29	8.56	8 37	8.37	8.26	8.56	8 40	8 41	8 33
EEGWH TPC	£000	33	48	47	47	46	53	52	52	52
EEGWH annual cost of capital	£000 p.a.	3.3	4 8	4 7	4 7	4 6	5.3	5 2	5 2	5 1
EEGWH other operating costs	£000 p.a.	12.6	13 8	13 8	13 7	13 7	14 3	14.2	14.2	14 1
Total hot water production	kg/s	17.84	19 92	19 74	20 02	20.03	20 37	20.21	20 53	20.54
TPC	£000	135	153	149	147	144	159	155	153	151
Annual cost of capital	£000 p.a.	13.5	15 2	14 8	14 6	14 4	15 8	15 5	15 3	15 0
Other operating costs	£000 p.a.	40.8	42.2	41.9	41 8	41 6	42 7	42 4	42 3	42 1

Grid Connection

TPC	£000	191	206	202	200	201	203	199	198	199
Annual cost of capital	£000 p.a.	19.0	20.5	20.1	19 9	20.1	20.3	19 9	19 7	19.9
Other operating costs	£000 p.a.	15.2	16 5	16.1	16 0	16 1	16.3	16 0	15 9	16.0

WHOLE SYSTEM

Net electrical output	MW	2.70	3.12	3.00	2.97	3.00	3.05	2 94	2.91	2.94
Hot water production	kg/s	17.84	19 92	19 74	20.02	20 03	20 37	20 21	20 53	20 54
Hot water production	MW	3.74	4.17	4 13	4.19	4.20	4.27	4.23	4 30	4 30
Overall electrical efficiency	%	26.2	28.1	27.0	26.7	27.0	27 5	26 5	26.2	26 5
Overall combined efficiency	%	62.5	65 6	64 2	64 4	64.7	65.9	64 6	64 9	65.2
Total plant cost	£000	4446	4524	4513	4495	4486	4502	4493	4476	4468
Total plant cost	£/kW	690	620	632	628	624	615	626	621	617
Biomass cost	£000 p.a.	1320	1320	1320	1320	1320	1320	1320	1320	1320
Annual cost of capital	£000 p.a.	443	451	449	448	447	448	447	446	445
Other operating costs	£000 p.a.	848	779	814	830	851	777	812	829	850
Total operating costs	£000 p.a.	2611	2550	2583	2598	2618	2546	2580	2595	2615
Revenue from heat sales	£000 p.a.	290	320	318	322	322	327	325	329	329
Total sales revenue	£000 p.a.	990	1127	1095	1089	1097	1117	1086	1082	1091
Cost of electricity (CHP)	£/kWh	0 122	0 102	0 108	0 109	0.109	0.104	0.109	0 111	0.111

A2.13 Worksheet Data Flows

Table A2.1 Data flows - Inputs sub-model

Sub-model: **Inputs**			
IN	**FROM**	**OUT**	**TO**
DC_B, m_B, X_{B2}, X_{B4}, $[O_2]_{A9}$	User	DC_B	Results
LF, d, l, F, N, EP		m_B	RSS, RD, RDB, BD, RFSG, UGETC
			RD, RDB, BD, Results
		X_{B2}	RD, RDB, BD, RFSG, UGETC, Results
		X_{B4}	AOEP, RFSG, Results
		$[O_2]_{A9}$	RSS, RD, RDB, BD, AOEP, RFSG, Results
		LR, AF	UGETC, PGWH, PGQ, ICE, ECWH, EEGWH, GC
		F	RFSG
		EP	Results

Table A2.2 Data flows - Results sub-model

Sub-model: **Results**			
IN	**FROM**	**OUT**	**TO**
DC_B, m_B, X_{B2}, X_{B4}, $[O_2]_{A9}$, EP	Inputs	DC_B, m_B, X_{B2}, X_{B4}, $[O_2]_{A9}$, TPC_1,	User
TPC_1, ACC_1, OOC_1	RSS	ACC_1, OOC_1, P_3, TPC_3, ACC_3,	
P_3, TPC_3, ACC_3, OOC_3	RD, RDB, BD	OOC_3, P_7, TPC_7, ACC_7, LC_7,	
P_7, TPC_7, ACC_7, LC_7, OOC_7	AEOP	OOC_7, η_{10}, TPC_{10}, ACC_{10}, OOC_{10},	
η_{10}, TPC_{10}, ACC_{10}, OOC_{10}	RFSG, UGETC	m_{W18}, TPC_{18}, ACC_{18}, OOC_{18}, TPC_{20},	
m_{W18}, T_{W19}, TPC_{18}, ACC_{18}, OOC_{18}	PGWH	ACC_{20}, OOC_{20}, P_{23}, η_{22}, TPC_{22},	
TPC_{20}, ACC_{20}, OOC_{20}	PGQ	ACC_{22}, OOC_{22}, TPC_{28}, ACC_{28},	
P_{23}, η_{22}, TPC_{22}, ACC_{22}, OOC_{22}	ICE	OOC_{28}, m_{W31}, TPC_{31}, ACC_{31},	
T_{W27}, TPC_{28}, ACC_{28}, OOC_{28}	ECWH	OOC_{31}, TPC_{34}, ACC_{34}, OOC_{34}, P_{33},	
m_{W31}, TPC_{31}, ACC_{31}, OOC_{31}	EEGWH	m_{35}, Q_{35}, η_{36}, TPC_{36}, ACB, ACC_{36},	
TPC_{34}, ACC_{34}, OOC_{34}	GC	OCC_{36}, AR_E, AR_H, AR_T, AP, COE	

Table A2.3 Data flows - Reception, Storage, Screening sub-model

Sub-model: **Reception, Storage, Screening (RSS)**			
IN	**FROM**	**OUT**	**TO**
m_B, LR, AF	Inputs	TPC_1, ACC_1, OOC_1	Results

Table A2.4 Data flows - Rotary Dryer without Burner sub-model

Sub-model: **Rotary Dryer without Burner (RD)**			
IN	**FROM**	**OUT**	**TO**
m_B, X_{B2}, X_{B4}, LR, AF	Inputs	T_{G2}	EEGWH
m_{23G}, T_{G23}, $[CO_2,N_2,H_2O,O_2]_{G23}$	ICE	P_3, TPC_3, ACC_3, OOC_3	Results

Table A2.5 Data flows - Rotary Dryer with Burner sub-model

Sub-model: **Rotary Dryer with Burner (RDB)**			
IN	**FROM**	**OUT**	**TO**
m_B, X_{B2}, X_{B4}, LR, AF	Inputs	T_{G6}, m_{G6}, T_{G6}, $[CO_2,N_2,H_2O,O_2]_{G6}$	EEGWH
m_{G23}, T_{G23}, $[CO_2,N_2,H_2O,O_2]_{G23}$	ICE	P_3, TPC_3, ACC_3, OOC_3	Results
m_{G32}, T_{G32}, $[CO_2,N_2,H_2O,O_2]_{G32}$	EEGWH		
Q_{35}	Results		

Table A2.6 Data flows - Band Dryer sub-model

Sub-model: **Band Dryer (BD)**			
IN	**FROM**	**OUT**	**TO**
$m_B, X_{B2}, X_{B4}, LR, AF$	Inputs	m_{A2}	ECR
T_{A26}	ECR	P_3, TPC_3, ACC_3, OOC_3	Results

Table A2.7 Data flows - Air Oxygen Enrichment Plant sub-model

Sub-model: **Air Oxygen Enrichment Plant (AOEP)**			
IN	**FROM**	**OUT**	**TO**
m_{A9}	RFSG, UGETC	$P_7, TPC_7, ACC_7, LC_7, OOC_7$	Results
$[O_2]_{A9}, LR, AF$	Inputs		
$m_{A21}, [O_2]_{A21}$	ICE		

Table A2.8 Data flows - Reverse Flow Slagging Gasifier sub-model

Sub-model: **Reverse Flow Slagging Gasifier (RFSG)**			
IN	**FROM**	**OUT**	**TO**
$m_B, X_{B4}, [O_2]_{A9}, LR, AF, F$	Inputs	m_{A9}	AOEP
		$m_{G11}, [H_2O]_{G11}$	PGWH, PGQ, ICE
		$[H_2, CO, CO_2, CH_4, N_2]_{G11}$	PGWH, ICE
		T_{G11}	PGWH
		$\eta_{10}, TPC_{10}, ACC_{10}, OOC_{10}$	Results

Table A2.9 Data flows - Updraft Gasifier with External Tar Cracking sub-model

Sub-model: **Updraft Gasifier with External Tar Cracking (UGETC)**			
IN	**FROM**	**OUT**	**TO**
m_B, X_{B4}, LR, AF	Inputs	m_{A9}	AOEP
		$m_{G11}, [H_2O]_{G11}$	PGWH, PGQ, ICE
		$[H_2, CO, CO_2, CH_4, N_2]_{G11}$	PGWH, ICE
		T_{G11}	PGWH
		$\eta_{10}, TPC_{10}, ACC_{10}, OOC_{10}$	Results

Table A2.10 Data flows - Product Gas Water Heater sub-model

Sub-model: **Product Gas Water Heater (PGWH)**			
IN	**FROM**	**OUT**	**TO**
LR, AF	Inputs	m_{W18}	EEGWH
$m_{G11}, T_{G11}, [H_2, CO, CO_2, CH_4, N_2, H_2O]_{G11}$	RFSG, UGETC	$m_{W18}, T_{W19}, TPC_{18},$	Results
$m_{W28}, T_{W27}, T_{W29}$	ECWH	ACC_{18}, OOC_{18}	

Table A2.11 Data flows - Product Gas Quench sub-model

Sub-model: **Product Gas Quench (PGQ)**			
IN	**FROM**	**OUT**	**TO**
LR, AF	Inputs	$TPC_{20}, ACC_{20}, OOC_{20}$	Results
$m_{G11}, [H_2O]_{G11}$	RFSG, UGETC		

A63

Table A2.12 Data flows - IC Engine sub-model

Sub-model: IC Engine (ICE)			
IN	**FROM**	**OUT**	**TO**
LR, AF m_{G11}, $[H_2, CO, CO_2, CH_4, N_2]_{G11}$	Inputs RFSG, UGETC	m_{23G}, T_{G23}, $[CO_2, N_2, H_2O, O_2]_{G23}$ m_{A21}, $[O_2]_{A21}$ m_{C22} P_{23}, η_{22}, TPC_{22}, ACC_{22}, OOC_{22}	RD, RDB, EEGWH AOEP ECR, ECWH Results

Table A2.13 Data flows - Engine Coolant Radiator sub-model

Sub-model: **Engine Coolant Radiator (ECR)**			
IN	**FROM**	**OUT**	**TO**
m_{C22} m_{A2}	ICE BD	T_{A26} m_{C25}	BD ECWH

Table A2.14 Data flows - Engine Coolant Water Heater sub-model

Sub-model: **Engine Coolant Water Heater (ECWH)**			
IN	**FROM**	**OUT**	**TO**
LR, AF m_{C22} m_{C25}	Inputs ICE ECR	m_{W28}, T_{W27}, T_{W29} T_{W27}, TPC_{28}, ACC_{28}, OOC_{28}	PGWH, ECWH Results

Table A2.15 Data flows - Engine Exhaust Gas Water Heater sub-model

IN	FROM	OUT	TO
Sub-model: **Engine Exhaust Gas Water Heater (EEGWH)**			
LR, AF	Inputs	$m_{G32}, T_{G32}, [CO_2,N_2,H_2O,O_2]_{G32}$	RDB
$m_{G23}, T_{G23}, [CO_2,N_2,H_2O,O_2]_{G23}$	ICE	$m_{W31}, TPC_{31}, ACC_{31}, OOC_{31}$	Results
$T_{G6}, m_{G6}, T_{G6}, [CO_2,N_2,H_2O,O_2]_{G6}$	RDB		
T_{G2}	RD		
$m_{W28}, T_{W27}, T_{W29}$	ECWH		
m_{W18}	PGWH		

Table A2.16 Data flows - Grid Connection sub-model

IN	FROM	OUT	TO
Sub-model: **Grid Connection (GC)**			
LR, AF	Inputs	$TPC_{34}, ACC_{34}, OOC_{34}$	Results
P_{33}	Results		